AD-A038 758 NAVAL POSTGRADUATE SCHOOL MONTEREY CALIF F/G 13/10.1
AUTOMATIC DEPTH AND PITCH CONTROL FOR SUBMARINES.(U)
DEC 76 V NITSCHE, K J LUESSOW

UNCLASSIFIED NL

1 OF 3
AD A038758

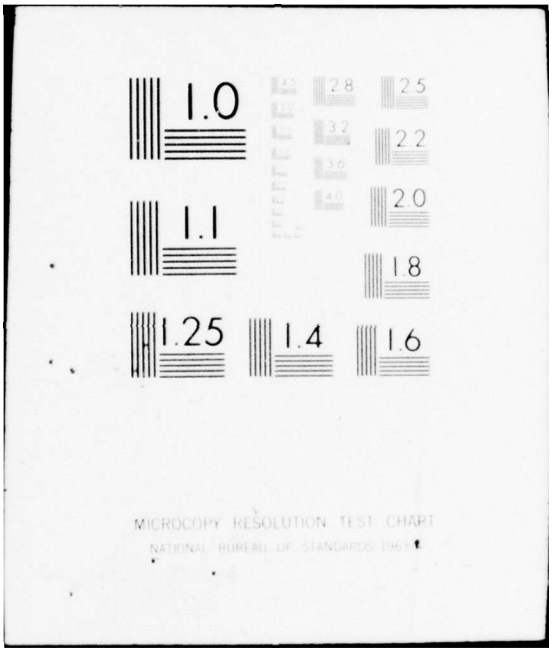
1.0
1.1
1.25
1.4
1.6
2.8
2.5
3.2
2.2
3.6
2.0
4.0
1.8
MICROCOPY RESOLUTION TEST CHART
NATIONAL BUREAU OF STANDARDS 1963

NAVAL POSTGRADUATE SCHOOL
Monterey, California

THESIS

AUTOMATIC DEPTH AND PITCH CONTROL SYSTEMS

FOR SUBMARINES

by

Volkmar Nitsche

Klaus J.C. Luessow

December 1976

Thesis Advisor: G.J. Thaler

Approved for public release; distribution unlimited.

SECURITY CLASSIFICATION OF THIS PAGE (When Data Entered)

REPORT DOCUMENTATION PAGE		READ INSTRUCTIONS BEFORE COMPLETING FORM
1. REPORT NUMBER	2. GOVT ACCESSION NO.	3. RECIPIENT'S CATALOG NUMBER
4. TITLE (and Subtitle) Automatic Depth and Pitch Control for Submarines,		5. TYPE OF REPORT & PERIOD COVERED Master's Thesis; December 1976 6. PERFORMING ORG. REPORT NUMBER
7. AUTHOR(s) Volkmar Nitsche Klaus J.C. Luessow		8. CONTRACT OR GRANT NUMBER(s)
9. PERFORMING ORGANIZATION NAME AND ADDRESS Naval Postgraduate School Monterey, California 93940		10. PROGRAM ELEMENT, PROJECT, TASK AREA & WORK UNIT NUMBERS
11. CONTROLLING OFFICE NAME AND ADDRESS Naval Postgraduate School Monterey, California 93940		12. REPORT DATE December 1976 13. NUMBER OF PAGES 259 (12) 260 pp.
14. MONITORING AGENCY NAME & ADDRESS(if different from Controlling Office) Naval Postgraduate School Monterey, California 93940		15. SECURITY CLASS. (of this report) Unclassified 15a. DECLASSIFICATION/DOWNGRADING SCHEDULE

16. DISTRIBUTION STATEMENT (of this Report)

Approved for public release; distribution unlimited.

17. DISTRIBUTION STATEMENT (of the abstract entered in Block 20, if different from Report)

18. SUPPLEMENTARY NOTES

19. KEY WORDS (Continue on reverse side if necessary and identify by block number)

20. ABSTRACT (Continue on reverse side if necessary and identify by block number)

Steady-state and total decoupling schemes for multivariable systems are used to develop two automatic control systems for the vertical motion of a fictitious submarine. A linearized mathematical model is derived from a non-linear model in six degrees of freedom. Both designs are simulated and evaluated with respect to performance, simplicity of design procedure, and grade of complexity. The controller, designed via the —OVER

DD FORM 1 JAN 73 1473 (Page 1)

EDITION OF 1 NOV 65 IS OBSOLETE
S/N 0102-014-6601

251 450

SECURITY CLASSIFICATION OF THIS PAGE (When Data Entered)

steady-state decoupling method, is implemented in the non-linear model and tested under various operating conditions.

AUTOMATIC DEPTH AND PITCH CONTROL SYSTEMS FOR SUBMARINES

by

Volkmar Nitsche
Lieutenant-Commander, Federal German Navy

Klaus J.C. Luessow
Lieutenant-Commander, Federal German Navy

Submitted in partial fulfillment of the
requirements for the degree of

MASTER OF SCIENCE IN APPLIED SCIENCE

from the

NAVAL POSTGRADUATE SCHOOL
December 1976

Authors: Volkmar Nitsche

Klaus Luessow

Approved by: Gerald A. Thaler
Thesis Advisor

D. E. Kirk
Chairman, Department of Electrical Engineering

Robert B. Testerman
Dean of Science and Engineering

ABSTRACT

Steady-state and total decoupling schemes for multivariable systems are used to develop two automatic control systems for the vertical motion of a fictitious submarine. A linearized mathematical model is derived from a non-linear model in six degrees of freedom. Both designs are simulated and evaluated with respect to performance, simplicity of design procedure, and grade of complexity. The controller, designed via the steady-state decoupling method, is implemented in the non-linear model and tested under various operating conditions.

TABLE OF CONTENTS

I. INTRODUCTION

The extreme importance of automatic control has become obvious for example in space vehicle control and missile guidance where manual control is not feasible. In addition it can provide means to relieve people from tedious routine and repetitive manual operations.

The complexity of a submarine offers a wide area of control problems. Deep water and near surface depth keeping, maneuvering, hovering, fuel economy, safety, crew comfort, etc. require precise controls.

Characteristic for a submarine is translation in three dimensions, where depth control is of essential importance. The automatic control of motion in the vertical plane, i.e. depth and pitch control, is the subject of this thesis.

Three sets of planes, the rudder, the fairwater and stern plane, the propulsion system, and a ballast system can be used to maneuver the submarine. The objective is to design a controller for depth changing maneuvers by automatic control of the fairwater and stern plane.

Previous designs were based on Optimal Control Theory, requiring feedback of both position and rate information. These informations are easily available when the submarine is equipped with an inertial guidance system. Rate information may be not available, as for example in the German coastal submarines. It may also be a desirable feature to have reduced sensor requirements. In these cases a different design approach must be used using position feedback only.

This thesis investigates two possible design methods, steady-state and total decoupling. As a basis for both designs a linear model is developed and validated.

Steady-state decoupling is achieved by designing a cascaded diagonal compensator matrix, using classical single-loop techniques. Based on the desired response characteristics the total decoupling scheme leads to a cascaded compensator matrix with off-diagonal terms. Both designs are simulated and evaluated with respect to performance, simplicity of design procedure, and grade of complexity.

II. SIMULATION MODELS

A. STANDARD MODEL

A set of " Standard Equations of Motion for Submarine Simulation " was developed by NSRDC (Ref. 1). Equations and additional auxiliary equations are repeated in Appendix A.

These equations are referred to a right-hand orthogonal system of moving axes, fixed in the body with its origin located at the center of mass (CG) of the body. The x-z-plane is the principle plane of symmetry (vertical center plane for submarines); the x-axis is parallel to the baseline of the body. Angular velocity components, forces, and moments are shown in Fig. 1.

The equations are written in a form utilizing nondimensionalized hydrodynamic coefficients and are applicable to the rigid body motions of submarines and other submerged vehicles. Complete sets of hydrodynamic coefficients have been determined by NSRDC. The coefficients for a fictitious submarine used in this thesis stem from a submarine simulation program developed in Ref. 2. A notation for the various terms in the equations including the hydrodynamic coefficients is given in Appendix B. Numerical values of coefficients and parameters are given in Appendix C. All coefficients of the terms containing (-1) and UC are set to zero. These terms reflect the incremental changes in forces and moments - generated by propeller rpm - due to either over or underpropulsion. For

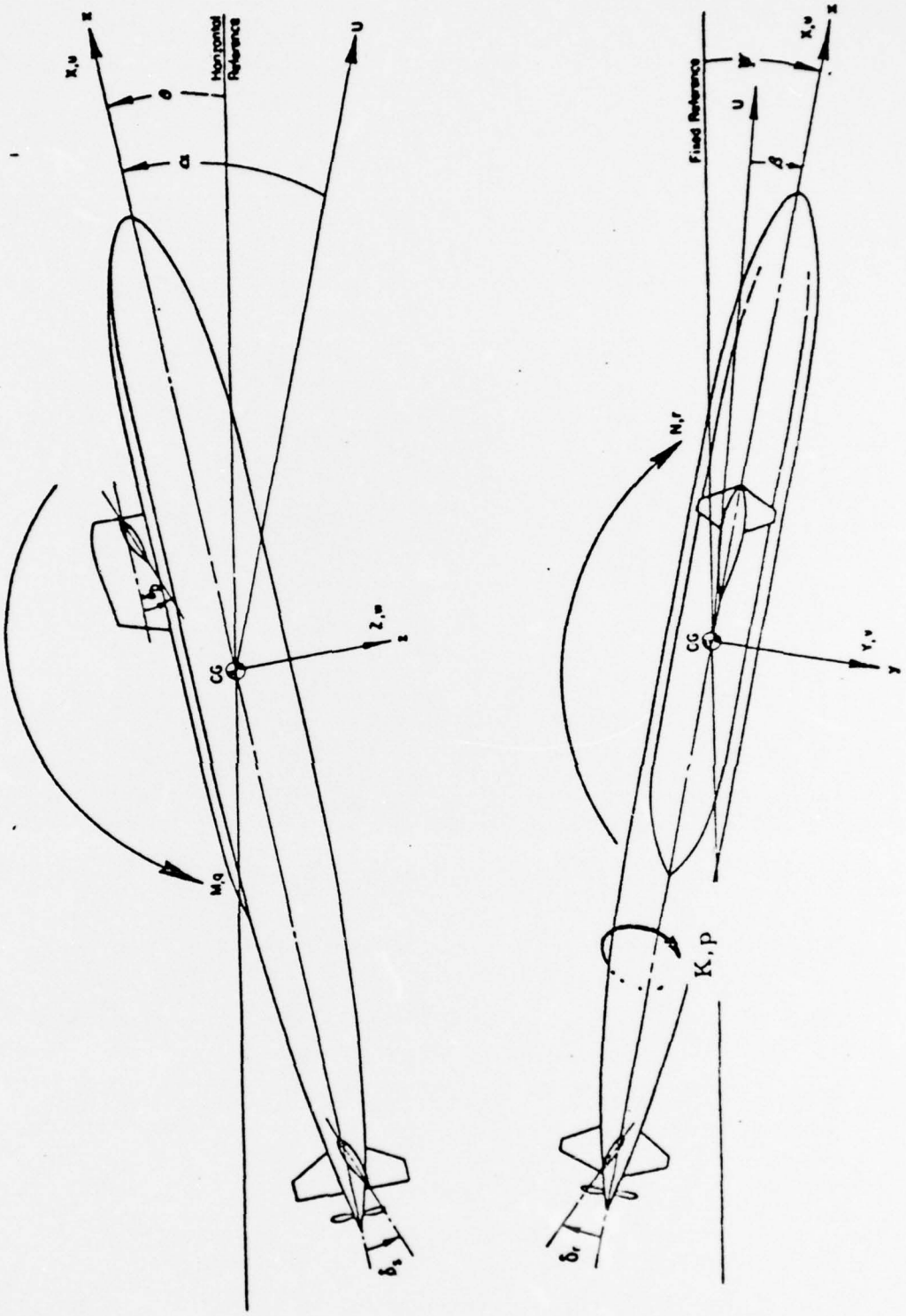

Figure 1 - SUBMARINE AXES

the moderate changes in ahead speed involved in most normal maneuvers all terms can be neglected. The coefficients used in this thesis apply only to the deeply submerged case, free of near-surface, bottom, and wall effects.

As Ref. 1 points out, correlation studies and preliminary comparisons have shown that the "Standard Equations" together with a given set of coefficients yield accurate predictions of normal maneuvers in submerged ahead motion. The "Standard Equations of Motion" will be referred to as "Non-linear Model".

In Ref. 2 H.L.Drurey translated these equations into Digital Simulation Language (DSL). The system of six equations was solved simultaneously by an approach using Cramer's rule developed and programmed by Ref. 3. The cofactors for the set of hydrodynamic coefficients used in this thesis were calculated by Drurey and are used as parameters. The validity of the DSL implementation has been shown by Ref. 2.

As this model contains non-linear terms it is not appropriate for the chosen design approach which is based on the linearity of the system. It was necessary to find a linear, representative approximation of the "Non-linear Model".

B. DERIVATION OF THE LINEARIZED MODEL

This section describes the assumptions, procedures, and tests to validate the linear model.

1. Assumptions

* Forward speed is constant

An attempt to linearize about the axial speed, u, which affects nearly every term in the standard equations, would imply a great deal of complexity. Thus the forward speed was assumed to be constant. This means that either the forward speed variations are small and can be neglected or if variations are large they impose a control problem and will be solved accordingly.

* Roll angle is small

In submarine maneuvering large roll angles occur only in the form of " Snap Roll ", i.e. high speed plus hard over rudder. Under normal conditions depth-changing and -keeping maneuvers produce very small roll angles. Therefore the roll angle can be neglected.

* Cross products of inertia may be neglected

This assumption is common to all submarine simulations because the hull and interior layout of submarines is approximately symmetric.

* All terms involving W_i are neglected

This is possible because the submarine was assumed to be in trim.

* The submarine can be approximated by a linear model

The linear equations are assumed to be a valid representation in the depth-keeping and depth-changing mode of operation respectively. This assumption is not obvious but will be verified via simulation.
These assumptions lead to the decoupling of the vertical plane from the remaining equations.

2. Derivation of state equations

As this thesis is only concerned with the vertical plane, the linearization of the horizontal plane is omitted.

Thus the linear equations are (FORTRAN-Notation, see Appendix D) :

$$\begin{aligned} M*WDCT - UC*M*Q &= L^4*ZQDOT*QDOT + L^3*ZWDOT*WDCT + \\ &\quad L^3*ZQDOT*UC*Q + L^2*ZW*UC*W + \\ &\quad L^2*UC^2*(ZDS*DS + ZDB*DB) \qquad (1) \end{aligned}$$

$$\begin{aligned} IY*QDOT &= L^5*MQDOT*QDOT + L^4*MQ*UC*Q + \\ &\quad L^4*MWDOT*WDOT + L^3*MW*UC*W + \\ &\quad L^3*UC^2(MDS*DS + MDB*DB) + \\ &\quad B*ZB*PITCH \qquad (2) \end{aligned}$$

The linearized auxiliary equations are :

$$\text{LPIDOT} = \text{LQ} \tag{3}$$

$$\text{LZDOT} = \text{W} - \text{UC}*\text{LPITCH} \tag{4}$$

Solving equation (1) and (2) for WDOT and LQDOT respectively and substituting into each other yields the following relations :

$$\begin{bmatrix} \text{WDOT} \\ \text{IQDOT} \\ \text{IC} \end{bmatrix} = \begin{bmatrix} a_{11} & a_{12} & a_{13} \\ a_{21} & a_{22} & a_{23} \\ a_{31} & a_{32} & a_{33} \end{bmatrix} \begin{bmatrix} \text{W} \\ \text{LQ} \\ \text{LPITCH} \end{bmatrix} + \begin{bmatrix} b_{11} & b_{12} \\ b_{21} & b_{22} \\ b_{31} & b_{32} \end{bmatrix} \begin{bmatrix} \text{DS} \\ \text{DB} \end{bmatrix} \tag{5}$$

which can be written as

$$\dot{\underset{\sim}{x}} = \underset{\sim\sim}{A}\underset{\sim}{x} + \underset{\sim\sim}{B}\underset{\sim}{R} \tag{6}$$

where

$$a_{11} = [L^2*ZW*UC + L^7*ZQDOT*MW*UC/(IY-L^5*MQDOT)]/\gamma$$

$$a_{12} = [L^3*ZQ*UC + M*UC + L^8*ZQDOT*MQ*UC/(IY-L^5*MQDOT)]/\gamma$$

$$a_{13} = -[L^4*ZQDOT*ZB*B/(IY-L^5*MQDOT)]/\gamma$$

$$a_{21} = [L^3*MW*UC + L^6*MWDOT*ZW*UC/(M-L^3*ZWDOT)]/\epsilon$$

$$a_{22} = [L^4*MQ*UC + L^7*MWDOT*ZQ*UC + L^4*MWDOT*M*UC/(M-L^3*ZWDOT)]/\epsilon$$

$$a_{23} = -B*ZB/\epsilon$$

$$a_{31} = 0.0$$

$$a_{32} = 1.0$$

$$a_{33} = 0.0$$

$$b_{11} = [L^2*ZDS*UC^2 + L^7*ZQDOT*MDS*UC^2/(IY-L^5*MQDOT)]/$$

$$b_{12} = [L^2*ZDE*UC^2 + L^7*ZQDOT*MDB*UC^2/(IY-L^5*MQDOT)]/$$

$$b_{21} = [L^3*MDS*UC^2 + L^6*MWDOT*ZDS*UC^2/(M-L^3*ZWDOT)]/$$

$$b_{22} = [L^3*MDE*UC^2 + L^6*MWDOT*ZDB*UC^2/(M-L^3*ZWDOT)]/$$

$$b_{31} = 0.0$$

$$b_{32} = 0.0$$

with

$$\gamma = M - L^3*ZWDOT - L^8*ZQDOT*MWDOT/(IY-L^5*MQDOT)$$

$$\mathcal{E} = IY - L^5*MQDOT - L^8*MWDOT*ZQDOT/(M - L^3*ZWDOT)$$

Vector equation (5) describes the state variable representation of the linearized, vertical plane equations of motion. However the state vector does not contain ZDOT but W. W represents the component of u in the z-direction, in order to make the depth a state variable one wants to use LZDOT which represents the depth change in the z-direction. Thus the linearized auxiliary equation (4) is used for the transformation

$$LZDOT = W - UC*LPITCH$$

By definition

$$\hat{\underset{\sim}{X}} = \begin{bmatrix} LZDCT \\ LQ \\ LPITCH \end{bmatrix} \qquad \underset{\sim}{X} = \begin{bmatrix} W \\ LQ \\ LPITCH \end{bmatrix}$$

Using the linear operator M, the new set of state variables is formed

$$\hat{\underset{\sim}{X}} = \underset{\sim}{M}\underset{\sim}{X}$$

where

$$\underset{\sim}{M} = \begin{bmatrix} 1 & 0 & -UC \\ 0 & 1 & 0 \\ 0 & 0 & 1 \end{bmatrix}$$

equations (6) become

$$\underset{\sim}{M}^{-1}\dot{\hat{\underset{\sim}{X}}} = \underset{\sim}{A}\underset{\sim}{M}^{-1}\hat{\underset{\sim}{X}} + \underset{\sim}{B}\underset{\sim}{R}$$

then

$$\dot{\hat{\underset{\sim}{X}}} = \underset{\sim}{M}\underset{\sim}{A}\underset{\sim}{M}^{-1}\hat{\underset{\sim}{X}} + \underset{\sim}{M}\underset{\sim}{B}\underset{\sim}{R}$$

but

$$\underset{\sim}{M}\underset{\sim}{B} = \hat{\underset{\sim}{B}} = \underset{\sim}{B}$$

thus

$$\dot{\hat{\underset{\sim}{X}}} = \underset{\sim}{M}\underset{\sim}{A}\underset{\sim}{M}^{-1}\hat{\underset{\sim}{X}} + \underset{\sim}{B}\underset{\sim}{R}$$

which can be rewritten as

$$\dot{\hat{\underset{\sim}{X}}} = \hat{\underset{\sim}{A}}\hat{\underset{\sim}{X}} + \hat{\underset{\sim}{B}}\underset{\sim}{R} \qquad (7)$$

where

$$\hat{\underset{\sim}{A}} = \begin{bmatrix} a_{11} & [a_{12}-UC] & [a_{13}+a_{11}*UC] \\ a_{21} & a_{22} & [a_{21}*UC+a_{23}] \\ 0.0 & 1.0 & 0.0 \end{bmatrix}$$

this can be written as

$$\hat{\underset{\sim}{A}} = \begin{bmatrix} A11*UC & A12*UC & [A13+A14*UC^2] \\ A21*UC & A22*UC & [A23*UC^2+A24] \\ 0.0 & 1.0 & 0.0 \end{bmatrix}$$

and

$$\hat{\underset{\sim}{B}} = UC^2 \begin{bmatrix} B11 & B12 \\ B21 & B22 \\ 0.0 & 0.0 \end{bmatrix}$$

Using the numerical values for the hydrodynamic coefficients given in Appendix C and letting UC still be variable, the constants of the A and B matrices are

$A11 = -1.728\ 10^{-3}$

$A12 = -0.7062$

$A13 = 0.01289$

$A14 = -1.728\ 10^{-3}$

$A21 = 1.884\ 10^{-5}$

$A22 = -6.365\ 10^{-3}$

$A23 = 1.884\ 10^{-5}$

$A24 = -2.522\ 10^{-3}$

$$B11 = -6.668\ 10^{-4}$$

$$B12 = -3.871\ 10^{-4}$$

$$B21 = -1.465\ 10^{-5}$$

$$B22 = 3.190\ 10^{-6}$$

C. VALIDATION OF LINEAR MODEL

The objective of this section is to compare the dynamics of the standard model with the developed linear model.

In order to compare both models, they should be in the same initial state, i.e. besides the identical initial conditions both models have to be " in trim ". One linearizing assumption was that the model will be in trim at all times. Therefore the standard model was brought into "neutral conditions" for the given test speeds, in order to avoid additional forcing terms. This procedure will be described explicitly in a later chapter.

Any total system response can be viewed as having two components: forced and free. The forced component includes the complex frequencies of the forcing functions, the free component the complex or natural frequencies of the system. Both response components were checked via simulation.

1. Initial condition response

It was expected that for small perturbations the deviations between both models should be small. Therefore initial conditions of 2.5° in pitch where tested first. The initial value of the second variable LZDOT was defined as -UC*sin(initial pitch), based on the auxiliary equation for depth change.

Test runs over 400 sec in the speed range 3 - 15 knots were performed simultaneously for both models. Table 01 shows the max. differences between the model responses. Fig. 2-11 are a representative selection of the depth change and the pitch behavior. In each figure curve 1 represents the non-linear, curve 2 the linear model.

Table 01 - Initial condition response to 2.5 ° pitch

Run	Speed in kn	Maximal deviation in				Fig.
		Pitch in °	Lzdot ft/s	Depth in ft	Speed in kn	
1	3	$3.04\ 10^{-2}$	$1.27\ 10^{-3}$	$1.10\ 10^{-1}$	$2.48\ 10^{-3}$	2,3
2	5	$8.20\ 10^{-2}$	$1.02\ 10^{-3}$	$6.54\ 10^{-1}$	$3.23\ 10^{-3}$	
3	7	$2.17\ 10^{-2}$	$3.08\ 10^{-3}$	$7.52\ 10^{-1}$	$4.03\ 10^{-3}$	4,5
4	9	$6.27\ 10^{-3}$	$5.19\ 10^{-3}$	$7.32\ 10^{-1}$	$5.18\ 10^{-3}$	6,7
5	11	$1.21\ 10^{-2}$	$4.47\ 10^{-3}$	$6.34\ 10^{-1}$	$7.26\ 10^{-3}$	8,9
6	13	$1.73\ 10^{-2}$	$1.78\ 10^{-2}$	1.53	$8.65\ 10^{-3}$	
7	15	$1.21\ 10^{-2}$	$5.39\ 10^{-3}$	$8.06\ 10^{-1}$	$1.09\ 10^{-2}$	10,11

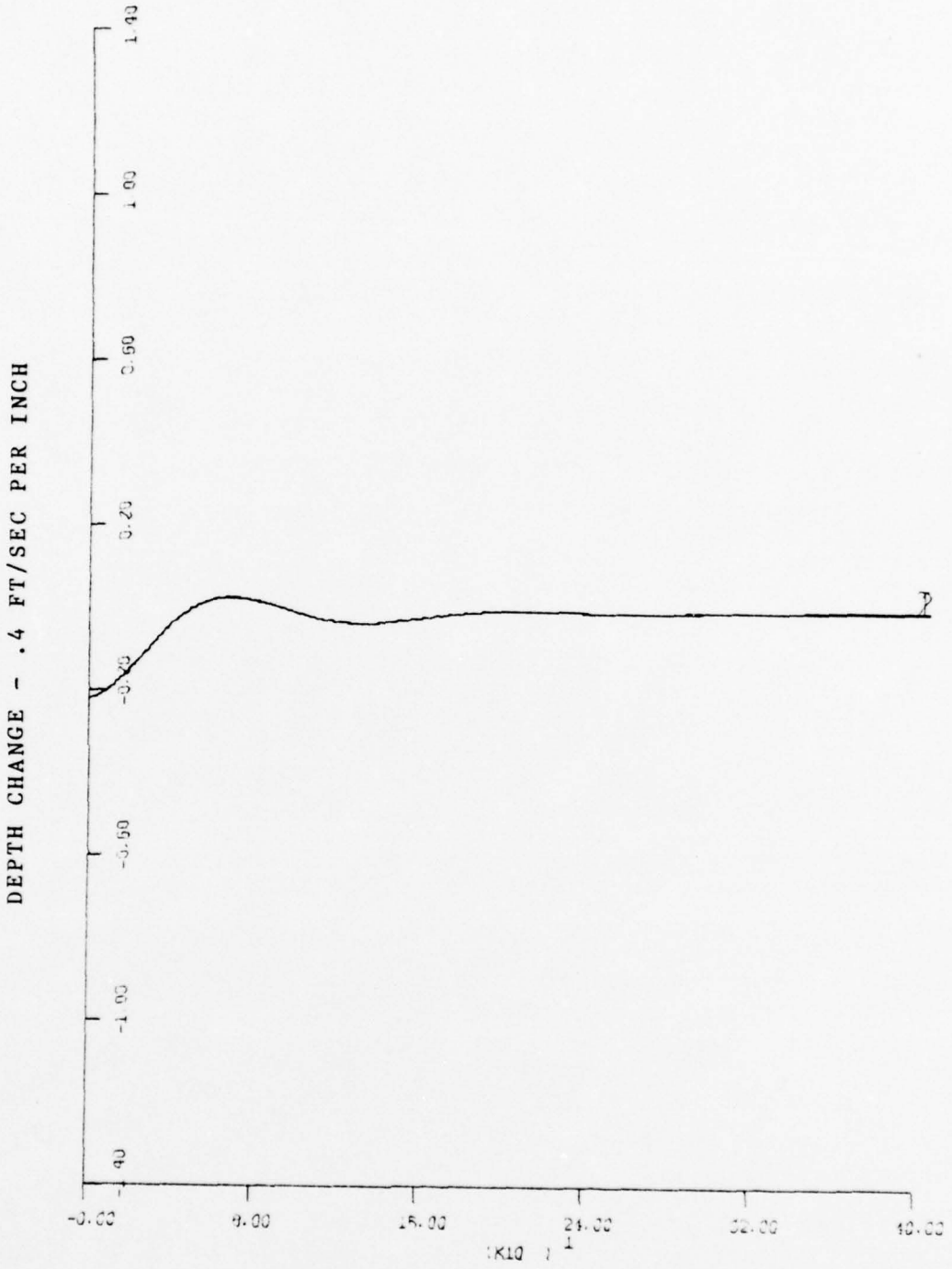

Figure 2 - INITIAL CONDITION RESPONSE
INITIAL PITCH = 2.5 °, SPEED = 3 KN

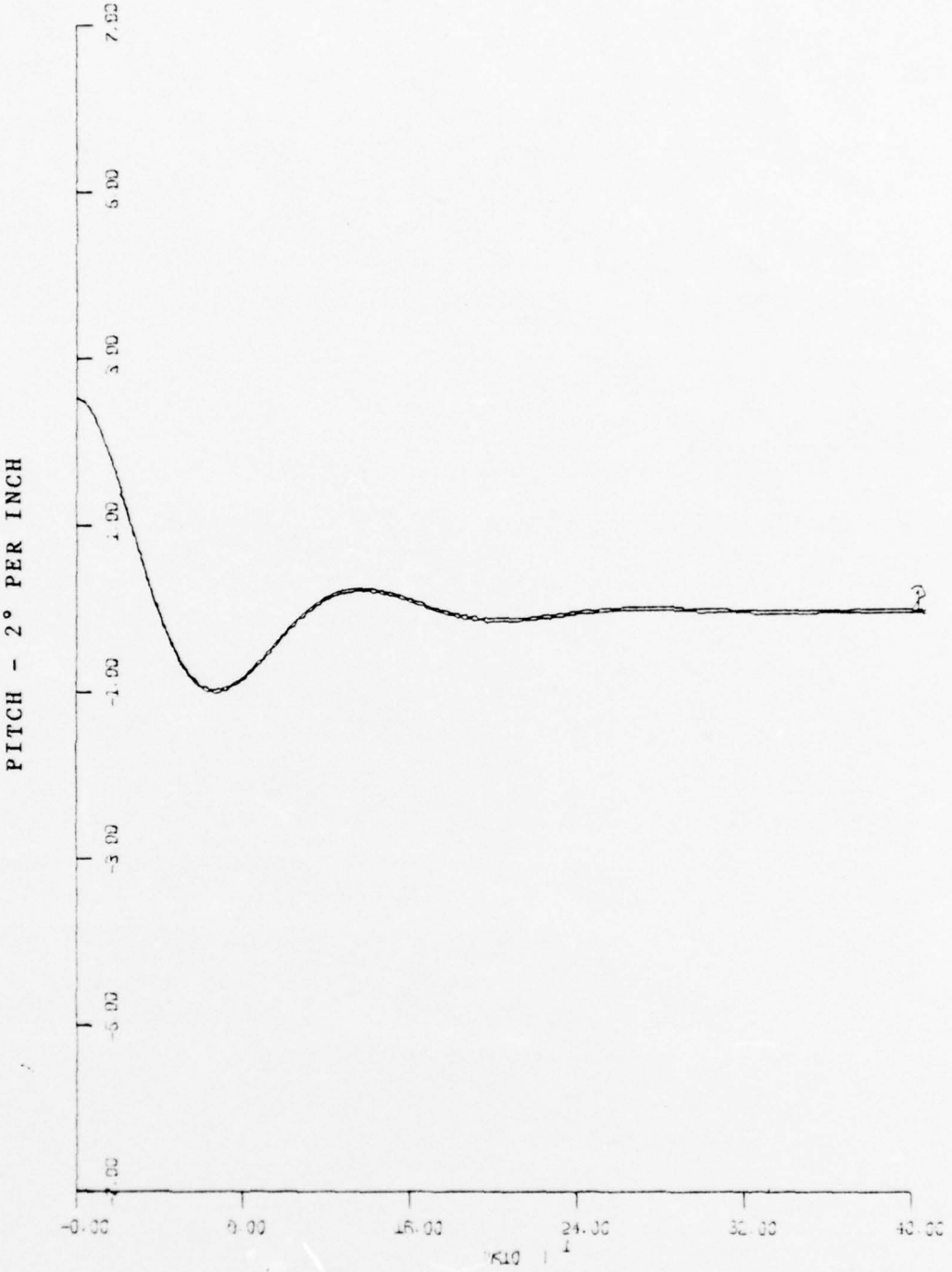

Figure 3 - INITIAL CONDITION RESPONSE
INITIAL PITCH = 2.5 °, SPEED = 3 KN

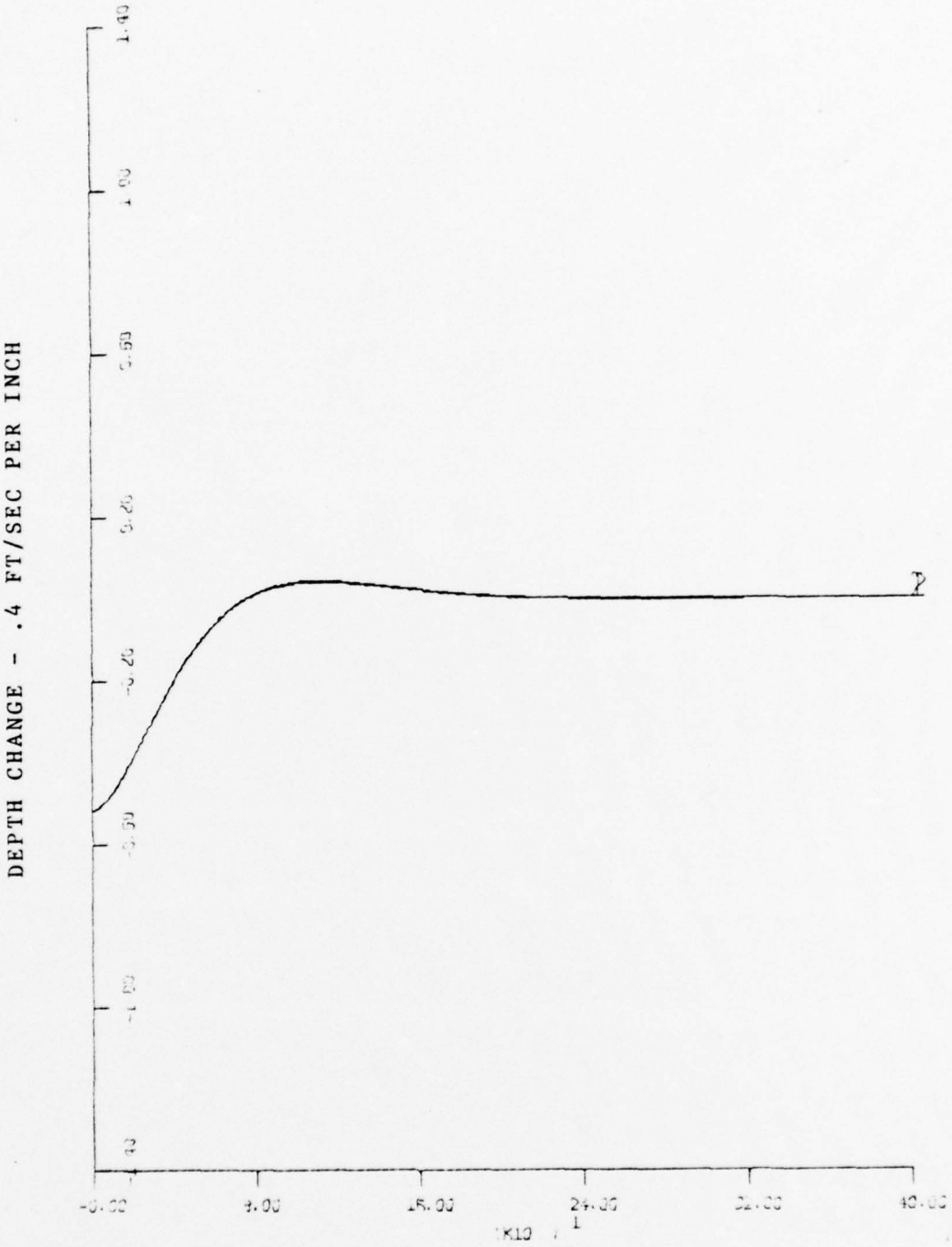

Figure 4 - INITIAL CONDITION RESPONSE
INITIAL PITCH = 2.5 °, SPEED = 7 KN

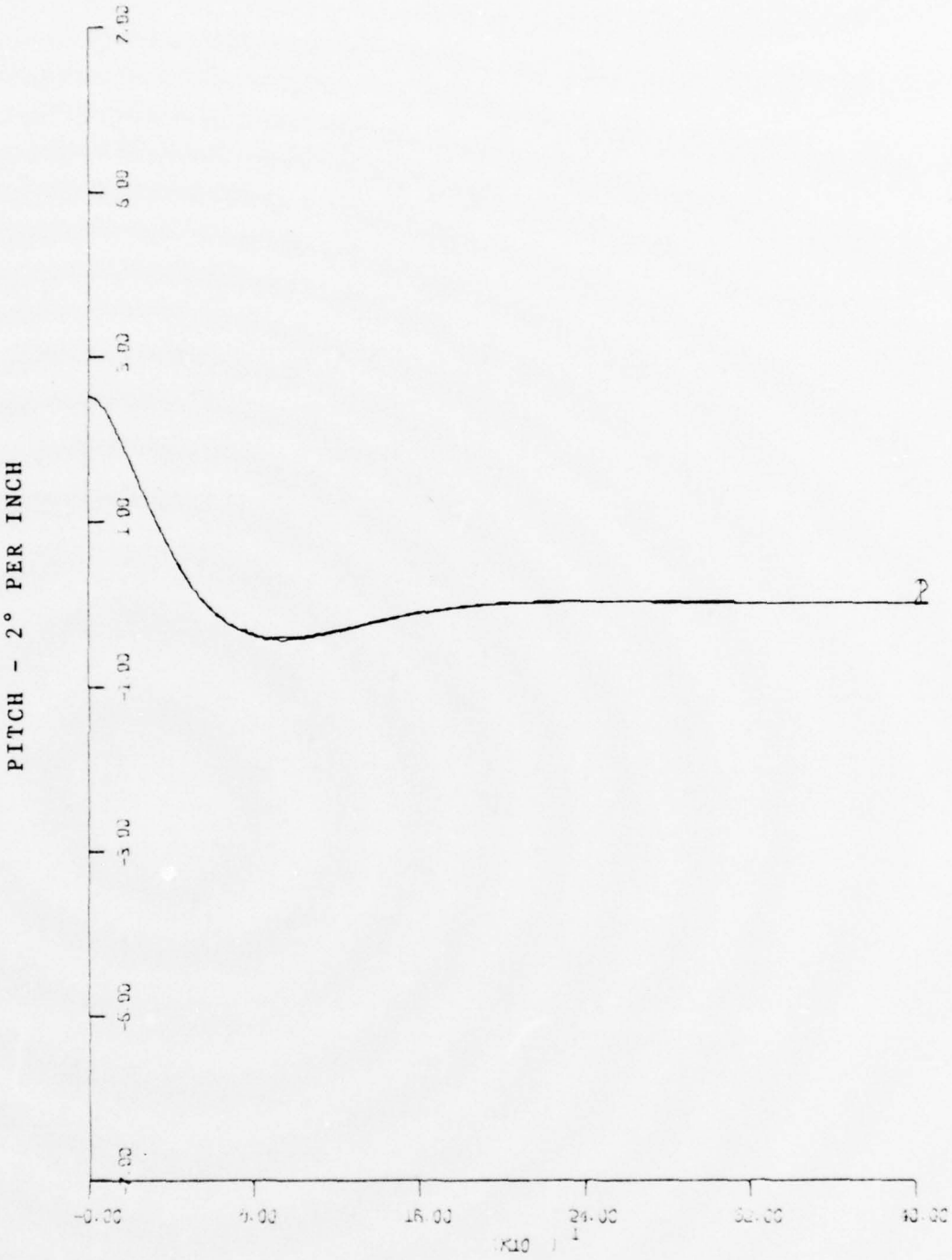

Figure 5 - INITIAL CONDITION RESPONSE
INITIAL PITCH = 2.5 °, SPEED = 7 KN

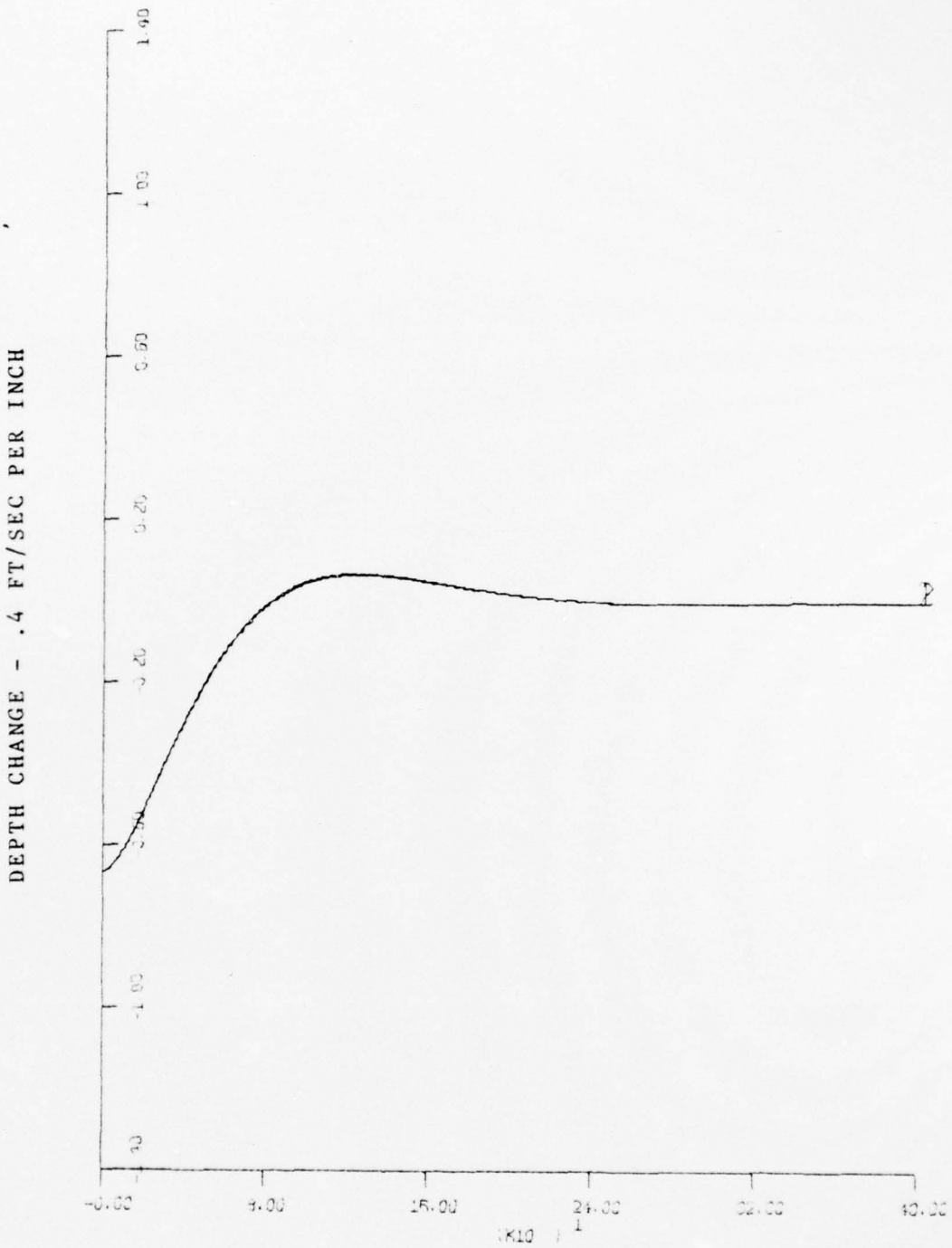

Figure 6 - INITIAL CONDITION RESPONSE
INITIAL PITCH = 2.5 °, SPEED = 9 KN

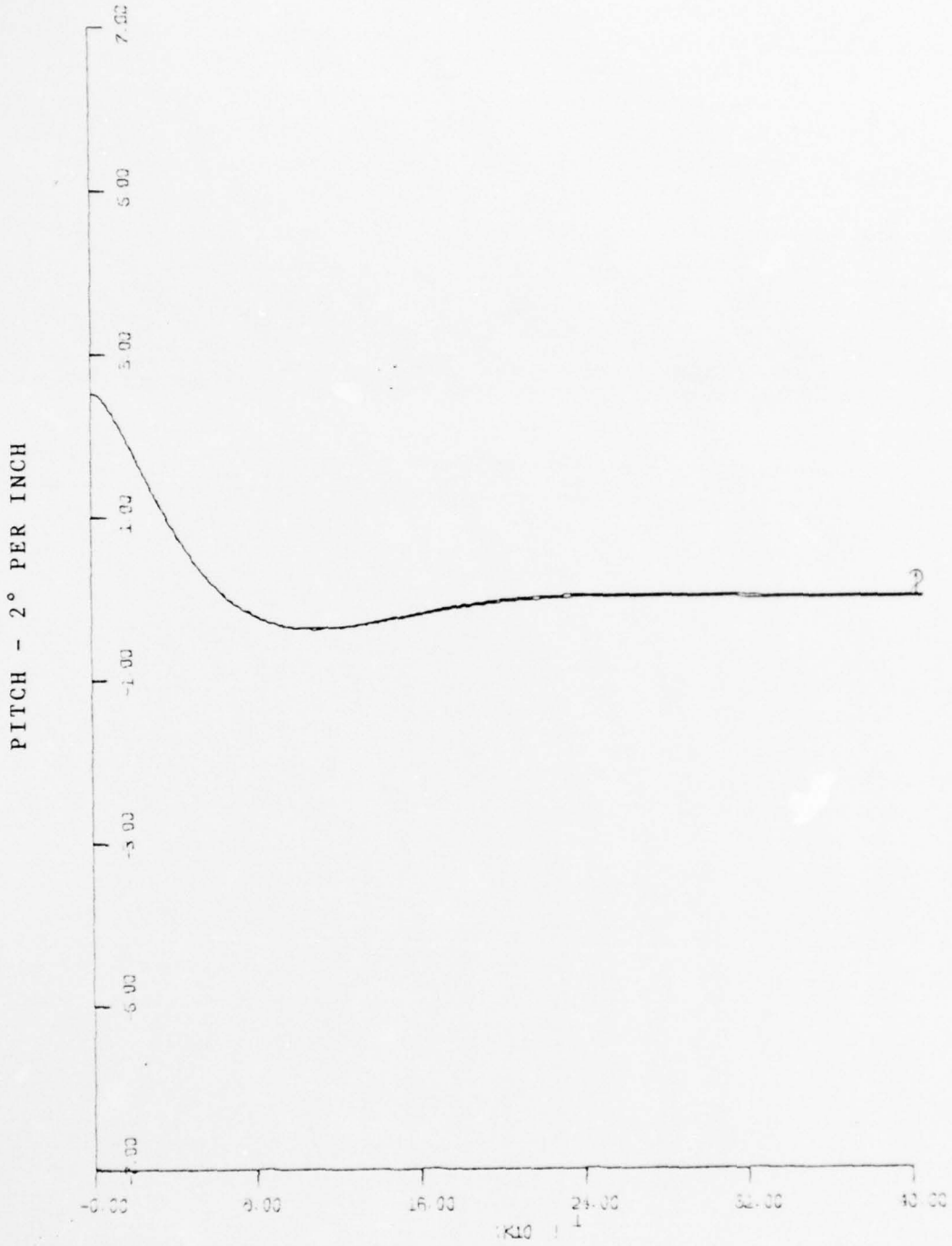

Figure 7 - INITIAL CONDITION RESPONSE
INITIAL PITCH = 2.5 °, SPEED = 9 KN

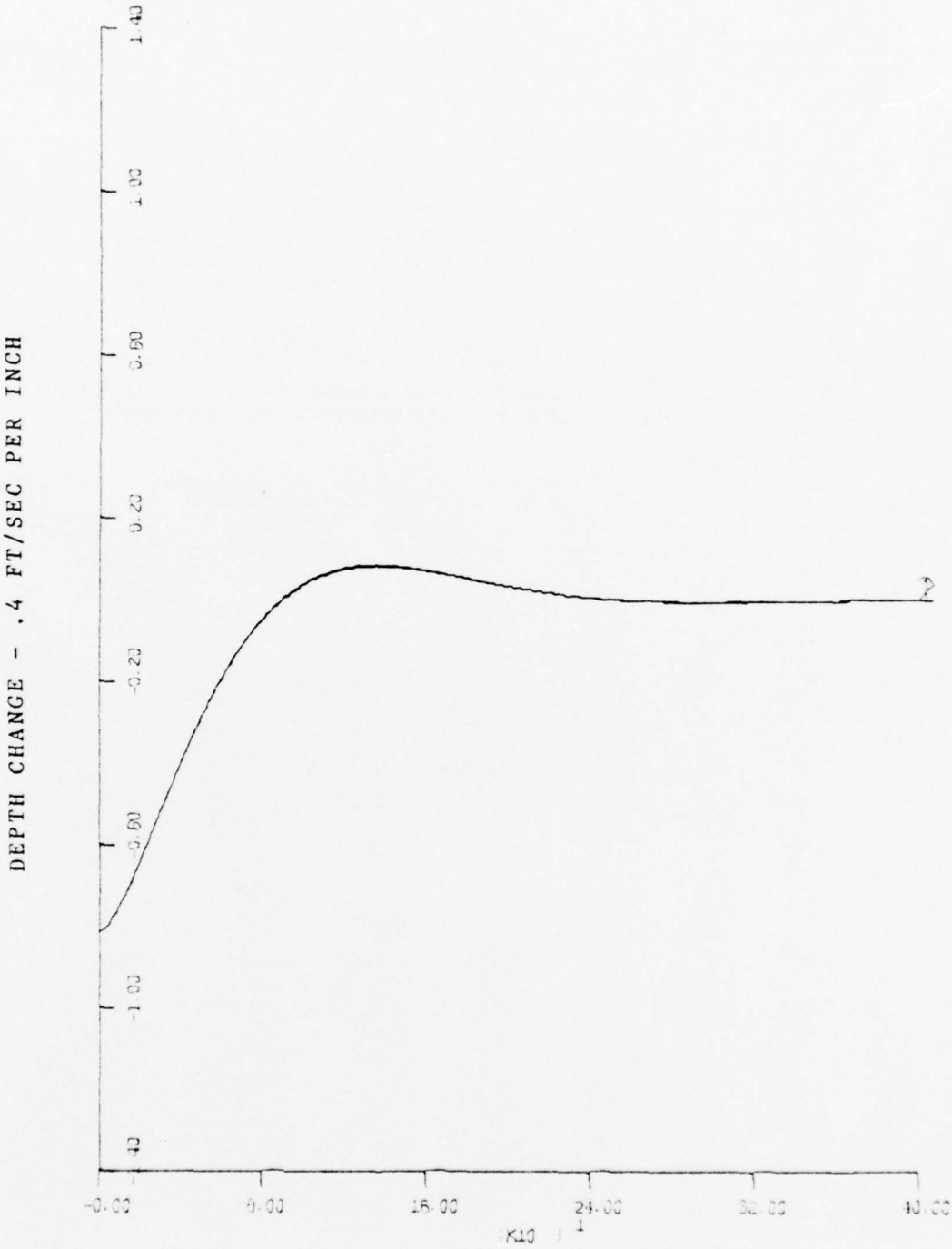

Figure 8 - INITIAL CONDITION RESPONSE
INITIAL PITCH = 2.5 °, SPEED = 11 KN

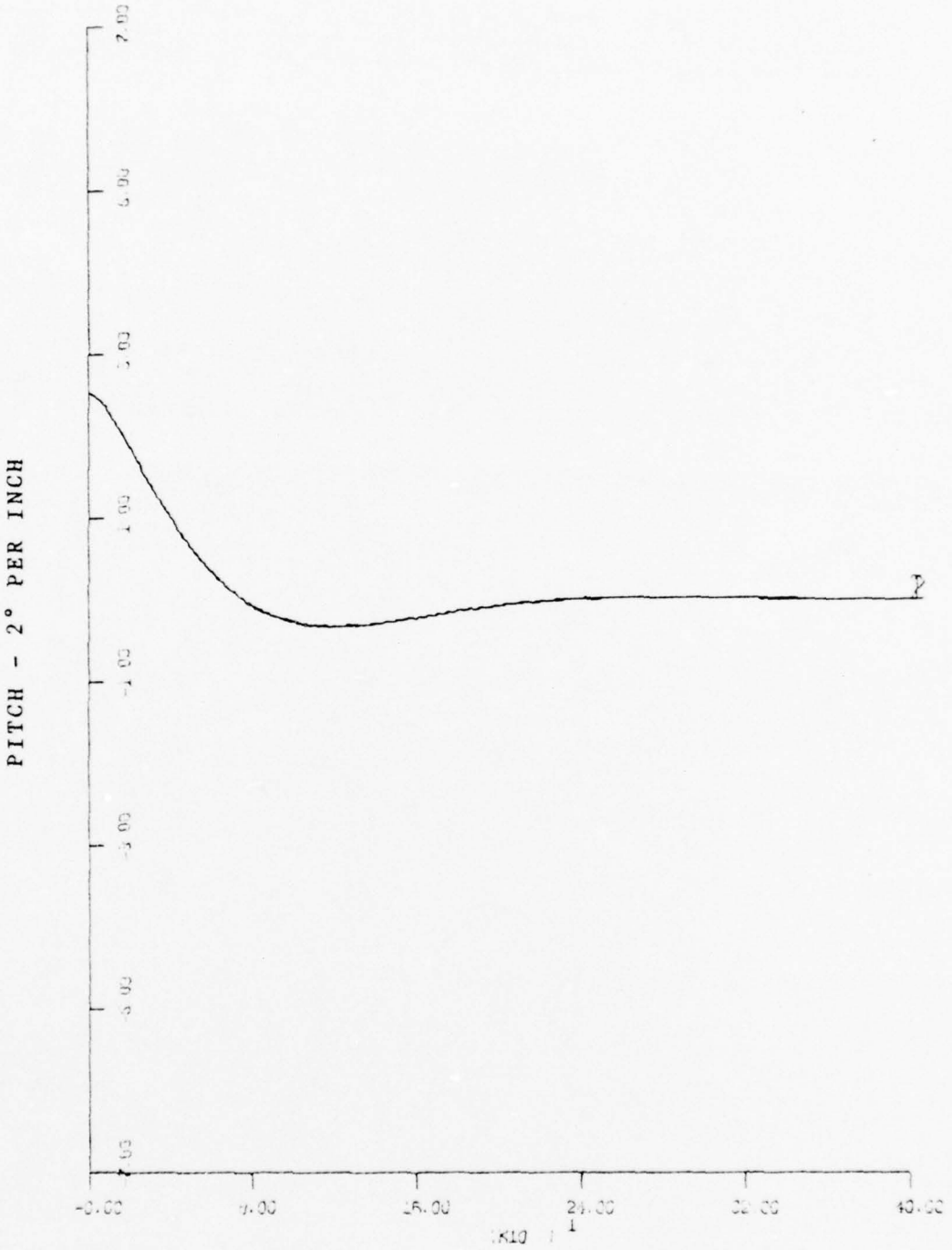

Figure 9 - INITIAL CONDITION RESPONSE
INITIAL PITCH = 2.5 °, SPEED = 11 KN

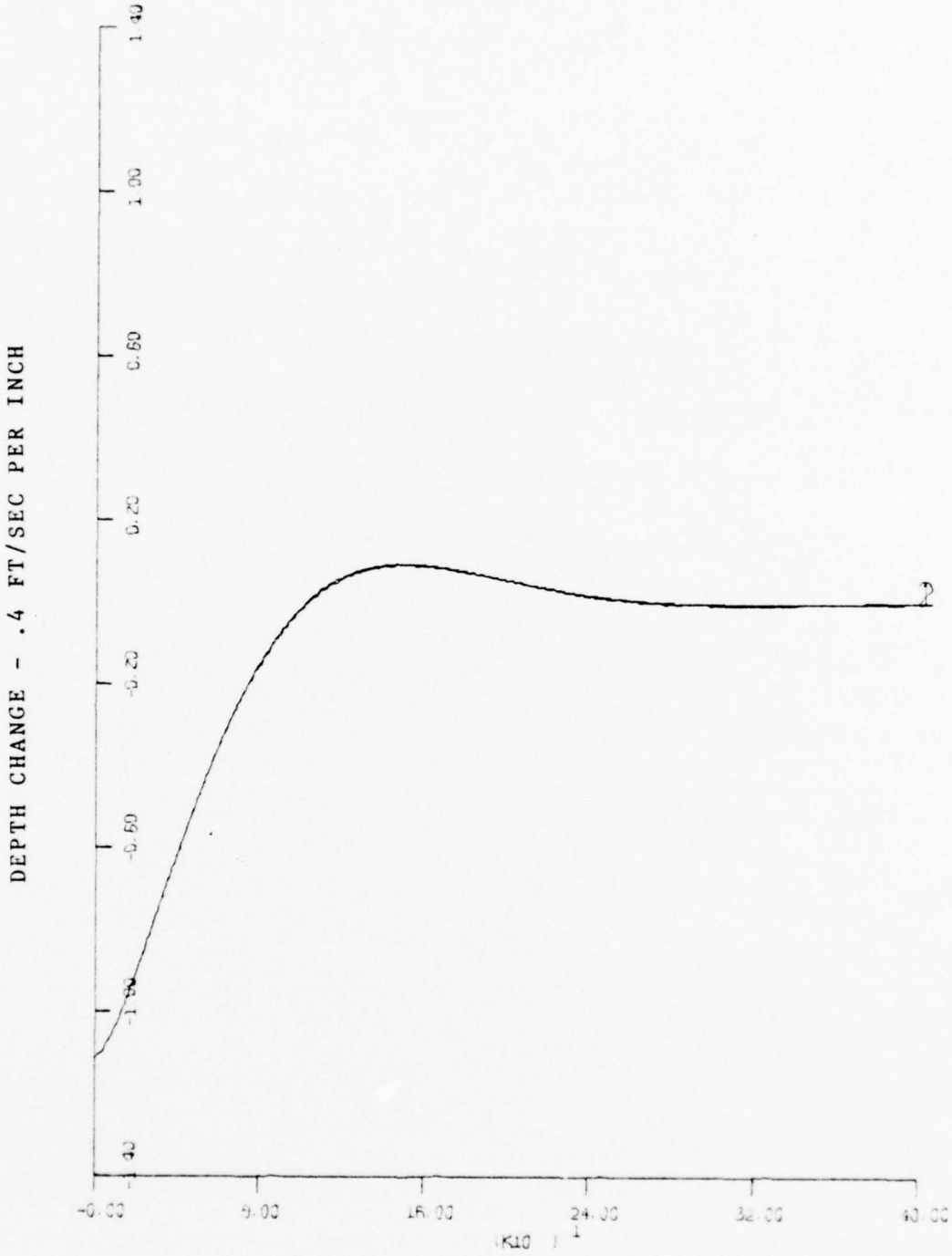

Figure 10 - INITIAL CONDITION RESPONSE
INITIAL PITCH = 2.5 °, SPEED = 15 KN

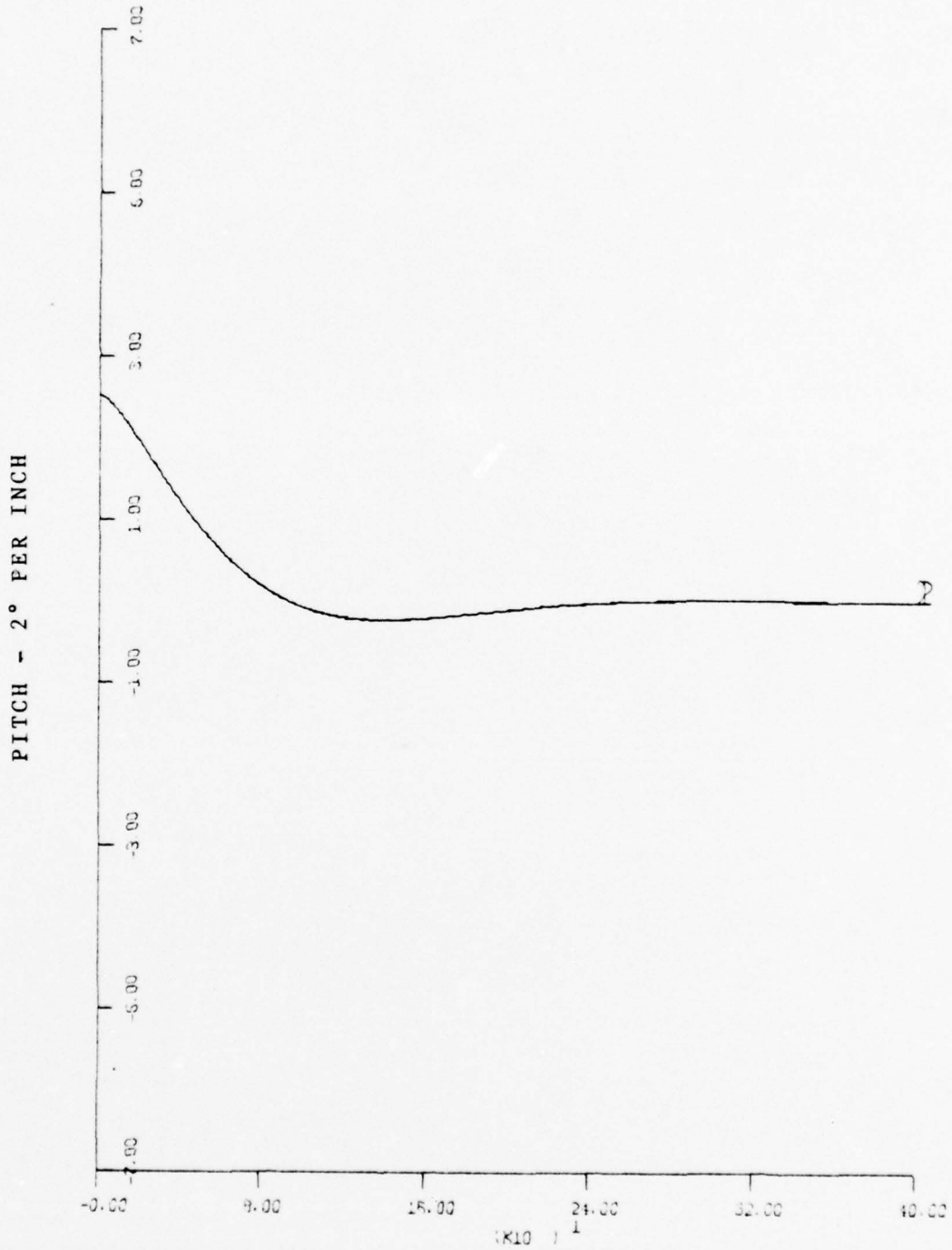

TIME - 80 SEC PER INCH

Figure 11 - INITIAL CONDITION RESPONSE
INITIAL PITCH = 2.5 °, SPEED = 15 KN

As one can readily observe, all deviations are small for this initial condition, which indicates that the dynamics are nearly identical for small perturbations.

The maximum pitch angle expected in normal operations is limited to about 45 °. Therefore this initial condition was simulated as well. As for the initial condition of 2.5° the max. deviations are summarized in Table 02. In Fig. 12-23 curve 1 represents the non-linear, curve 2 the linear model.

The second set of initial conditions, which represents rather large perturbations, still leads to very similar dynamic behavior, but the deviations increased substantially. This was expected as the angle approximation

$$\sin \Theta = \Theta$$

is rather crude for angles of this magnitude. In addition to that the constant speed assumption is not as valid as for IC = 2.5°. For both sets of initial condition it is observed that increasing speed tends to increase the deviations between both trajectories.

Table 02 - Initial condition response to 45. ° pitch

Run	Speed in kn	Maximal deviation in				Fig.
		Pitch in °	Lzdot ft/s	Depth in ft	Speed in kn	
1	3	1.64	$2.52\ 10^{-1}$	17.4	$5.68\ 10^{-1}$	12,13
2	5	0.85	$2.41\ 10^{-1}$	18.63	$5.92\ 10^{-1}$	14,15
3	7	1.13	$1.61\ 10^{-1}$	14.75	$5.76\ 10^{-1}$	16,17
4	9	1.23	$3.24\ 10^{-1}$	17.76	$5.51\ 10^{-1}$	18,19
5	11	2.05	$7.30\ 10^{-1}$	46.9	$5.30\ 10^{-1}$	
6	13	2.84	1.22	82.77	$5.07\ 10^{-1}$	20,21
7	15	3.63	1.85	131.25	$5.05\ 10^{-1}$	22,23

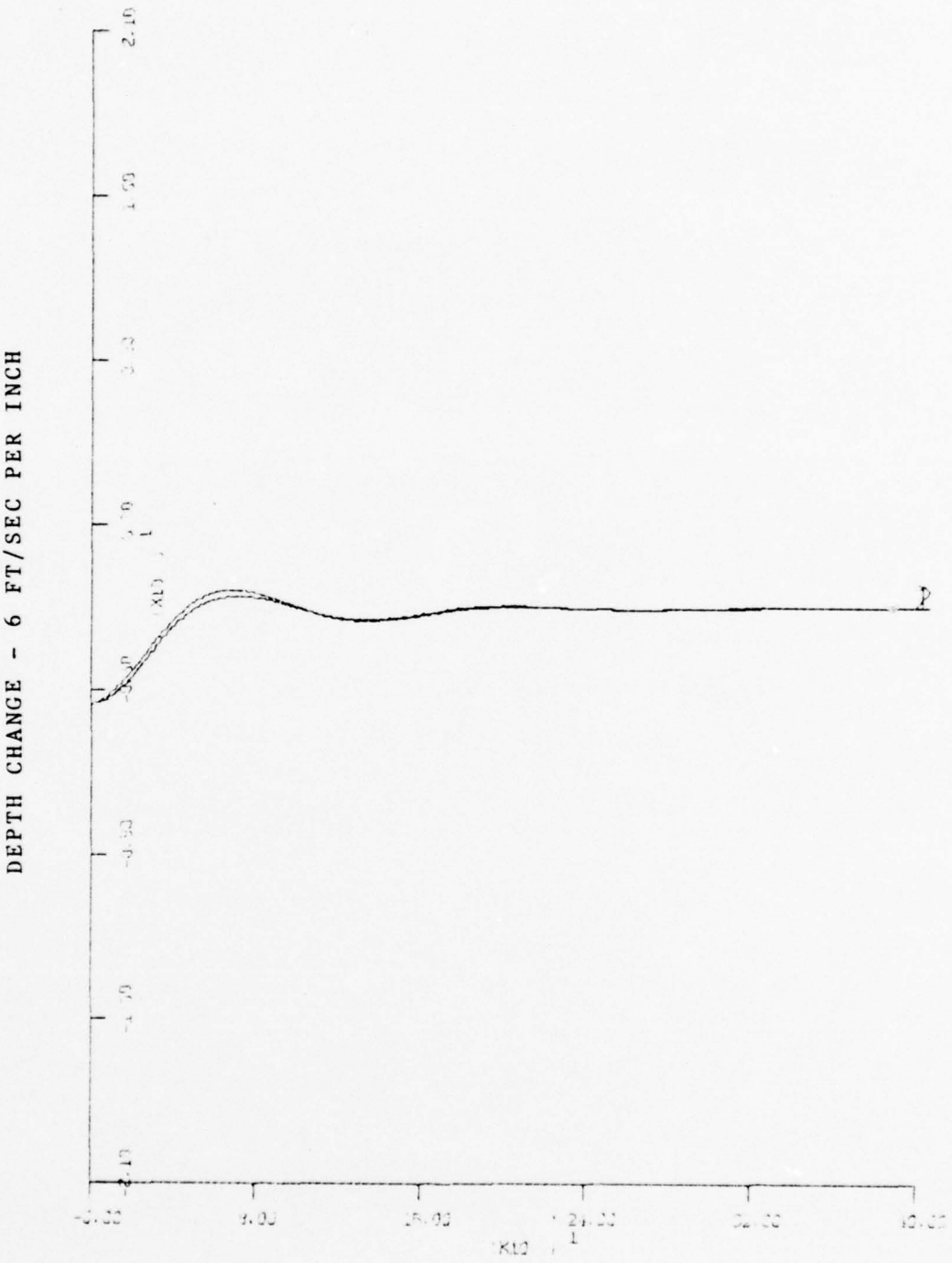

Figure 12 - INITIAL CONDITION RESPONSE
INITIAL PITCH = 45 °, SPEED = 3 KN

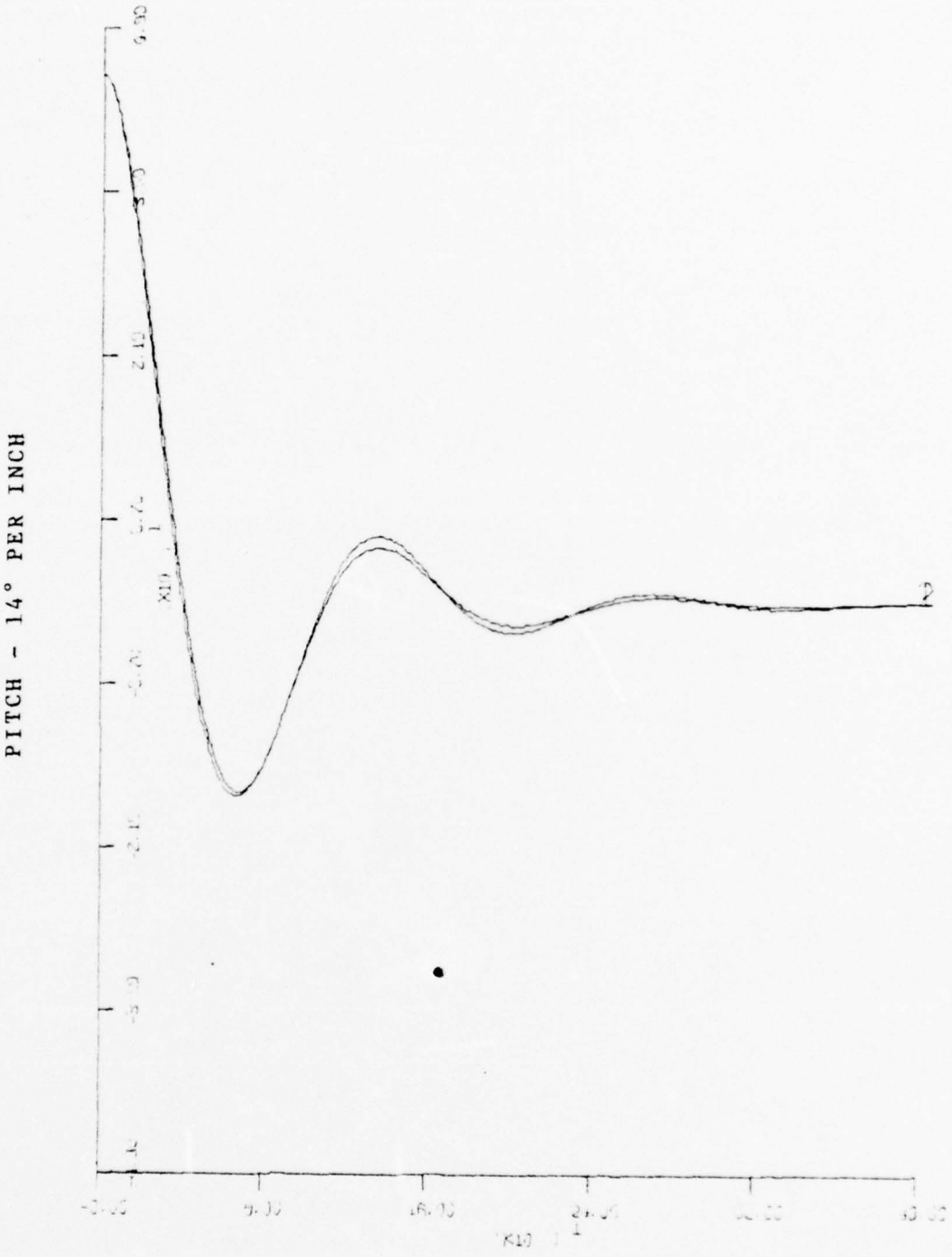

Figure 13 - INITIAL CONDITION RESPONSE
INITIAL PITCH = 45 °, SPEED = 3 KN

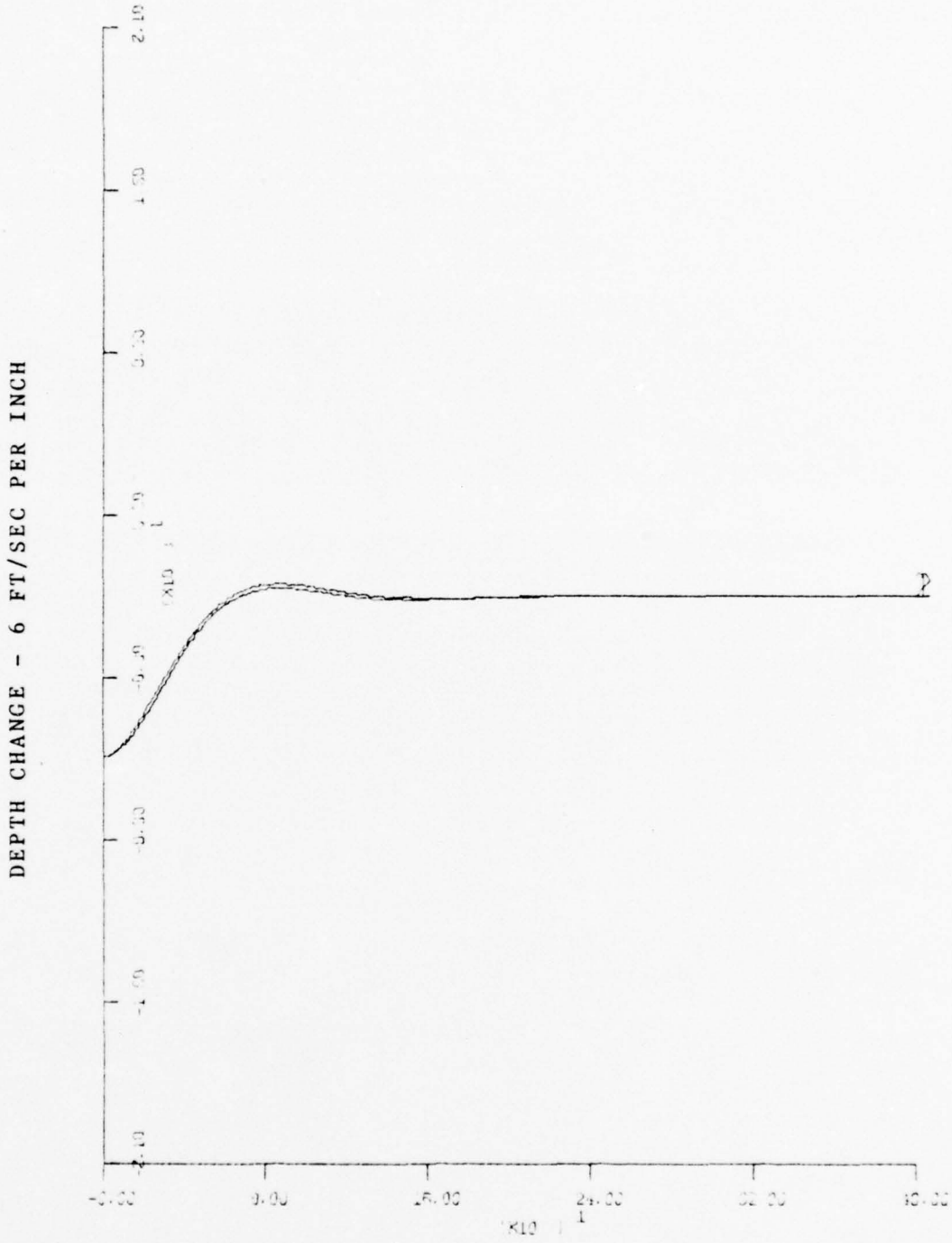

Figure 14 - INITIAL CONDITION RESPONSE
INITIAL PITCH = 45 °, SPEED = 5 KN

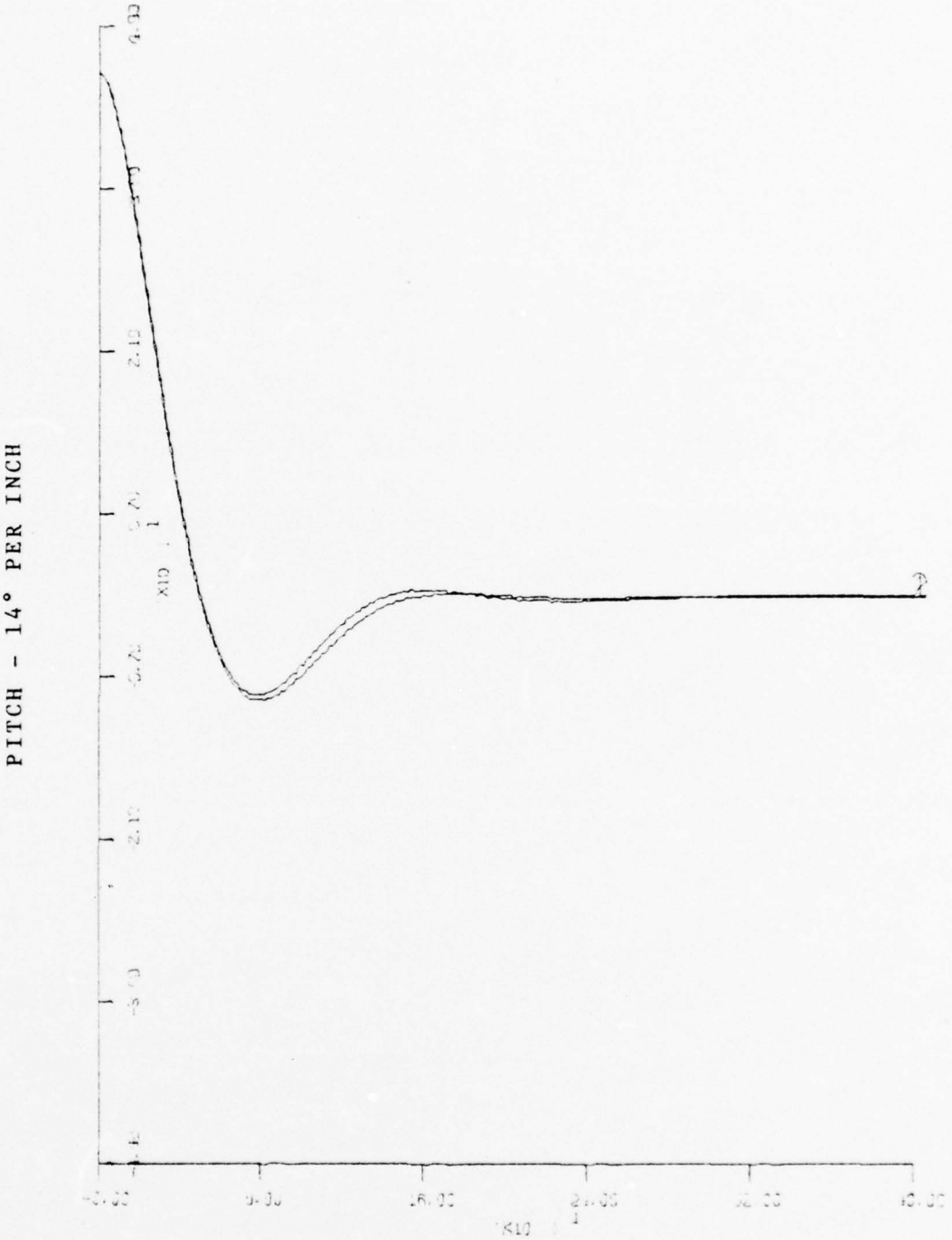

Figure 15 - INITIAL CONDITION RESPONSE
INITIAL PITCH = 45 °, SPEED = 5 KN

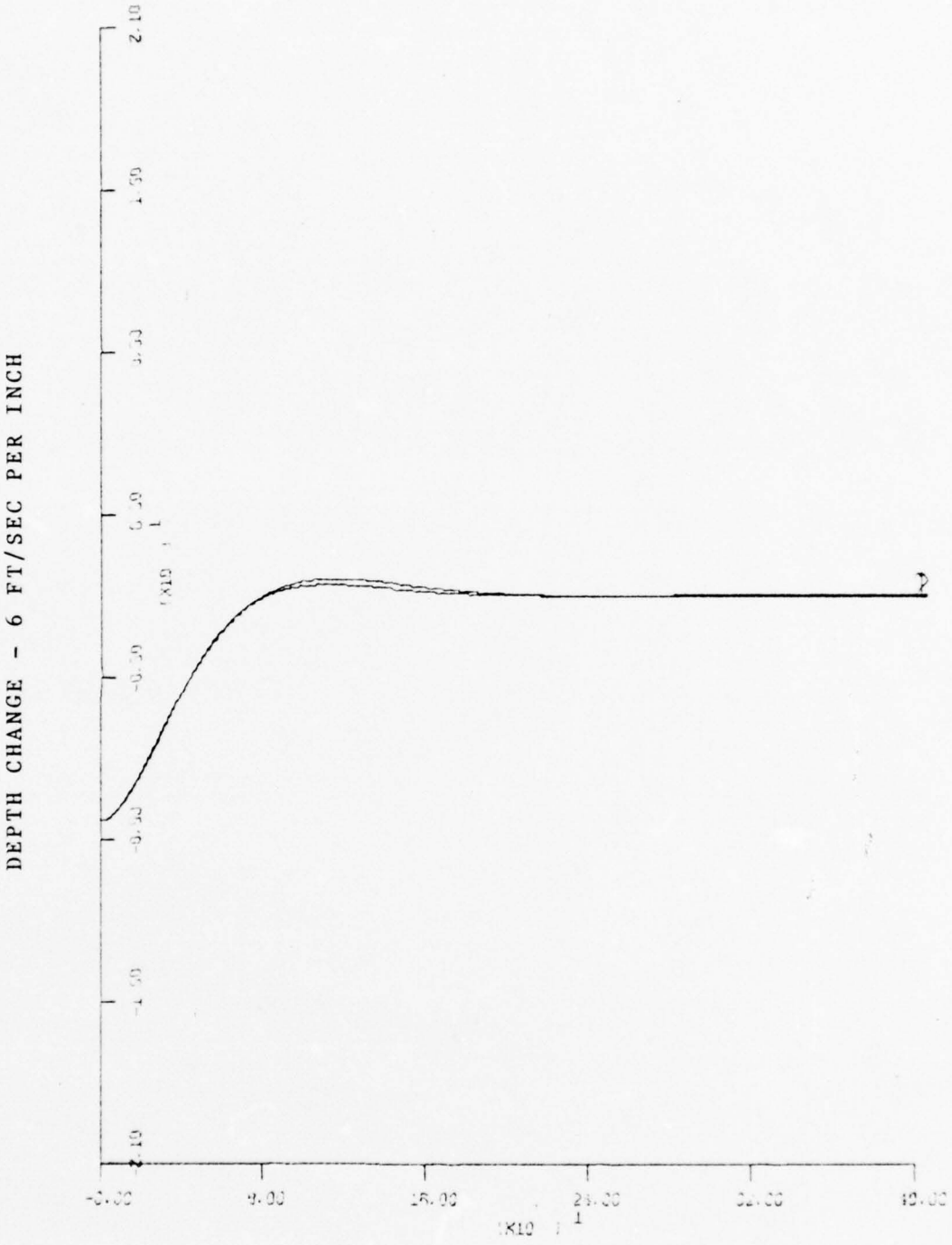

Figure 16 - INITIAL CONDITION RESPONSE
INITIAL PITCH = 45 °, SPEED = 7 KN

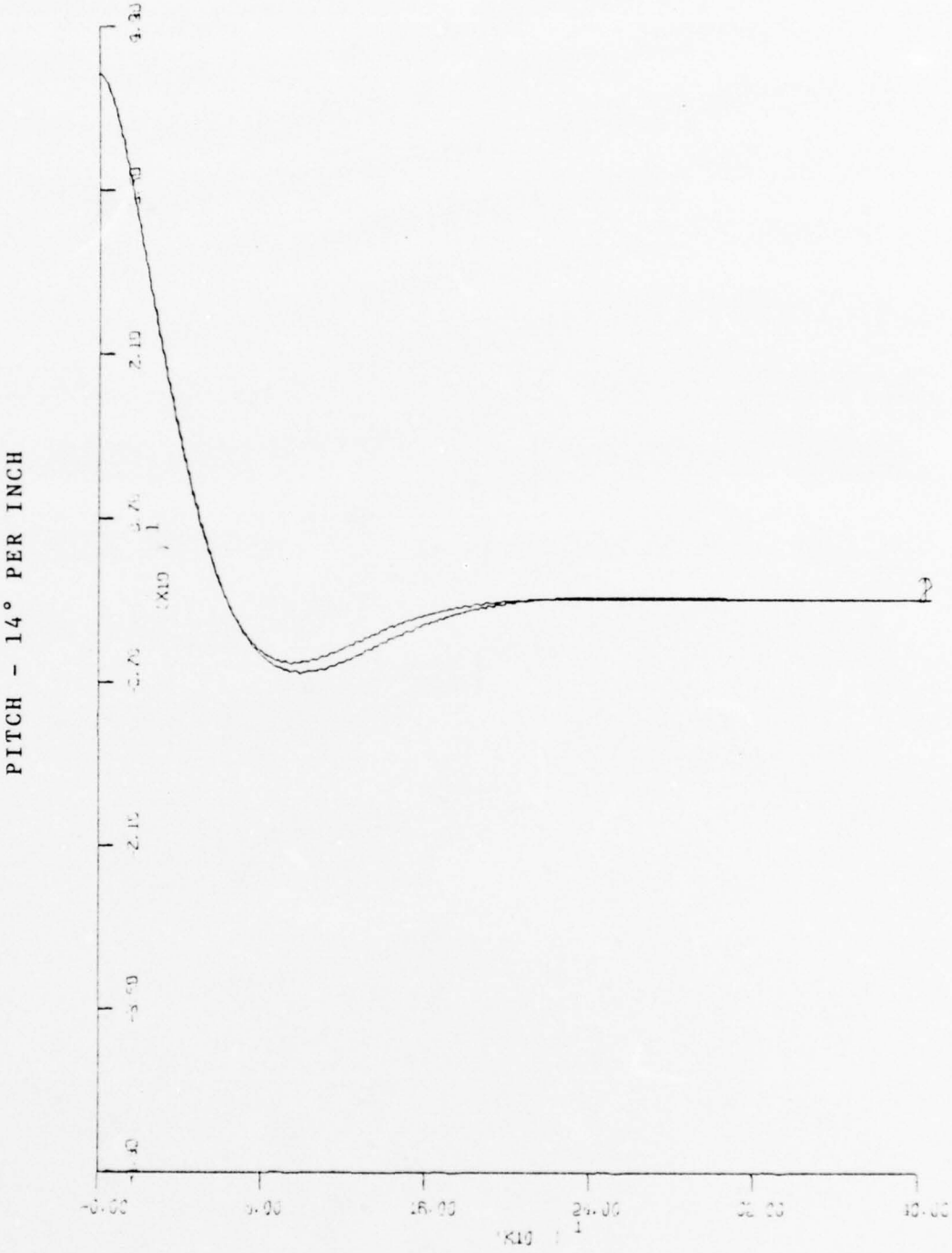

Figure 17 - INITIAL CONDITION RESPONSE
INITIAL PITCH = 45 °, SPEED = 7 KN

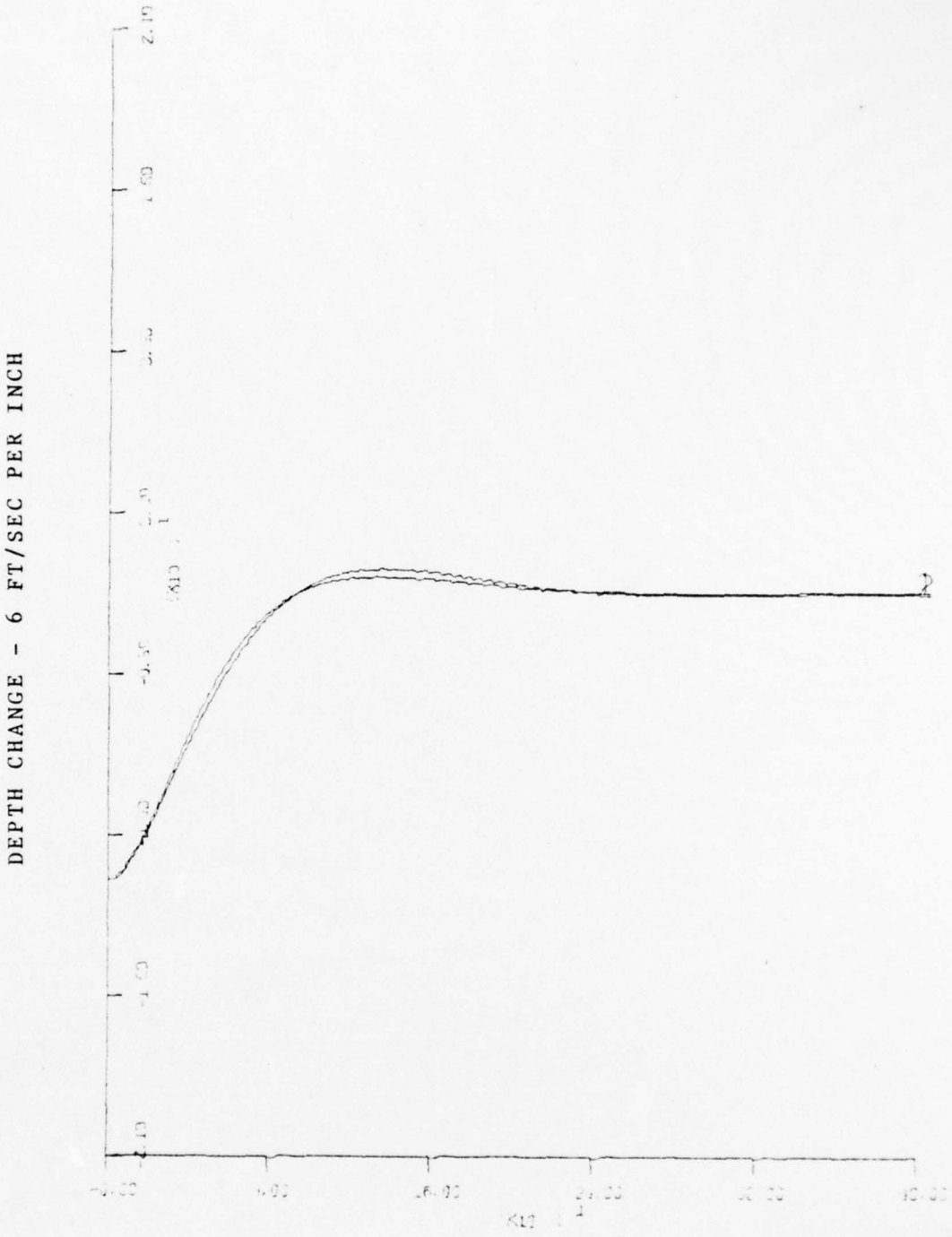

Figure 18 - INITIAL CONDITION RESPONSE
INITIAL PITCH = 45 °, SPEED = 9 KN

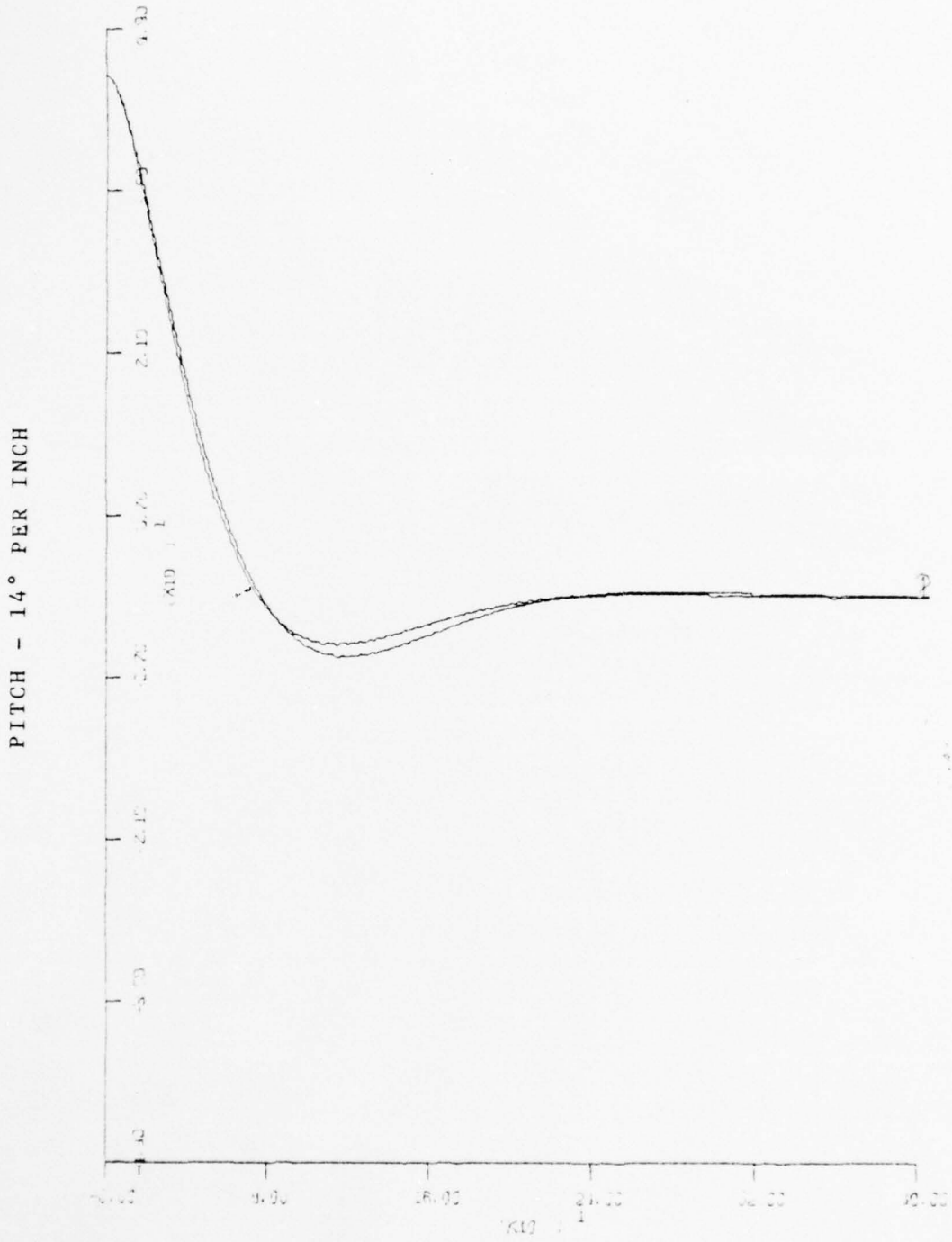

Figure 19 - INITIAL CONDITION RESPONSE
INITIAL PITCH = 45 °, SPEED = 9 KN

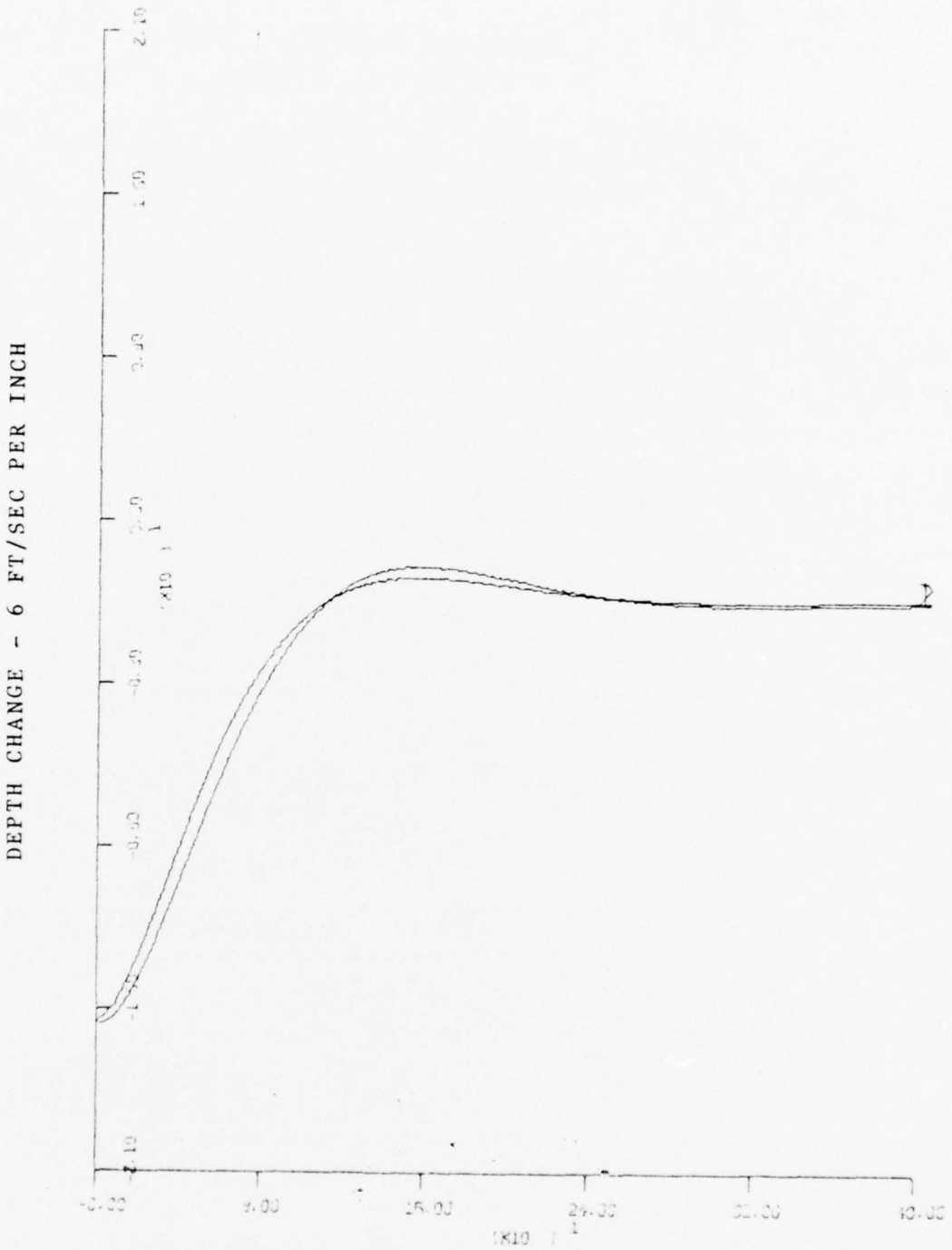

Figure 20 - INITIAL CONDITION RESPONSE
INITIAL PITCH = 45 °, SPEED = 13 KN

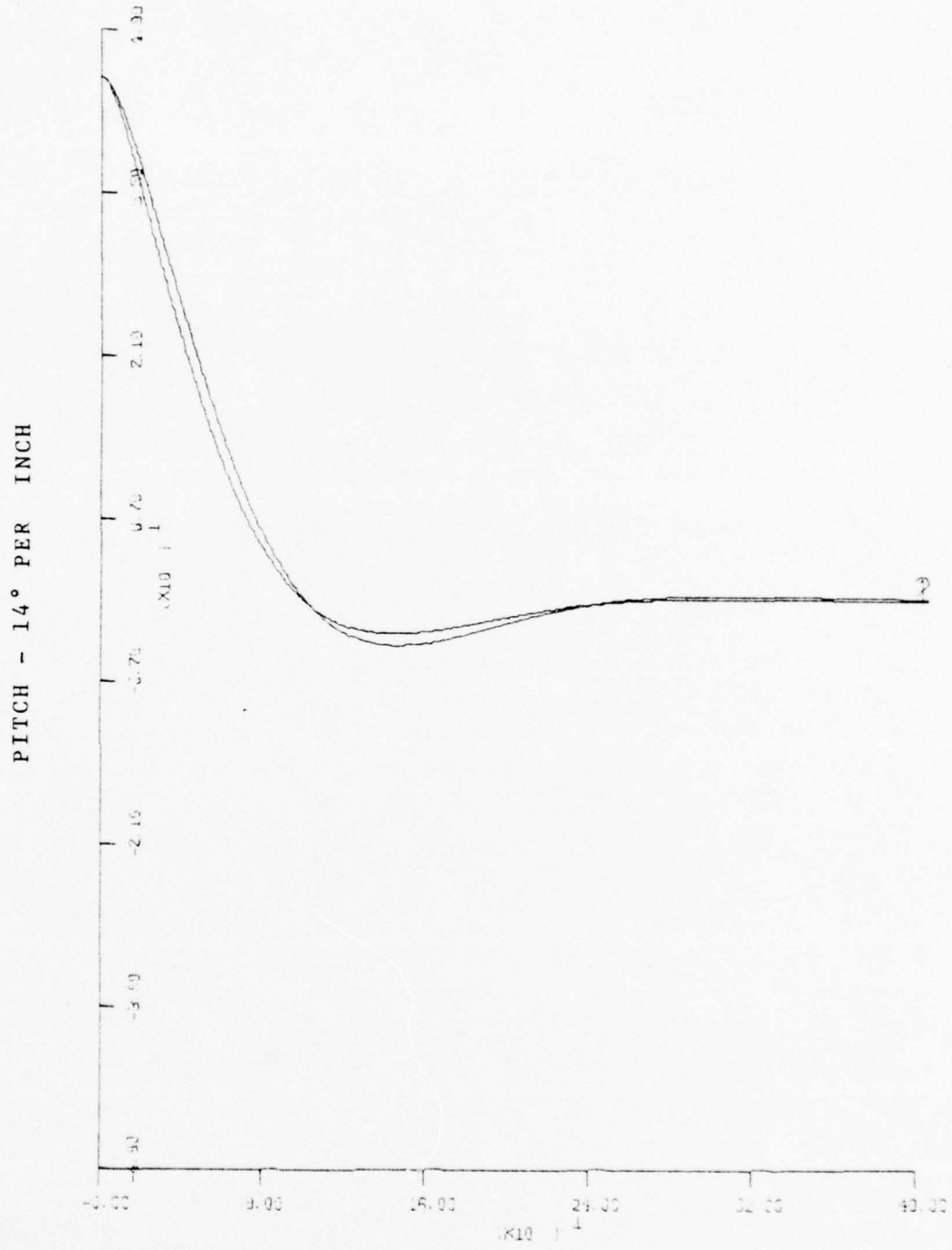

Figure 21 - INITIAL CONDITION RESPONSE
INITIAL PITCH = 45 °, SPEED = 13 KN

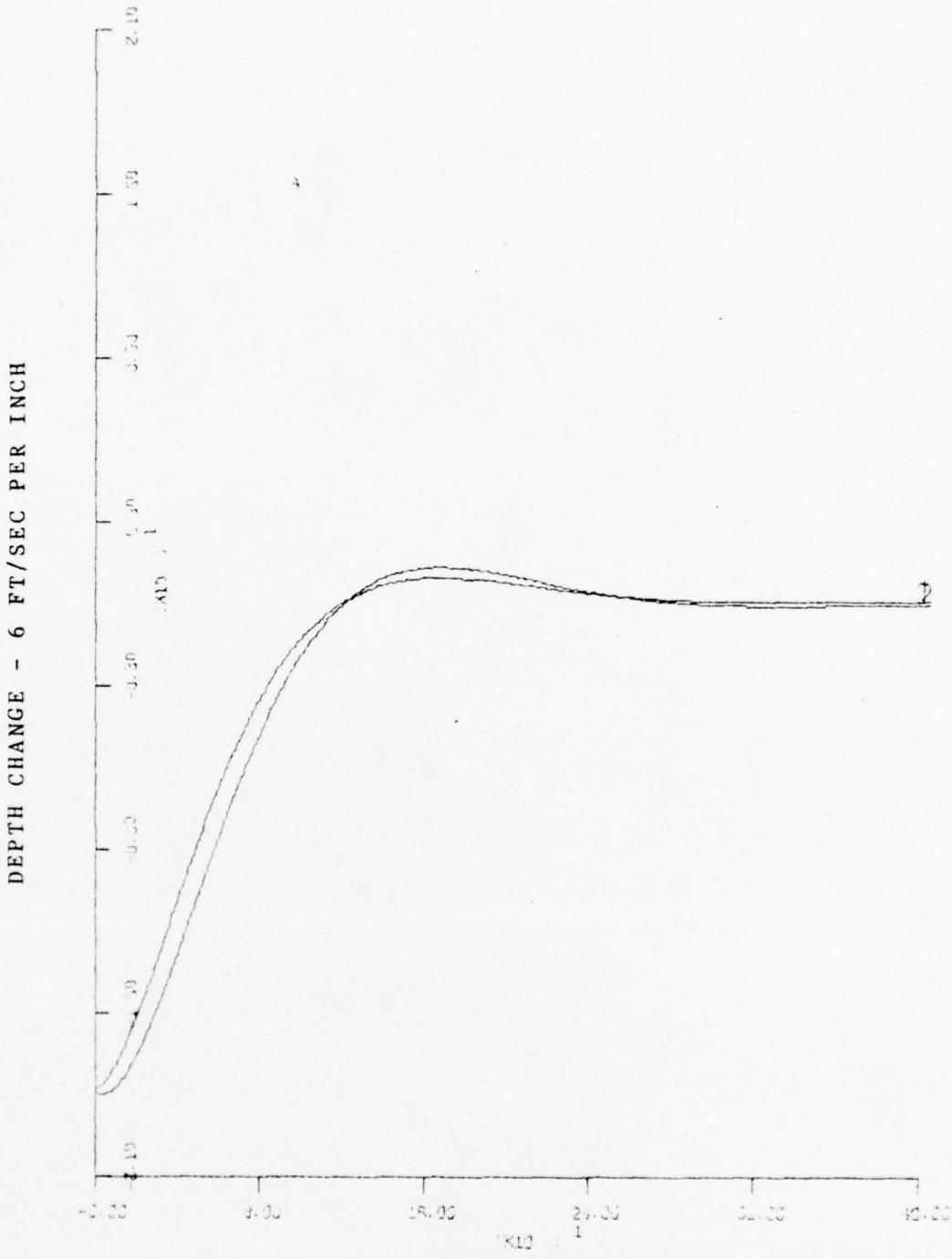

Figure 22 - INITIAL CONDITION RESPONSE
INITIAL PITCH = 45 °, SPEED = 15 KN

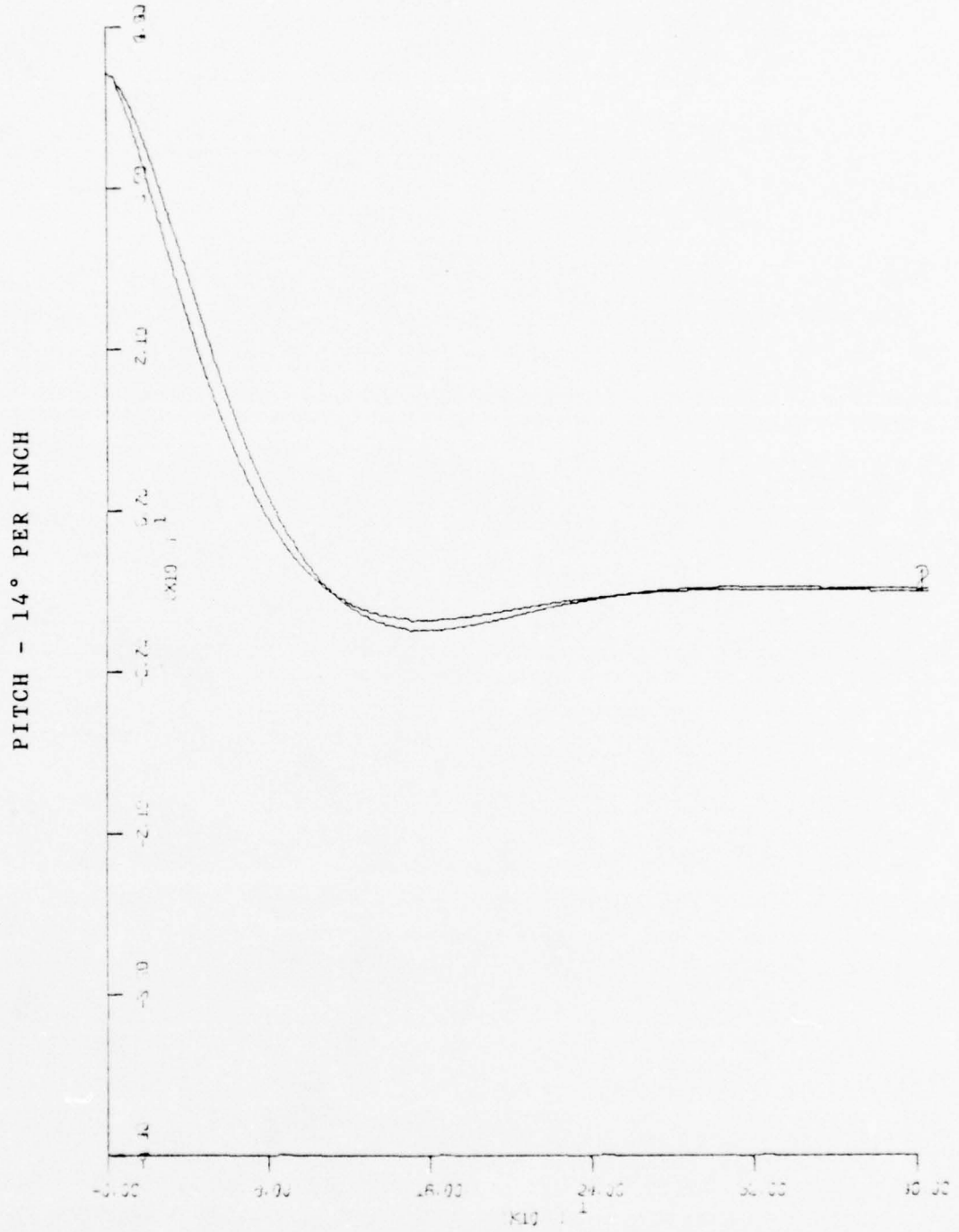

Figure 23 - INITIAL CONDITION RESPONSE
INITIAL PITCH = 45 °, SPEED = 15 KN

2. Forced response

As the models considered are deeply submerged and in trim, the planes exert the only relevant forces. It was considered best to test the response of both models (excluding actuators) to sinusoidal forcing functions, because in the controlled system the rudder excursions due to depth and pitch changes are expected to be sinusoidal.

The following forcing functions were chosen for both planes separately and three different speeds (3, 9, 15 knots):

$$A \cdot \sin(B \cdot t)$$

where $A = 35°, 15°, 5°$

and $B = 5.73, 2.87$ °/sec

The magnitude of the amplitude was limited to 35°, because this is an approximate, mechanical limit.
The max. deviations are summarized in Table 03-05. Curve 1 and 2 in Fig. 24-69 show the responses of the non-linear and linear model respectively.

Table 03 - Speed 3 kn

Run	Plane	Omega rad	Amp °	Max deviation in Speed in kn	Pitch in °	ZDOT in ft/s	Fig
1	LDB	0.1	5	$8.35\ 10^{-3}$	$3.88\ 10^{-2}$	$1.05\ 10^{-3}$	
2	LDB	0.1	15	$7.18\ 10^{-2}$	$4.34\ 10^{-2}$	$2.07\ 10^{-3}$	
3	LDB	0.1	35	$3.43\ 10^{-1}$	$1.16\ 10^{-1}$	$2.26\ 10^{-2}$	24,25
4	LDS	0.1	5	$8.75\ 10^{-3}$	$3.56\ 10^{-2}$	$1.01\ 10^{-3}$	26,27
5	LDS	0.1	15	$7.51\ 10^{-2}$	$6.60\ 10^{-2}$	$3.86\ 10^{-3}$	28,29
6	LDS	0.1	35	$3.54\ 10^{-1}$	$3.68\ 10^{-1}$	$3.90\ 10^{-2}$	
7	LDB	.05	5	$8.34\ 10^{-3}$	$3.53\ 10^{-2}$	$1.15\ 10^{-3}$	
8	LDB	.05	15	$7.16\ 10^{-2}$	$5.27\ 10^{-2}$	$4.82\ 10^{-3}$	30,31
9	LDB	.05	35	$3.43\ 10^{-1}$	$2.16\ 10^{-1}$	$5.07\ 10^{-2}$	
10	LDS	.05	5	$9.28\ 10^{-3}$	$4.21\ 10^{-2}$	$8.83\ 10^{-4}$	
11	LDS	.05	15	$8.09\ 10^{-2}$	$1.62\ 10^{-1}$	$1.04\ 10^{-2}$	32,33
12	LDS	.05	35	$3.80\ 10^{-1}$	1.19	$9.42\ 10^{-2}$	

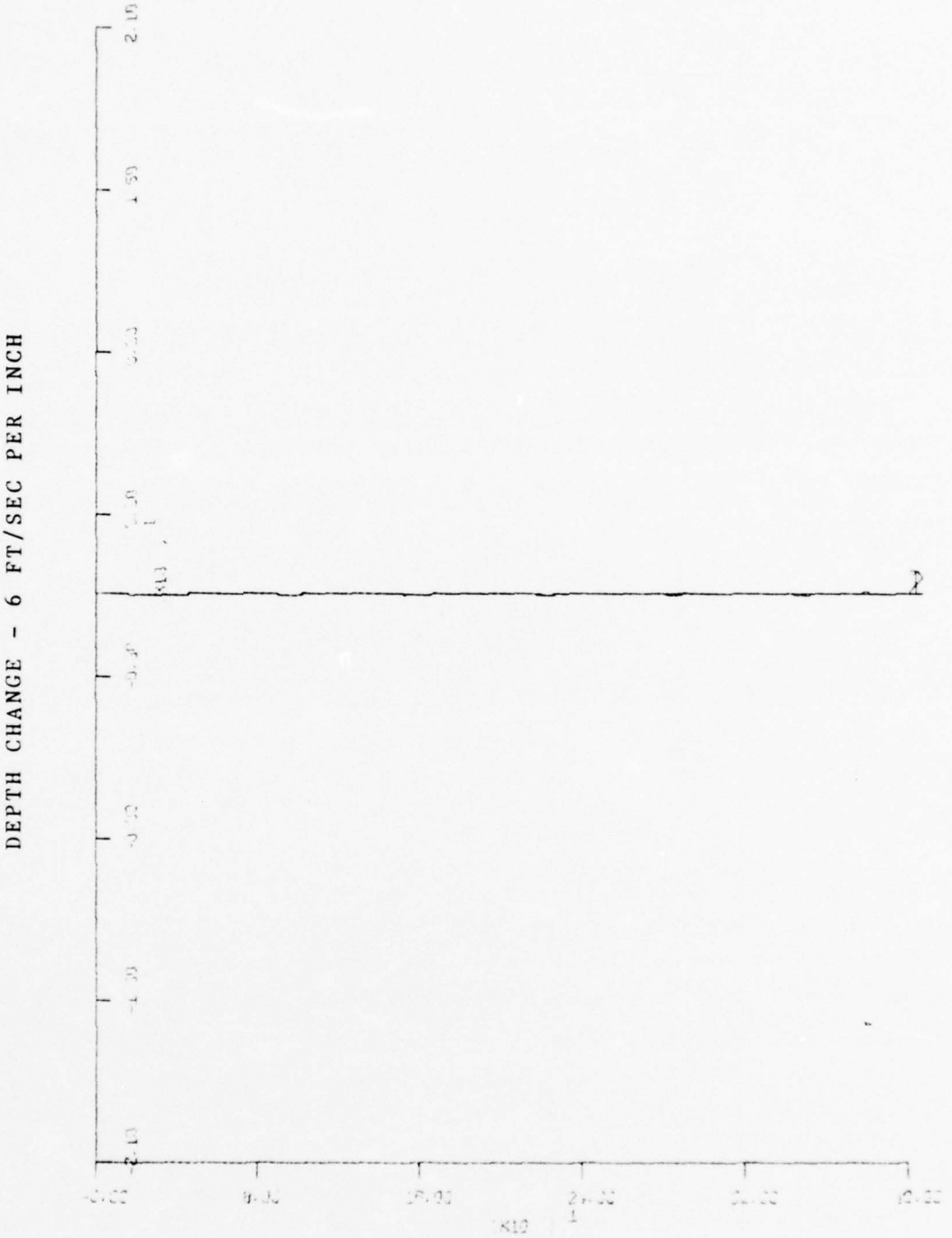

Figure 24 - FORCED RESPONSE, 3 KN
LDB = 35 °SIN .1 t

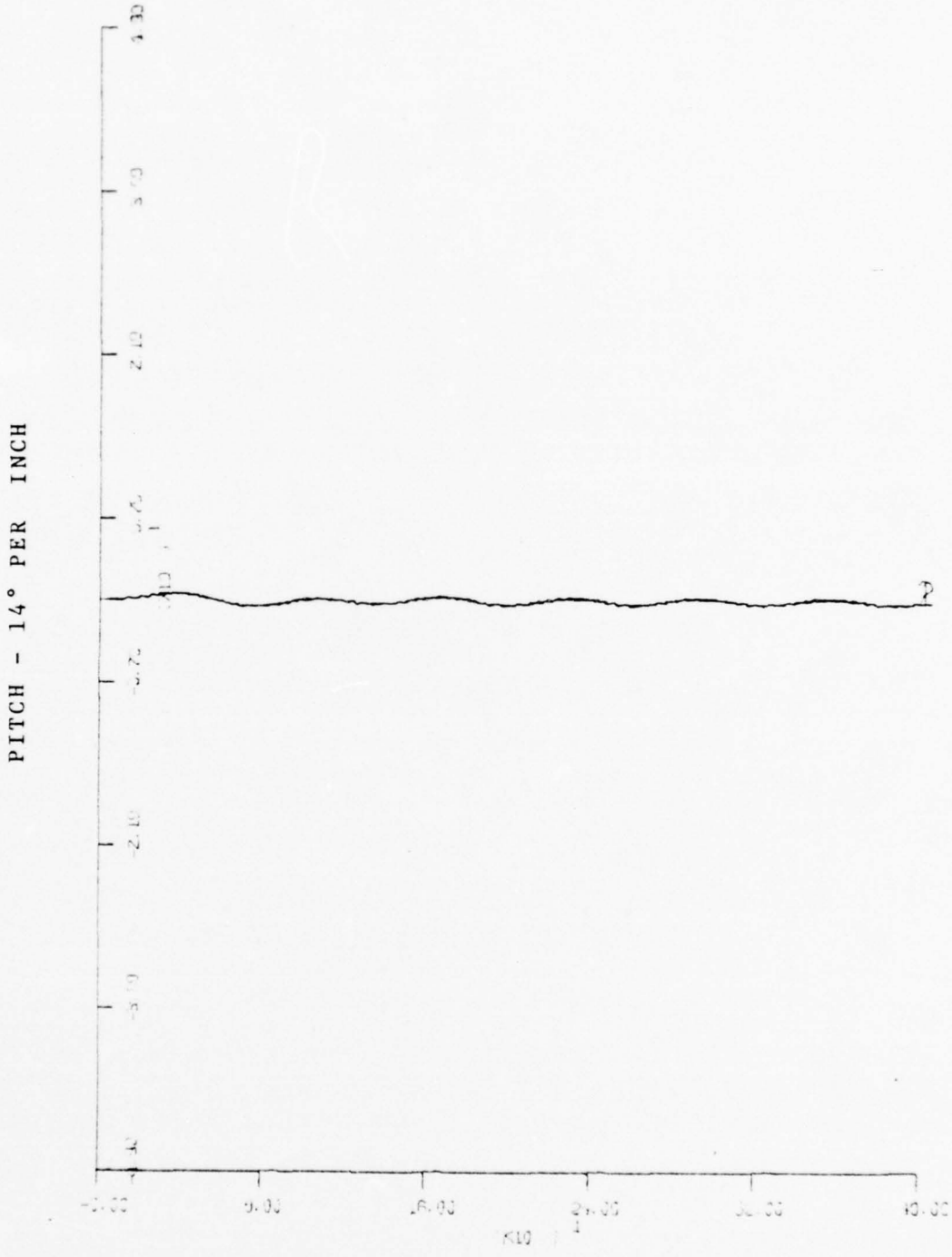

Figure 25 - FORCED RESPONSE, 3 KN
LDB = 35 °SIN .1 t

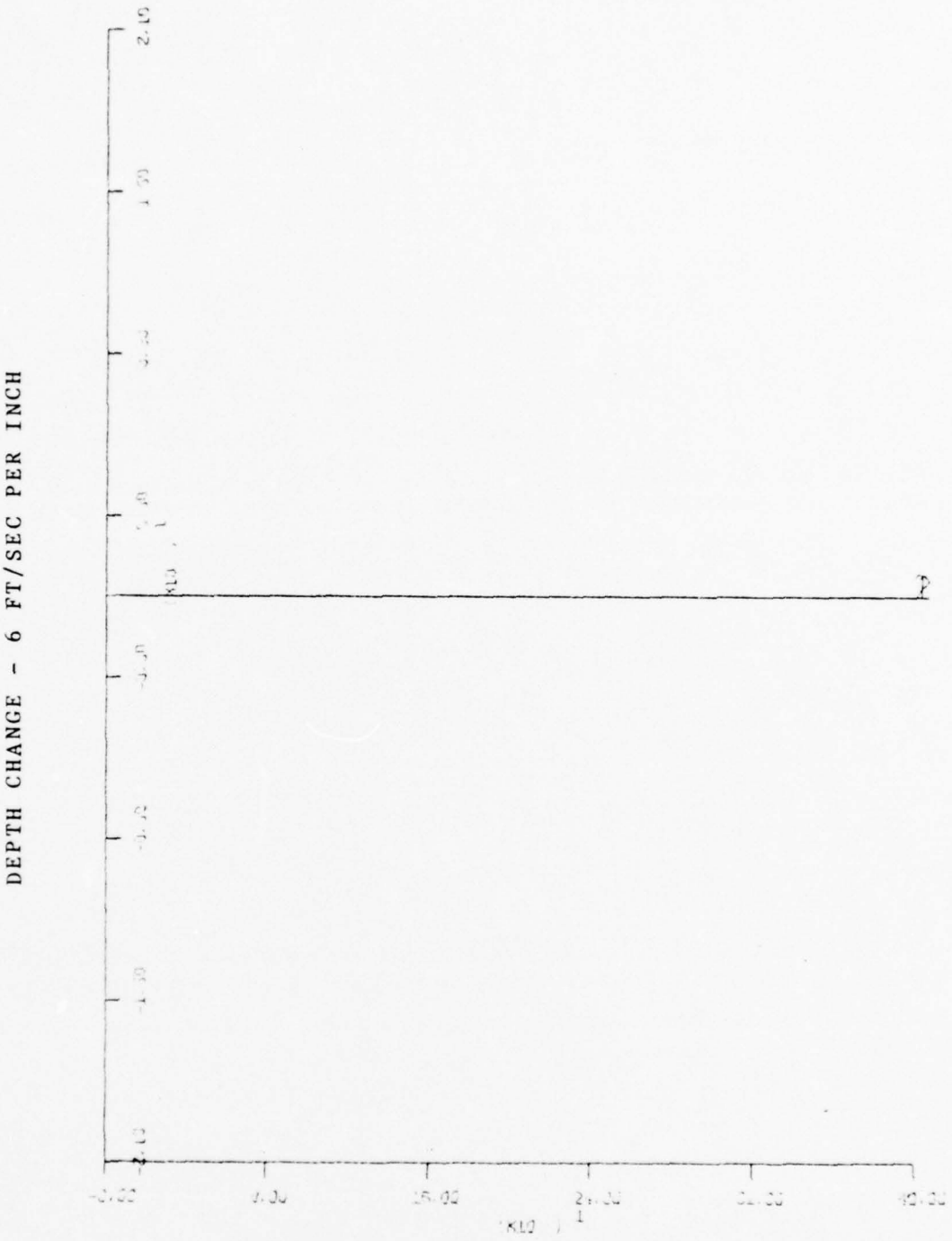

Figure 26 - FORCED RESPONSE, 3 KN
LDS = 5 °SIN .1 t

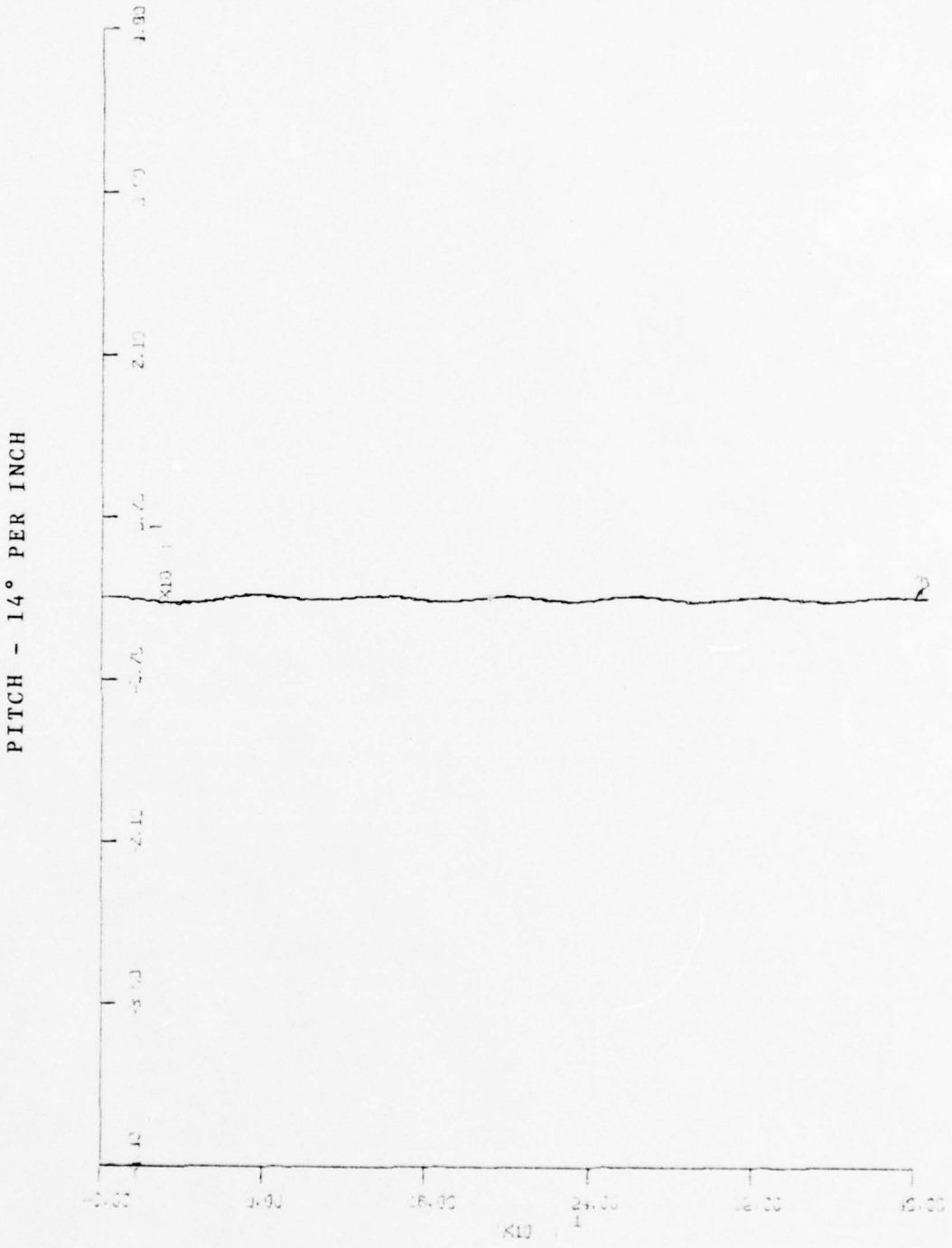

Figure 27 - FORCED RESPONSE, 3 KN
LDS = 5 °SIN .1 t

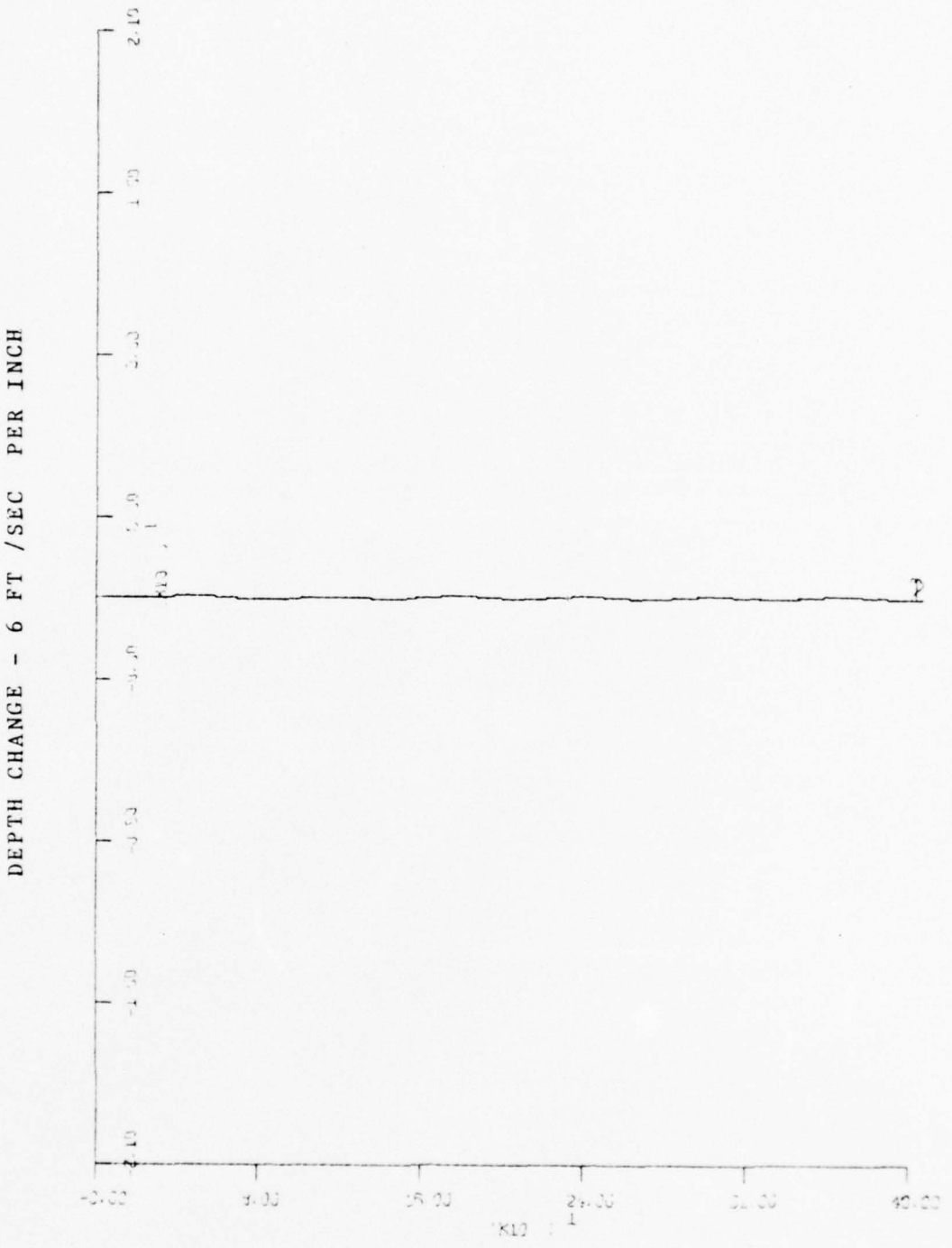

Figure 28 - FORCED RESPONSE, 3 KN
LDS = 15 °SIN .1 t

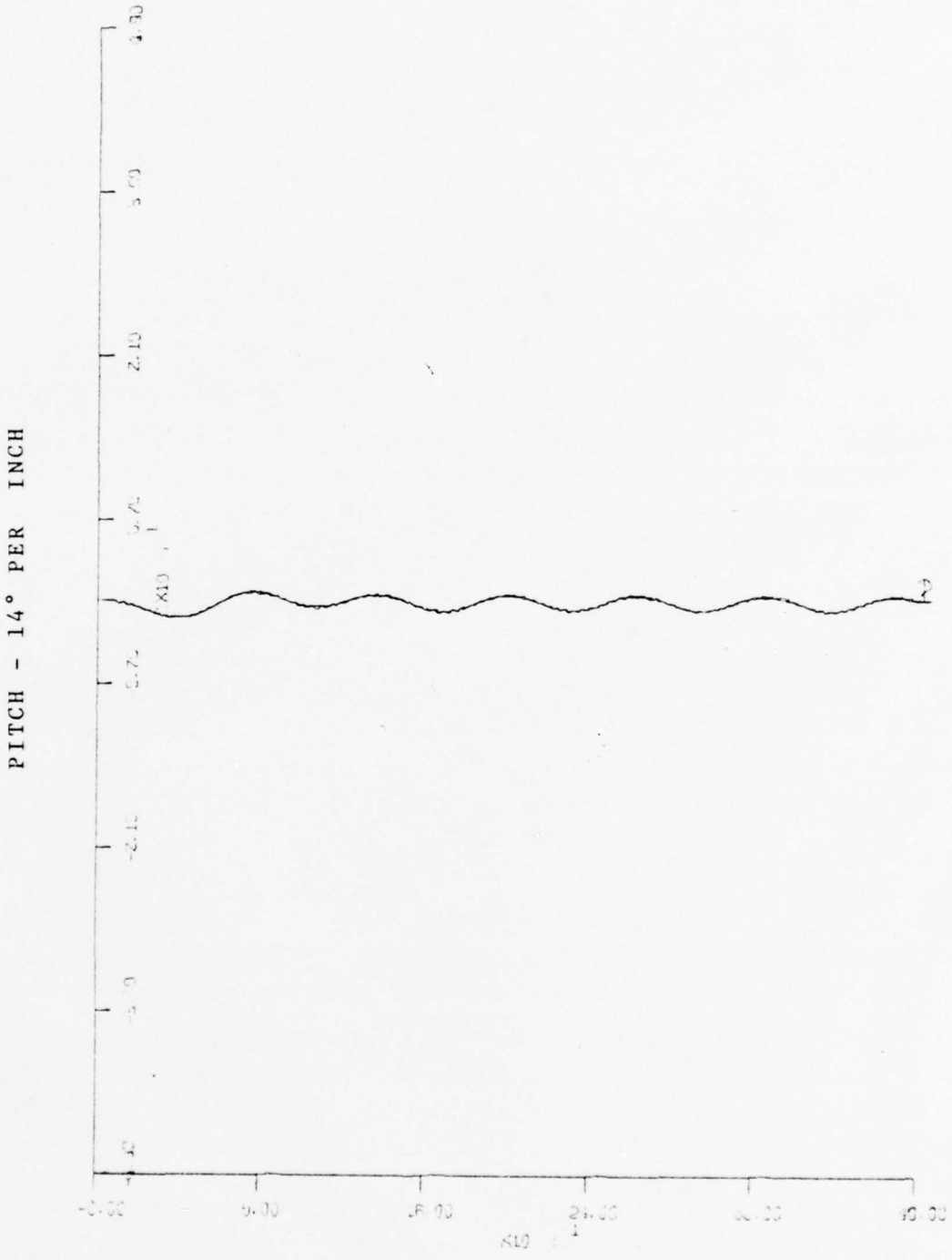

Figure 29 - FORCED RESPONSE, 3 KN
LDS = 15 °SIN .1 t

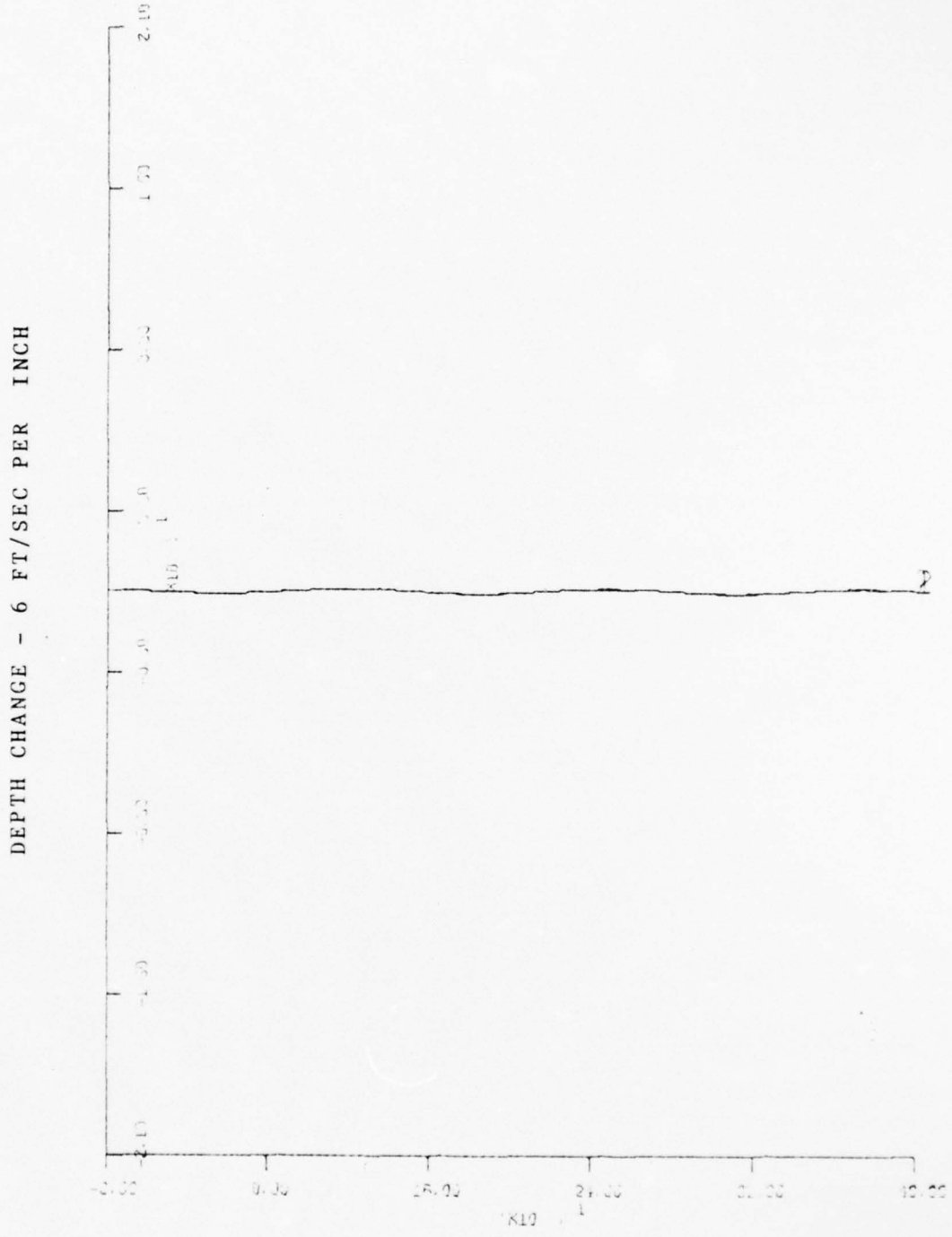

Figure 30 - FORCED RESPONSE, 3 KN
LDB = 15 °SIN .05 t

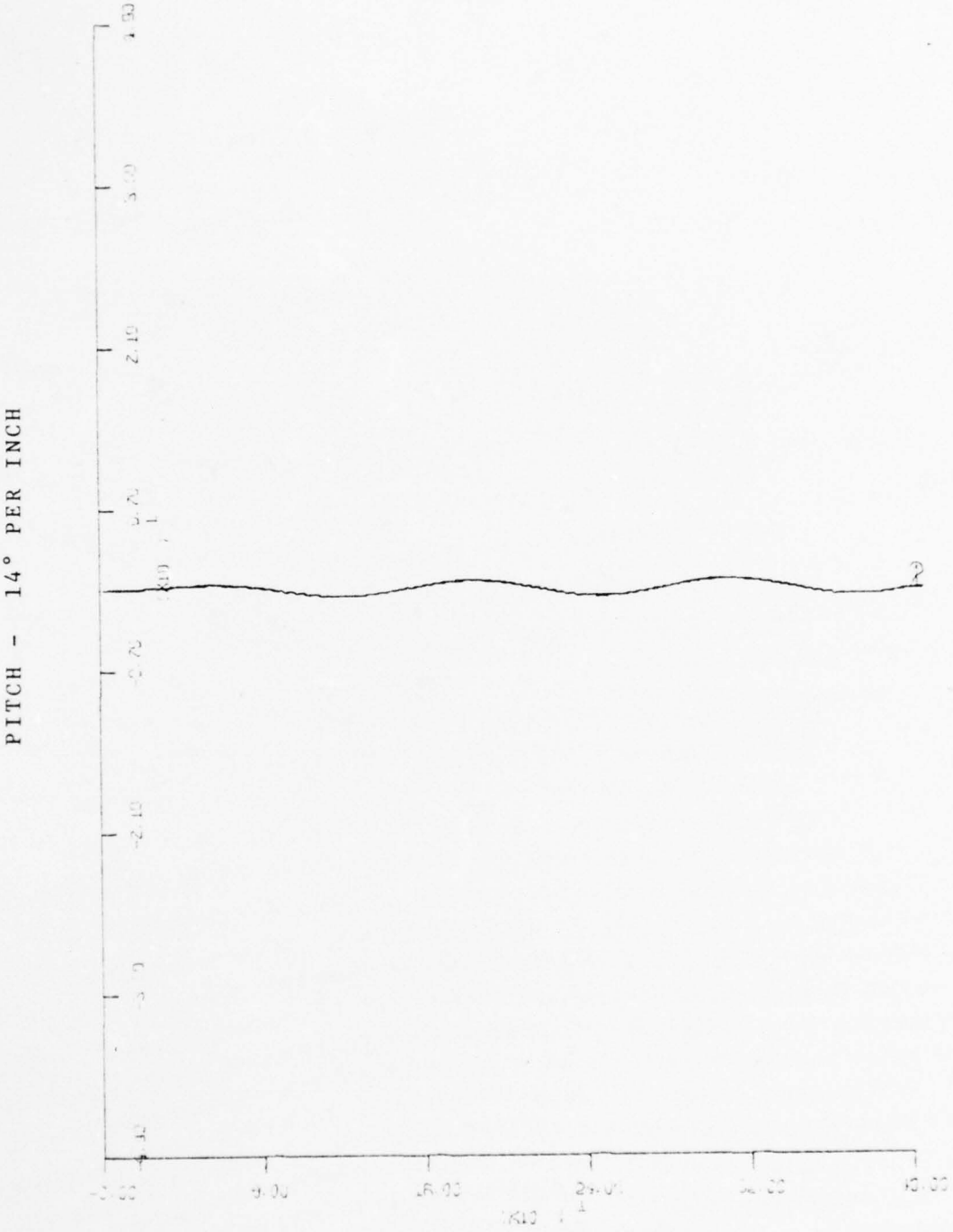

Figure 31 - FORCED RESPONSE, 3 KN
LDB = 15 °SIN .05 t

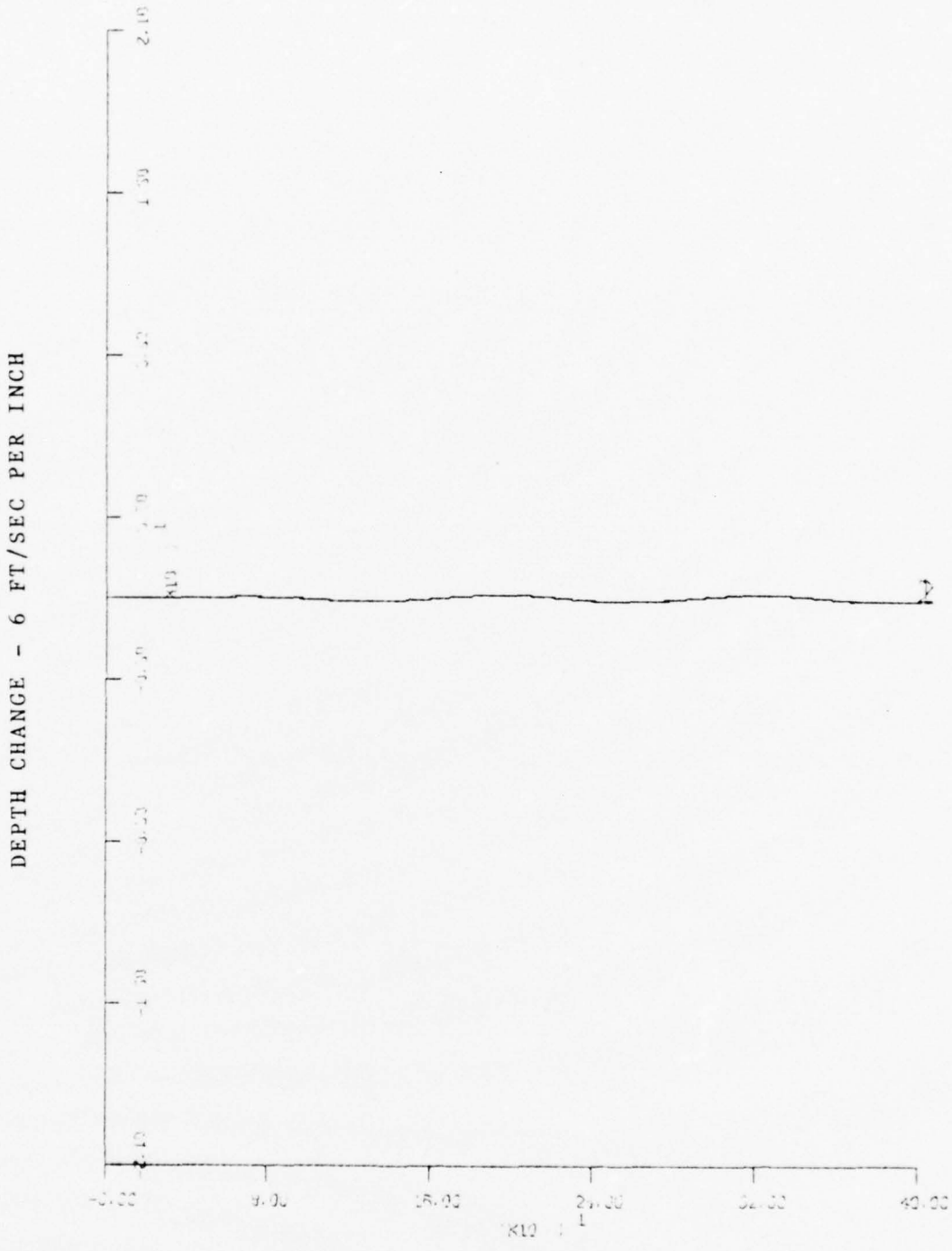

Figure 32 - FORCED RESPONSE, 3 KN
LDS = 15 °SIN .05 t

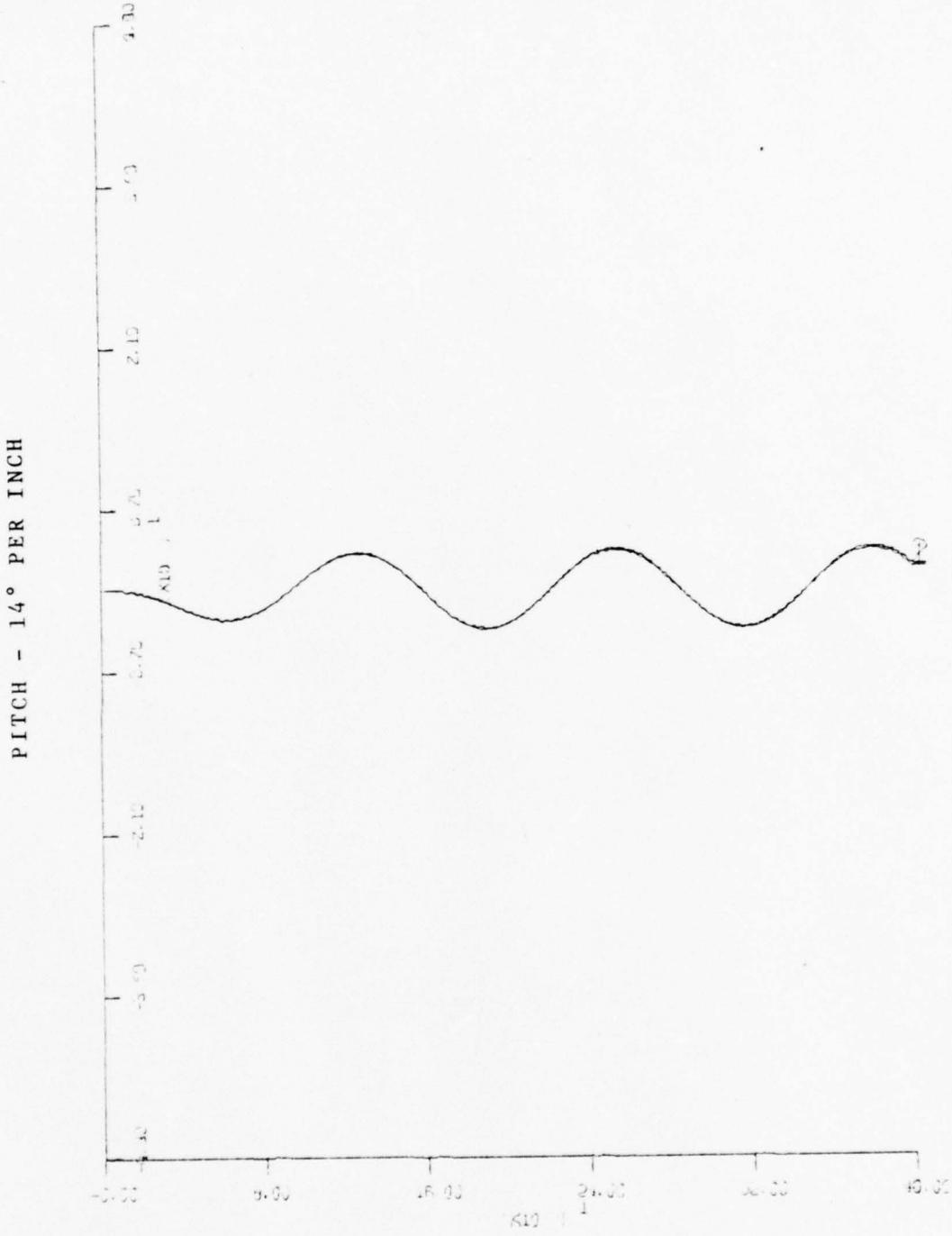

Figure 33 - FORCED RESPONSE, 3 KN
LDS = 15 °SIN .05 t

Table 04 - Speed 9 kn

Run	Plane	Omega rad	Amp °	Max deviation in Speed in kn	Pitch in °	ZDOT in ft/s	Fig
1	LDE	0.1	5	$3.00\ 10^{-2}$	$2.72\ 10^{-2}$	$5.00\ 10^{-3}$	
2	LDE	0.1	15	$2.65\ 10^{-1}$	$8.55\ 10^{-2}$	$3.63\ 10^{-2}$	34,35
3	LDE	0.1	35	1.20	$5.26\ 10^{-1}$	$2.85\ 10^{-1}$	
4	LDS	0.1	5	$4.50\ 10^{-2}$	$7.88\ 10^{-1}$	$1.78\ 10^{-2}$	36,37
5	LDS	0.1	15	$3.75\ 10^{-1}$	$6.10\ 10^{-1}$	$1.18\ 10^{-1}$	38,39
6	LDS	0.1	35	1.52	3.10	$4.25\ 10^{-1}$	40,41
7	LDE	.05	5	$3.30\ 10^{-2}$	$3.26\ 10^{-2}$	$6.92\ 10^{-3}$	42,43
8	LDE	.05	15	$2.87\ 10^{-1}$	$1.84\ 10^{-1}$	$7.52\ 10^{-2}$	44,45
9	LDB	.05	35	1.29	11.15	$6.07\ 10^{-1}$	46,47
10	LDS	.05	5	$8.40\ 10^{-2}$	$3.10\ 10^{-1}$	$6.18\ 10^{-2}$	48,49
11	LDS	.05	15	$6.56\ 10^{-1}$	2.59	$4.45\ 10^{-1}$	50,51
12	LDS	.05	35	2.24	12.70	2.76	52,53

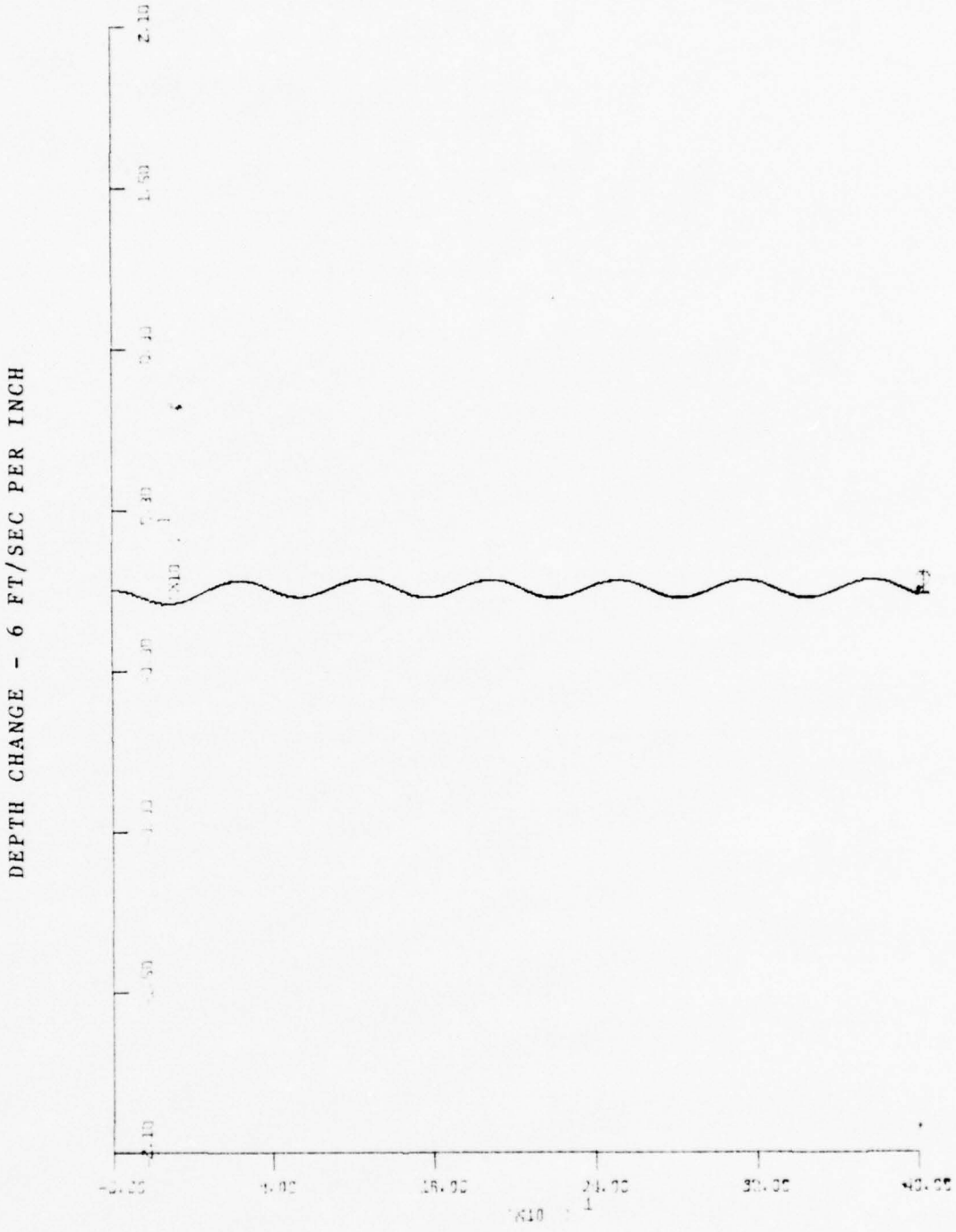

Figure 34 - FORCED RESPONSE, 9 KN
LDB = 15 °SIN .1 t

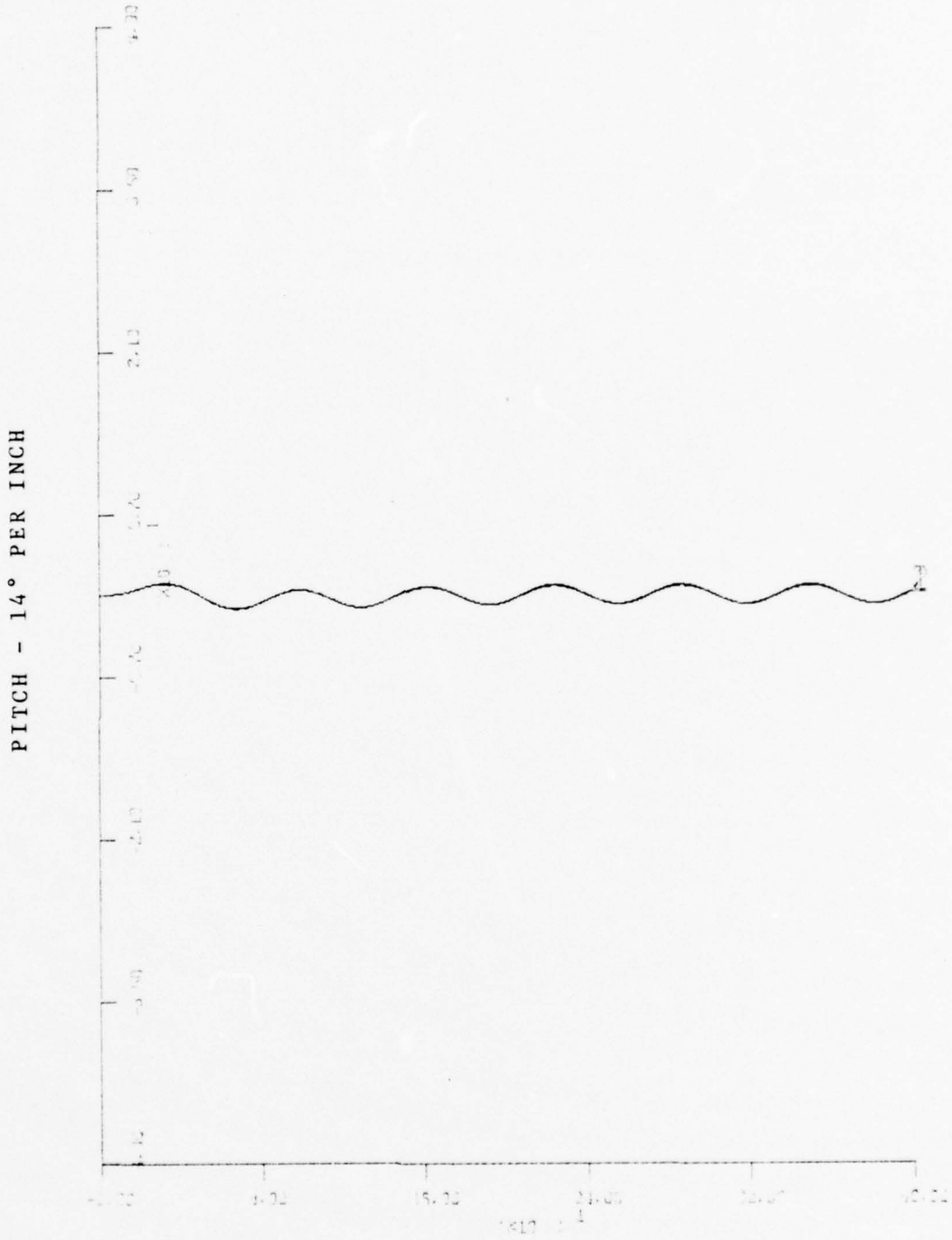

Figure 35 - FORCED RESPONSE, 9 KN
LDB = 15 °SIN .1 t

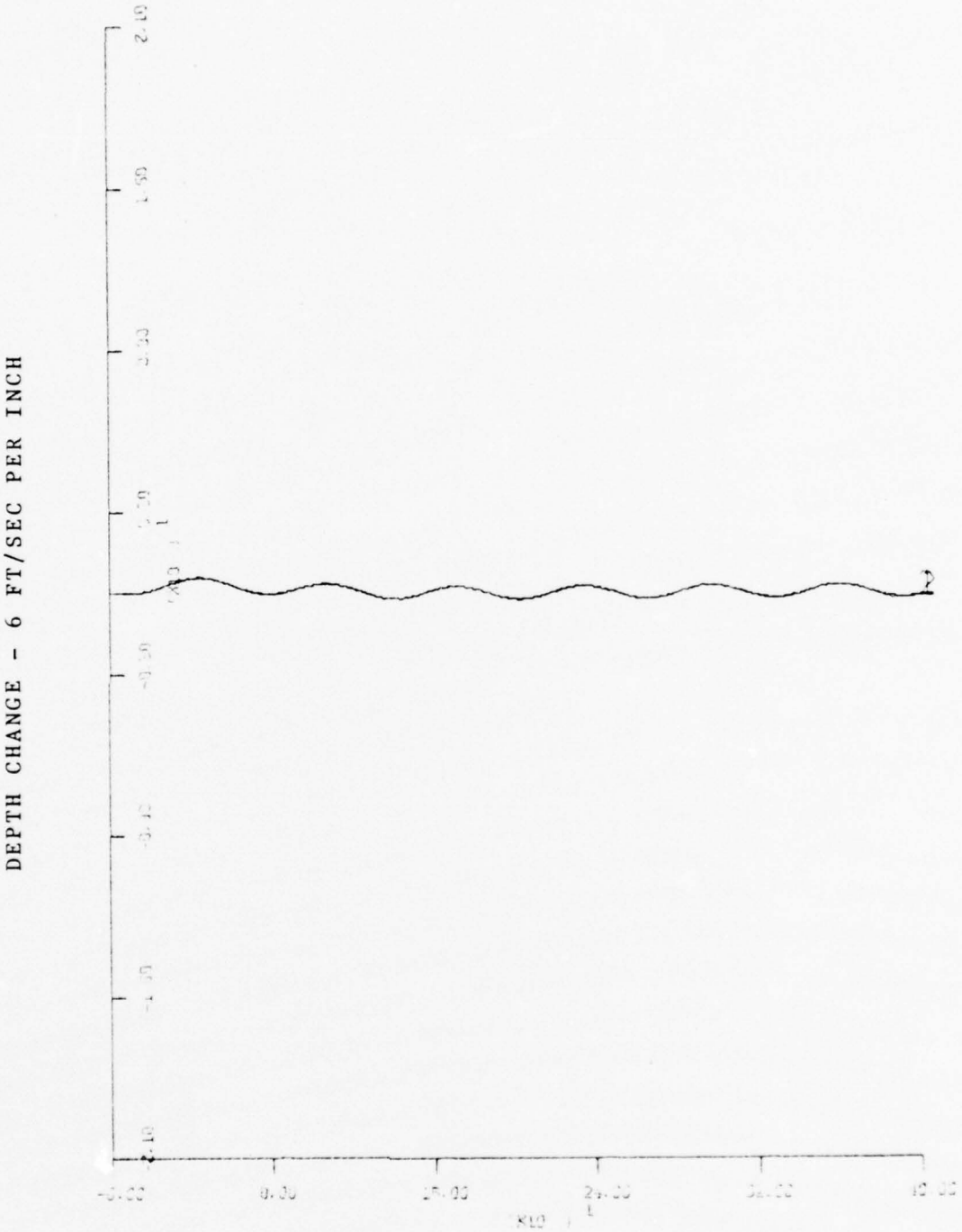

Figure 36 - FORCED RESPONSE, 9 KN
LDS = 5 °SIN .1 t

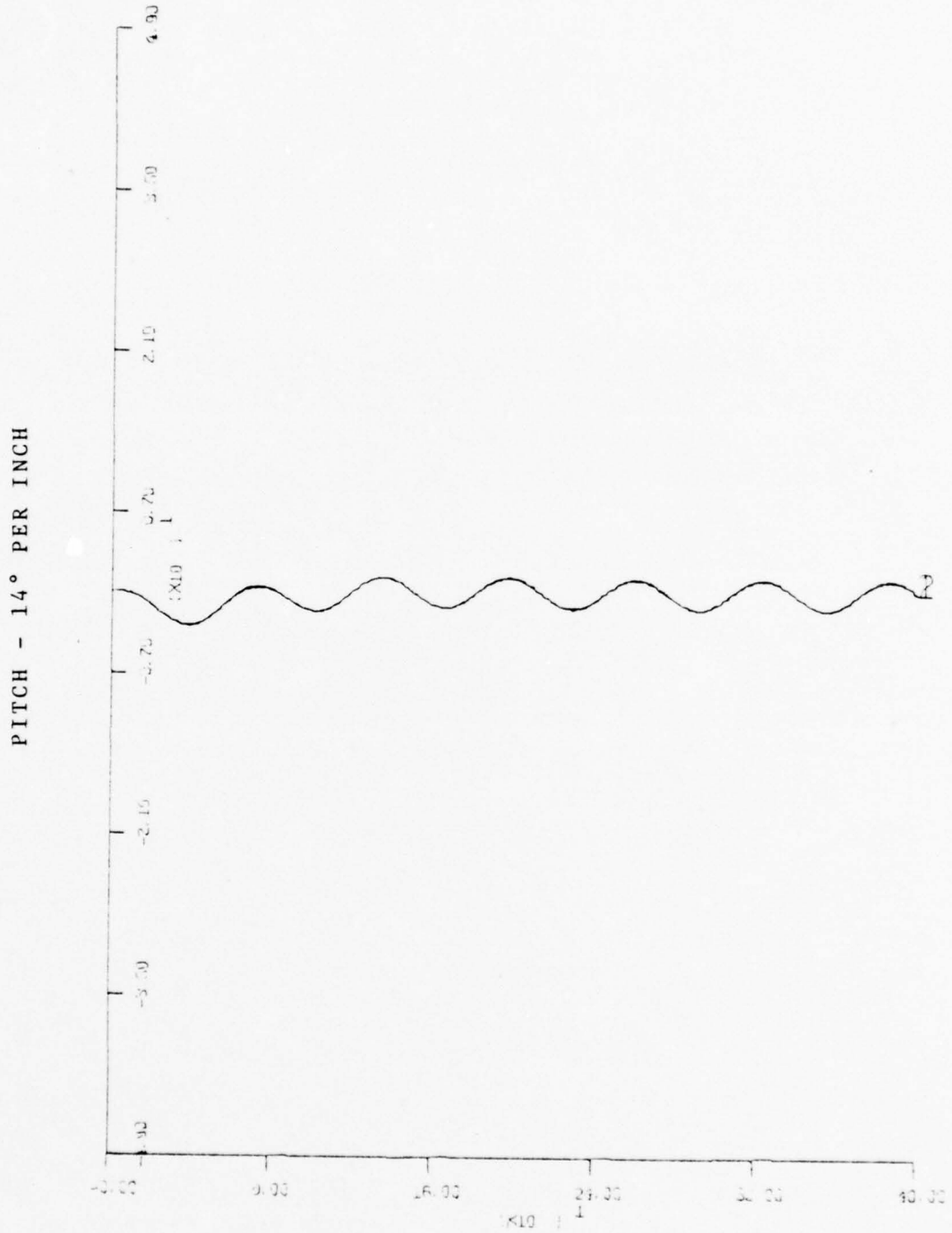

Figure 37 - FORCED RESPONSE, 9 KN
LDS = 5 °SIN .1 t

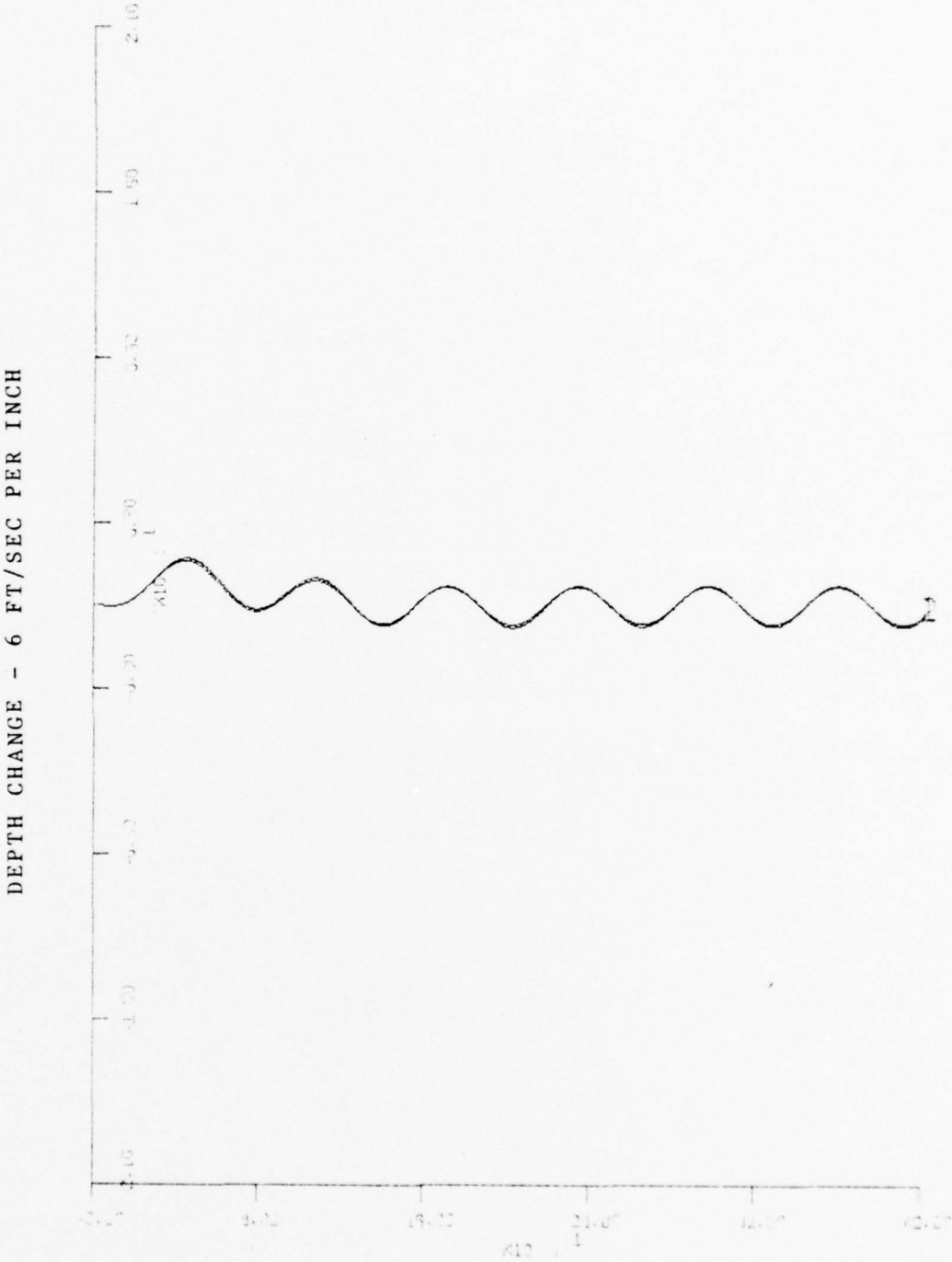

Figure 38 - FORCED RESPONSE, 9 KN
LDS = 15 °SIN .1 t

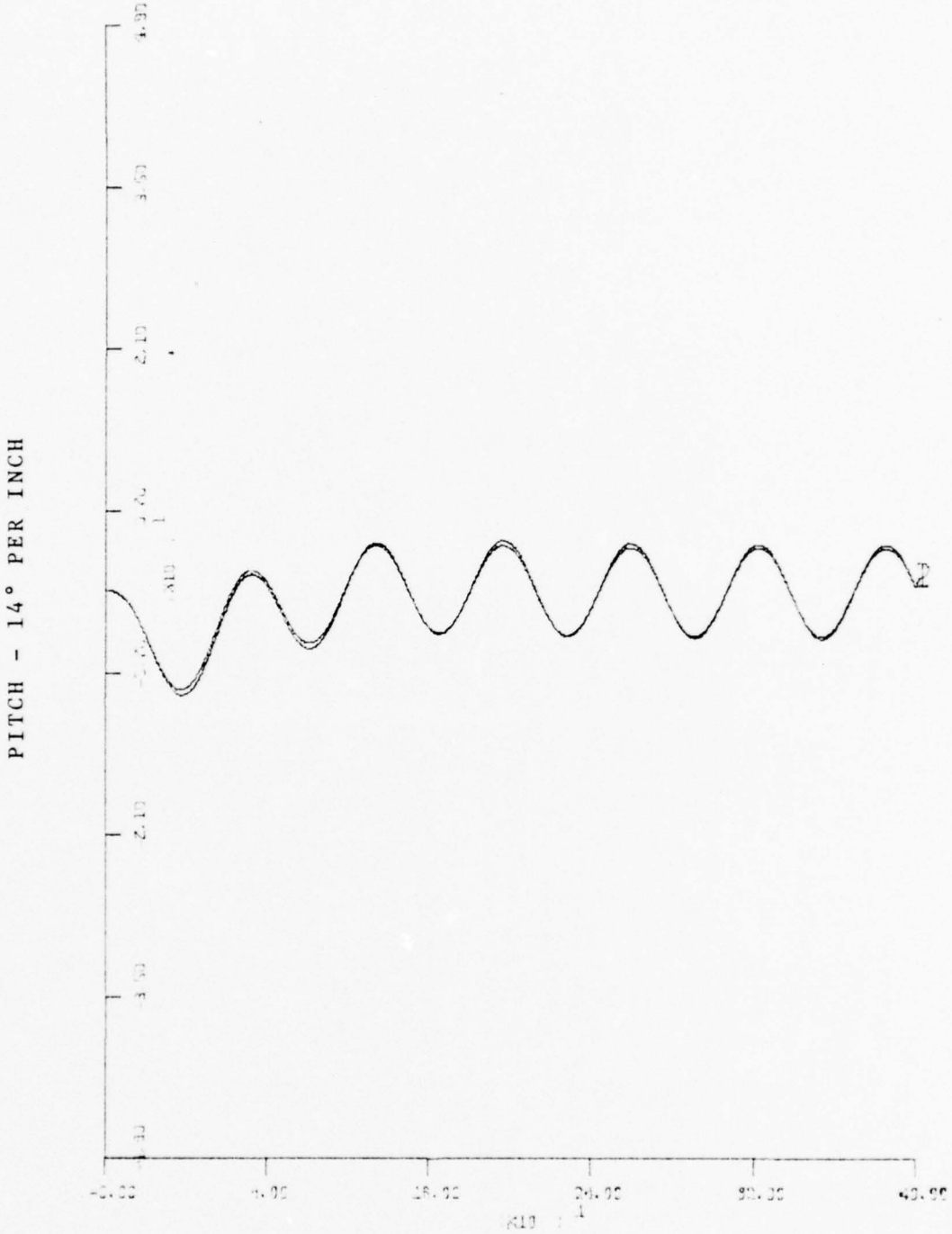

Figure 39 - FORCED RESPONSE, 9 KN
LDS = 15 °SIN .1 t

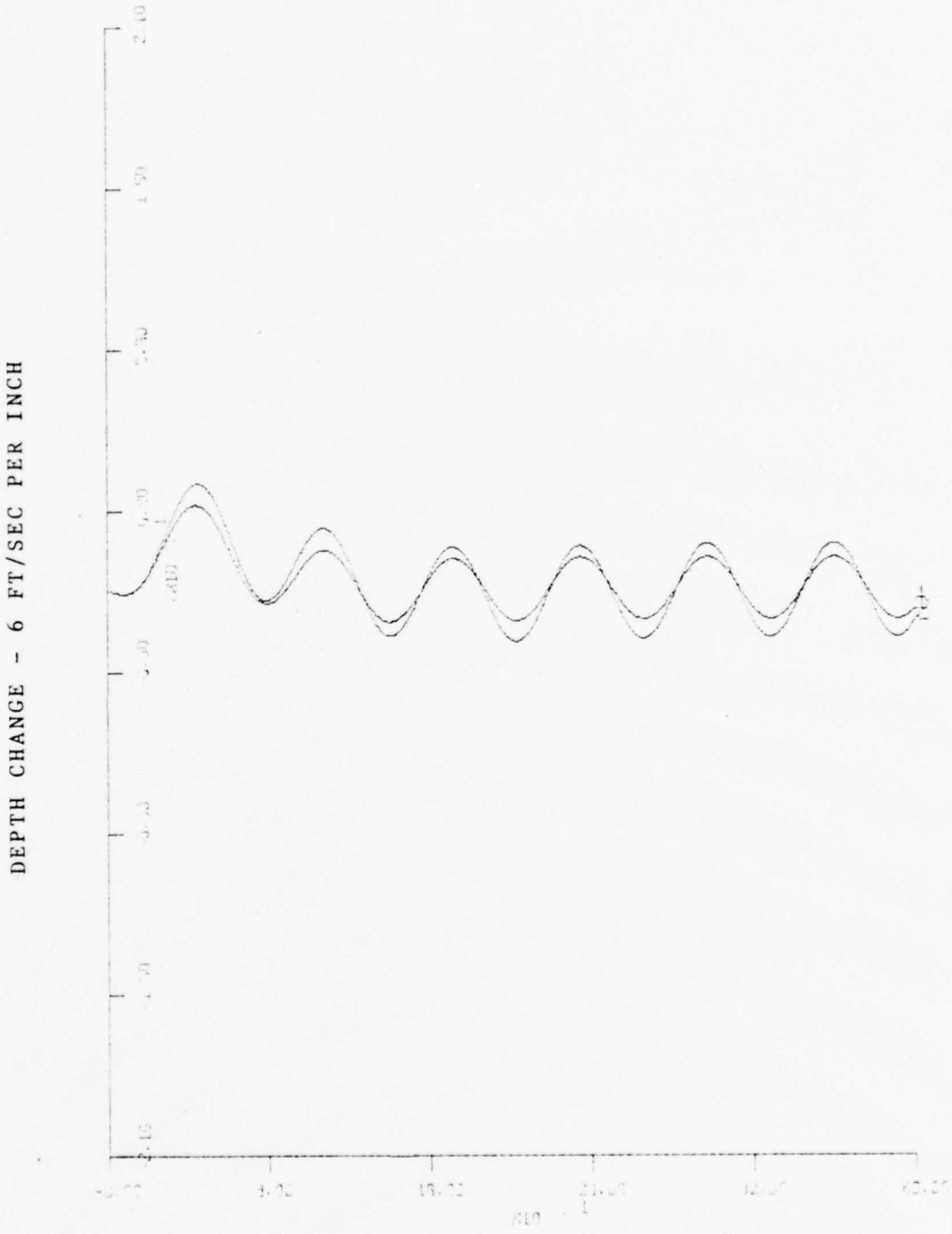

Figure 40 - FORCED RESPONSE, 9 KN
LDS = 35 °SIN .1 t

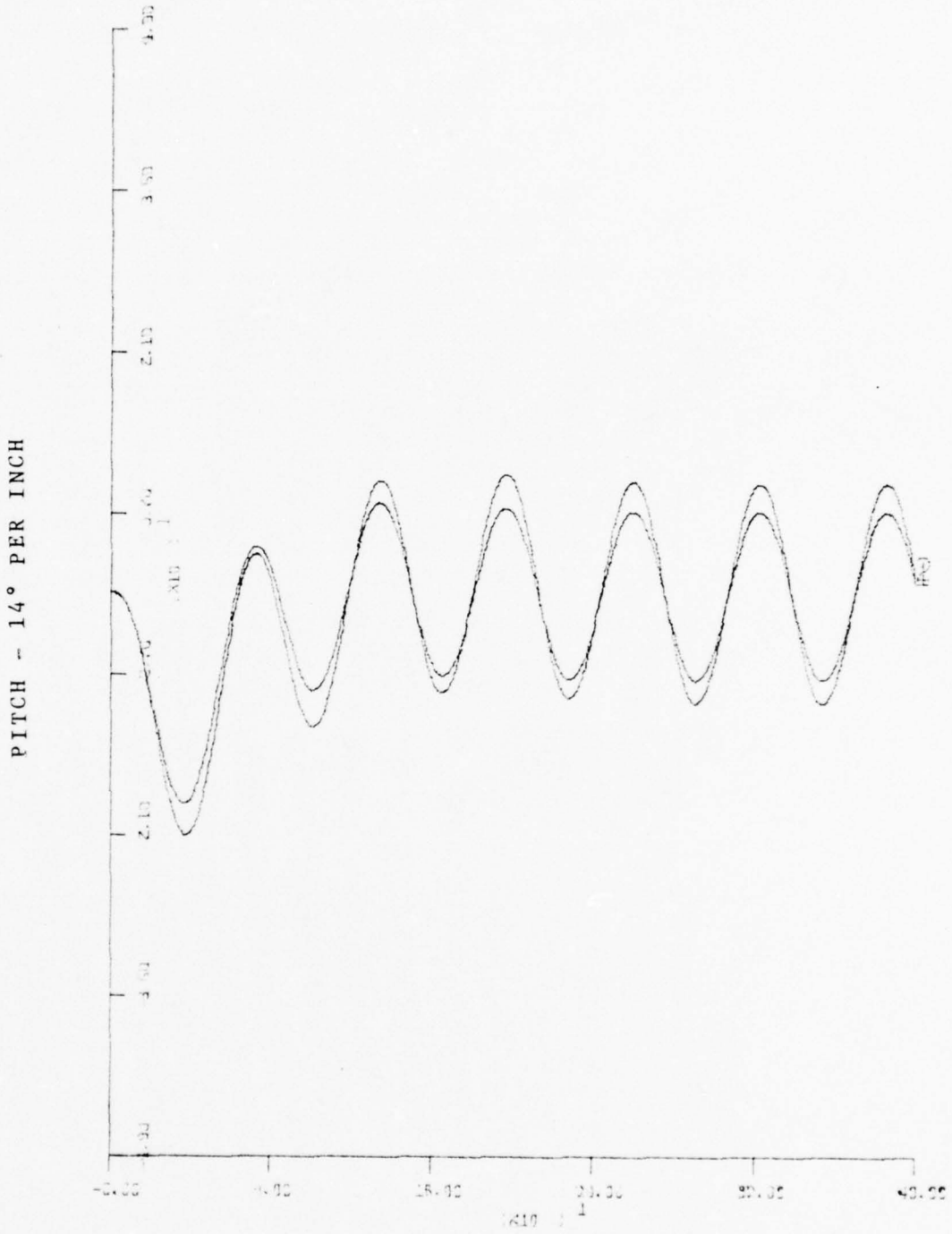

Figure 41 - FORCED RESPONSE, 9 KN
LDS = 35 °SIN .1 t

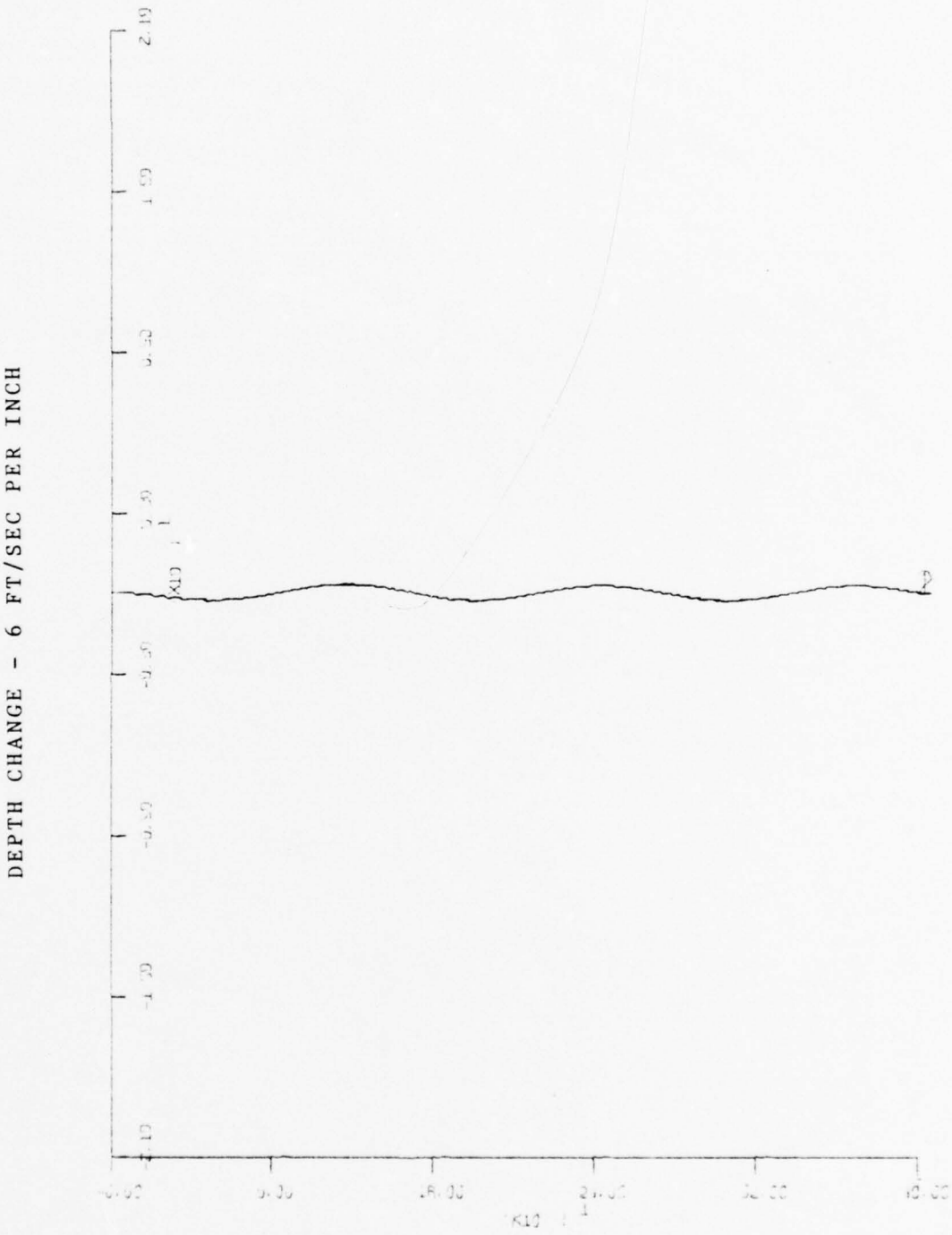

Figure 42 - FORCED RESPONSE, 9 KN
LDB = 5 °SIN .05 t

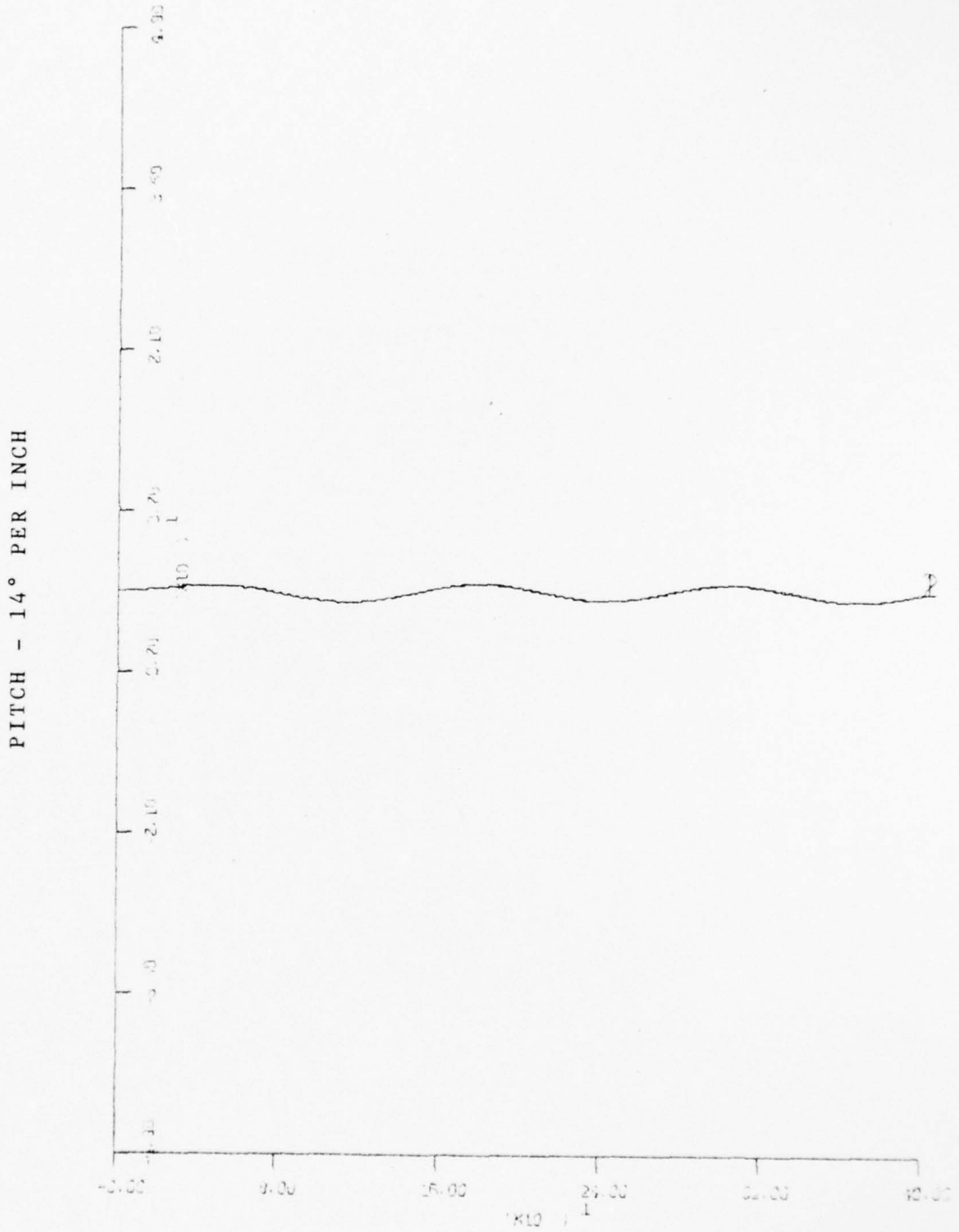

Figure 43 - FORCED RESPONSE, 9 KN
LDB = 5 °SIN .05 t

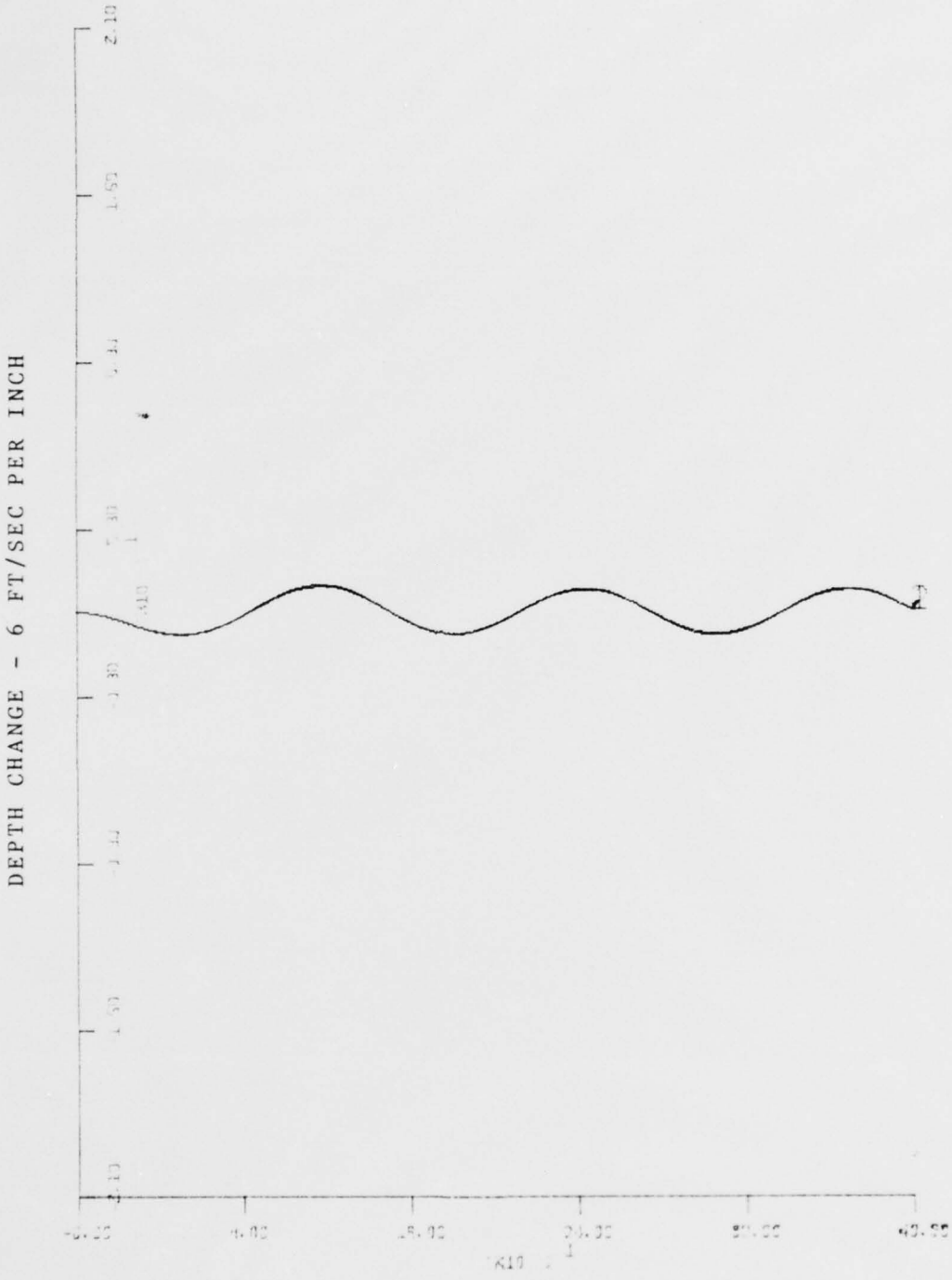

Figure 44 - FORCED RESPONSE, 9 KN
LDB = 15 °SIN .05 t

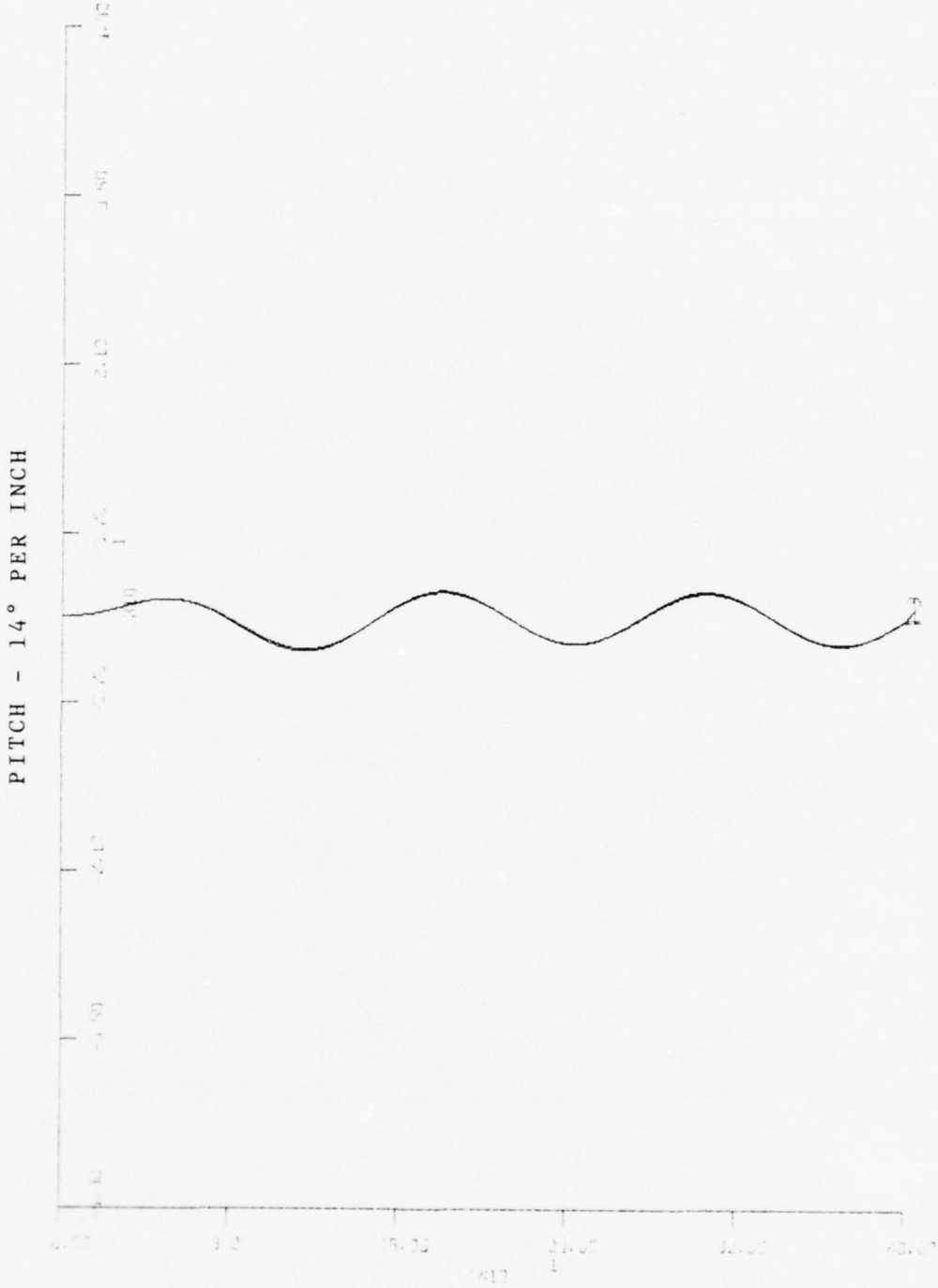

Figure 45 - FORCED RESPONSE, 9 KN
LDB = 15 °SIN .05 t

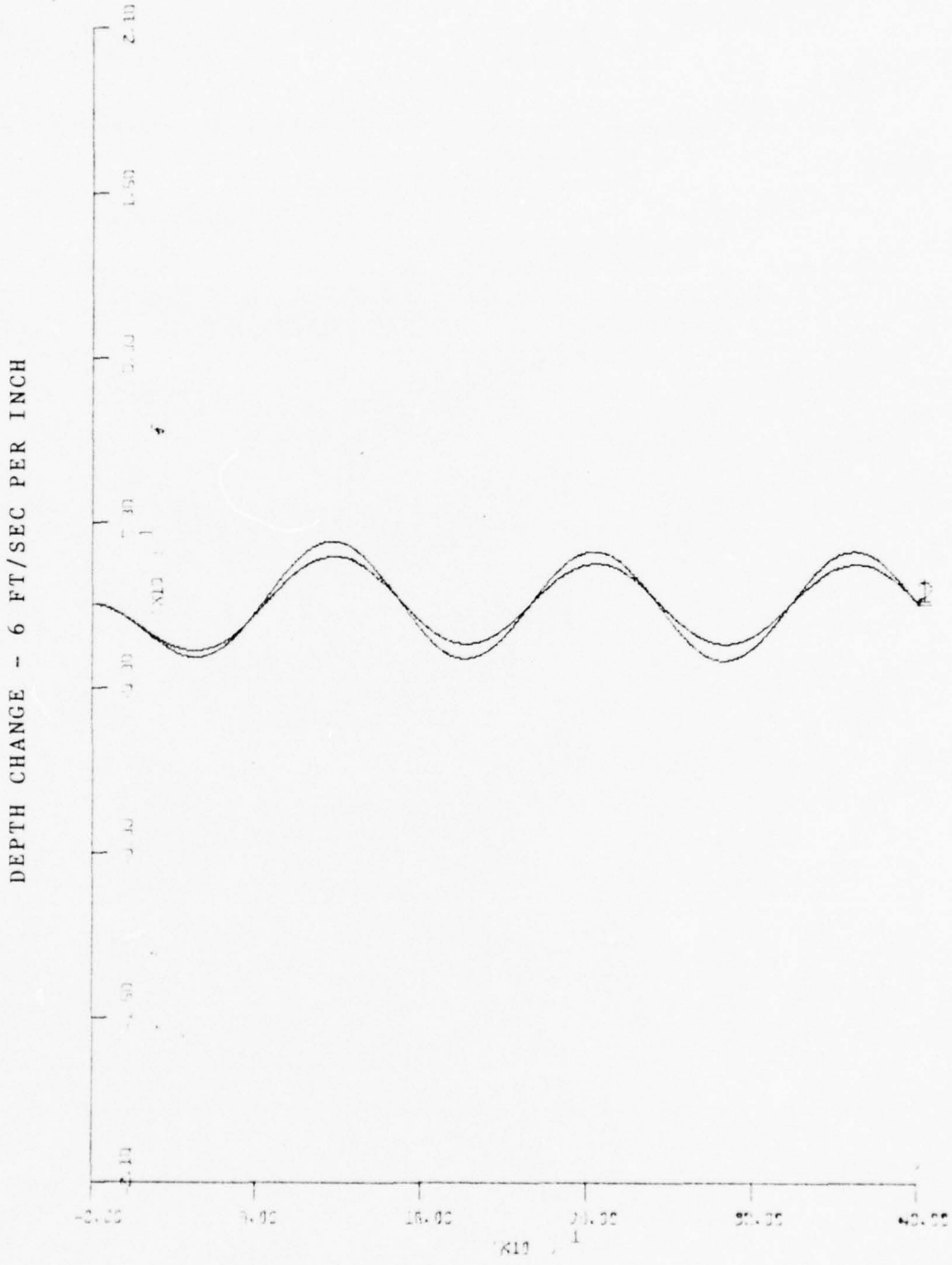

Figure 46 - FORCED RESPONSE, 9 KN
LDB = 35 °SIN .05 t

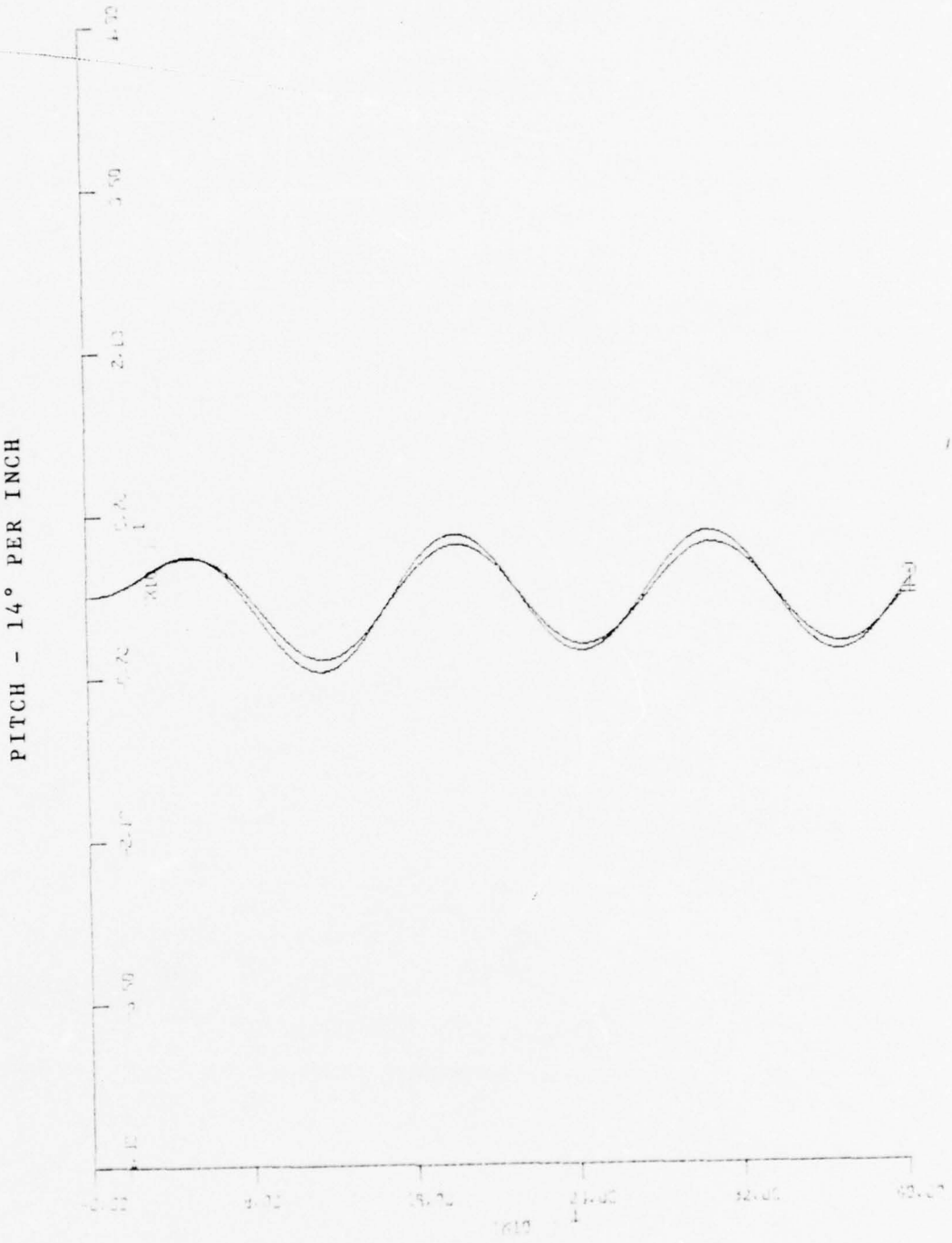

Figure 47 - FORCED RESPONSE, 9 KN
LDB = 35 °SIN .05 t

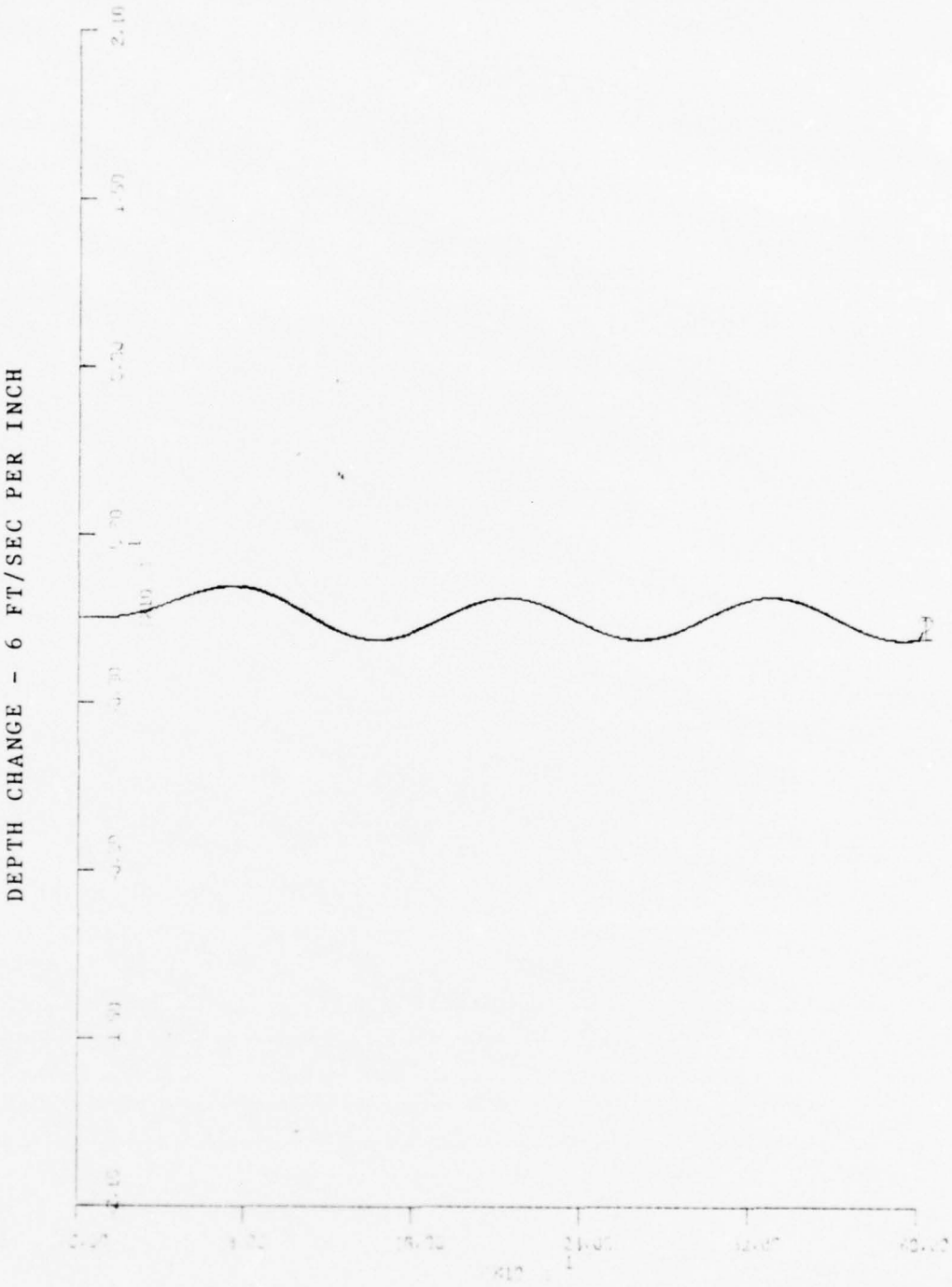

Figure 48 - FORCED RESPONSE, 9 KN
LDS = 5 °SIN .05 t

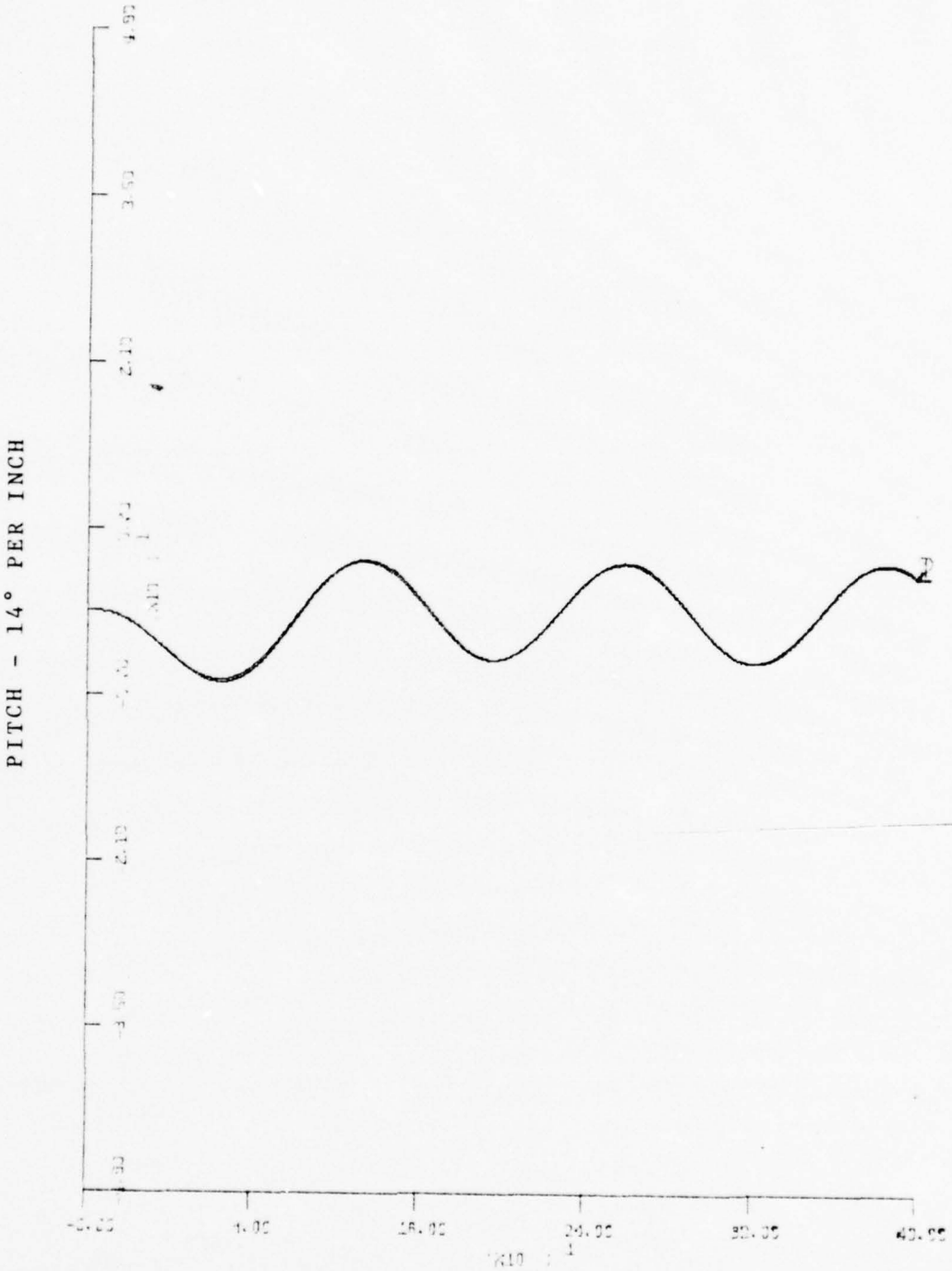

Figure 49 - FORCED RESPONSE, 9 KN
LDS = 5 °SIN .05 t

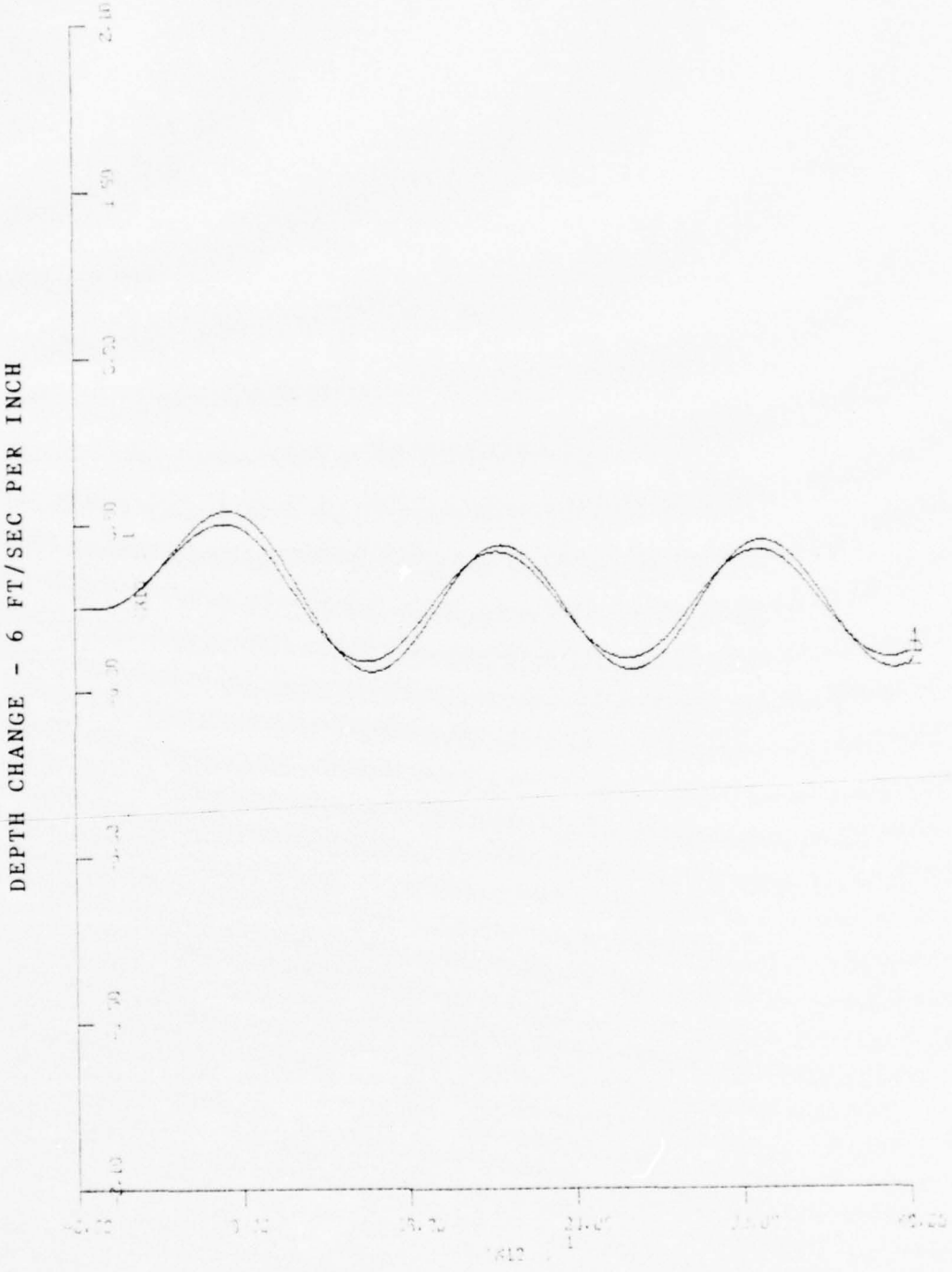

Figure 50 - FORCED RESPONSE, 9 KN
LDS = 15 °SIN .05 t

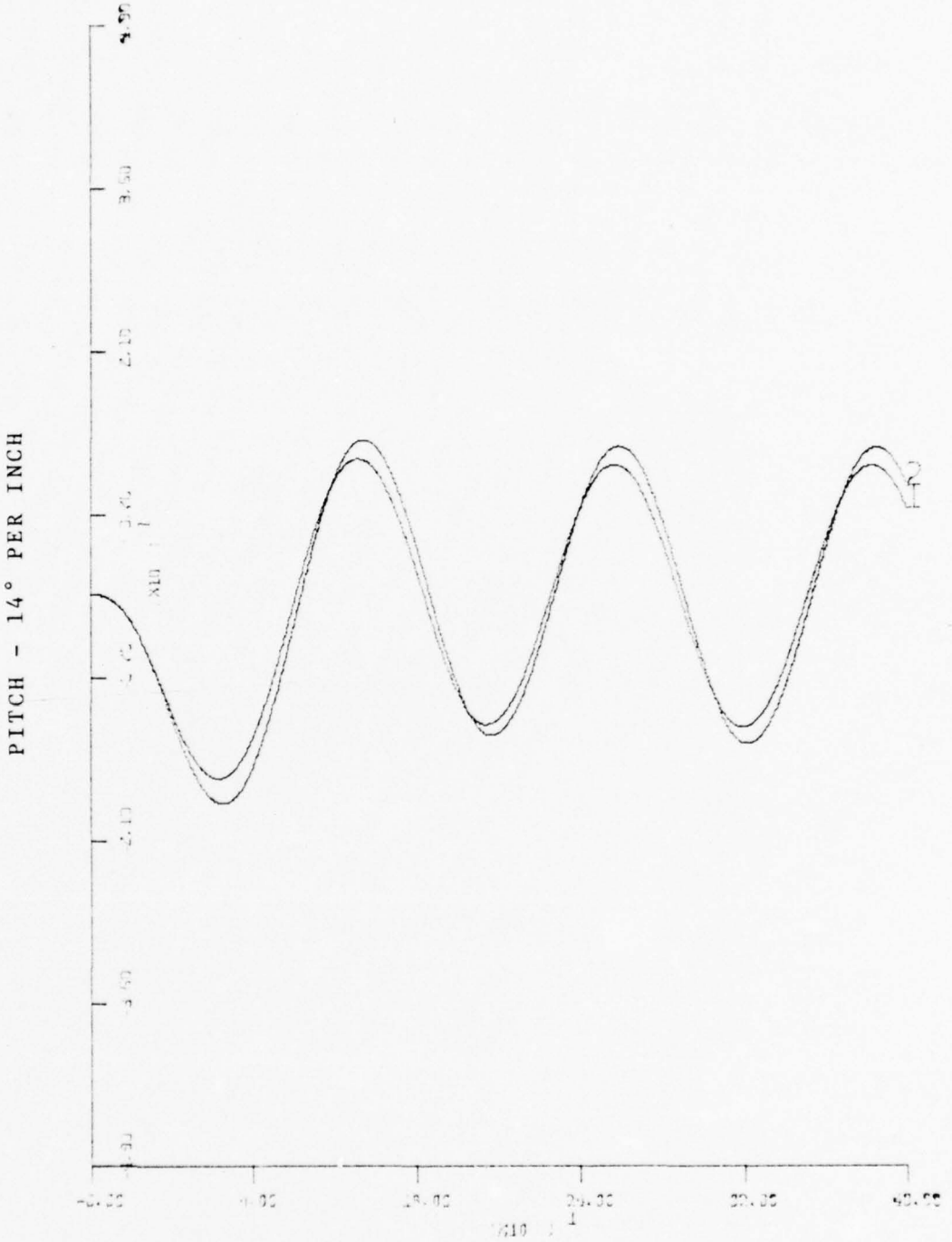

Figure 51 - FORCED RESPONSE, 9 KN
LDS = 15 °SIN .05 t

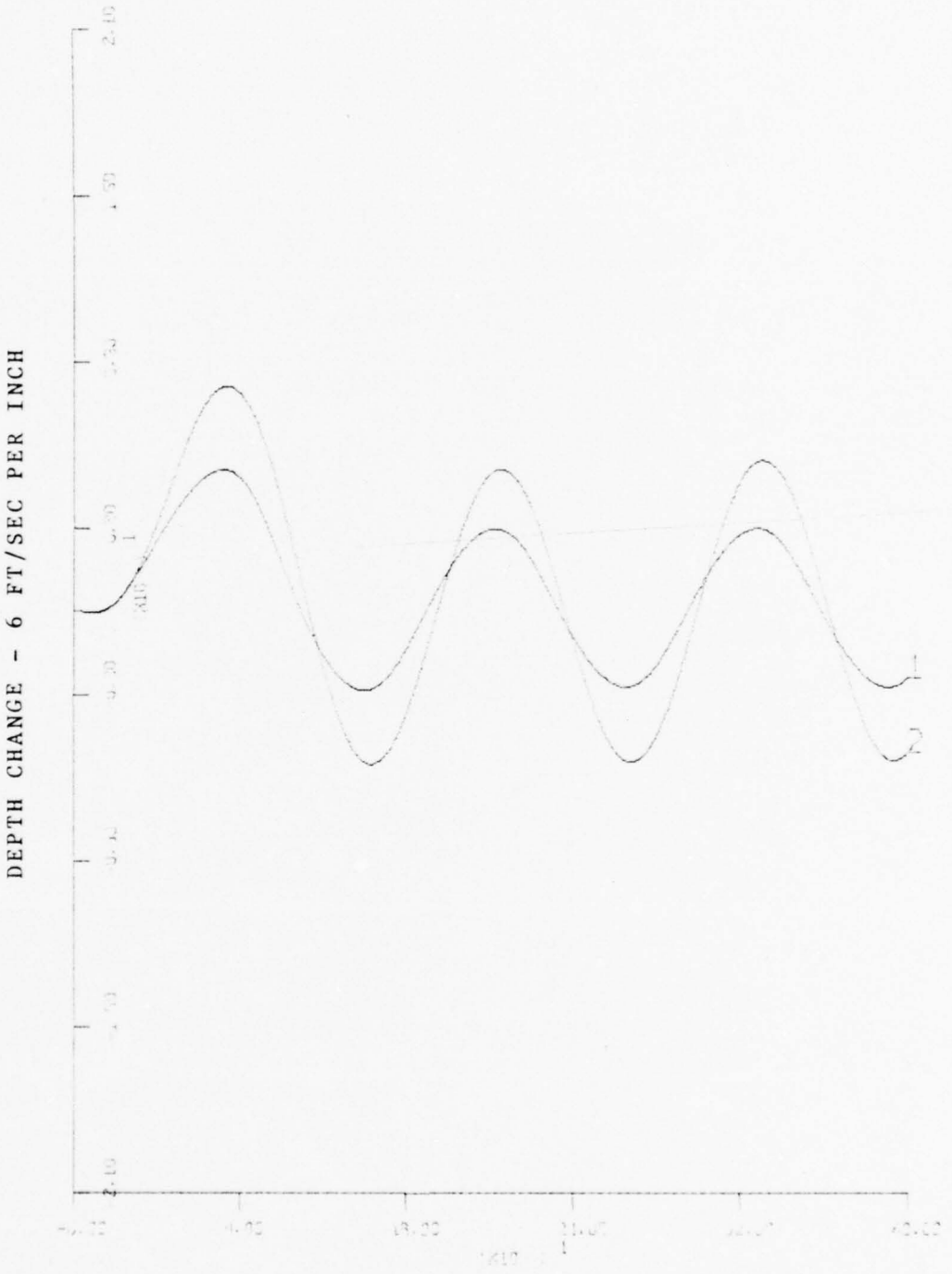

Figure 52 - FORCED RESPONSE, 9 KN
LDS = 35 °SIN .05 t

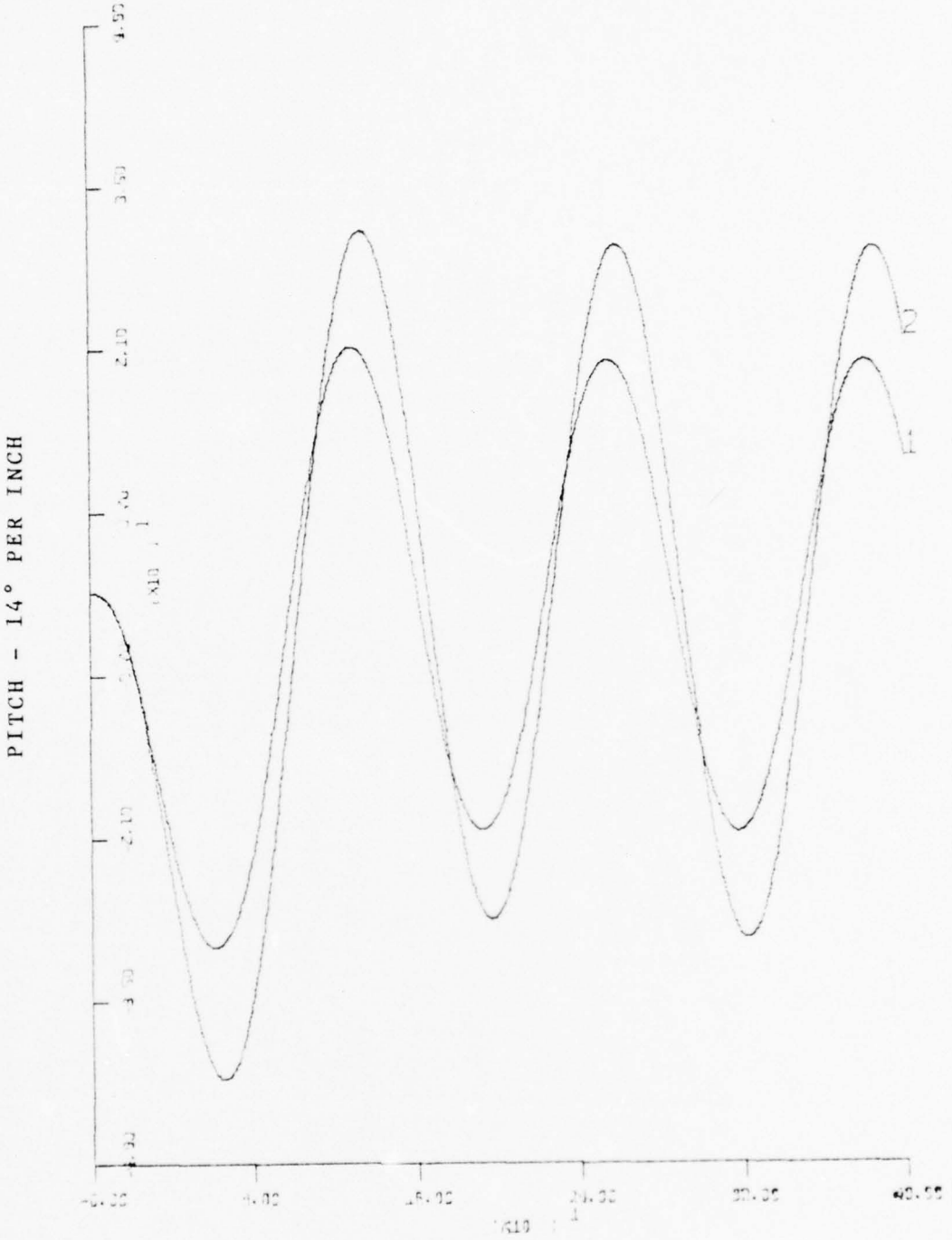

Figure 53 - FORCED RESPONSE, 9 KN
LDS = 35 °SIN .05 t

Table 05 - Speed 15 kn

Run	Plane	Omega rad	Amp °	Max deviation in Speed in kn	Pitch in °	ZDOT in ft/s	Fig
1	LDB	0.1	5	$5.47\ 10^{-2}$	$1.80\ 10^{-2}$	$8.80\ 10^{-3}$	
2	LDB	0.1	15	$4.61\ 10^{-1}$	$1.54\ 10^{-1}$	$1.23\ 10^{-1}$	
3	LDB	0.1	35	2.08	$9.38\ 10^{-1}$	$8.87\ 10^{-1}$	54,55
4	LDS	0.1	5	$1.16\ 10^{-1}$	$4.30\ 10^{-1}$	$1.67\ 10^{-1}$	56,57
5	LDS	0.1	15	$8.98\ 10^{-1}$	3.00	1.27	58,59
6	LDS	0.1	35	3.21	12.83	6.74	60,61
7	LDB	.05	5	$6.36\ 10^{-2}$	$8.51\ 10^{-2}$	$3.73\ 10^{-2}$	62,63
8	LDB	.05	15	$5.13\ 10^{-1}$	$7.01\ 10^{-1}$	$3.69\ 10^{-1}$	64,65
9	LDB	905	35	2.28	3.2	2.24	
10	LDS	.05	5	$2.87\ 10^{-1}$	1.58	$6.38\ 10^{-1}$	66,67
11	LDS	.05	15	1.76	10.76	4.87	68,69
12	LDS	.05	35	4.89	44.15	22.12	

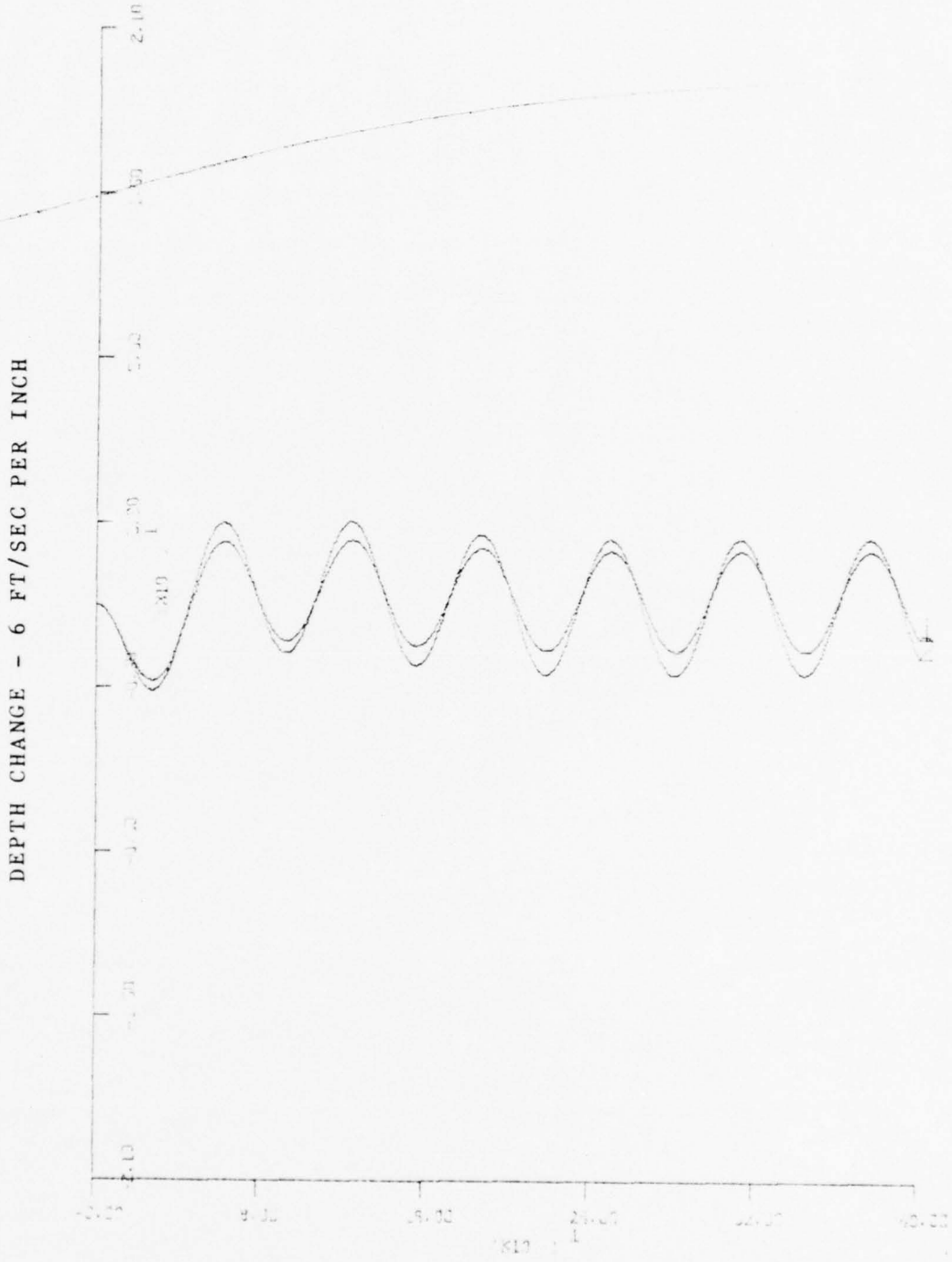

Figure 54 - FORCED RESPONSE, 15 KN
LDB = 35 °SIN .1 t

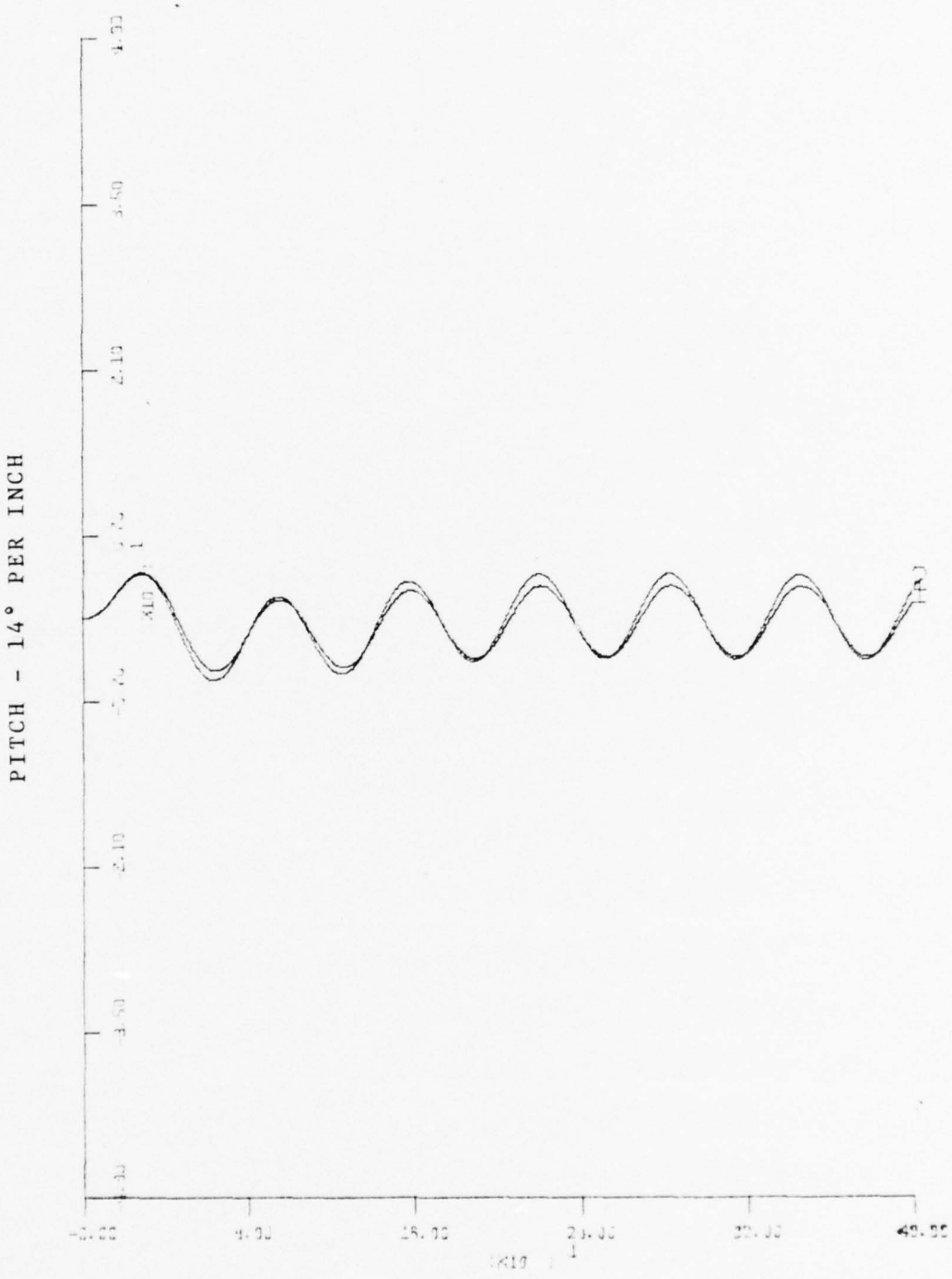

Figure 55 - FORCED RESPONSE, 15 KN
LDB = 35 °SIN .1 t

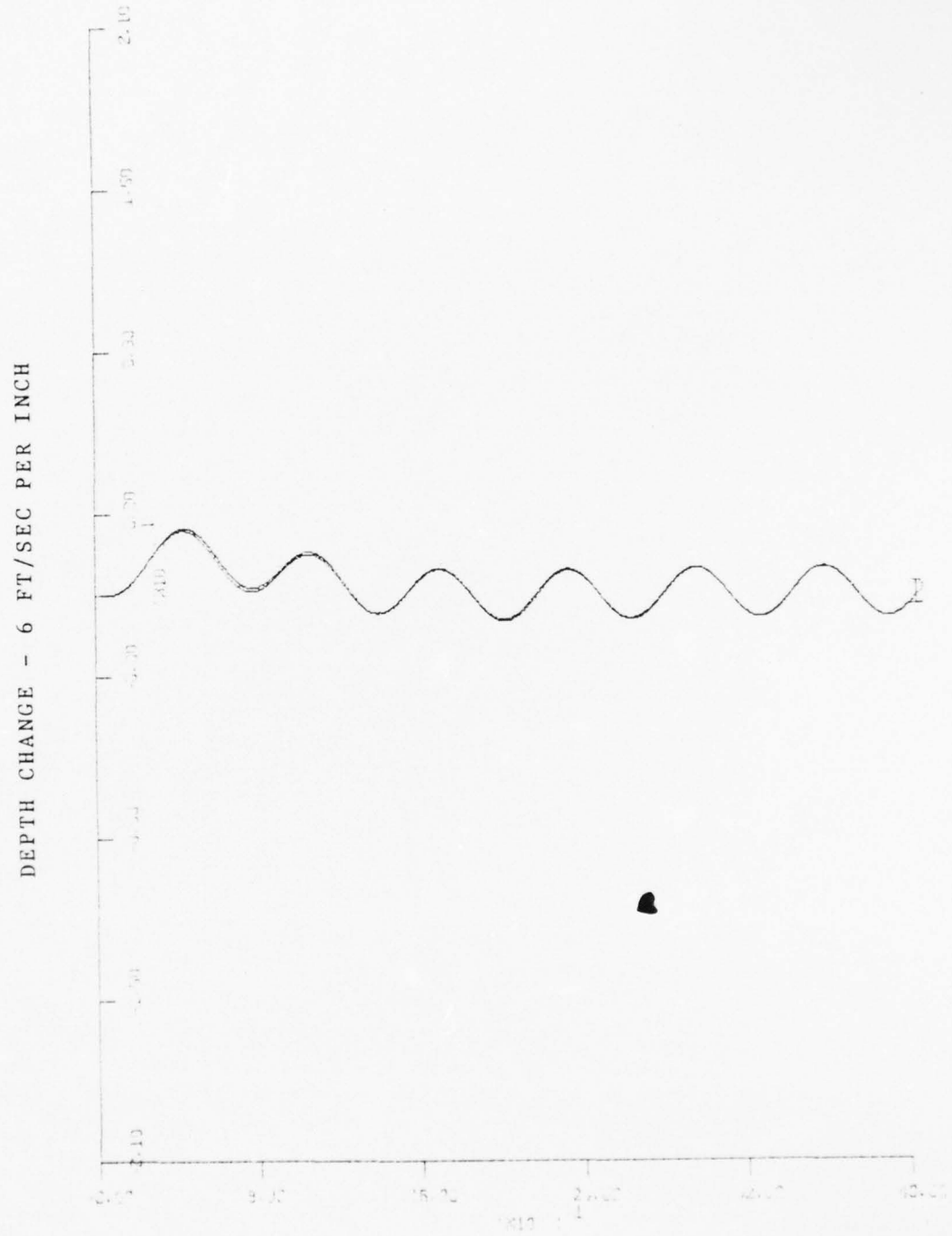

Figure 56 - FORCED RESPONSE, 15 KN
LDB = 5 °SIN .1 t

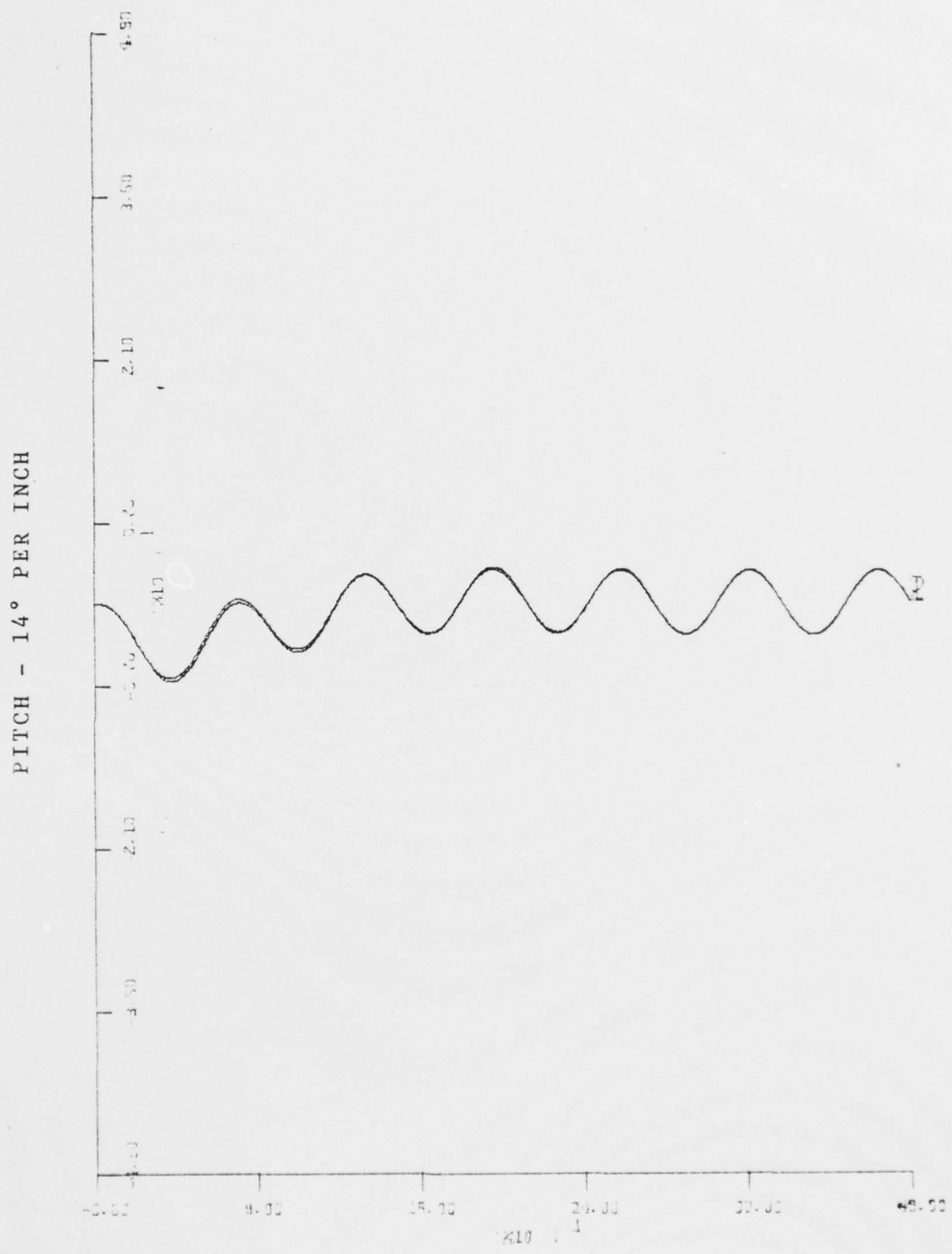

Figure 57 - FORCED RESPONSE, 15 KN
LDB = 5 °SIN .1 t

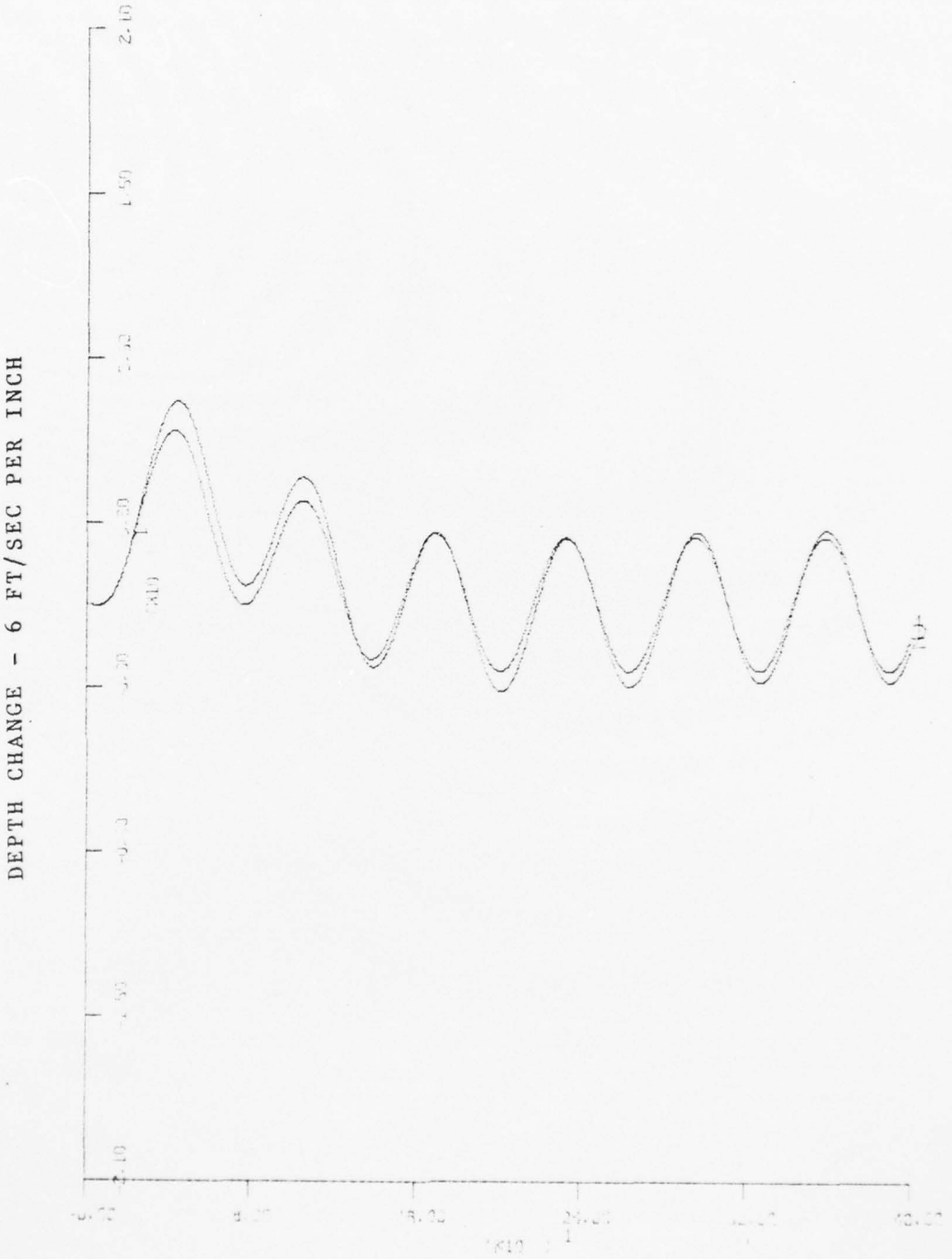

Figure 58 - FORCED RESPONSE, 15 KN
LDB = 15 °SIN .1 t

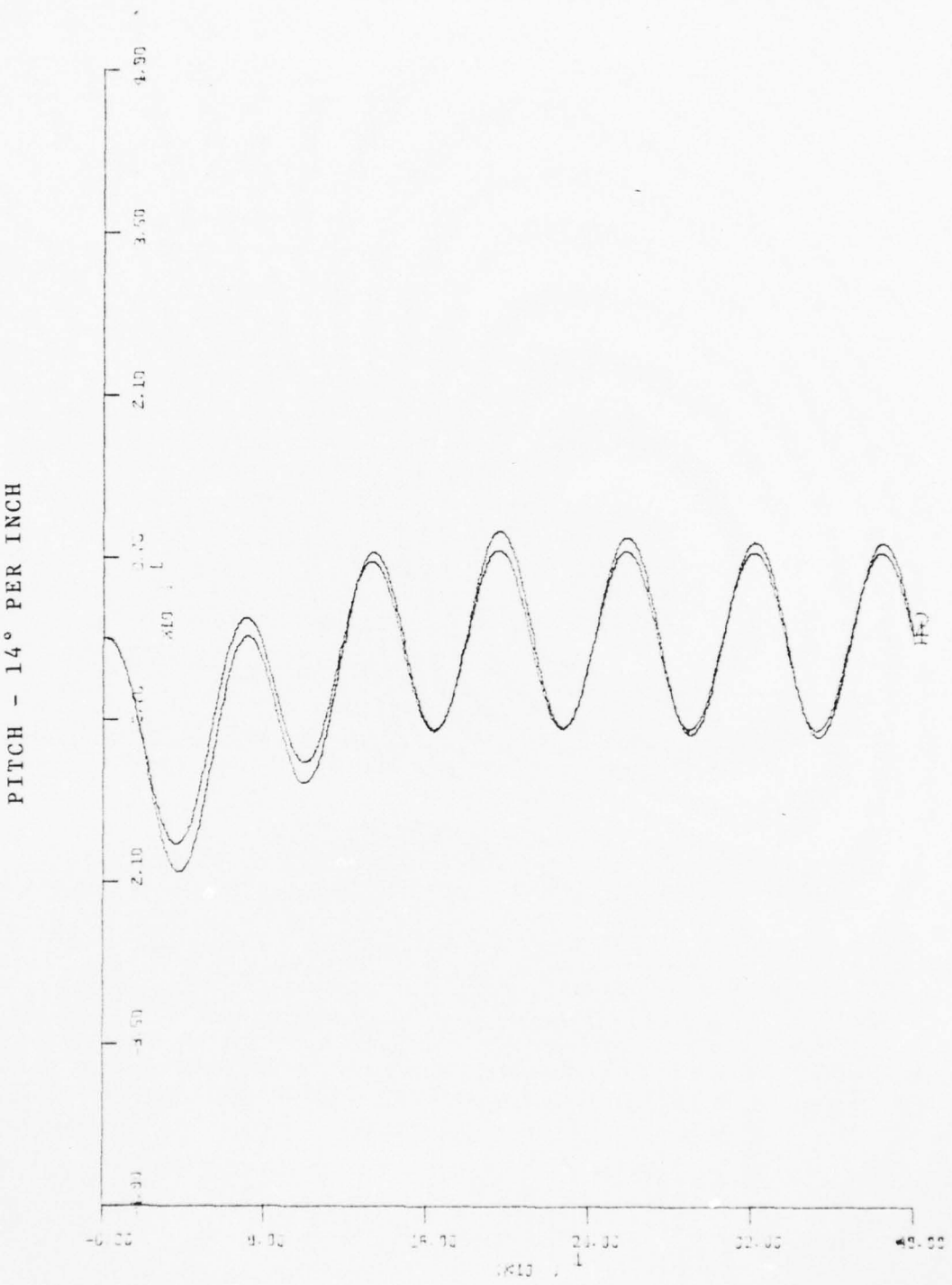

Figure 59 - FORCED RESPONSE, 15 KN
LDB = 15 °SIN .1 t

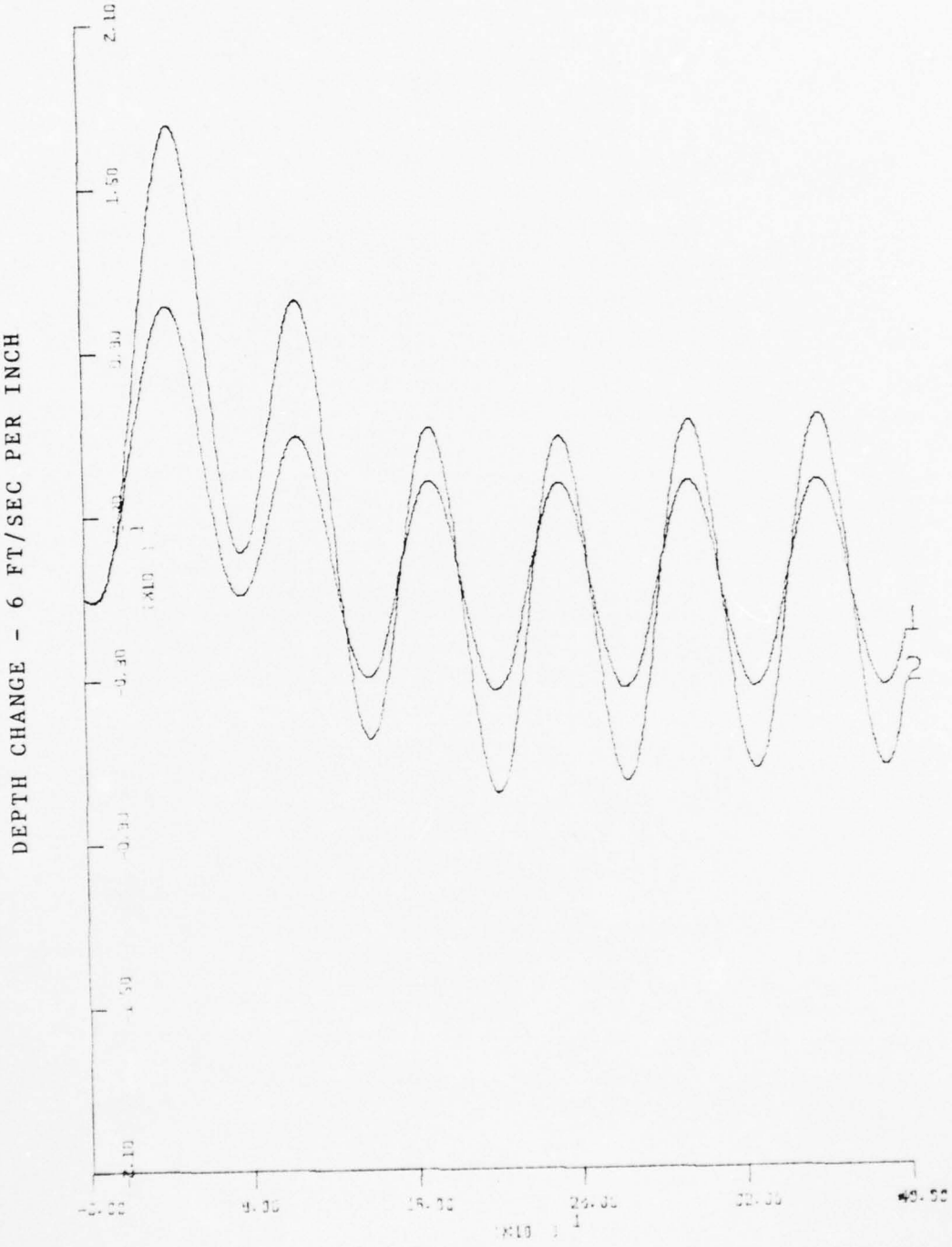

Figure 60 - FORCED RESPONSE, 15 KN
LDB = 35 °SIN .1 t

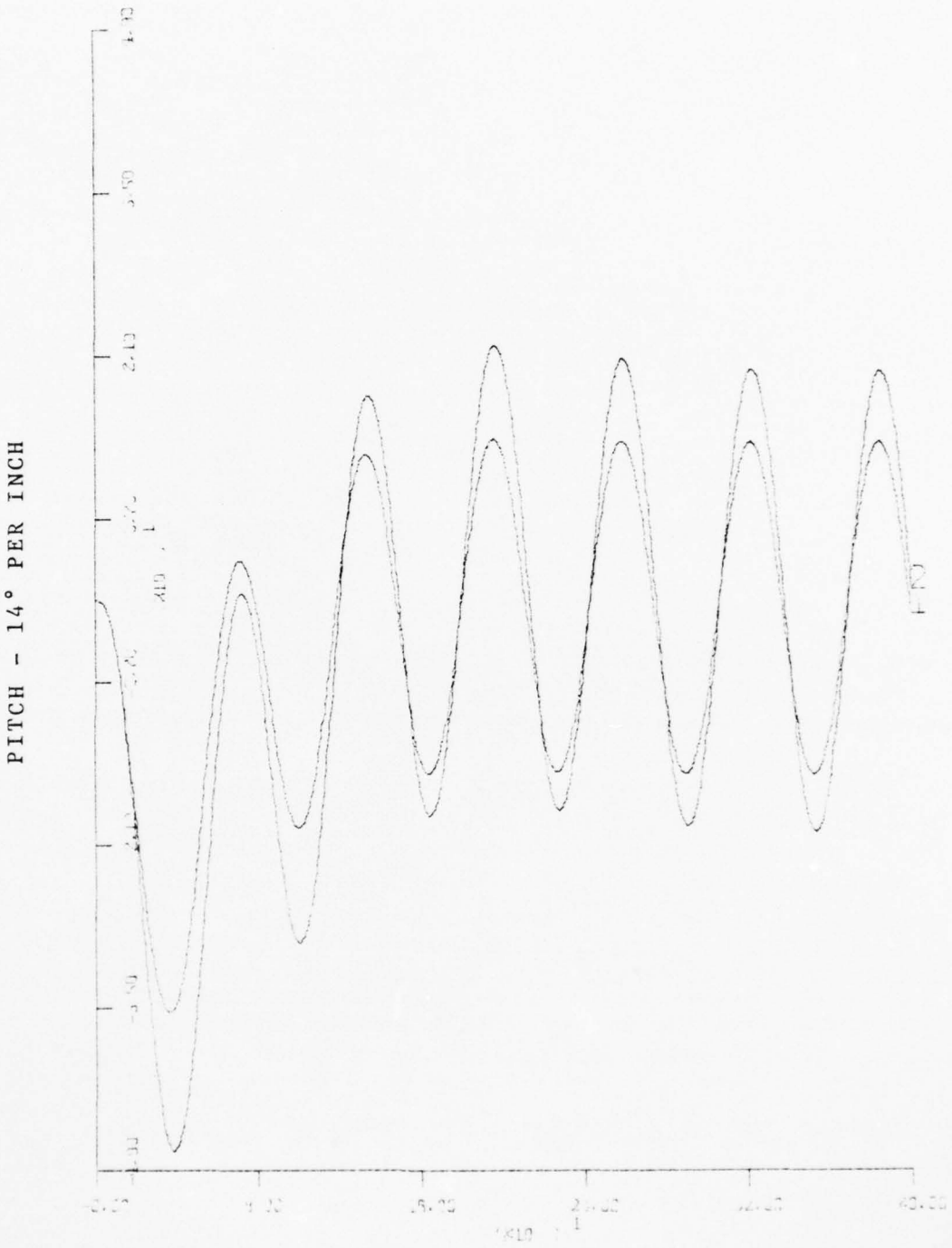

Figure 61 - FORCED RESPONSE, 15 KN
LDB = 35 °SIN .1 t

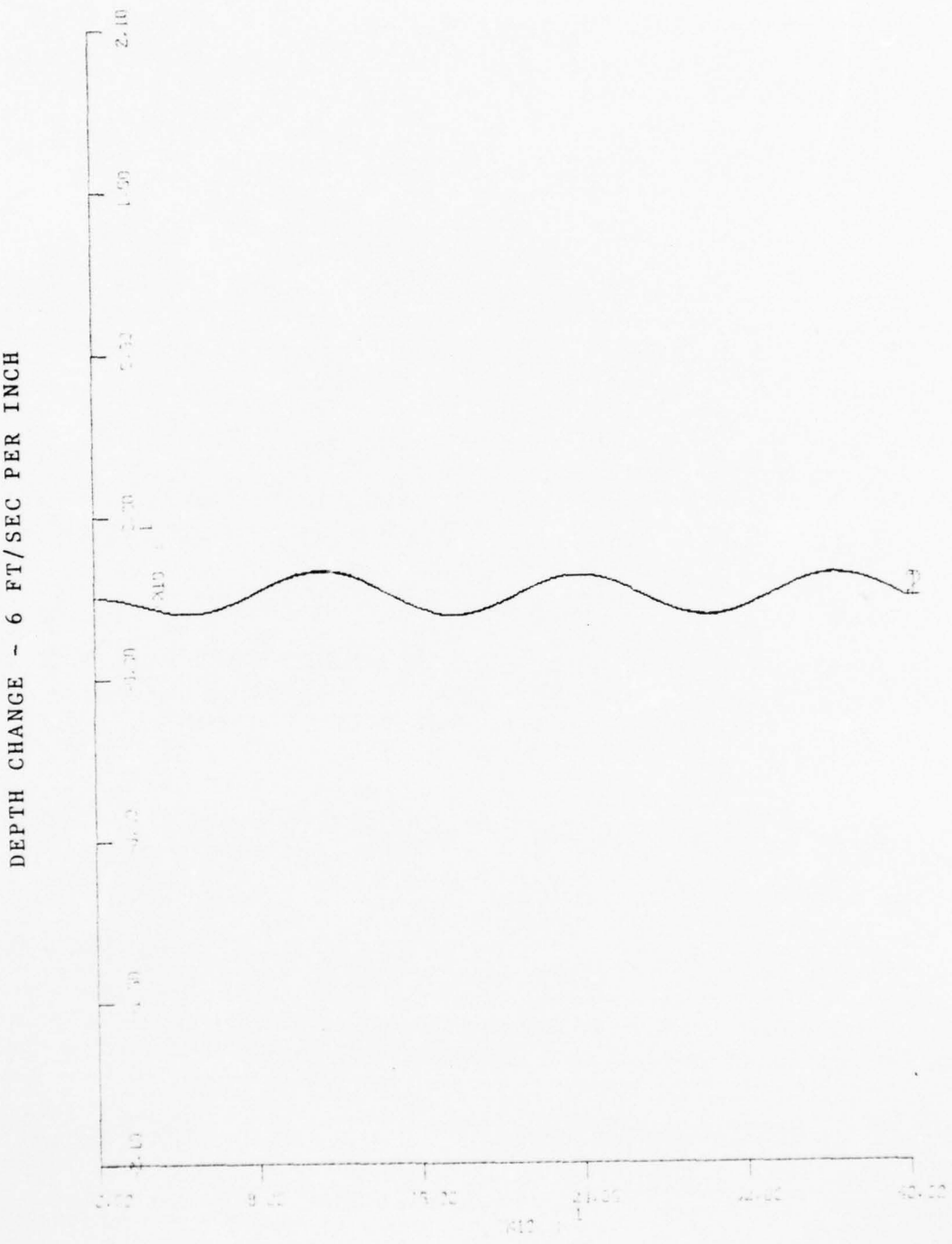

Figure 62 - FORCED RESPONSE, 15 KN
LDB = 5 °SIN .05 t

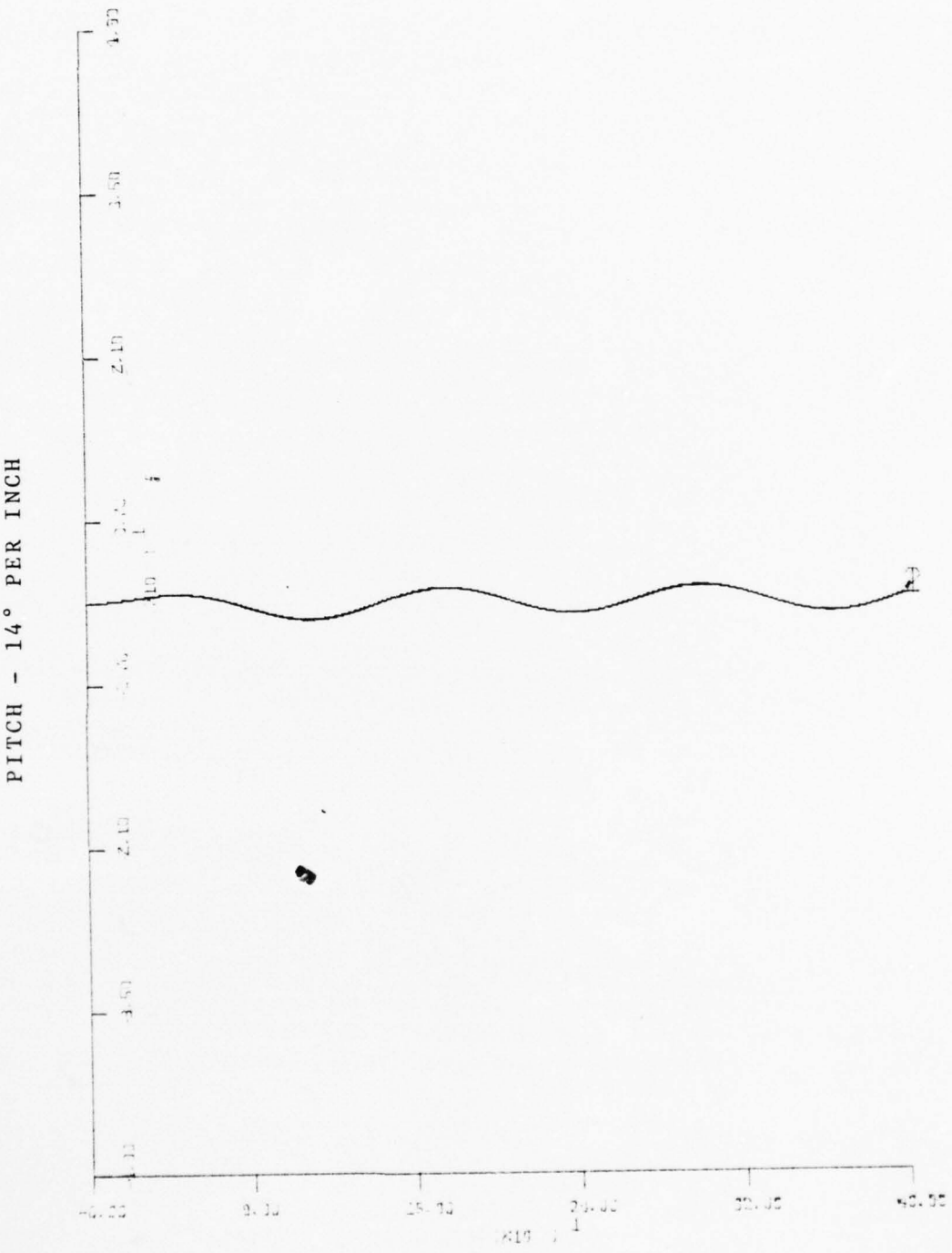

Figure 63 - FORCED RESPONSE, 15 KN
LDB = 5 °SIN .05 t

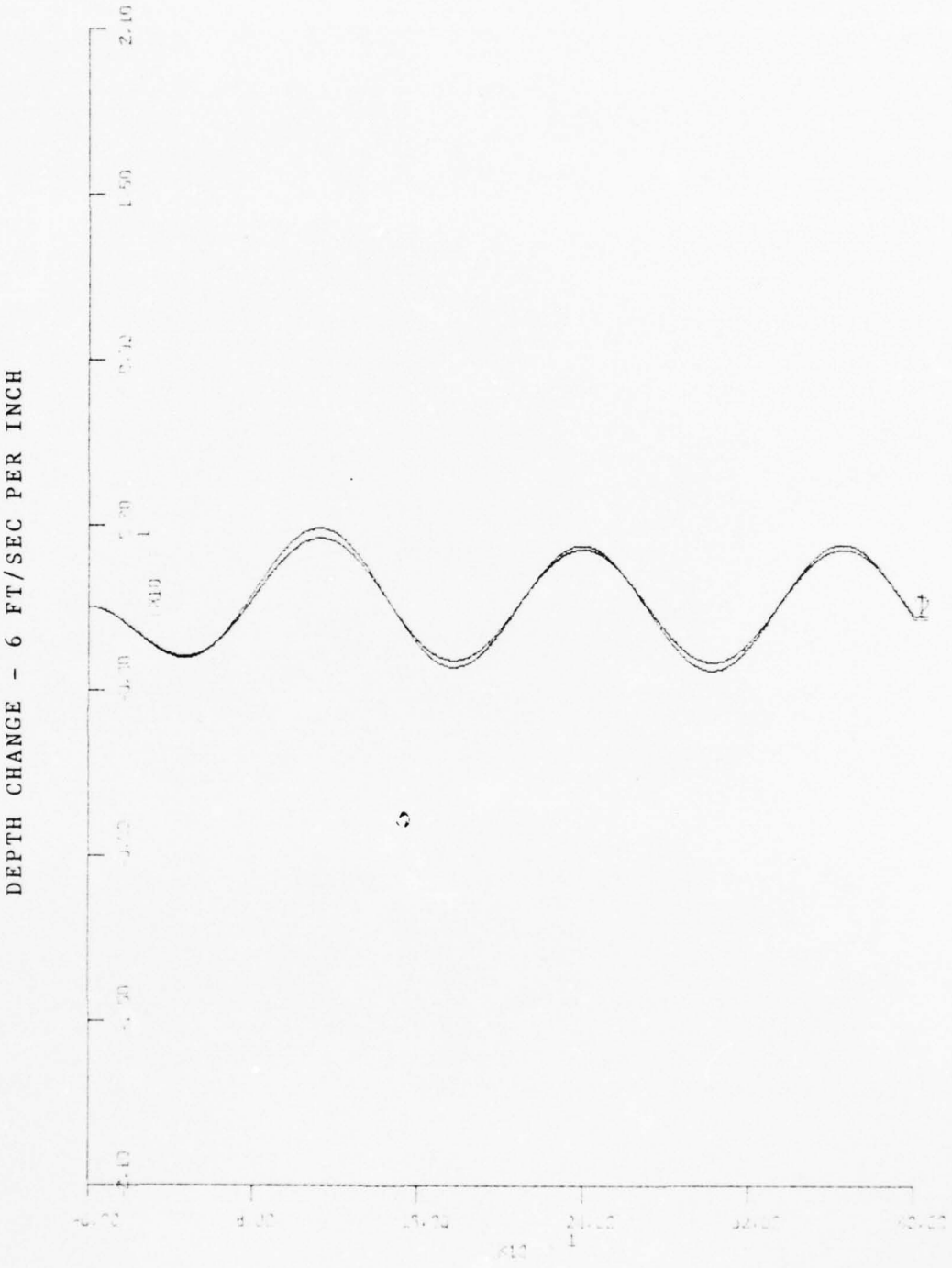

Figure 64 - FORCED RESPONSE, 15 KN
LDB = 15 °SIN .05 t

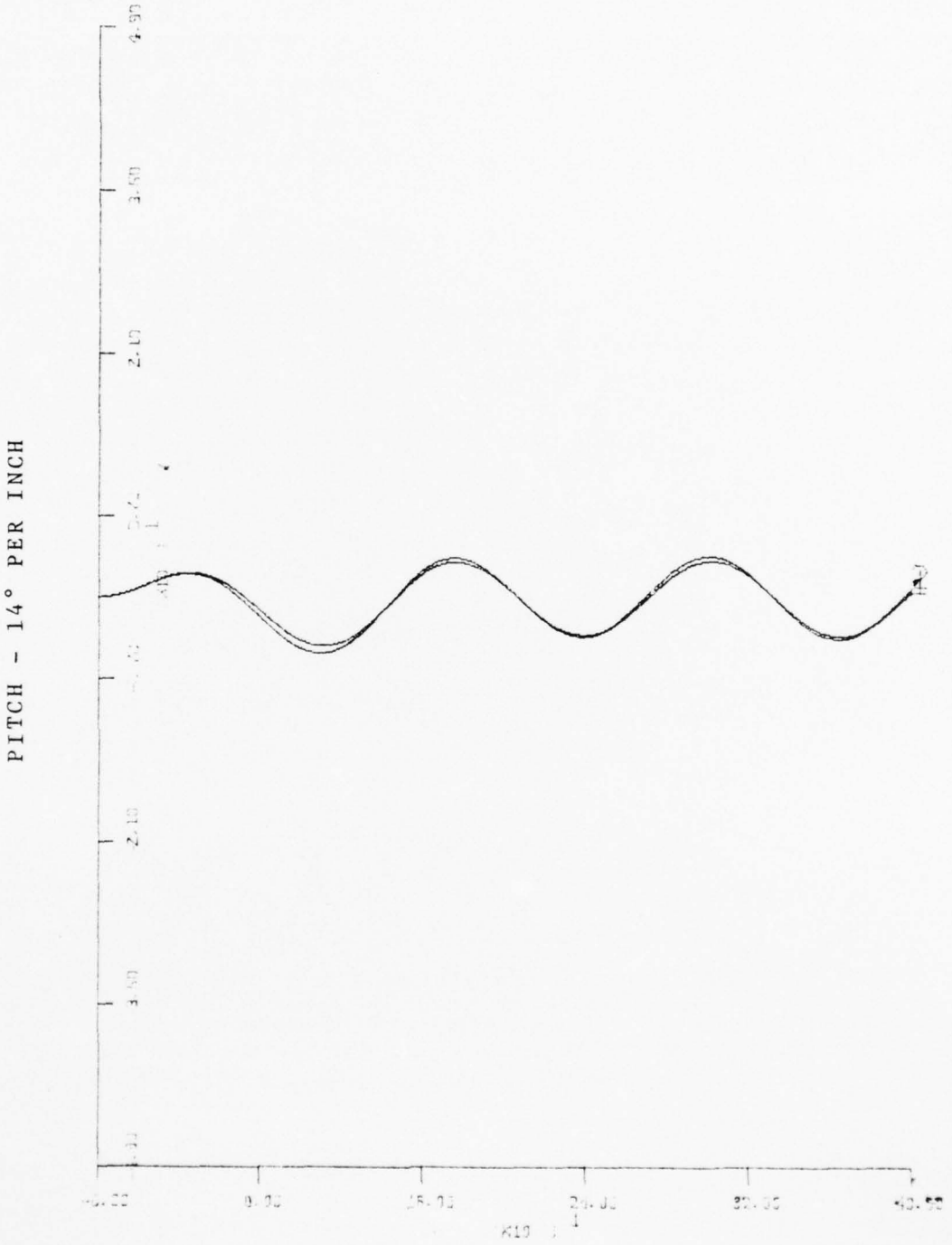

Figure 65 - FORCED RESPONSE, 15 KN
LDB = 15 °SIN .05 t

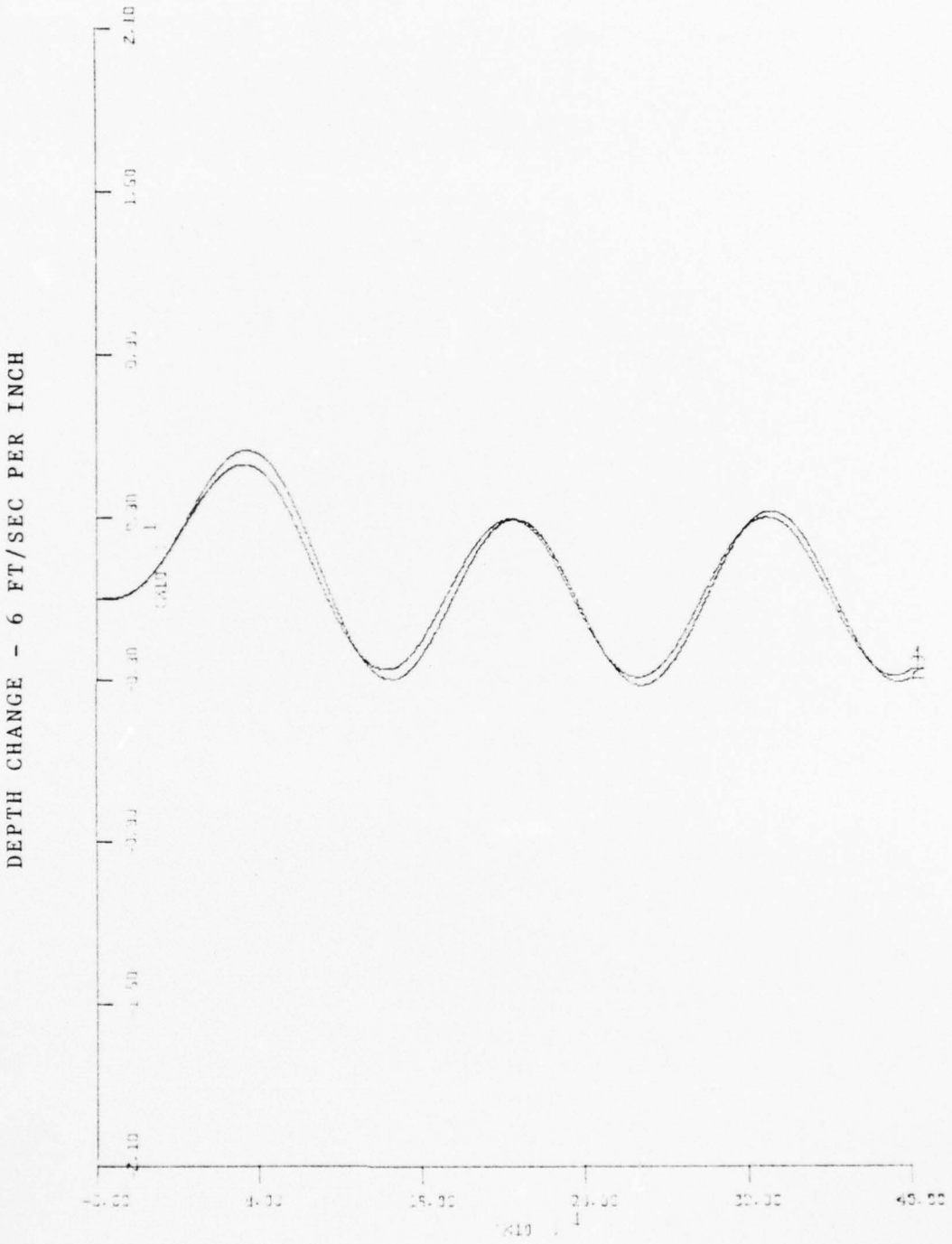

Figure 66 - FORCED RESPONSE, 15 KN
LDS = 5 °SIN .05 t

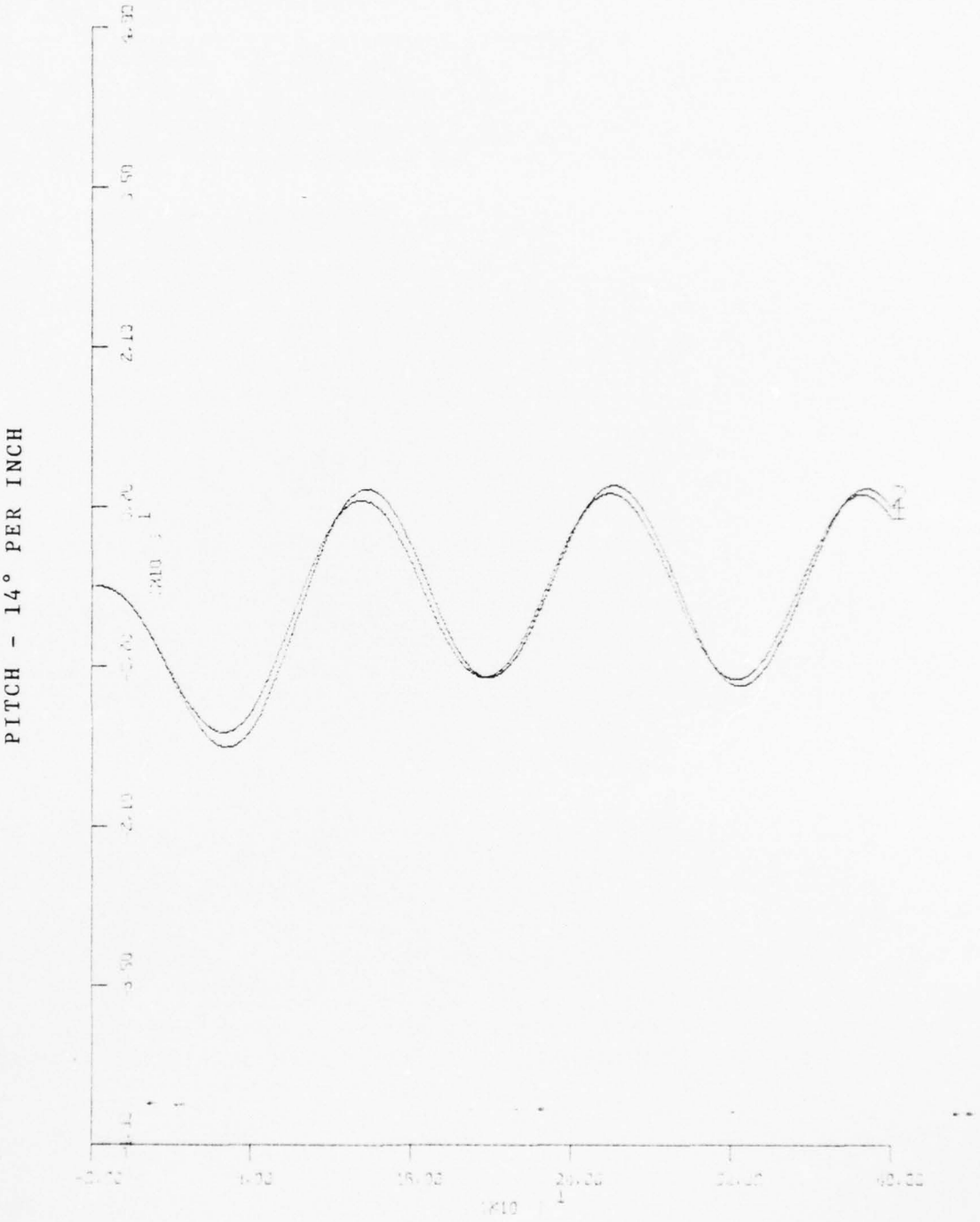

Figure 67 - FORCED RESPONSE, 15 KN
LDS = 5 °SIN .05 t

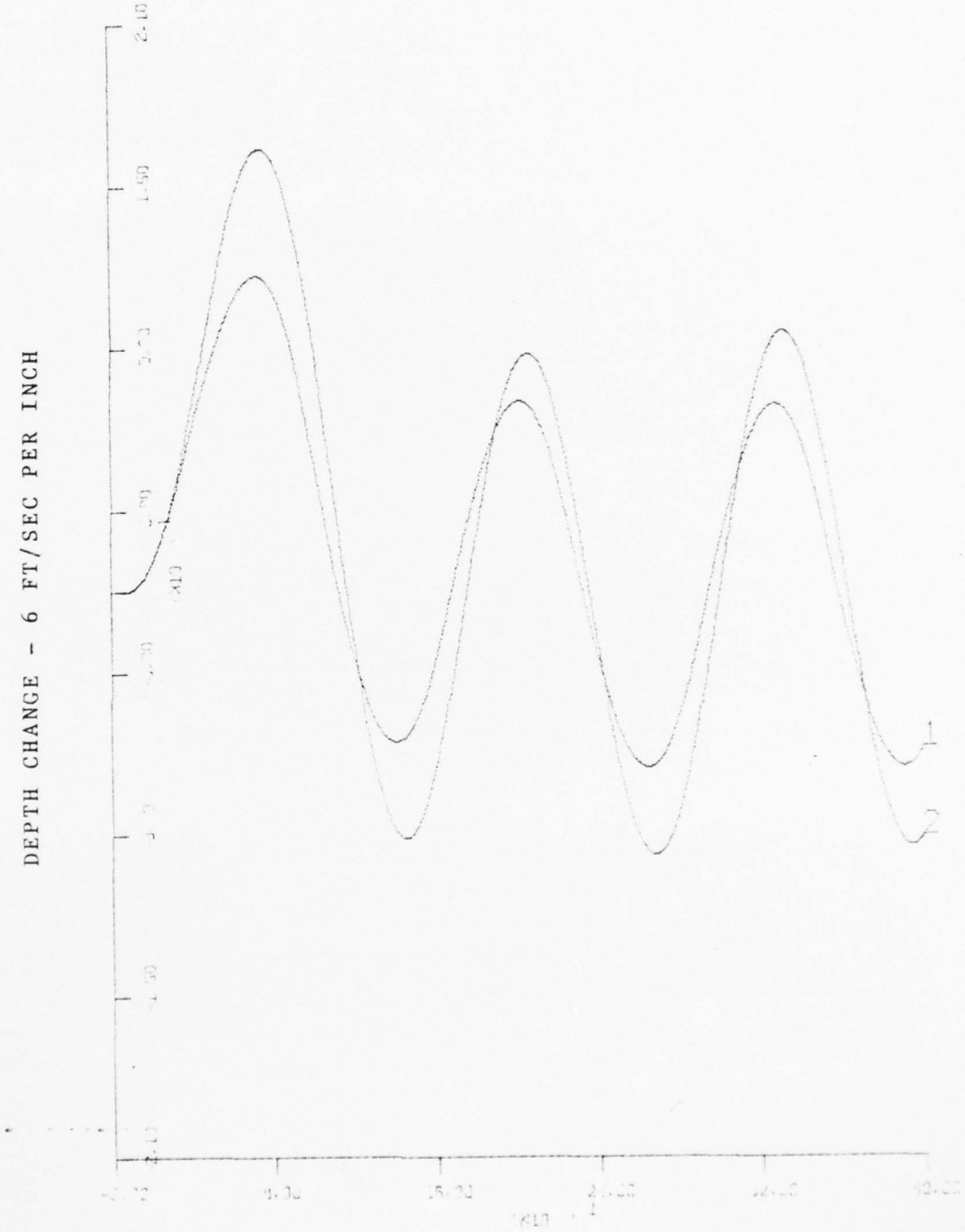

Figure 68 - FORCED RESPONSE, 15 KN
LDS = 15 °SIN .05 t

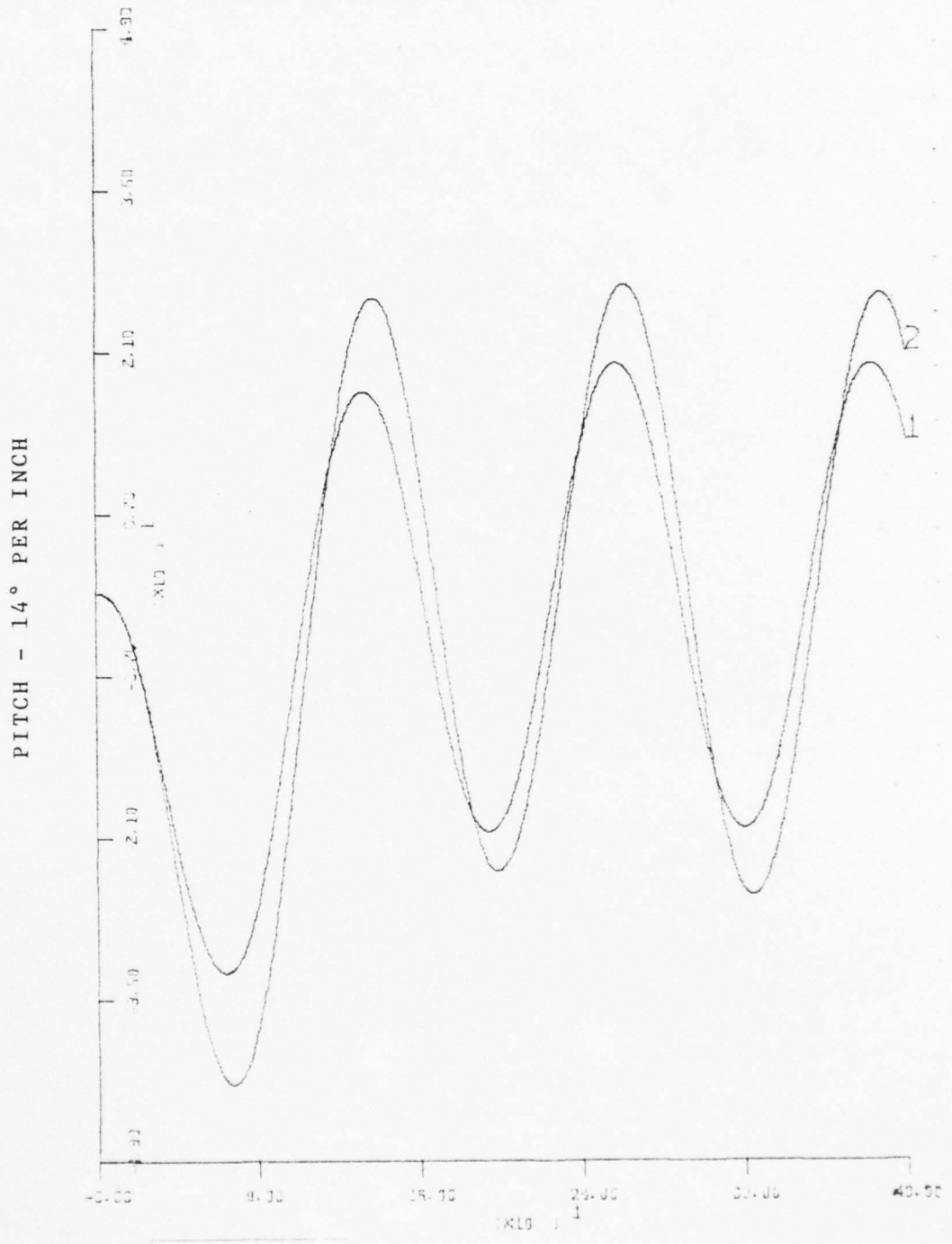

Figure 69 - FORCED RESPONSE, 15 KN
LDS = 15 °SIN .05 t

* 3 knots

The response to the sternplane showed an increasing deviation in pitch and depth change with increasing amplitude. With decreasing frequency the gain was increased. The percent deviation stayed about the same.

The response to the fairwater plane shows the same behavior except that the gain ratio DS/DB = 3.5 for pitch and 1.6 for depth change. The absolute magnitude of all deviations is considered negligibly small.
This can be expected, because the pitch involved is relatively small and the speed is about constant (max. decrease in speed is .38 kn for 35° plane deflection).

* 9 kncts

The speed decreases substantially (up to 2.2 kn) for large plane angles, which causes bigger deviations in pitch and depth change (up to 12.7°).
But it could be observed that the linearized model was still a good approximation for small perturbations.

* 15 knots

At this speed the decrease of U was even bigger (up to 32% at 35° plane deflection), which resulted in larger deviations in both variables. For small perturbations the approximation is still very good.

Thus it has been shown that:
- Approximation by linear model is valid for small perturbations at all speeds.
- The dynamics of both models are compatible.

In addition it has been observed, that the

AD-A038 758 NAVAL POSTGRADUATE SCHOOL MONTEREY CALIF F/G 13/10.1
AUTOMATIC DEPTH AND PITCH CONTROL FOR SUBMARINES.(U)
DEC 76 V NITSCHE, K J LUESSOW

UNCLASSIFIED NL

2 OF 3
AD A038758

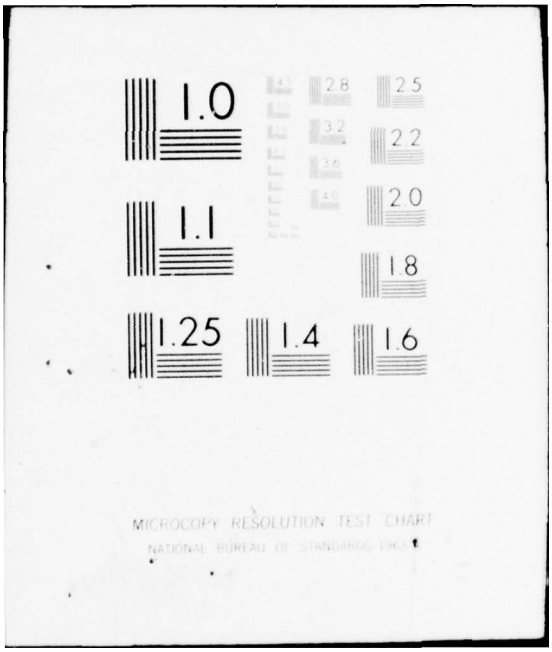
1.0
1.1
1.25
1.4
1.6
2.8
2.5
3.2
2.2
3.6
2.0
4.0
1.8
MICROCOPY RESOLUTION TEST CHART
NATIONAL BUREAU OF STANDARDS 1963

linearized mcdel is still valid for large perturbations applied cver a short period of time (initial condition response). When large plane angles were applied over a long period, the speed of the standard model decreased substantially, which made the constant speed assumption invalid.

3. Actuator model

The linearized model does not include the dynamics of the plane actuators, which are force and moment producers. Including the actuators would increase the ccmplexity of the system. The actuator dynamics may be ignored in the analysis and initial design phase, if and only if their dynamics are " fast " compared with the system dynamics.

Frcm our own experience, we know that the response of the hydraulic systems to a unit step input looks like an exponential function of the form:

$$(1 - e^{-\alpha t})$$

which has the Laplace transform of

$$\frac{1}{s} * \frac{1}{(s+\alpha)}$$

Thus the actuator dynamics will be represented by:

$$\frac{1}{(s+\alpha)}$$

α represents the inverse of the time constant, which has to be determined. As the rate of the rudder deflection depends on the magnitude of the desired angle the maximum rate limit is determined by the mechanical limits of the rudder, which are assumed to be $\pm$ 35 ^{o} for this model. It was assumed that the maximum deflection is reached in 5 time constants. As the needed time is about 3 to 3.5 sec, the time constant was determined to be 2/3 sec.

The actuator time constant is fast compared to those of the system. Therefore the actuators will be neglected in the design of the compensators, but will be included in the simulation of the compensated system.

III. DESIGN SPECIFICATIONS

The objective is to design an automatic controller for maneuvering in the vertical plane, i.e. depth and pitch control. The submarine is considered deeply submerged and therefore free from all external disturbances like surface-, bottom-, and wall-effects. The dynamics for a depth change include the depth and pitch dynamics. The depth response to an ordered depth change should basicly look like a second order overdamped or highly damped system response. The pitch shall be kept as close as possible to the ordered pitch, which under regular conditions will be zero. This submarine has no inertial guidance system (as for example the German coastal submarines). Rate information is not available and the only states to be used as feedback are depth, pitch, and speed. Due to this limited instrumentation the controller will have to use cascaded filters.

* Time requirements.

Depth changes at even keel for speeds

- $\leq$ 9 kn 10 ft in $\leq$ 120 sec
  100 ft in $\leq$ 240 sec

- $\geq$ 9 kn 10 ft in $\leq$ 60 sec
  100 ft in $\leq$ 100 sec

* Overshoot requirements

For depth changes

≤ 100 ft	≤ 5 %
≥ 100 ft	≤ 5 ft

* Pitch deviations

Always less than ± 2 ° from ordered pitch.

* Mechanical constraints

- plane angle limits according to diagram

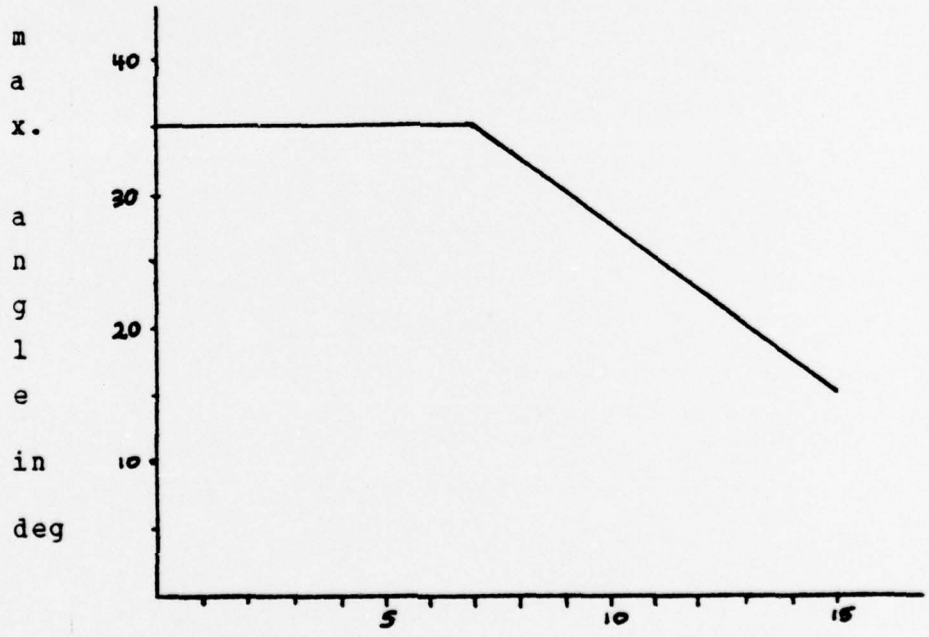

- maximum possible pitch ≤ 45 °

IV. DESIGN

A. TRANSFER FUNCTION

The design approach chosen for this thesis requires the system description by the transfer function matrix. Matrix equation (7) is the state variable representation of the system. The signal flowgraph equivalent for this system is given below. An additional integration is included, because the depth is a desired output.

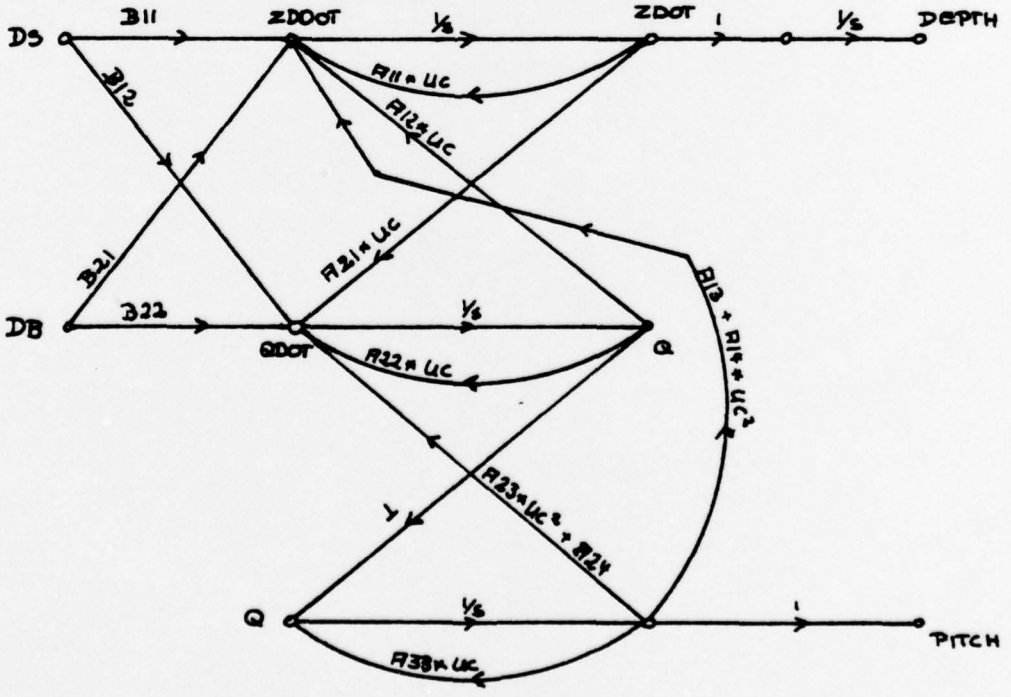

The input-output relations of interest are DEPTH/DS, DEPTH/DB, PITCH/DS, and PITCH/DB, because depth and pitch will be the measurable quantities and will be used for the control.

Applying Mason's gain rule the input-output relations have the form

$$\frac{Y(s)}{X(s)} = \frac{N2*s^2 + N1*s + N0}{D4*s^4 + D3*s^3 + D2*s^2 + D1*s + D0} \qquad (8)$$

The coefficients for equation (8) are:

ZDOT/DS :

$N2 = B11*UC^2$

$N1 = (A22*B11 - A12*B21)*UC^3$

$N0 = (E21*(A13 + A14*UC^2) - B11*(A23*UC^2 + A24))*UC^2$

$D4 = 1$

$D3 = -(A11 + A22)*UC$

$D2 = A11*A22*UC^2 - (A23*UC^2 + A24) - A12*A21*UC^2$

$D1 = A11*(A23*UC^2 + A24)*UC - A21*UC*(A13 + A14*UC^2)$

$D0 = 0.0$

ZDOT/DB :

$N2 = B12*UC^2$

$N1 = -(A22*B12 - A12*B22)*UC^3$

$N0 = (E22*(A13 + A14*UC^2) - B12*(A23*UC^2 + A24))*UC^2$

$D4 = 1$

$D3 = -(A11 + A22)*UC$

$$D2 = A11*A22*UC^2 - (A23*UC^2 + A24) - A12*A21*UC^2$$

$$D1 = A11*(A23*UC^2 + A24)*UC - A21*UC*(A13 + A14*UC^2)$$

$$D0 = 0.0$$

PITCH/DS :

$$N1 = E21*UC^2$$

$$N0 = (A21*B11 - A11*B21)*UC^3$$

$$D3 = 1$$

$$D2 = -(A11 + A22)*UC$$

$$D1 = A11*A22*UC^2 - (A23*UC^2 + A24) - A12*A21*UC^2$$

$$D0 = A11*(A23*UC^2 + A24)*UC - A21*UC*(A13 + A14*UC^2)$$

PITCH/DB :

$$N1 = E22*UC^2$$

$$N0 = (A21*B12 - A11*B22)*UC^3$$

$$D3 = 1$$

$$D2 = -(A11 + A22)*UC$$

$$D1 = A11*A22*UC^2 - (A23*UC^2 + A24) - A12*A21*UC^2$$

$$D0 = A11*(A23*UC^2 + A24)*UC - A21*UC*(A13 + A14*UC^2)$$

Table 06 through 10 show the root-locations for the speed range 1 kn - 15 kn. The characteristic roots move closer to the origin and the damping reduces with decreasing speed. This indicates that the overall response of the uncompensated submarine will be much slower for 3 kn than for 9 kn or 15 kn.

Table 06 - Characteristic roots

Speed	Root	Complex roots
1	$-0.2774\ 10^{-2}$	$-0.5452\ 10^{-2} \pm j\ 0.4978\ 10^{-1}$
2	$-0.5650\ 10^{-2}$	$-0.1085\ 10^{-1} \pm j\ 0.4841\ 10^{-1}$
3	$-0.8768\ 10^{-2}$	$-0.1613\ 10^{-1} \pm j\ 0.4604\ 10^{-1}$
4	$-0.1235\ 10^{-1}$	$-0.2114\ 10^{-1} \pm j\ 094245\ 10^{-1}$
5	$-0.1705\ 10^{-1}$	$-0.2563\ 10^{-1} \pm j\ 0.3716\ 10^{-1}$
6	$-0.2527\ 10^{-1}$	$-0.2835\ 10^{-1} \pm j\ 0.2908\ 10^{-1}$
7	$-0.4872\ 10^{-1}$	$-0.2347\ 10^{-1} \pm j\ 0.2116\ 10^{-1}$
8	$-0.7068\ 10^{-1}$	$-0.1933\ 10^{-1} \pm j\ 0.2032\ 10^{-1}$
9	$-0.8812\ 10^{-1}$	$-0.1744\ 10^{-1} \pm j\ 0.2014\ 10^{-1}$
10	-0.1038	$-0.1643\ 10^{-1} \pm j\ 0.1999\ 10^{-1}$
11	-0.1186	$-0.1586\ 10^{-1} \pm j\ 0.1982\ 10^{-1}$
12	-0.1328	$-0.1557\ 10^{-1} \pm j\ 0.1963\ 10^{-1}$
13	-0.1467	$-0.1546\ 10^{-1} \pm j\ 0.1940\ 10^{-1}$
14	-0.1603	$-0.1549\ 10^{-1} \pm j\ 0.1915\ 10^{-1}$
15	-0.1738	$-0.1562\ 10^{-1} \pm j\ 0.1887\ 10^{-1}$

Table 07 - Zeros of Pitch/DS

Speed	Gain	Root
1	$-0.4184\ 10^{-4}$	$-0.4370\ 10^{-2}$
2	$-0.1674\ 10^{-3}$	$-0.8739\ 10^{-2}$
3	$-0.3766\ 10^{-3}$	$-0.1311\ 10^{-1}$
4	$-0.6675\ 10^{-3}$	$-0.1745\ 10^{-1}$
5	$-0.1044\ 10^{-2}$	$-0.2182\ 10^{-1}$
6	$-0.1503\ 10^{-2}$	$-0.2619\ 10^{-1}$
7	$-0.2047\ 10^{-2}$	$-0.3056\ 10^{-1}$
8	$-0.2674\ 10^{-2}$	$-0.3493\ 10^{-1}$
9	$-0.3385\ 10^{-2}$	$-0.3929\ 10^{-1}$
10	$-0.4179\ 10^{-2}$	$-0.4367\ 10^{-1}$
11	$-0.5057\ 10^{-2}$	$-0.4804\ 10^{-1}$
12	$-0.6013\ 10^{-2}$	$-0.5238\ 10^{-1}$
13	$-0.7058\ 10^{-2}$	$-0.5675\ 10^{-1}$
14	$-0.8187\ 10^{-2}$	$-0.6112\ 10^{-1}$
15	$-0.9400\ 10^{-2}$	$-0.6549\ 10^{-1}$

Table C8 - Zeros of Pitch/DB

Speed	Gain	Root
1	$0.9111\ 10^{-5}$	$0.9434\ 10^{-3}$
2	$0.3644\ 10^{-4}$	$0.1887\ 10^{-2}$
3	$0.8200\ 10^{-4}$	$0.2831\ 10^{-2}$
4	$0.1453\ 10^{-3}$	$0.3768\ 10^{-2}$
5	$0.2272\ 10^{-3}$	$0.4713\ 10^{-2}$
6	$0.3274\ 10^{-3}$	$0.5654\ 10^{-2}$
7	$0.4457\ 10^{-3}$	$0.6599\ 10^{-2}$
8	$0.5822\ 10^{-3}$	$0.7542\ 10^{-2}$
9	$0.7370\ 10^{-3}$	$0.8484\ 10^{-2}$
10	$0.9100\ 10^{-3}$	$0.9428\ 10^{-2}$
11	$0.1101\ 10^{-2}$	$0.1037\ 10^{-1}$
12	$0.1309\ 10^{-2}$	$0.1131\ 10^{-1}$
13	$0.1537\ 10^{-2}$	$0.1225\ 10^{-1}$
14	$0.1783\ 10^{-2}$	$0.1319\ 10^{-1}$
15	$0.2047\ 10^{-2}$	$0.1414\ 10^{-1}$

Table 09 - Zeros of Depth/DS

Speed	Gain	Root	Root
1	$-0.1904\ 10^{-2}$		$-0.7732\ 10^{-2} \pm j\ 0.5083\ 10^{-1}$
2	$-0.7618\ 10^{-2}$		$-0.1546\ 10^{-1} \pm j\ 0.4378\ 10^{-1}$
3	$-0.1714\ 10^{-1}$		$-0.2320\ 10^{-1} \pm j\ 0.2841\ 10^{-1}$
4	$-0.3038\ 10^{-1}$	$0.5803\ 10^{-1}$	$-0.3740\ 10^{-2}$
5	$-0.4749\ 10^{-1}$	$0.9089\ 10^{-1}$	$-0.1366\ 10^{-1}$
6	$-0.6843\ 10^{-1}$	0.1183	$-0.2557\ 10^{-1}$
7	$-0.9316\ 10^{-1}$	0.1438	$-0.3567\ 10^{-1}$
8	-0.1217	0.1685	$-0.4489\ 10^{-1}$
9	-0.1541	0.1926	$-0.5356\ 10^{-1}$
10	-0.1902	0.2165	$-0.6190\ 10^{-1}$
11	-0.2302	0.2400	$-0.7001\ 10^{-1}$
12	-0.2737	0.2633	$-0.7790\ 10^{-1}$
13	-0.3213	0.2866	$-0.8572\ 10^{-1}$
14	-0.3726	0.3097	$-0.9343\ 10^{-1}$
15	-094278	0.3329	-0.1011

Table 10 - Zeros of Depth/DB

Speed	Gain	Root	Root
1	$-0.1106\ 10^{-2}$		$-0.1030\ 10^{-1} \pm j\ 0.4792\ 10^{-1}$
2	$-0.4422\ 10^{-2}$		$-0.2059\ 10^{-1} \pm j\ 0.4404\ 10^{-1}$
3	$-0.995C\ 10^{-2}$		$-0.3089\ 10^{-1} \pm j\ 0.3665\ 10^{-1}$
4	$-0.1764\ 10^{-1}$		$-0.4112\ 10^{-1} \pm j\ 0.2269\ 10^{-1}$
5	$-0.2757\ 10^{-1}$	$-0.7499\ 10^{-1}$	$-0.2784\ 10^{-1}$
6	$-0.3972\ 10^{-1}$	-0.1049	$-0.1853\ 10^{-1}$
7	$-0.5408\ 10^{-1}$	-0.1304	$-0.1359\ 10^{-1}$
8	$-0.7065\ 10^{-1}$	-0.1544	$-0.1020\ 10^{-1}$
9	$-0.8944\ 10^{-1}$	-0.1775	$-0.7620\ 10^{-2}$
10	-0.1104	-0.2003	$-0.5510\ 10^{-2}$
11	-0.1336	-0.2227	$-0.3718\ 10^{-2}$
12	-0.1589	-0.2447	$-0.2156\ 10^{-2}$
13	-0.1865	-0.2667	$-0.7480\ 10^{-3}$
14	-0.2163	-0.2886	$0.5368\ 10^{-3}$
15	-0.2484	-0.3088	$0.1734\ 10^{-3}$

B. STEADY-STATE DECOUPLING

The derived model represents a linear, multivariable system. In order to allow the application of existing single-loop techniques, such as Nyquist-Bode-Nichol's methods and Root-Locus design, the equations must be decoupled. Decoupling requires the system to be characterized by a non-singular, diagonal transfer function matrix. When linear state variable feedback is applied, one necessary condition according to Wolovich (Ref. 12) is that a system characterized by a (n * m) transfer function matrix may not have poles at the origin. The developed linear system contains two transfer functions with such poles.

Ref. 4 develops another approach which decouples the steady-state only. This approach uses classical cascade compensation and allows the precluded poles at the origin. Actually, these poles are used for the decoupling of linear, multivariable systems.

A steady-state decoupled system is a system in which changes in each input are reflected in a corresponding output and only that output, when steady-state is reached. Thus mutual interactions are allowed during the transient period, but only during this period.

Using cascade compensation and a diagonal compensator matrix

$$G_c = \begin{bmatrix} g_{c11} & 0 \\ 0 & g_{c22} \end{bmatrix}$$

the model configuration becomes:

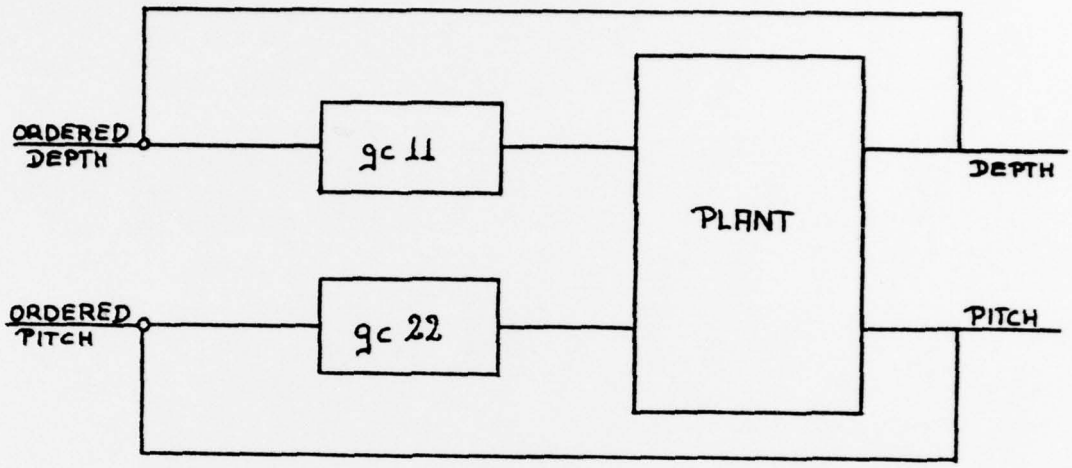

where

$$G_p = \begin{bmatrix} g_{p11} & g_{p12} \\ g_{p21} & g_{p22} \end{bmatrix}$$

By theorem 2.2 of Ref. 4 the system is steady-state decoupled if and only if

$$1. \lim_{s \to 0} 1/s^{(k-1)} * (I+G_p G_c)_{12} / \det(I+G_p G_c) = 0 \qquad (9)$$

and

$$2. \lim_{s \to 0} 1/s^{(k-1)} * (I+G_p G_c)_{21} / \det(I+G_p G_c) = 0 \qquad (10)$$

Since

$$G_p G_c = \begin{bmatrix} g_{p11}g_{c11} & g_{p12}g_{c22} \\ g_{p21}g_{c11} & g_{p22}g_{c22} \end{bmatrix}$$

we have

$$\det (I+G_p G_c) = 1+g_{p11}g_{c11}+g_{p22}g_{c22}+ g_{p11}g_{p22}g_{c11}g_{c22}- g_{p12}g_{p21}g_{c11}g_{c22} \quad (11)$$

and cofactors

$$(I+G_p G_c)_{12} = g_{p21}g_{c11} \quad (12)$$

$$(I+G_p G_c)_{21} = g_{p12}g_{c22} \quad (13)$$

K_1 and k_2 are defined according to

$$(\text{input}_j(t)) = 1/ s^{kj}$$

where the inputs are constants, steps, ramps etc., with arbitrary amplitude.

By substituting (11), (12), and (13) into (9) and (10), and assuming a step input for depth and constant pitch, we have the two necessary and sufficient conditions for steady-state decoupling :

1. $\lim_{s\to 0} g_{p21}g_{c11} / D = 0$ (14)

2. $\lim_{s\to 0} s*g_{12}g_{22} / D = 0$ (15)

where

$$D = \det (I + G_p G_c)$$

All g_p are known. Thus the design for steady-state decoupling is the determination of g_{c11} and g_{c22} such that (14) and (15) are satisfied.

Although the locations of the poles and zeros are dependent on the speed their number is independent. Therefore the poles will be called

$$p_{ijm} \qquad m = 1,2,3...$$

and the zeros

$$z_{ijm} \qquad m = 1,2,3...$$

where ij denotes the element of the matrix and m the m^{th} pole and zero of the element.

$$g_{p11} = k_{11} (s+z_{111}) (s+z_{112}) / s^2$$

$$g_{p12} = k_{12} (s+z_{121}) (s+z_{122}) / s^2$$

$$g_{p21} = k_{21} (s+z_{211}) / s^2$$

$$g_{p22} = k_{22} (s+z_{221}) / s^2$$

where

$$\gamma = (s+p_{111})\ (s+p_{112})\ (s+p_{113})$$

When these transfer functions are substituted into equations (14) and (15), both limits go to zero for all speeds.
Thus conditions (1) and (2) are satisfied for the specified inputs.

1. Design of closed-loop system

The previous section resulted in the decoupling of the steady-state of the system. However, one must realize, that:

1. the result does not guarantee stability.
2. steady-state decoupling is only meaningful, when the closed-loop system is stable.

Thus it is necessary to consider the stability of the closed-loop system after the steady-state decoupling has been achieved.

Ref.4 investigates a connection between single-loop and multivariable systems by properly factorizing the closed-loop characteristic equation. It allows the design of multivariable systems by using any suitable single-loop method. The primary method chosen will be the root-locus design.

2. Stability criterion

Ref.13 and 14 prove that the stability of this multivariable system is determined by the zeros of $N_1(s)$ and $N_2(s)$, where

$$N_1(s)/D_1(s) = \det(I + G_p(s)*G_c(s)) \tag{16}$$

and

$$N_2(s) = \Delta c(s)*\Delta p(s)/D_1(s) \tag{17}$$

$N_1(s)/D_1(s)$ is in irreducible form, i.e. all common factors are cancelled. $\Delta c(s)$ represents the characteristic polynomial of the transfer function matrix $G_c(s)$ and $\Delta p(s)$ represents the polynomial of the transfer function matrix $G_p(s)$. The characteristic polynomial of the transfer function is defined as the least common denominator of all minors.

However Ref.4 devises a method by which it is necessary to check equation (16) alone for stability, if:

1. cancellations are selected systematically by using equation (4.5) Ref. 4.

2. poles of G_c are carefully selected, which can be taken care of in the process of the design.

Thus

$$\det(I + G_p G_c) = 0 \qquad (18)$$

represents the characteristic equation of the multivariable system.

For the system under consideration equation (18) becomes:

$$\det(I + G_p G_c) = 1+g_{p11}g_{c11} + g_{p22}g_{c22} + \det(G_p)\, g_{c11}g_{c22}$$

which can be factored

$$\det(I + G_p G_c) = (1 + g_{p11}g_{c11})(1 + G_{eq}g_{c22})$$

where

$$G_{eq} = g_{p22}(1 + \det G_p * g_{c11}/g_{p22})/(1+g_{p11}g_{c11}) \qquad (19)$$

By cancellation of the common roots the equation determining the stability of the system becomes

$$1 + G_{eq}g_{c22} = 0 \ . \qquad (20)$$

Equation (20) still contains both g_{c11} and g_{c22} as unknown functions. It is possible for example to choose g_{c11} arbitrarily. In this case the only unknown left to be designed is g_{c22}, which means the design is reduced to a single-loop case. But if g_{c11} has not been chosen properly, G_{eq} may become very unstable. This can make the design of

g_{c22} very difficult. Thus it is preferable to have guidelines in choosing g_{c11} in order to get a reasonable pole-zero pattern for G_{eq}, which will make the design of g_{c22} much easier.

3. Design Guidelines

The roots of equation (19) are determined by the following expressions:

1. $G_2 = g_{p22} + \det(G_p) g_{c11}$

2. $G_1 = 1 + g_{p11} g_{c11}$

where

$$G_{eq} = G_1/G_2 \tag{21}$$

Then

$$\det(I + G_p G_c) = G_1 + G_2 g_{c22} \quad .$$

As the design is concerned with the poles and zeros of G_{eq} they must be identified. They can be found by considering the functions G_1 and G_2. From equation (21) it can be seen, that the zeros of G_{eq} are determined by:

$$Z_{Geq} = Z_{G1} + P_{G2} - (P_{G2} \cap P_{G1}) \tag{22}$$

$$P_{Geq} = Z_{G2} + P_{G1} - (P_{G2} \cap P_{G1}) \tag{23}$$

Poles and zeros of G_1 and G_2 are dependent on the function g_{c11} acccrding to:

$$1 + \det(G_p) * g_{c11} / g_{p22} = 0 \tag{24}$$

$$1 + g_{p11} g_{c11} = 0 \quad . \tag{25}$$

Therefore the design will proceed as follows:

1. Design g_{c11} to achieve a reasonable pole-zero pattern for G_{eq}.

   a.) Prepare root-locus studies for equation (24) and (25), where $g_{c11} = f(K_1, s)$. K_1 is a real parameter positive or negative. The poles and zeros of g_{c11} are determined by

      aa.) number of free integrators needed to decouple the system.

      ab.) the needs of compensation, which may arise, due to desired root locations.

   b.) From root-locus studies choose the parameter K_1, which fixes g_{c11}. This will be an iterative process as both root-locus studies in combination with equations (22) and (23) determine the final pole-zero pattern of G_{eq}.

2. Design of g_{c22} in order to meet the system specification. As G_{eq} is known equation (20), i.e.

$$1 + G_{eq} g_{c22} = 0$$

can be studied via root-locus, where $g_{c22} = f(K_2, s)$. The criteria which determine $f(K_2, s)$ are the same as mentioned above for $f(K_1, s)$.

3. With the proper choice of K_2

a.) system stability is guaranteed.
b.) the dynamics of the system are fixed.
c.) the diagonal compensator is determined.

4. The design is completed. Now simulation is required to check whether the design specifications have been met. If the specifications have not been met, a redesign of compensator g_{c22} or even g_{c11} may be necessary. But every trial provides some insight and helps with the next trial.

4. Root-locus design

Following the design guide lines the first step is a root-locus study for the equations (24) and (25). As shown in II.B no free integrators for g_{c11} and g_{c22} are required for the specified inputs.

The speed range of interest extends from 3 kn to 15

kn. As the root locations of the system change with varying speed, it is not certain whether one compensator set will cover the whole speed range. It seems reasonable to design for the medium speed of 9 kn. Afterwards it can be tested whether this compensator set is adequate for the whole speed range and whether the variations due to speed can be taken care of by either gain variations or other means. It may turn out that different compensators are required to meet the design specifications.

a.) Design of g_{c11}

The root-loci for $1+g_{c11}g_{p11}=0$ where $g_{c11}=K_1$ are shown in Fig. 70 K_1 = negative and Fig. 71 K_{21} = positive. K_1 = positive is clearly undesirable, because there will be one branch that extends along the positive real axis to + and will produce a pole on the positive real axis for G_{eq}.

The root-loci for $1 + \det(G_p)*g_{c11}/g_{p22} = 0$ are shown in Fig. 72 K_1 = negative and Fig. 73 K_1 = positive. For the same reason as above K_1 has to be negative.

From the root-loci for K_1 = negative it is obvious that further compensation is needed in order to achieve reasonable root locations. The following compensator was chosen

$$g_{c11}=K_1(s + 0.4)^2/(s + 4.0)^2$$

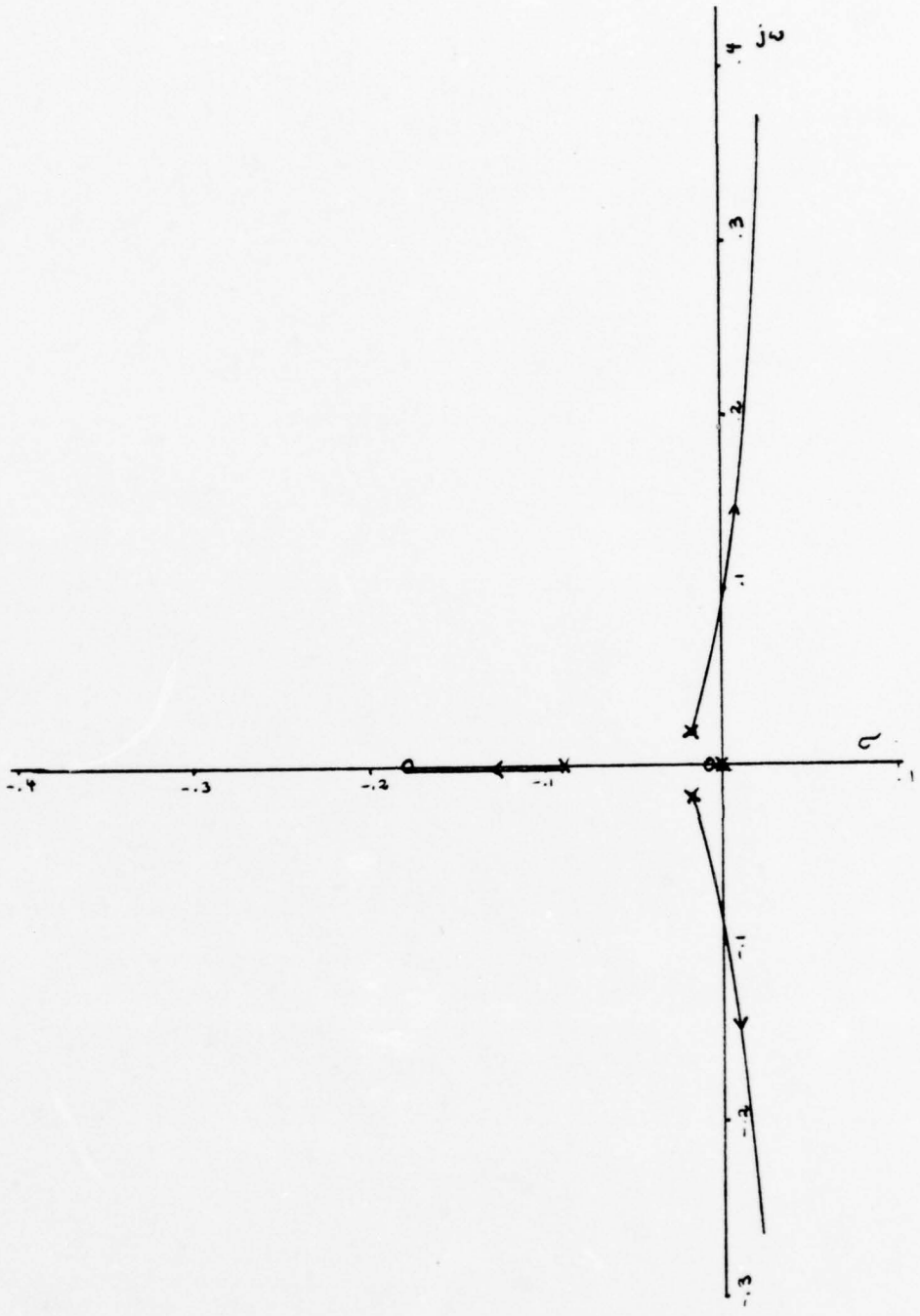

.1 UNITS PER INCH

Figure 70 - ROOT LOCUS 1+GP11*GC11 = 0
SPEED = 9 KN, K1 = NEG.

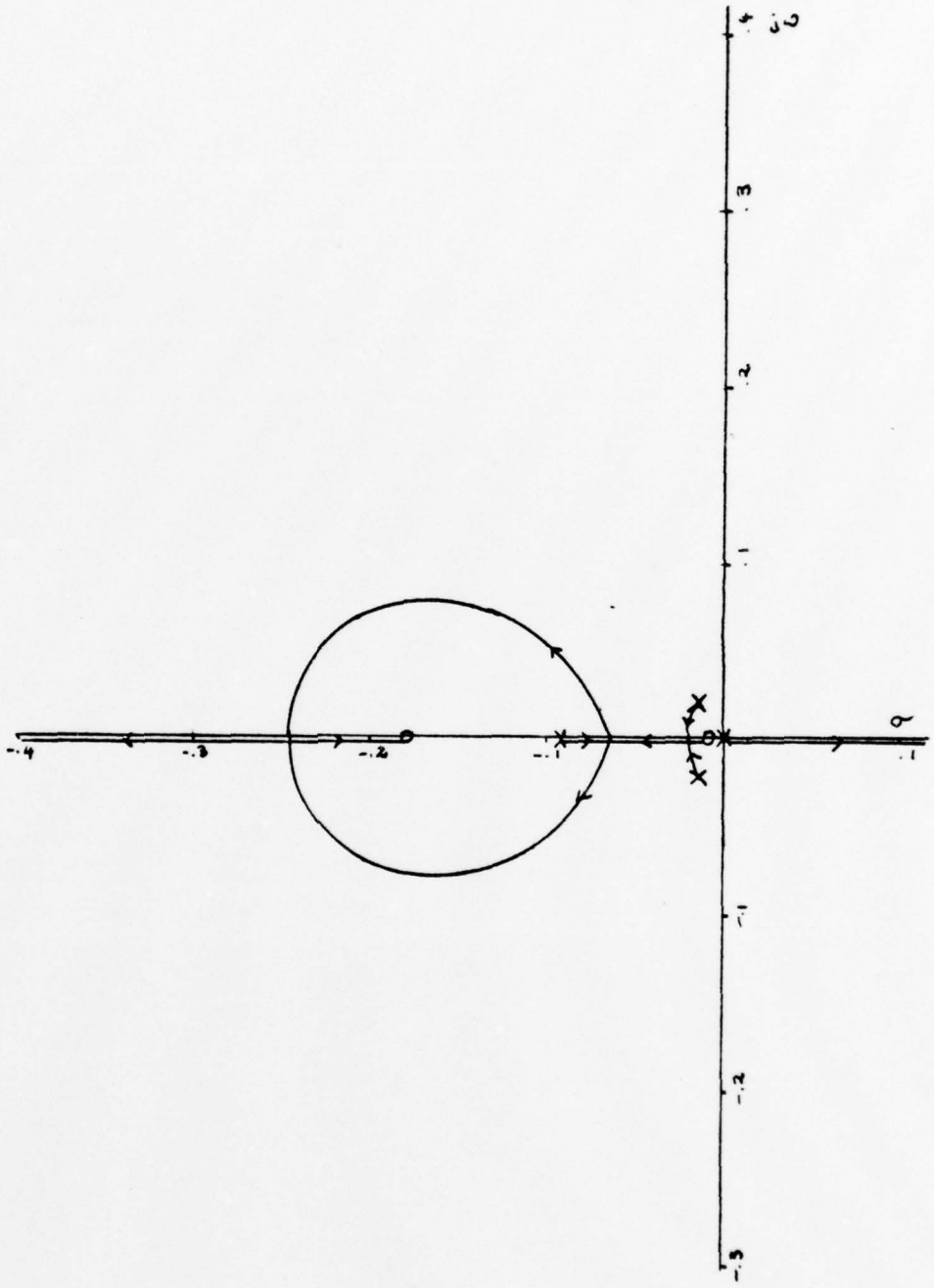

.1 UNITS PER INCH

Figure 71 - ROOT LOCUS 1+GP11*GC11 = 0
SPEED = 9 KN, K1 = POS.

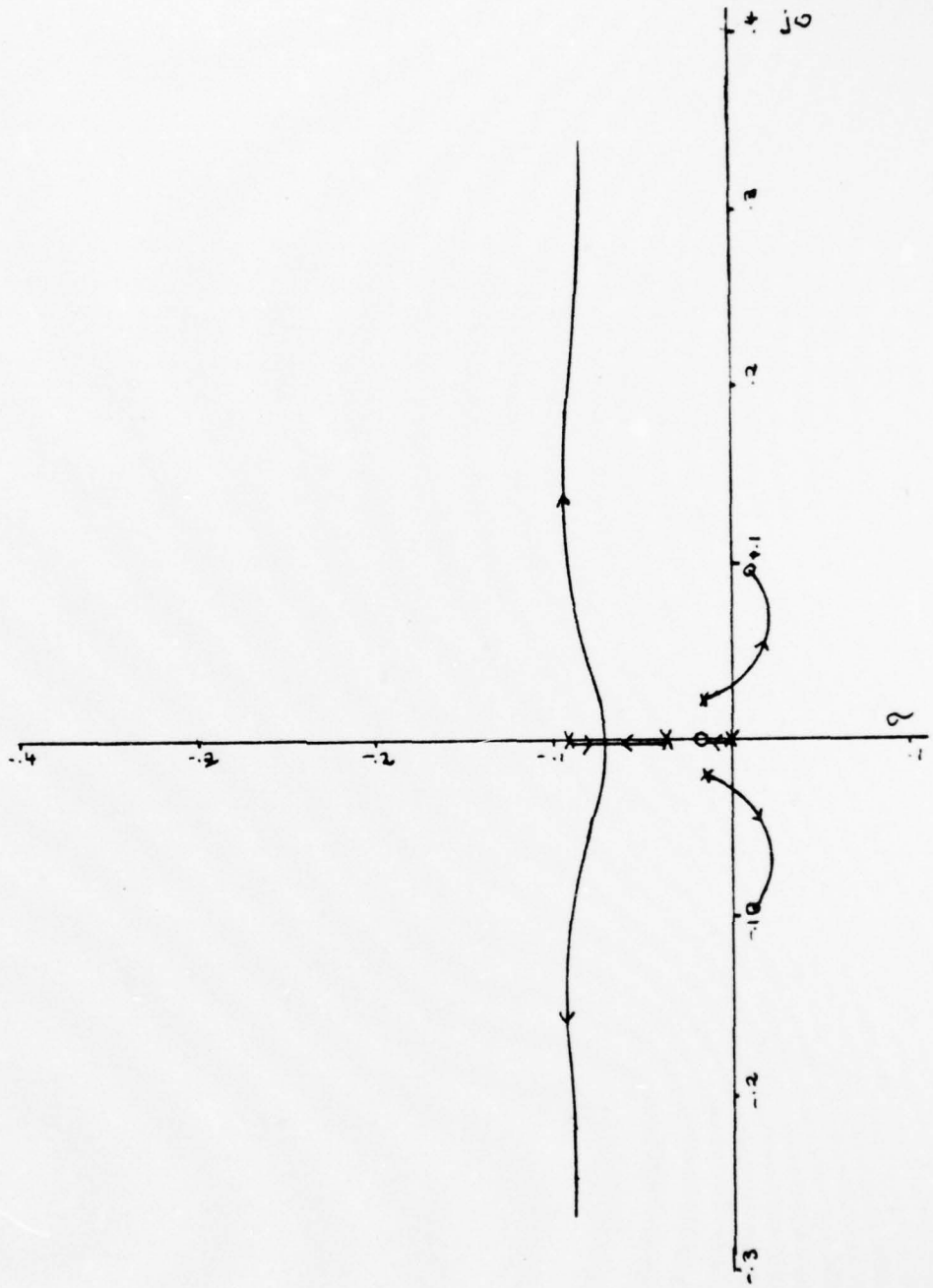

.1 UNITS PER INCH

Figure 72 - ROOT LOCUS 1+DET(GP)/GP22*GC11 = 0
SPEED = 9 KN, K1 = NEG.

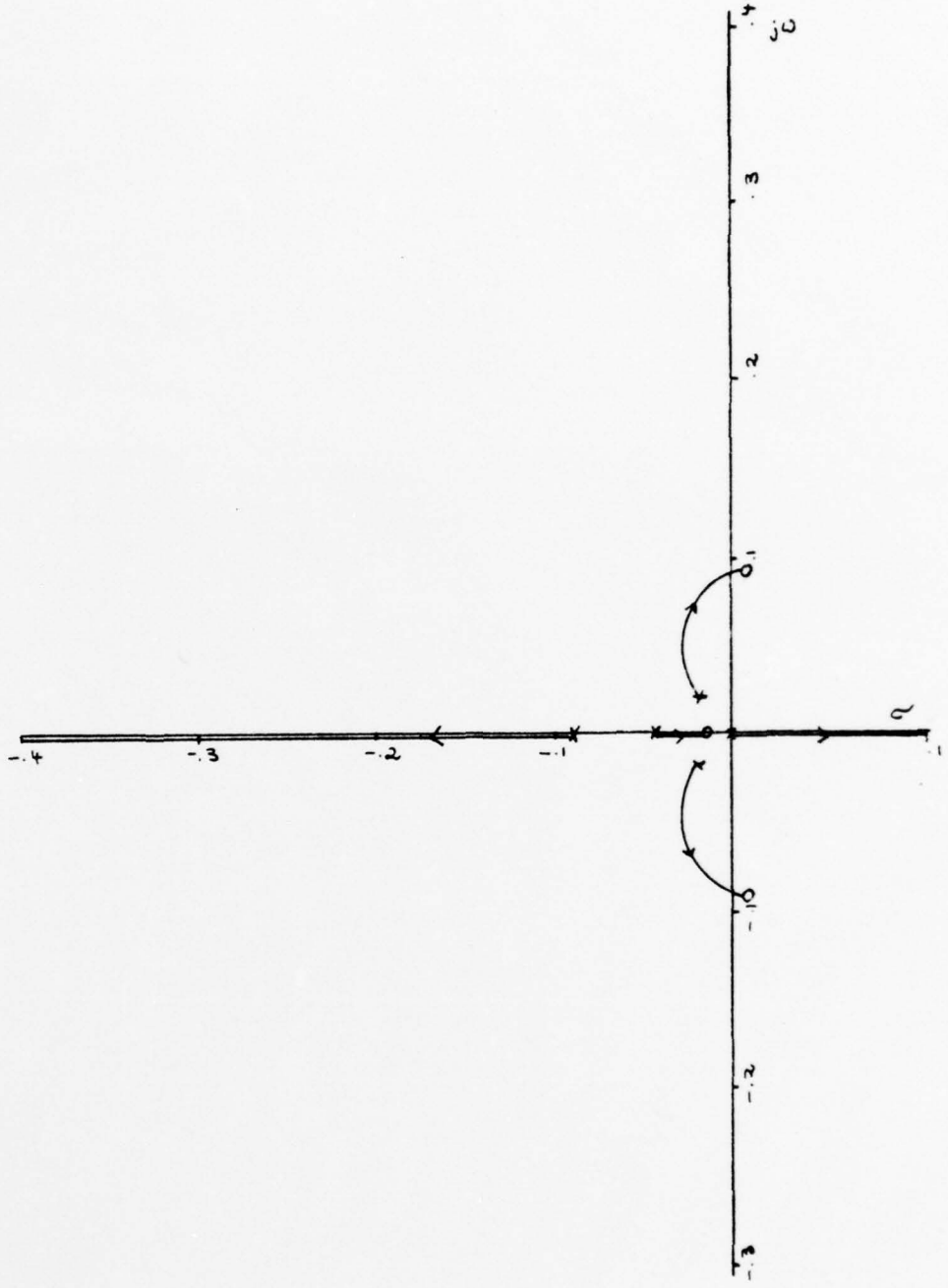

.1 UNITS PER INCH

Figure 73 - ROOT LOCUS 1+DET(GP)/GP22*GC11 = 0
SPEED = 9 KN, K1 = POS.

This compensation resulted in Fig. 74 for $1+g_{c11}g_{p11} = 0$ and Fig. 75 for $1+\det(G_p)g_{c11}g_{p11} = 0$. The roots of Fig. 74 represent part of the poles of G_{eq}. By means of the compensation all roots were constrained to the stable region. The roots of Fig. 75 will form the zeros of G_{eq}. Although this compensation did not pull the unstable branches considerably to the left half plane, it does not mean that the system will not be well behaved, because the system behavior will in the end be determined by the poles of G_{eq} and g_{c22}.

As Ref. 4 in equations (6-33) points out, the poles and zeros of G_{eq} are determined as follows:

$$\text{Poles: } P_{Geq} = Z_{G1}+P_{G2}-(P_{G2} \wedge P_{G1})$$

$$\text{Zeros: } Z_{Geq} = Z_{G2}+P_{G1}-(P_{G2} \wedge P_{G1})$$

$$P_{G1} = P_{gp11} + P_{gc11}$$

$$Z_{G1} = \{\text{roots from root-locus } 1+g_{p11}g_{c11}=0\}$$

$$P_{G2} = P_{gp22}+P(\det G_p)g_{c11}-(P_{gp22} \wedge P(\det G_p)g_{c11})$$

P_{G2} P_{G1} = P_{G1} for this system.

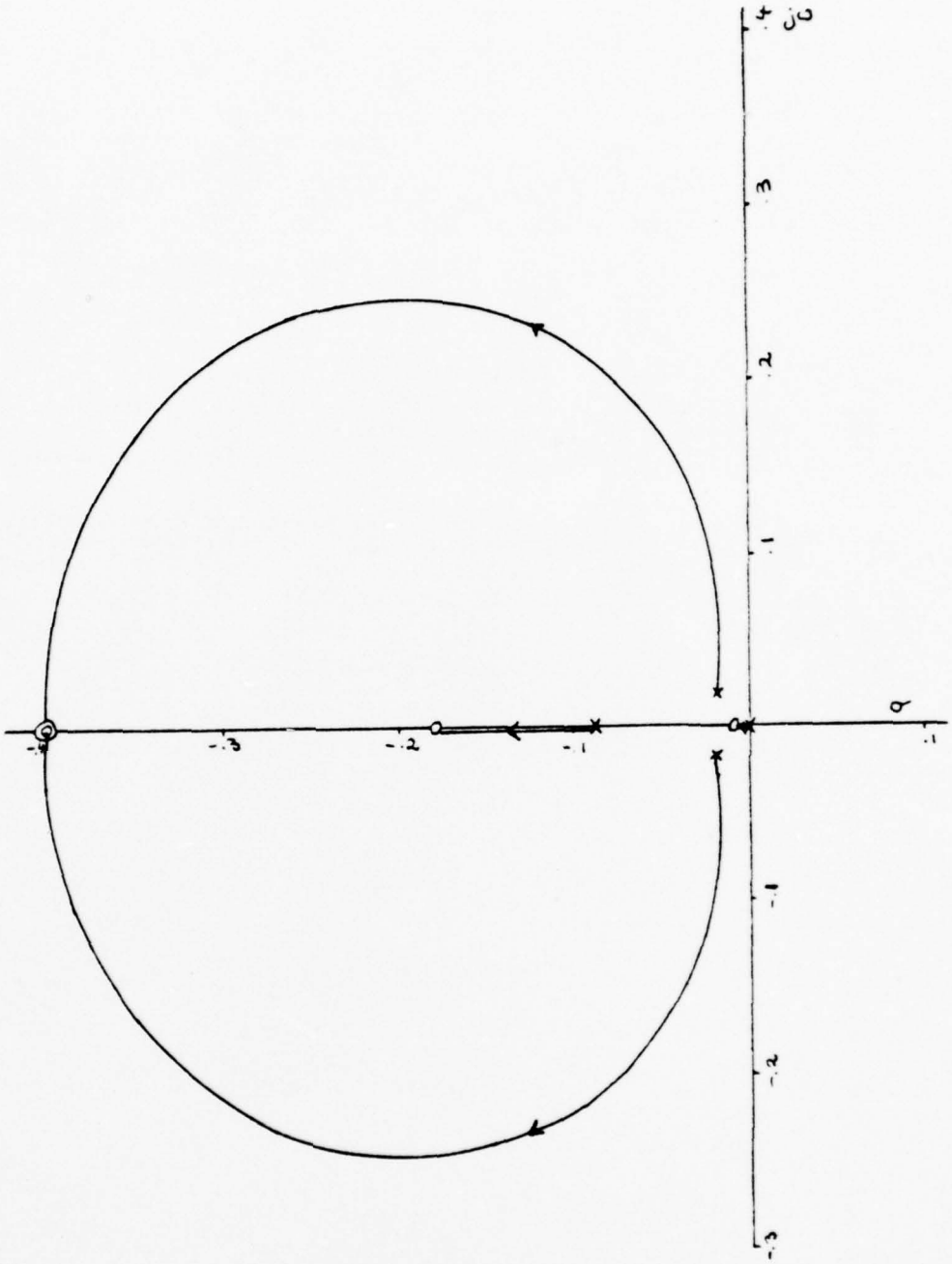

.1 UNITS PER INCH

Figure 74 - ROOT LOCUS 1+GP11*GC11 = 0
SPEED = 9 KN, K1 = NEG., COMPENSATED

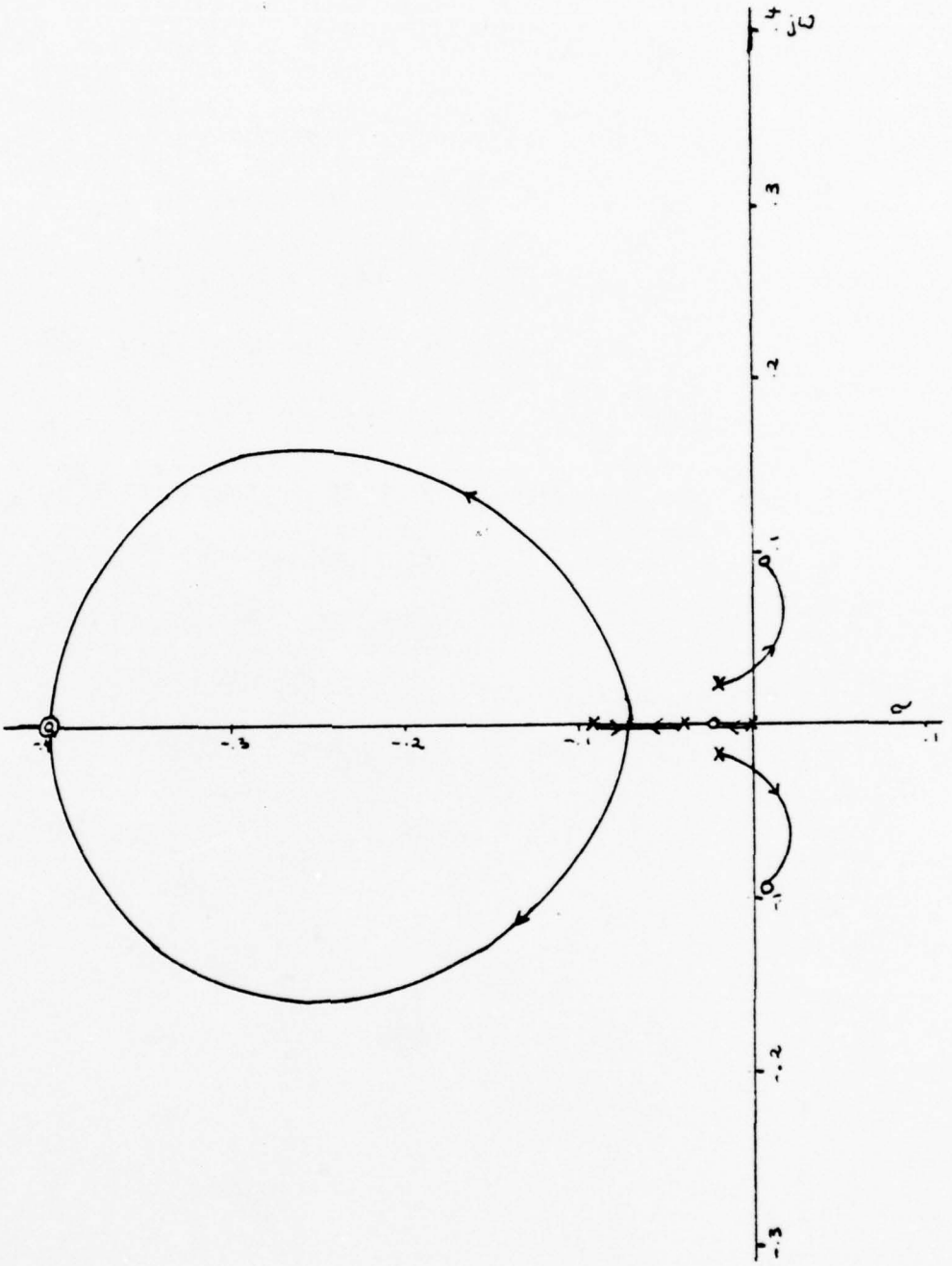

.1 UNITS PER INCH

Figure 75 - ROOT LOCUS 1+DET(GP)/GP22*GC11 = 0
SPEED = 9 KN, K1 = NEG., COMPENSATED

Thus the poles of G_{eq} are:

$$P_{Geq} = P_{gp11} - \{0.0\} + \{\text{roots from root-locus } 1 + g_{p11} g_{c11} = 0\}$$

and the zeros of G_{eq} are:

$$Z_{Geq} = \{\text{roots from root-locus } 1 + \det G_p \, g_{c11} / g_{p22} = 0\}.$$

G_{eq} has four known poles, namely the poles of the system transfer function g_{p11}. The remaining poles and zeros have to be determined from the compensated root-locus studies Fig. 74 and Fig. 75 .

To get an idea how the pole-zero pattern of G_{eq} will behave with varying K_1 both root-loci are superimposed in Fig. 76 The additional poles of $g_{p11} - \{0.0\}$ are added. They are independent of K_1 and therefore fixed.

b.) Design of g_{c22}

As the gain K_1 is important for the magnitude of the plane deflection of the fairwater planes the problem is not only to find adequate root locations, but also to pick the right gain. Two different gains for K_1 were chosen which determine two different sets of pole and zero locations for G_{eq}, thus the choice of K_1 fixes the dynamics of the

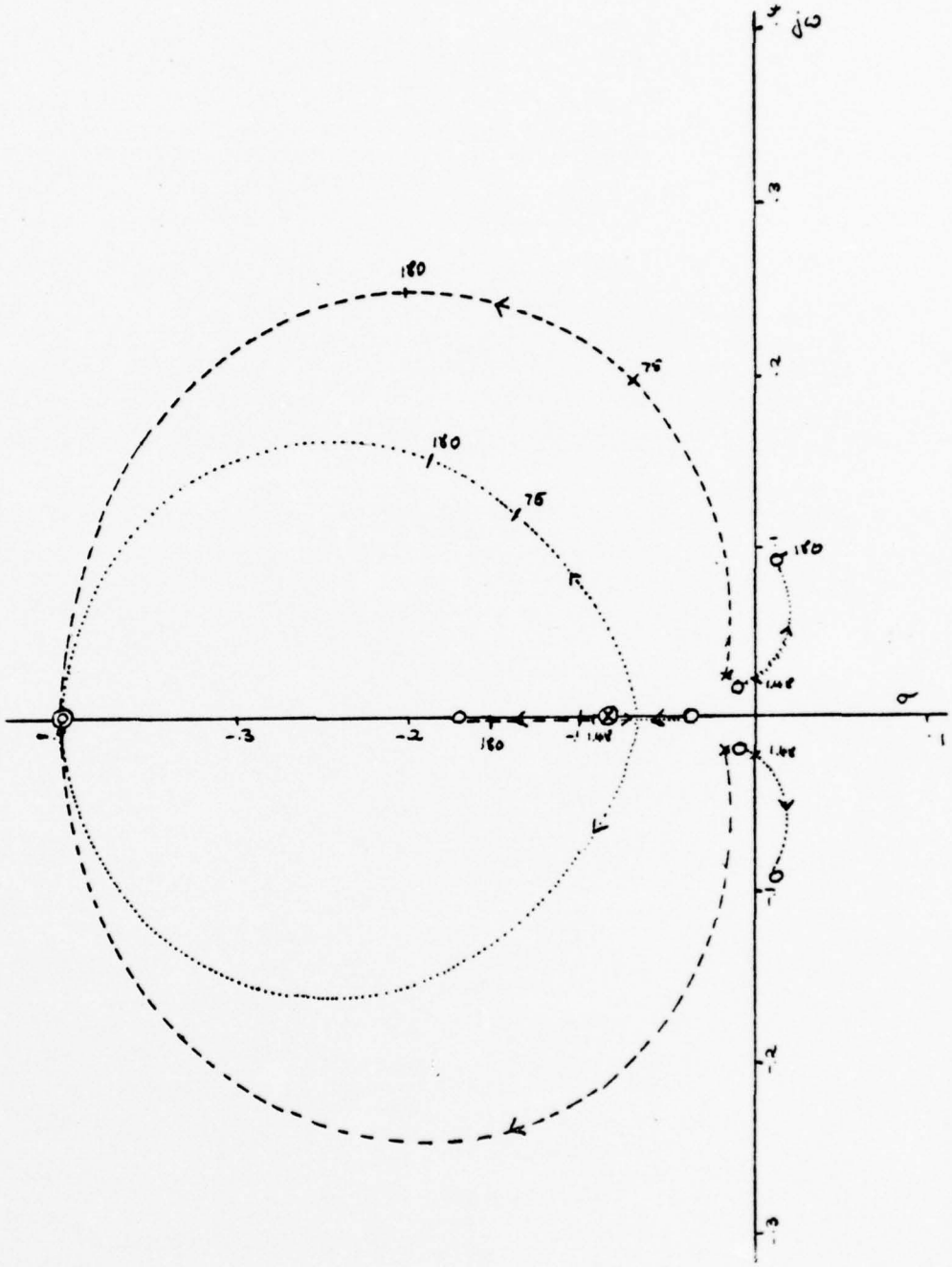

.1 UNITS PER INCH

Figure 76 - SUPERPOSITION OF FIG. 74 AND FIG. 75

open-loop system G_{eq}. The closed-loop poles are now determined by the root-locus study for $1+G_{eq}g_{c22} = 0$. Where $g_{c22} = K_2$. The gain-compensated studies for $K_1 = 1.48$ and $K_1 = 75.0$ are shown in Fig. 77 and Fig. 78 . Fig. 77 has complex roots close to the imaginary axis which go to ∞ asymptotically, which is not desirable as the damping gets too small. Fig. 78 shows very similar behavior. Therefore it is desired to move the asymptotes to the left, which is achieved by

$$g_{c22} = K_2(s+0.5)/(s+10.0).$$

The results of this compensation are shown in Fig. 79 and Fig. 80. for $K_1 = 1.48$ and $K_1 = 75.0$ respectively. As the compensated root-locus for $K_1 = 1.48$ indicates, G_{eq} will be stable for all values of $K_2 * K_{eq}$. The root-locus for $K_1 = 75.0$ has zeros in the right half plane and will limit the value of $K_2 * K_{eq}$ in order to maintain stability.

As many poles are clustered around the origin, it is difficult to tell which roots will be dominant. A time response could reveal the dominant roots, but as the system has to be simulated in order to check the compensation anyhow, because both outputs have to satisfy the design specifications, it seems more reasonable to simulate the total system. From the simulation results it will be judged whether the compensation was sufficient or if further compensation is necessary.

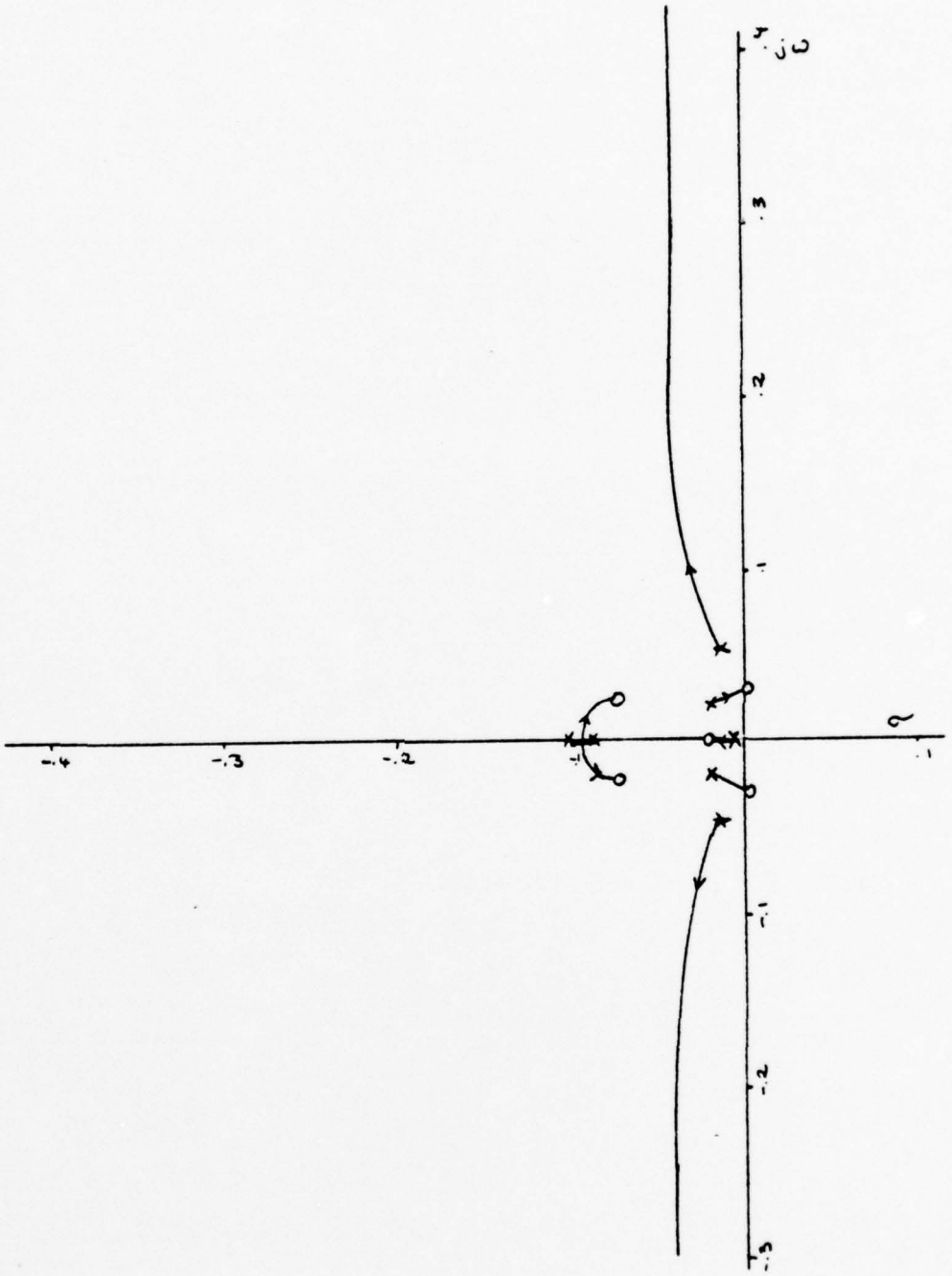

.1 UNITS PER INCH

Figure 77 - ROOT LOCUS 1+G(EQ)*GC22 = 0
SPEED = 9 KN, K1 = 1.48

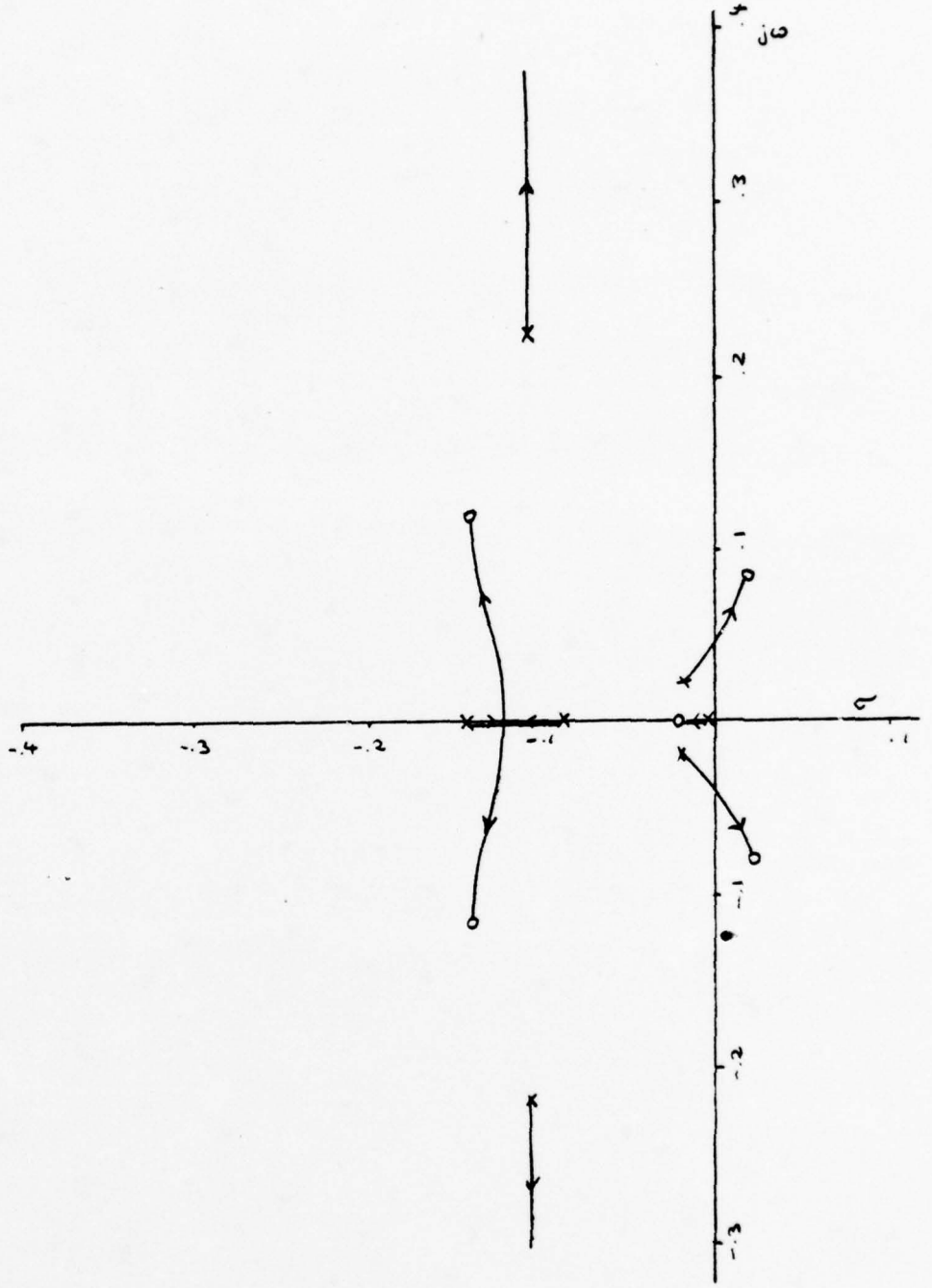

.1 UNITS PER INCH

Figure 78 - ROOT LOCUS 1+G(EQ)*GC22 = 0
SPEED = 9 KN, K1 = 75.

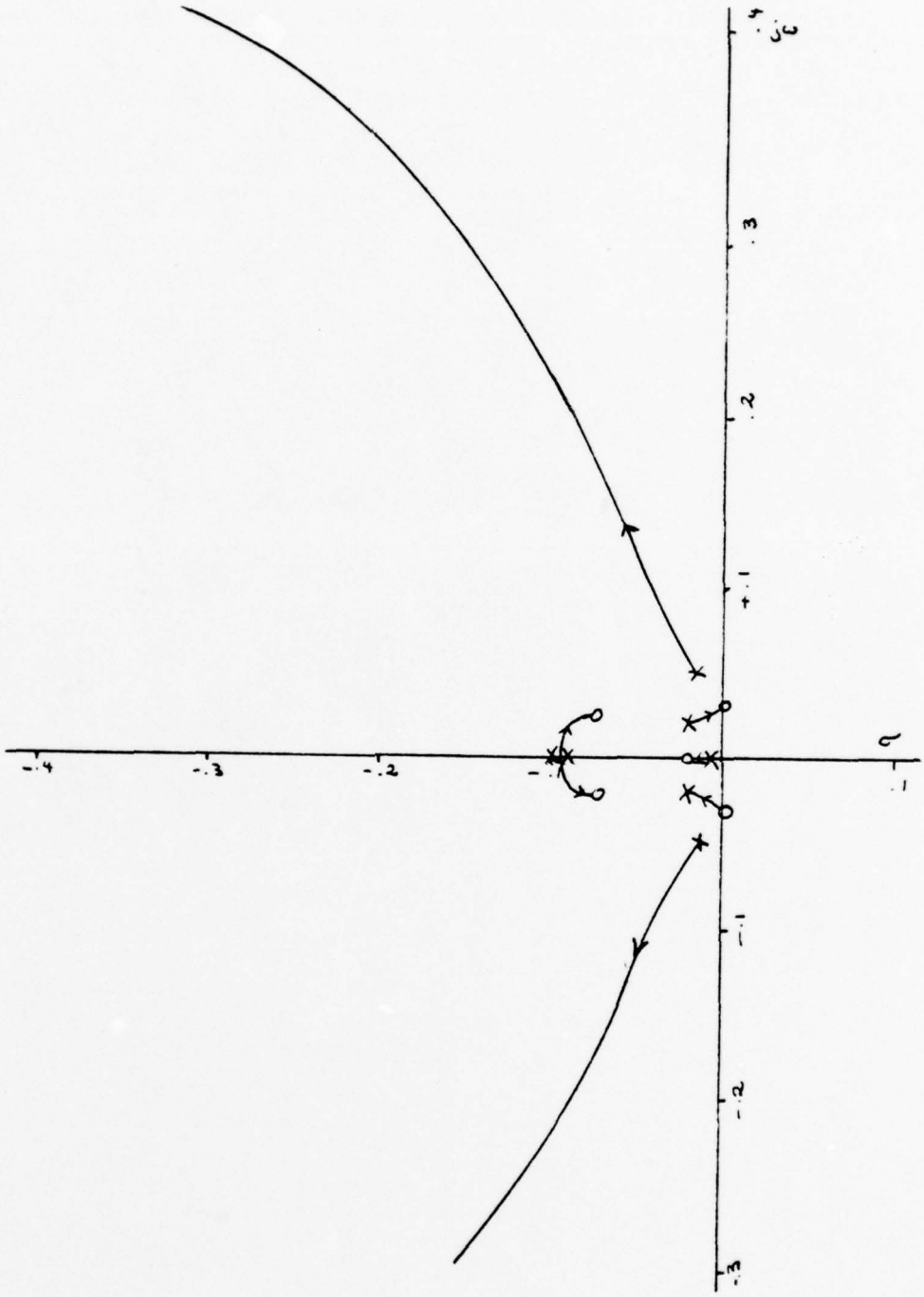

.1 UNITS PER INCH

Figure 79 - ROOT LOCUS 1+G(EQ)*GC22 = 0
SPEED = 9 KN, K1 = 1.48, COMPENSATED

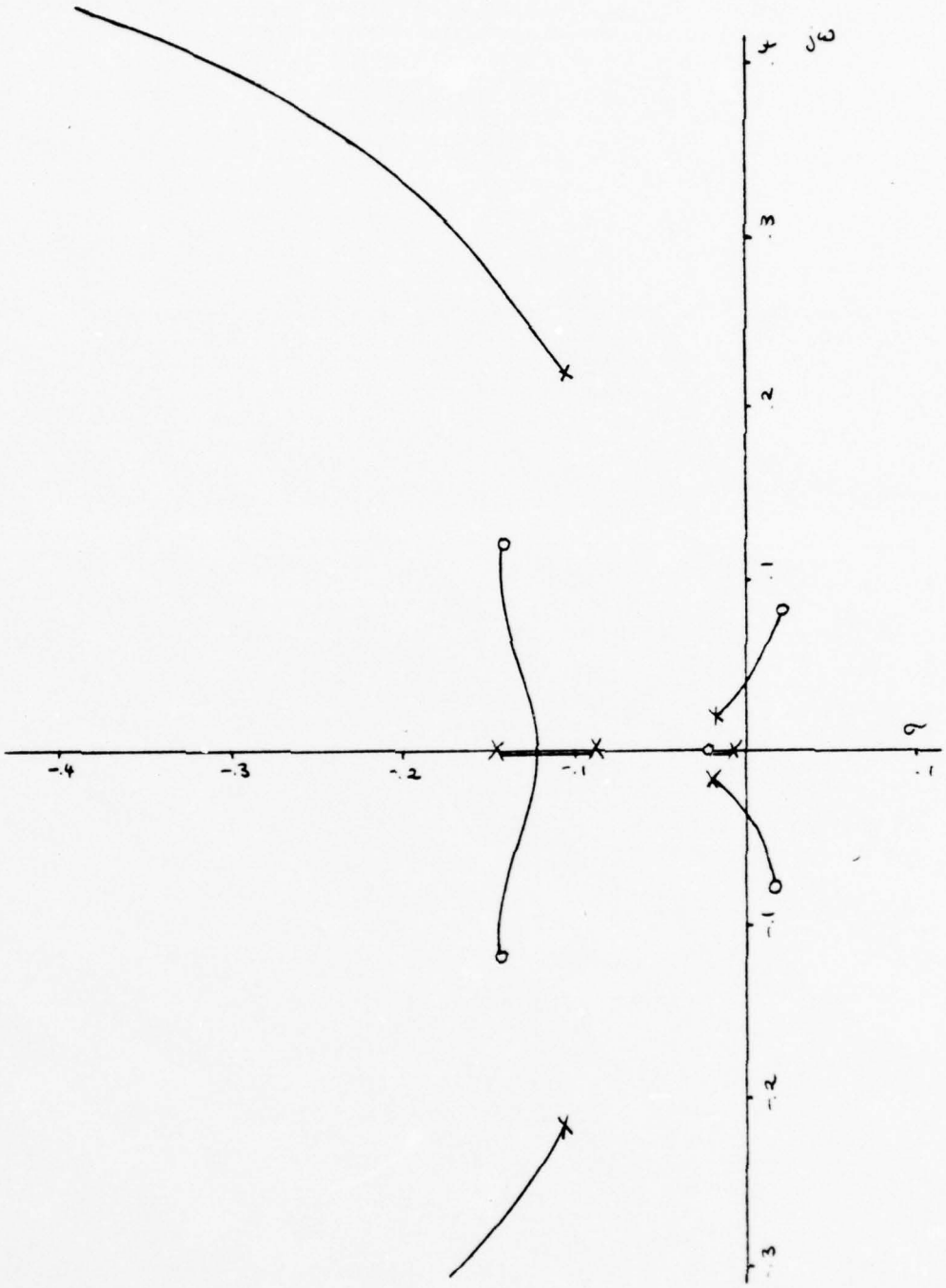

.1 UNITS PER INCH

Figure 80 - ROOT LOCUS 1+G(EQ)*GC22 = 0
SPEED = 9 KN, K1 = 75., COMPENSATED

5. Simulation of compensated linear model

a. Determination of gain constants

As mentioned above the roots of G_{eq} will always be stable if a value of $K_1 = 1.48$ is chosen. Thus this value was picked for the initial simulation trials. The root-locus for G_{eq} for this choice of K_1 is shown in Fig. 79 . The next step is to find the gain constant K_2. The gains shown in Fig. 79 represent $K_2 * K_{eq}$. In order to determine K_2, K_{eq} has to be found.

Because

$$G_{eq} = g_{p22} + \det(G_p) * g_{c22} / 1 + g_{p11} g_{c11}$$

$$= (-.3385\ 10^{-2})(s^7 + \ldots)/(s^9 + \ldots)$$

$$K_{eq} = -.3385\ 10^{-2}$$

Therefore

$$K_2 = (\text{gain from root-locus})/K_{eq}$$

The only roots which change significantly with increasing gain are those which go to ∞ . A reasonable value for K_2

seems to be $K_2 = 60$, because :

- K_2 is not too large (to avoid excessive rudder deflections)
- damping is greatest in this region.

Six simulation runs were performed using the chosen values as pointed out above and variatons of them. The ordered depth change is 10 ft., the ordered pitch is 0 °.
The results are shown in Table 11.

Table 11 - Parameter study for gains

Run	Gains	Depth reached after sec	Overshoot in ft	Max Pitch in °	Max DB in °	Max DS in °	Figure
1	$K_1 = 1.0$ $K_2 = 15.$	66.0	0.09	0.361	5.27	0.27	81
2	$K_1 = 1.5$ $K_2 = 15.$	42.5	1.41	0.534	7.62	0.4	82
3	$K_1 = 1.5$ $K_2 = 40.$	48.5	0.50	0.373	7.62	0.76	83
4	$K_1 = 2.0$ $K_2 = 40.$	36.5	1.33	0.508	9.79	0.957	
5	$K_1 = 2.0$ $K_2 = 60.$	39.0	0.94	0.403	9.79	1.24	
6	$K_1 = 1.5$ $K_2 = 60.$	54.0	0.36	0.286	7.62	0.975	84-86

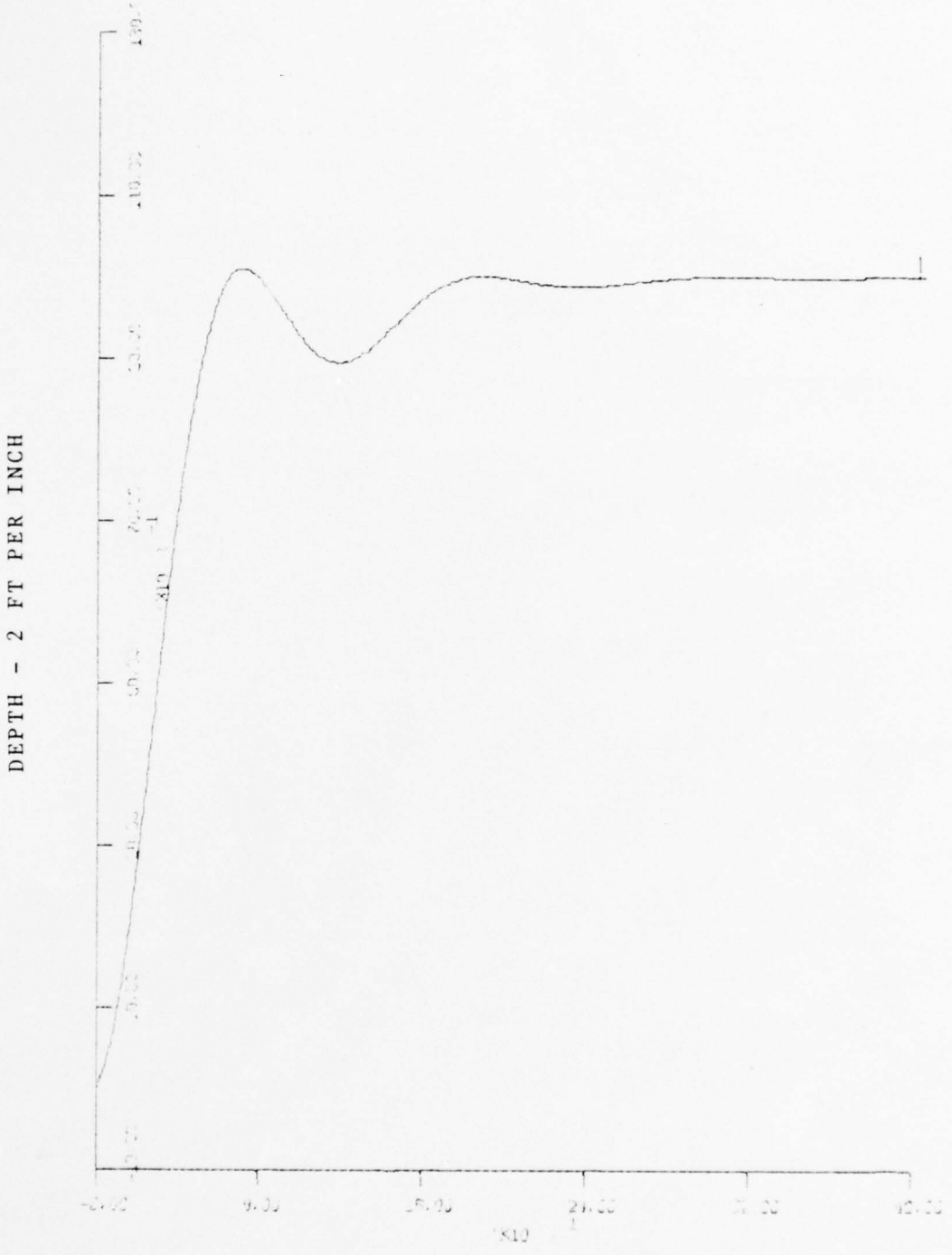

Figure 81 - RUN 1
10 FT DEPTH CHANGE, 9 KN

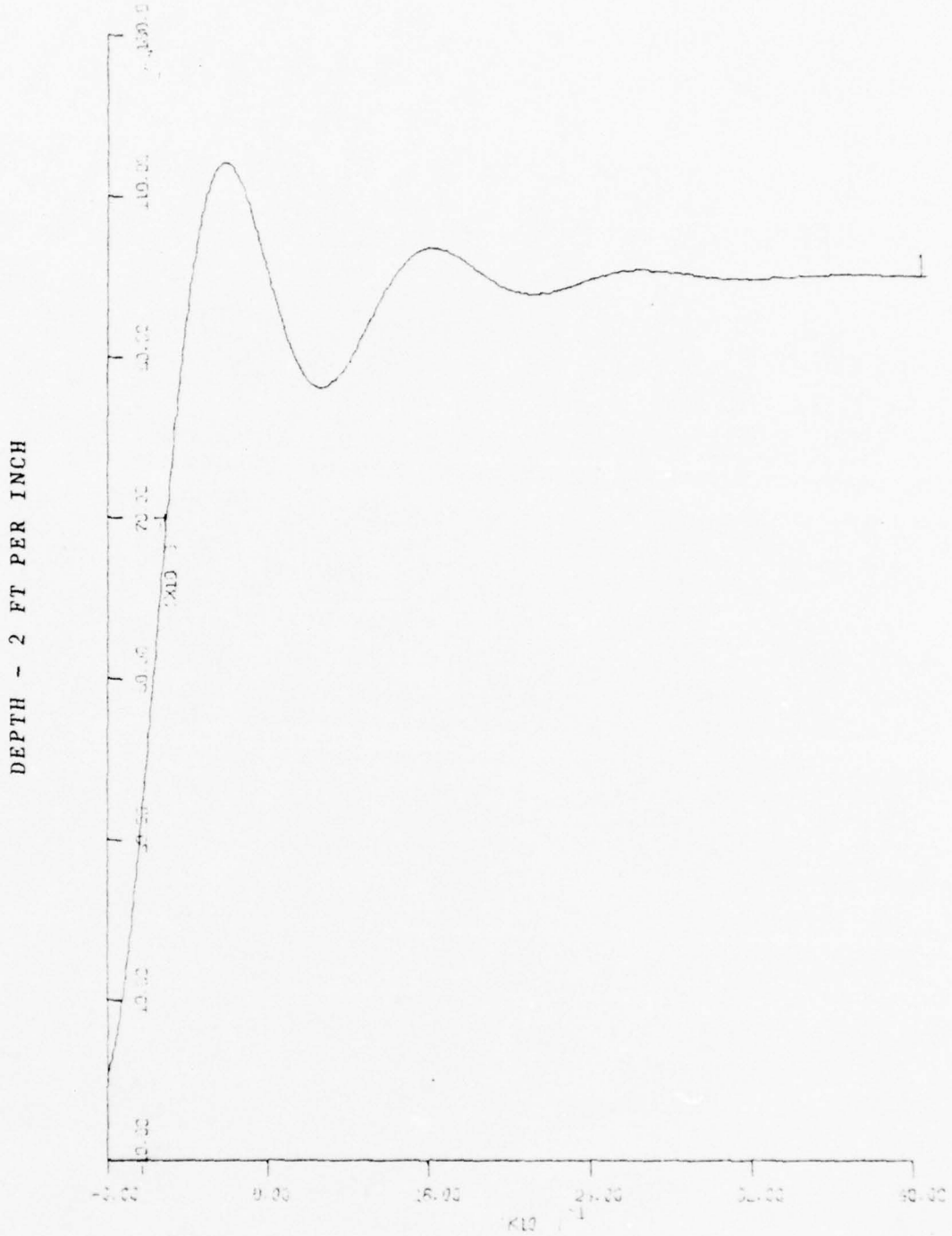

Figure 82 - RUN 2
10 FT DEPTH CHANGE, 9 KN

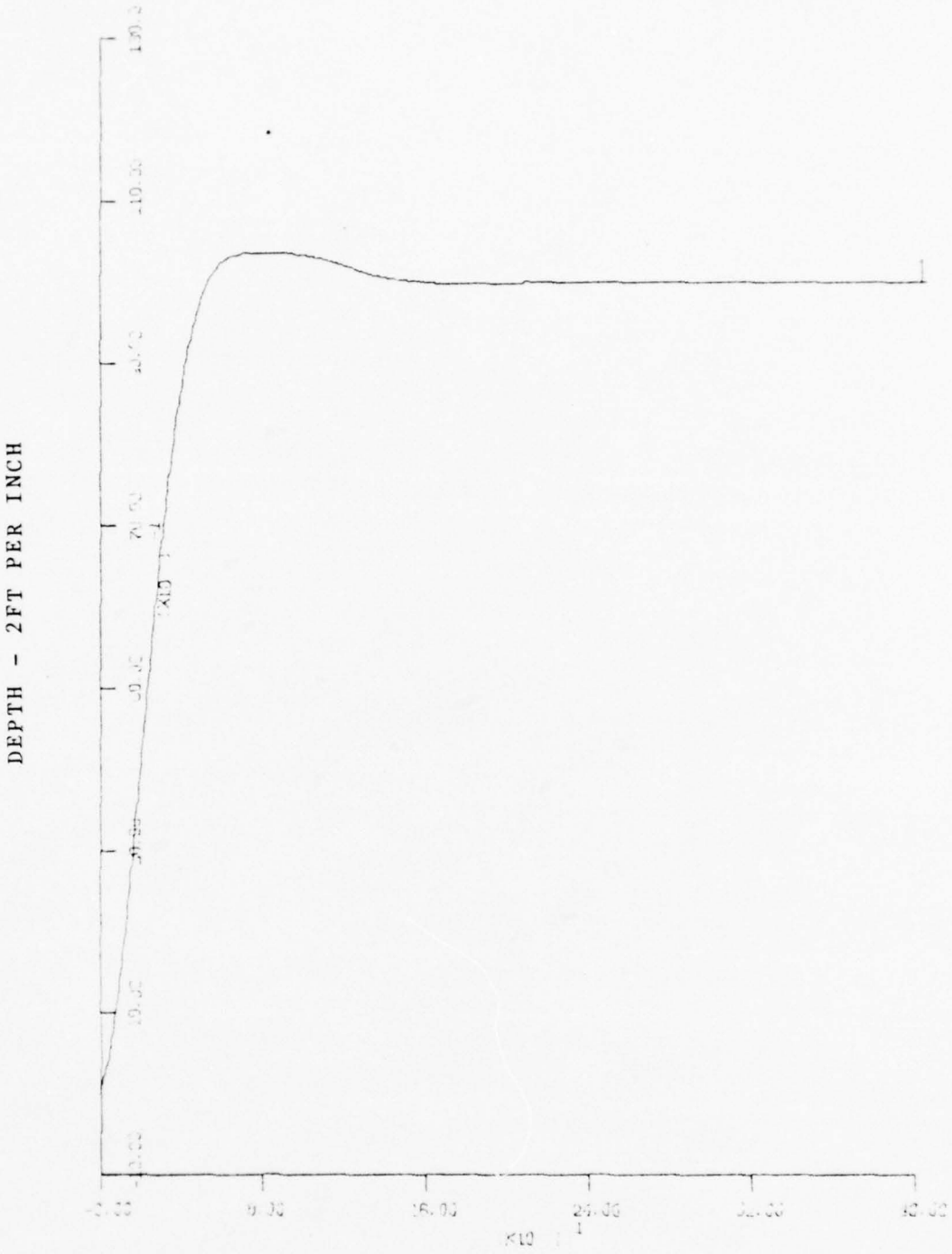

Figure 83 - RUN 3
10 FT DEPTH CHANGE, 9 KN

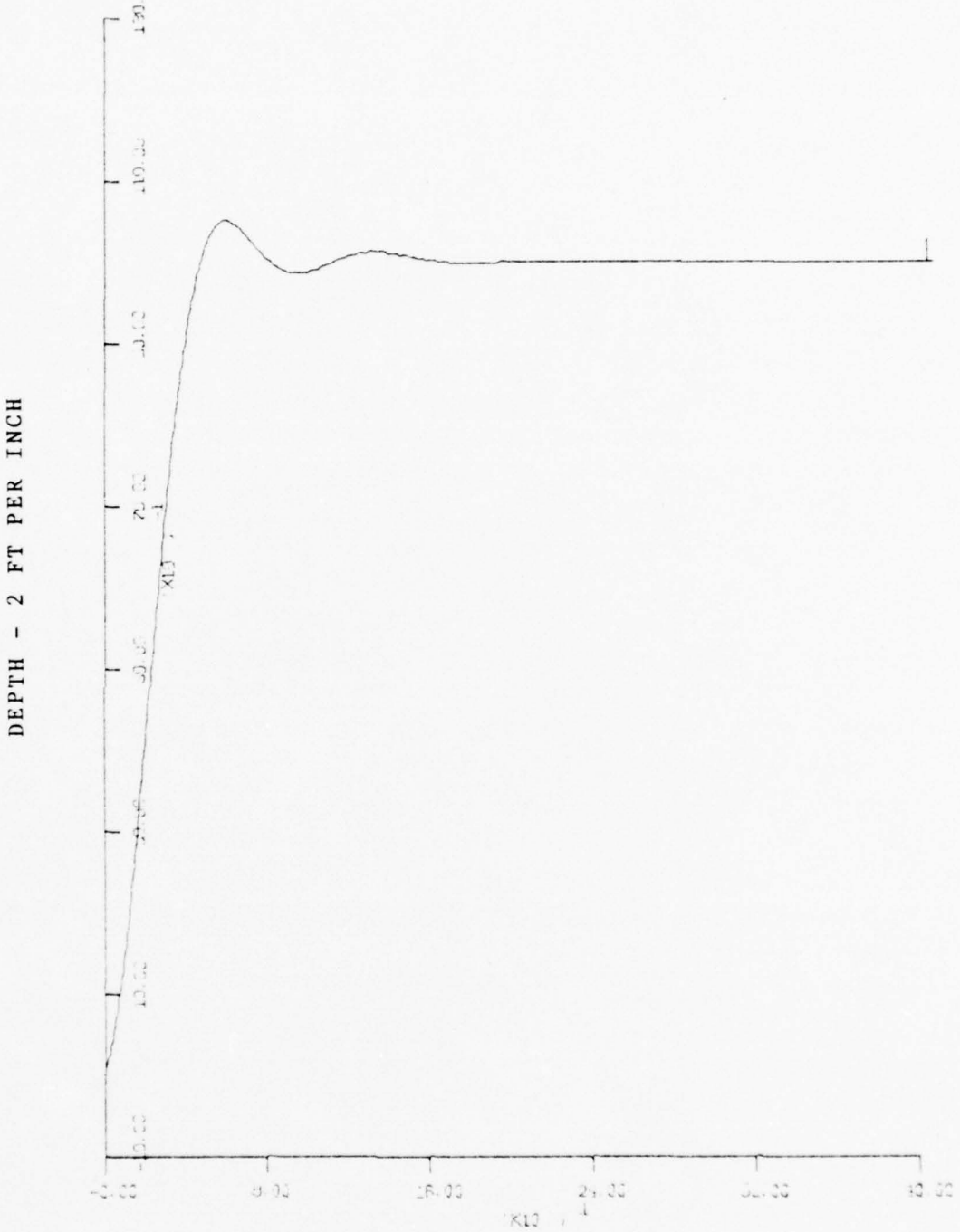

Figure 84 - RUN 6
10 FT DEPTH CHANGE, 9 KN

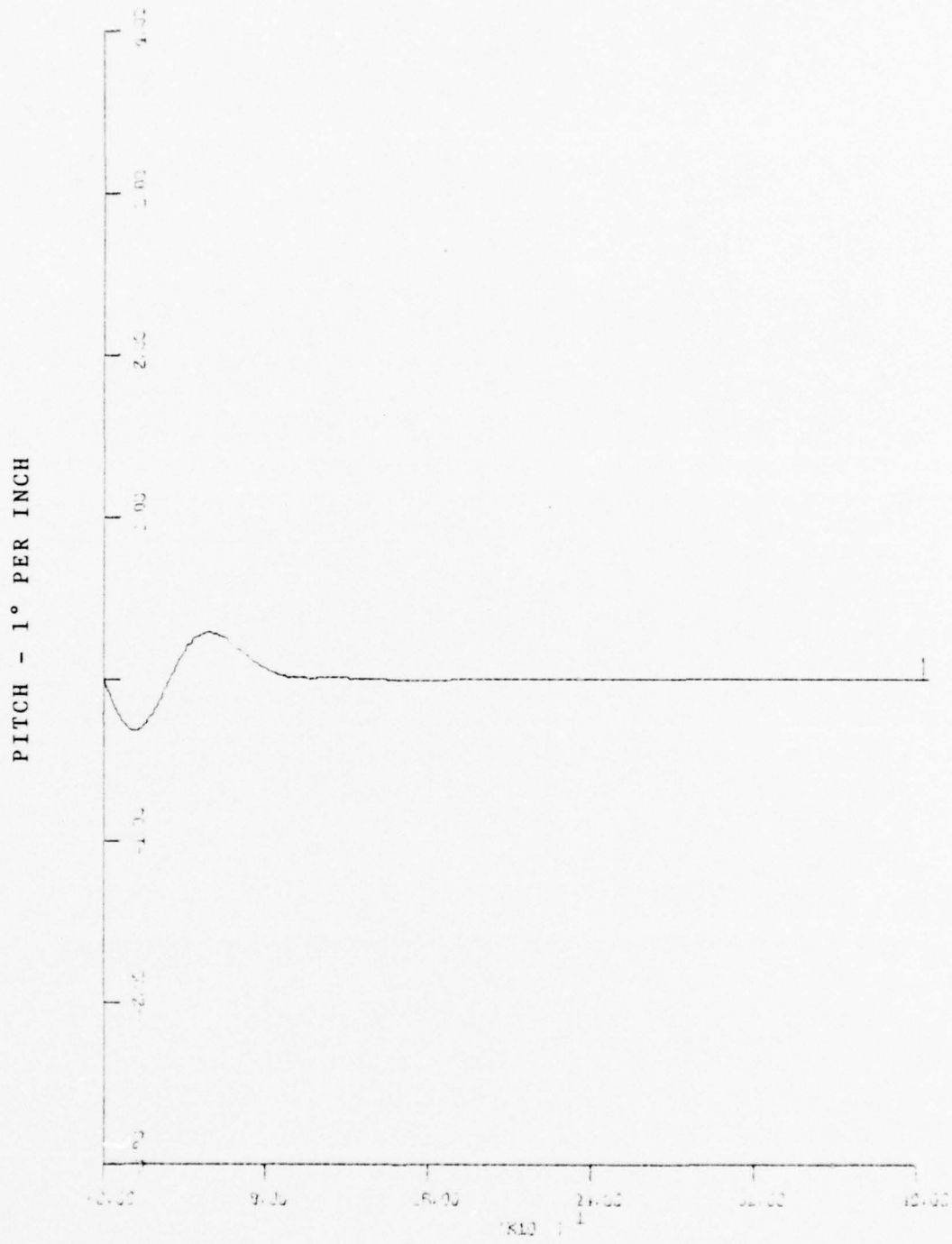

Figure 85 - RUN 6
10 FT DEPTH CHANGE, 9 KN

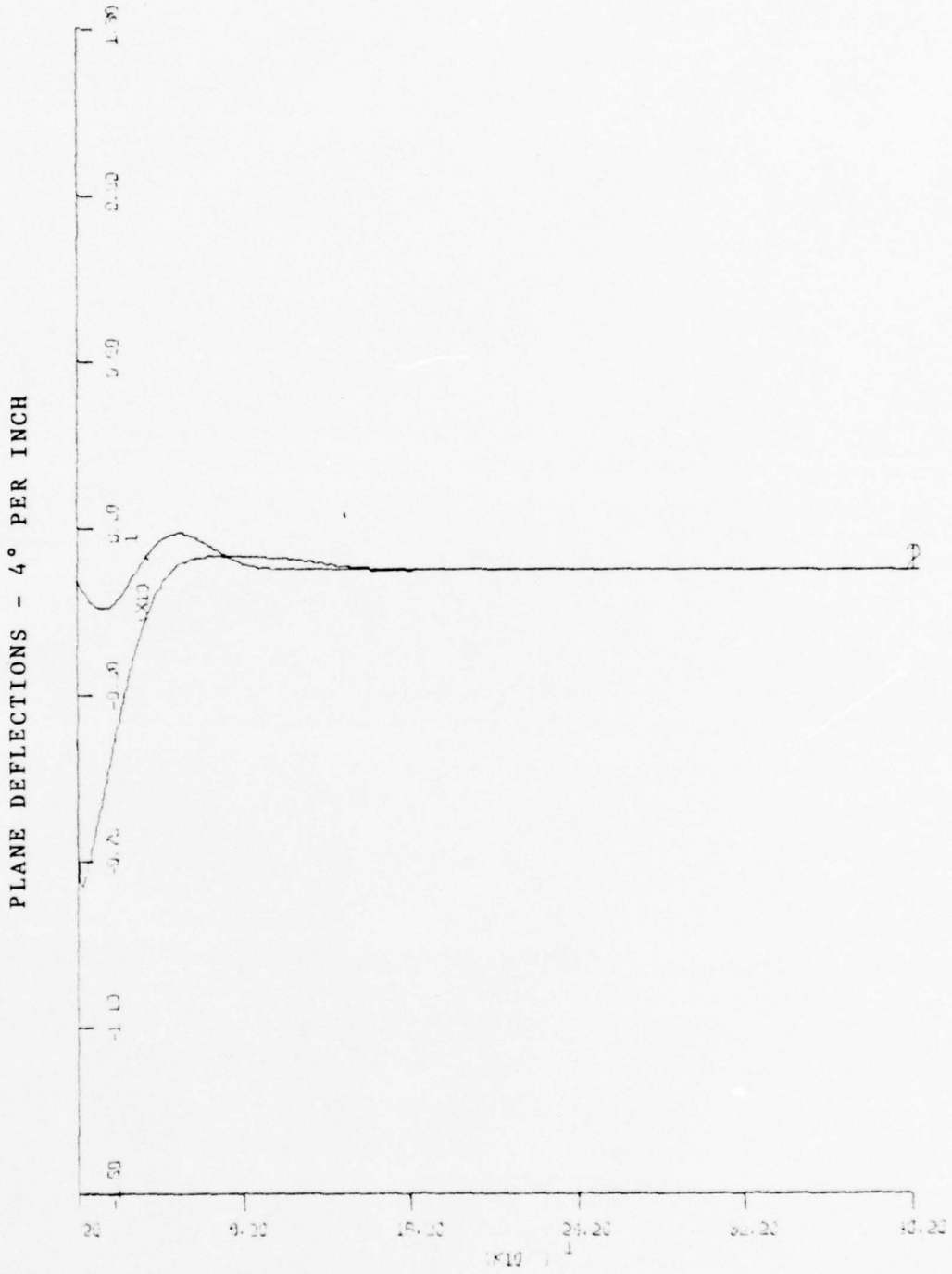

Figure 86 - RUN 6
10 FT DEPTH CHANGE, 9 KN

All these test runs showed that the compensated system is stable as expected and that the steady-states are reached independently without error. The plane angles increase with increasing gains. The pitch behavior has basically the same form for all runs. In the initial phase the submarine pitches in the direction of the depth change, which is counteracted by the stern planes. Before the ordered depth is reached the submarine pitches in the opposite direction and reaches steady-state in a sinusoidally damped motion. An increase in K_2 reduces the amplitude of the pitch.

The primary task of the stern planes is to maintain the ordered pitch, i.e. in this case even keel, and to counteract the moments generated by the fairwater planes. As the lever arm of the stern planes is greater than the one of the fairwater planes, the stern plane deflections are significantly smaller.

The fairwater plane angles exceed the design specifications in run 4 and 5, which eliminates those runs from further considerations and shows that K_1 should be smaller than 2.0.

Run 1 :

$$K_1 = 1. \qquad K_2 = 15.$$

The ordered depth was reached with very small overshoot, but the system showed a big undershoot of 10.8% after the first peak. This is due to the fact that at the time the ordered depth is reached, the pitch is greatest in the positive direction. This is not desirable.

Run 2 :

$$K_1 = 1.5 \qquad K_2 = 15.$$

The increase in K_1 leads to an increase in the fairwater plane deflection. The depth change is accelerated and the pitch deviations increase, which in turn leads to greater stern plane deflections. The amplitudes of the oscillations increase, the overshoot reaches 11.4% and the undershoot 11.4%. As the fairwater planes have reached about the allowed deflection limits K_1 will not be increased any further. The action taken will concern K_2 only.

Run 3 :

$$K_1 = 1.5 \qquad K_2 = 40.$$

The increase in K_2 resulted in larger stern plane deflections, which damped the pitch more than before. Due to the smaller pitch changes which at the same time support the depth response, the deviations are decreased significantly and die out rapidly. The trade-off which has to be considered is that increasing the damping will result in longer times until the ordered depth is reached.

Run 4 and 5 :

are not considered as mentioned above.

Run 6 :

$$K_1 = 1.5 \qquad K_2 = 60.$$

This further increase in K_2 confirmed the previously observed tendency. The overshoot is decreased to 3.6 % and there is essentially no undershoot. Both run 3 and 6 satisfy the design specifications. But run 6 shows clearly the more desirable behavior as the pitch is smaller, the overshoot is less and the depth accuracy is more important than the small sacrifice in time, as all these depth maneuvers represent standard depth changes and no emergency dives.

b. Check for valid speed range

So far the compensator is designed for 9 kn. The sensitivity of the compensated system to speed is important for two reasons. First, the constant speed assumption for the linear model is not quite accurate, because on our submarines the speed is ordered in form of rpm. The actual speed varies with rudder deflections and pitch angle. These influences result in small speed changes. This phenomenon was observed in the comparative test runs with the linear and non-linear models. Second, it is of interest to find the speed range where this compensator still yields a satisfactory behavior which is within the design specifications.

Therefore simulation runs with the compensator designed for 9 kn were performed for the speed range from 3 kn to 15 kn at 2 kn-intervals. The results are shown in Table 12.

Table 12 - 10 ft depth change

Run	Speed	Depth reached after sec	Overshoot in ft	Max Pitch in °	Max DB in °	Max DS in °	Figure
1	3	169.0	1.88	0.192	8.46	0.58	87
2	5	100.5	1.16	0.203	8.26	0.815	88
3	7	70.0	0.66	0.303	7.97	0.921	89
4	9	54.0	0.36	0.286	7.62	0.975	
5	11	44.5	0.20	0.328	7.19	1.01	90
6	13	39.5	0.13	0.335	6.71	1.04	91
7	15	39.0	0.10	0.342	6.17	1.08	92

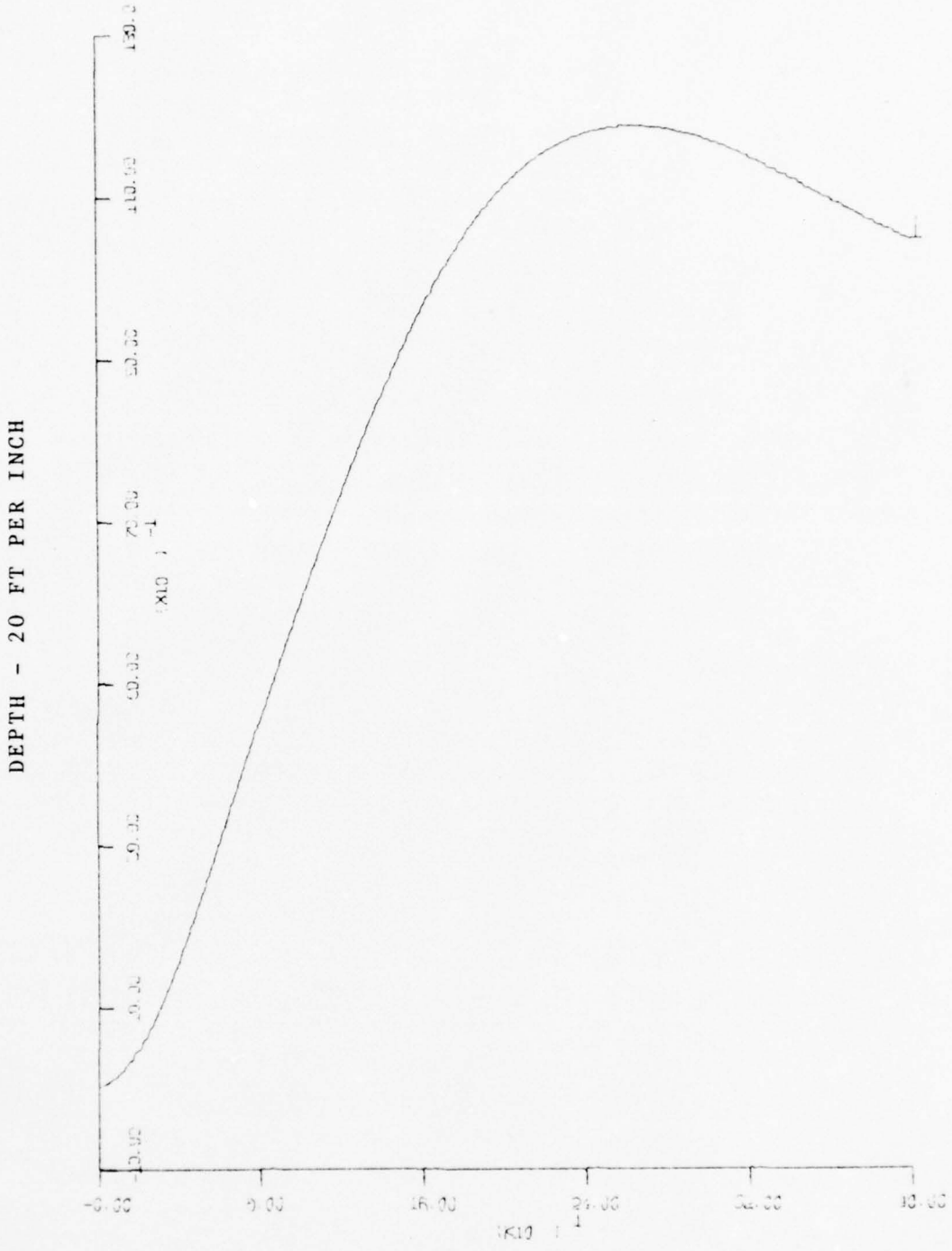

Figure 87 - RUN 1
100 FT DEPTH CHANGE, 3 KN

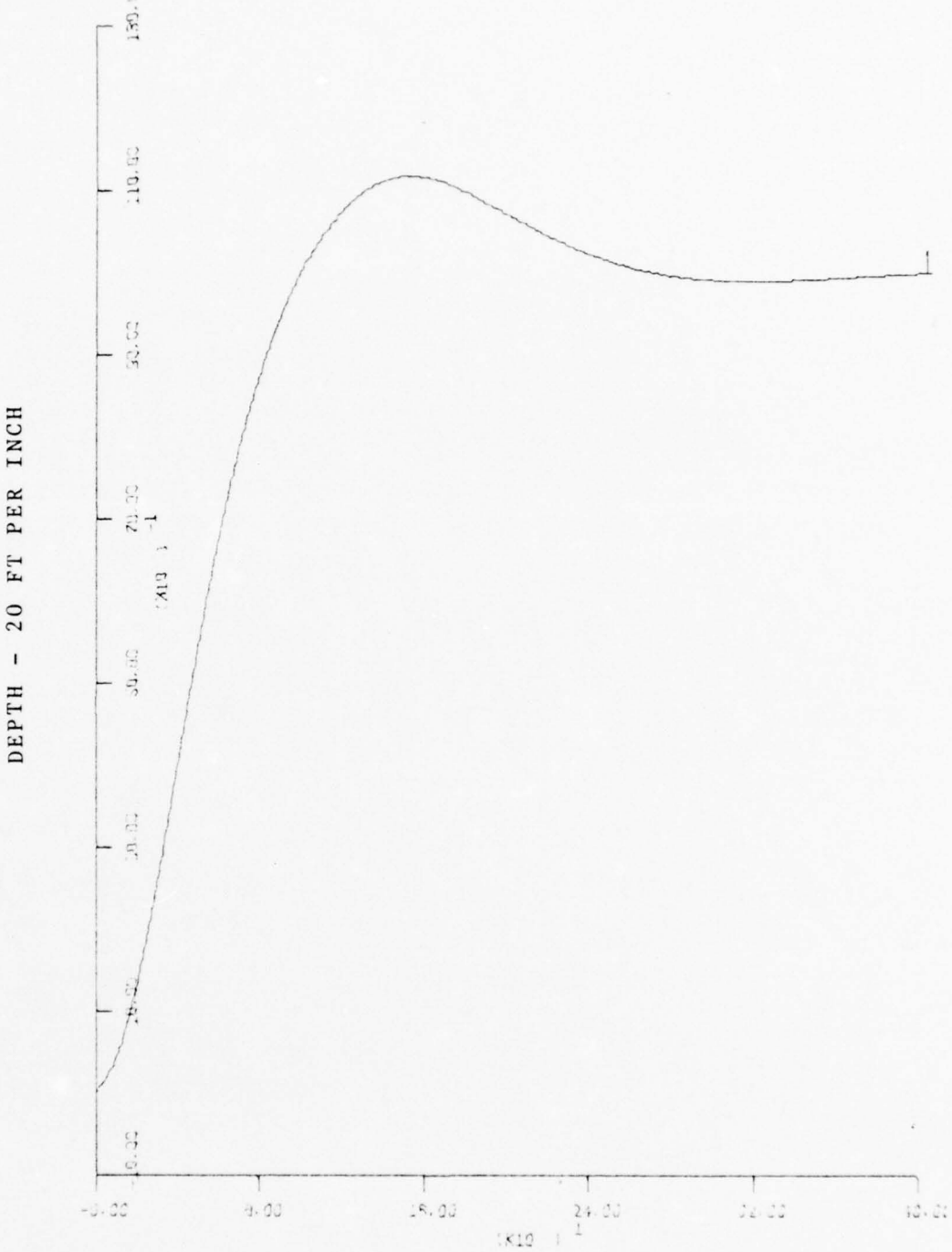

Figure 88 - RUN 2
100 FT DEPTH CHANGE, 5 KN

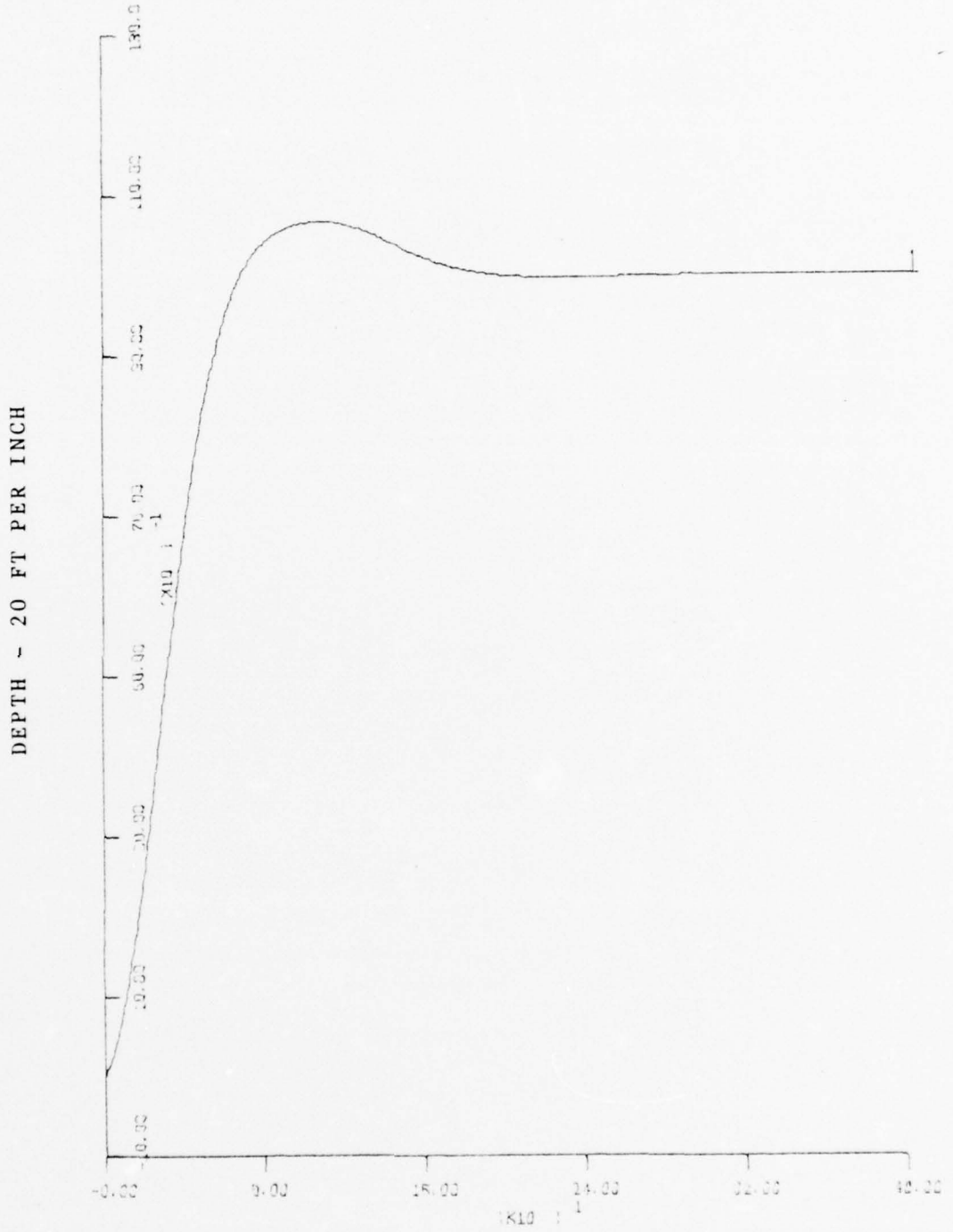

Figure 89 - RUN 3
100 FT DEPTH CHANGE, 7 KN

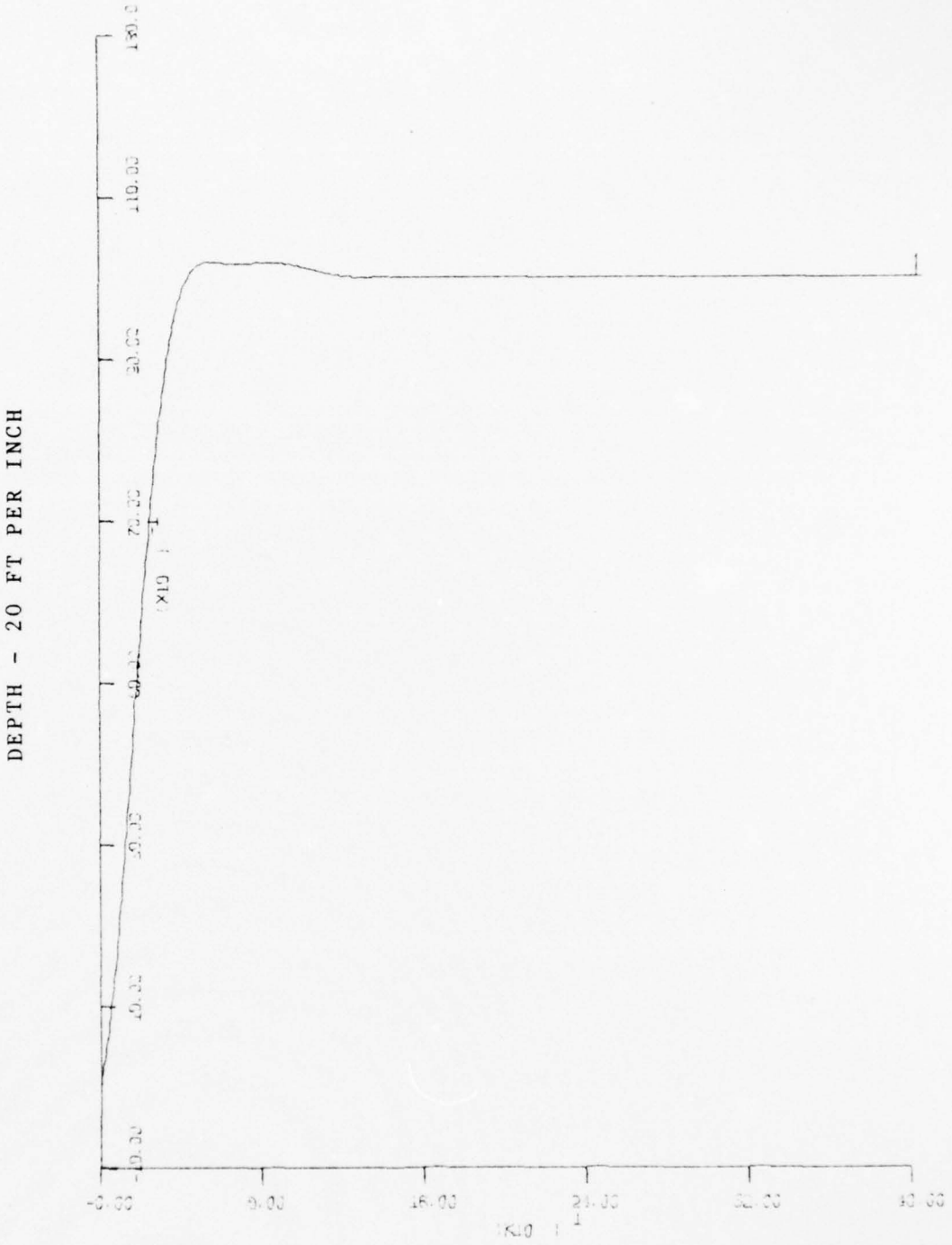

Figure 90 - RUN 5
100 FT DEPTH CHANGE, 11 KN

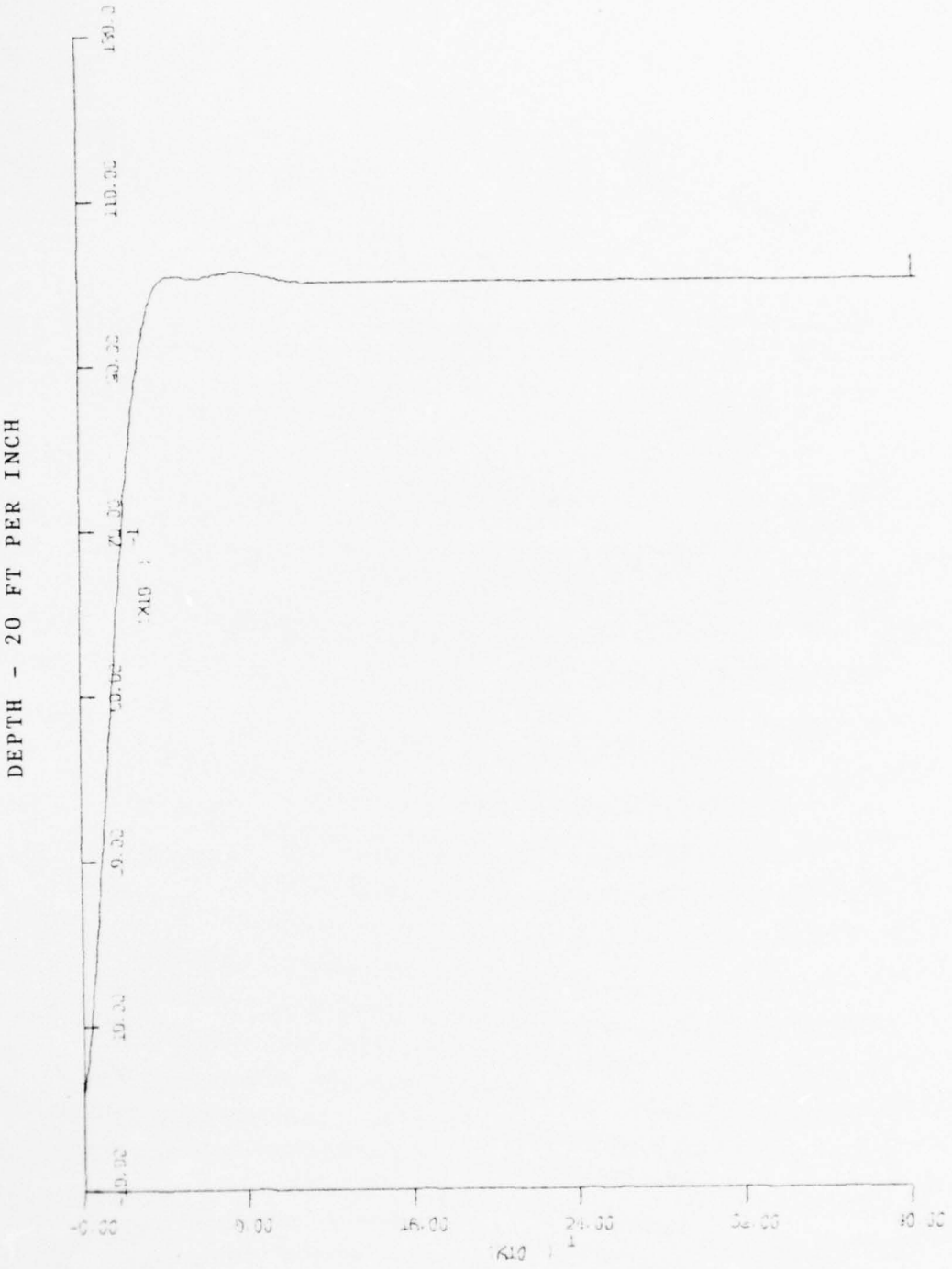

Figure 91 - RUN 6
100 FT DEPTH CHANGE, 13 KN

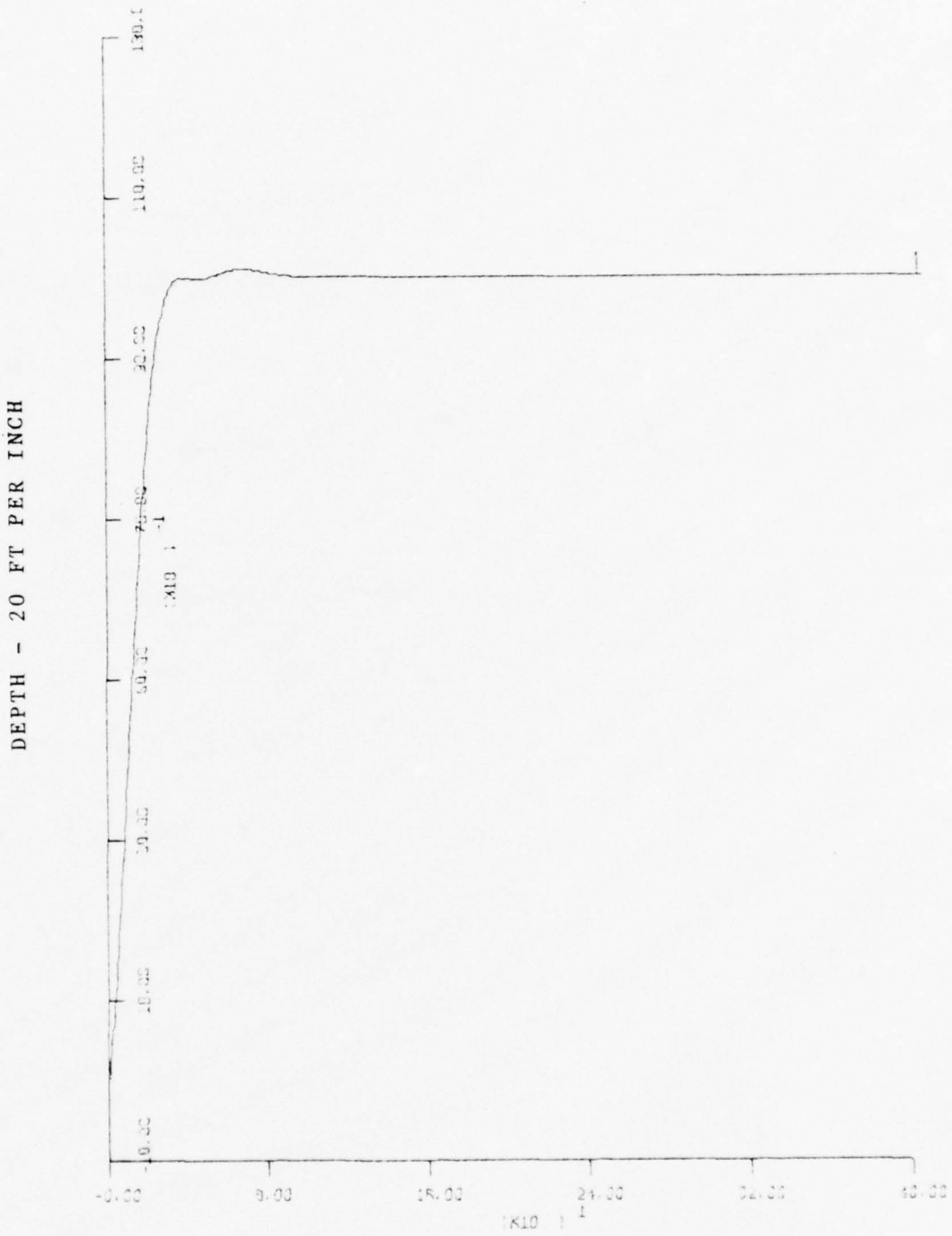

Figure 92 - RUN 7
100 FT DEPTH CHANGE, 15 KN

As can be seen from Table 06 the poles of the characteristic equation of the open loop system transfer functions move closer tc the origin of the s-plane with decreasing speeed, which should lead to a slower response. At the same time the damping-ratic decreases with decreasing speed. All test runs reflect this observed tendency.

* Run 4-7 :

The time, at which the ordered depth was reached for the first time, is acceptable. The overshoot is within the design specifications. The plane angles never exceeded the limits and the pitch is small. Small gain variations led to a shift in the trade-off between response time and overshoot. The improvements which resulted from tests were not significant enough to justify the complexity of gain switching. Thus the designed compensator will cover the entire speed range from 9 to 15 kn very satisfactorily.

* Run 3 :

The 7 kn depth response exceeds the design specifications slightly with respect to time and overshoot, while pitch and plane angles are still within the limits. This speed represents a borderline case where the compensator might be acceptable.

* Run 2 and 1 :

For these two speeds the overshoot of 11.58 % and 18.77 % respectively exceed the specifications by far and the times required are clearly not desired.

It was possible to improve the response time

with gain variations, but it was impossible to reduce the overshoot to an acceptable value. This indicated that for slow speeds gain switching can not be a sufficient measure to adjust this compensator. It seems that a redesign of the compensator is necessary.

3 kn and 5 kn are eliminated from further considerations as these speeds are not too important for submarine maneuvering.

c. Modification for major depth changes

The mechanical limit for both rudder deflections is 35 °. As outlined in the design specifications these limits are reduced to smaller values for higher speeds. Due to the linearity of the system major depth changes, which lead to proportional depth errors, will cause plane deflections exceeding these limits. Therefore it is necessary to prevent the planes from exceeding these limits. There are two possible actions one can take.

First, limit the planes. Test runs where this scheme was implemented led to unacceptable plane behavior.

Second, limiting of the error signals. The resultant block diagram is:

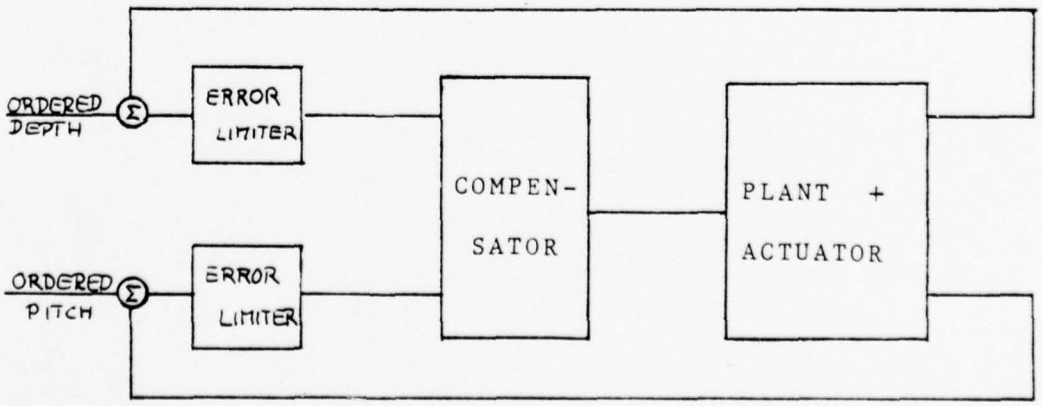

From the design specifications it was determined that the error limit function could be approximated by a straight line:

$$lim = -1.6655*UC + 59.6875$$

Where UC is in ft/s.

This function and the resulting maximum angles are shown in the following diagram

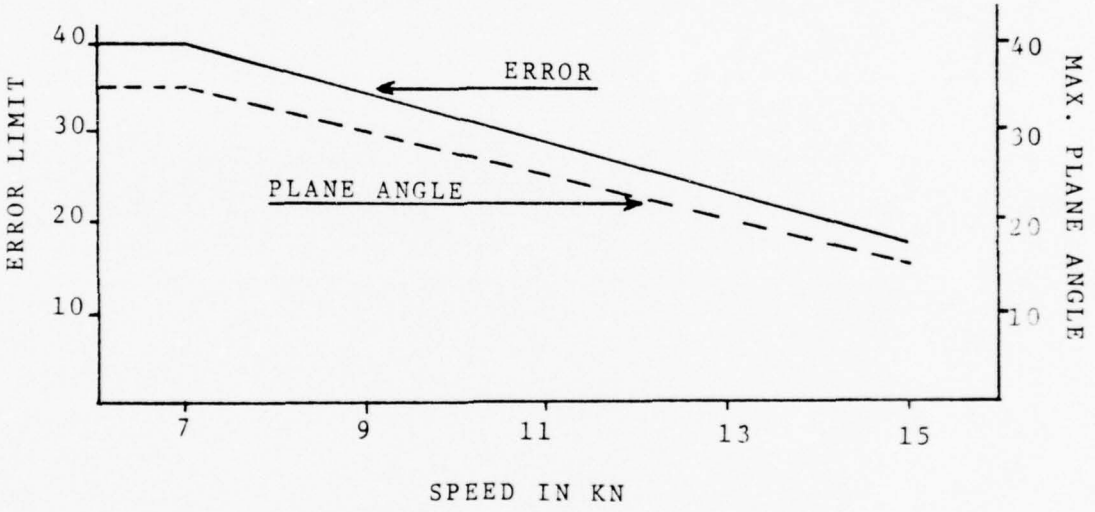

Table 13 shows the simulation runs for 100 ft depth change.

Table 13 - 100 ft depth change

Run	Speed	Depth reached after sec	Overshoot in ft	Max Pitch in °	Max DB in °	Max DS in °	Figure
1	7	105.5	5.30	1.41	34.4	4.26	93
2	9	91.0	3.0	1.30	29.5	3.94	94
3	11	86.0	1.71	1.16	24.7	3.50	95
4	13	87.0	0.80	0.97	19.9	2.96	96
5	15	97.0	0.31	0.75	15.0	2.28	97-99

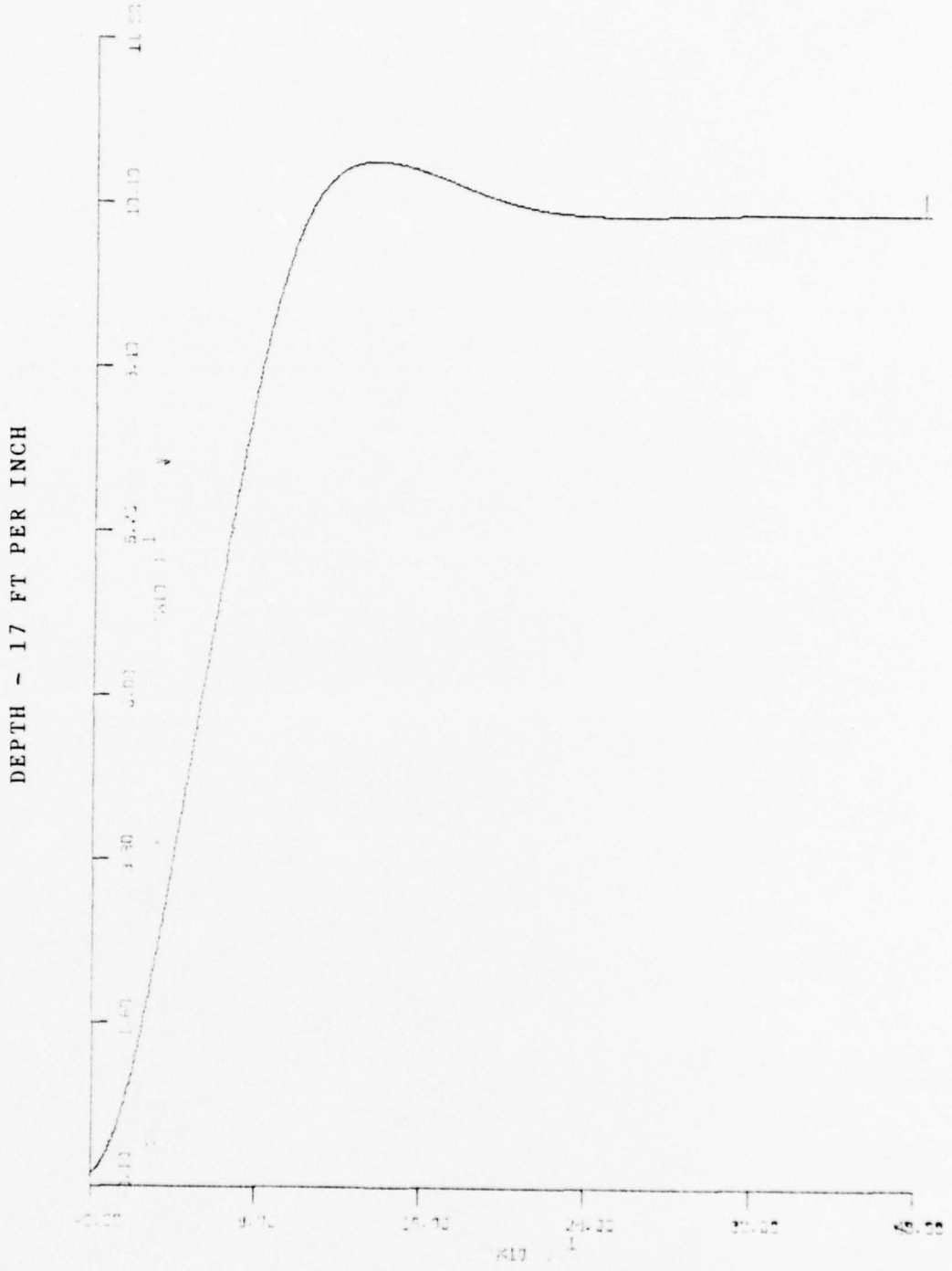

Figure 93 - RUN 1
100 FT DEPTH CHANGE, 7 KN

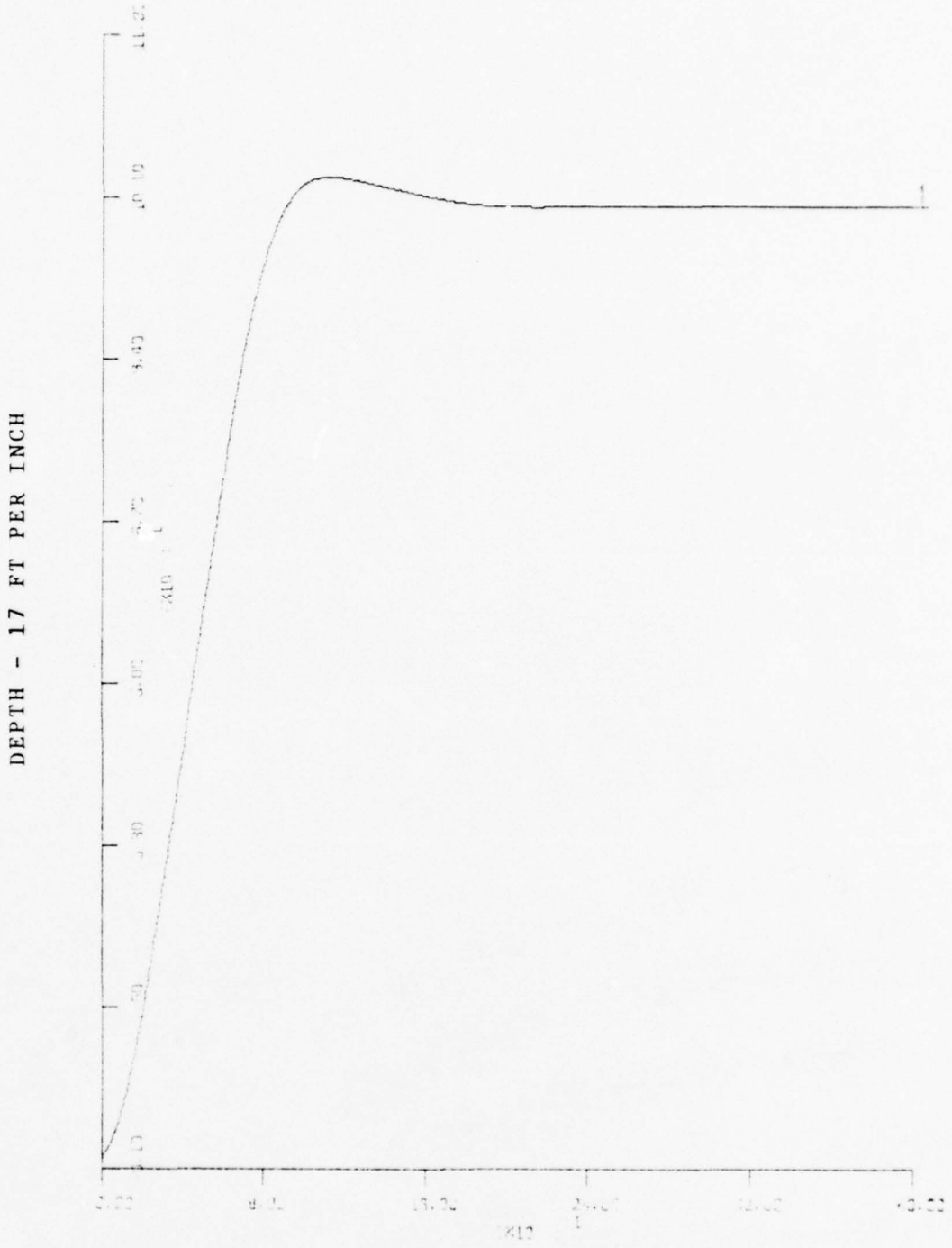

Figure 94 - RUN 2
100 FT DEPTH CHANGE, 9 KN

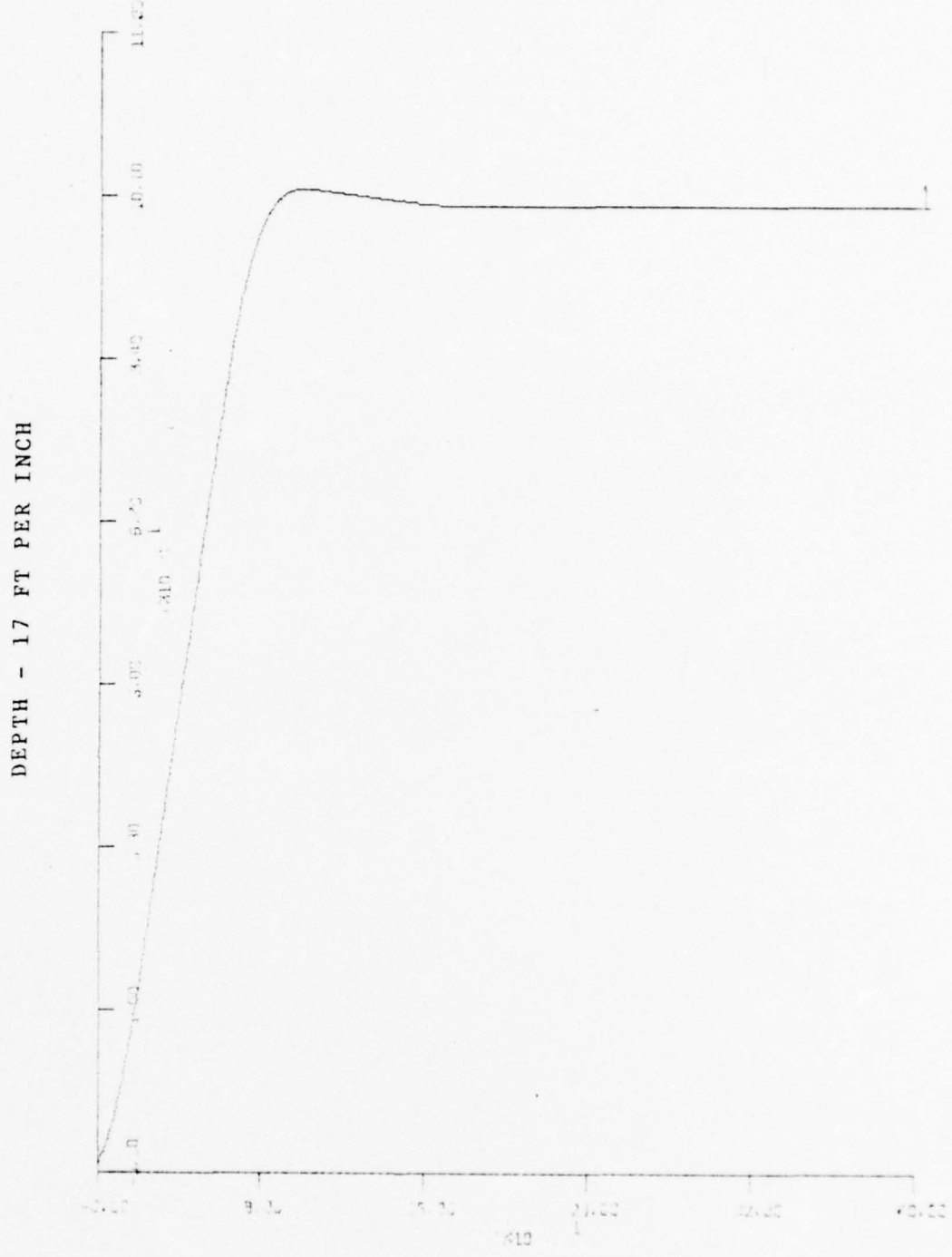

Figure 95 - RUN 3
100 FT DEPTH CHANGE, 11 KN

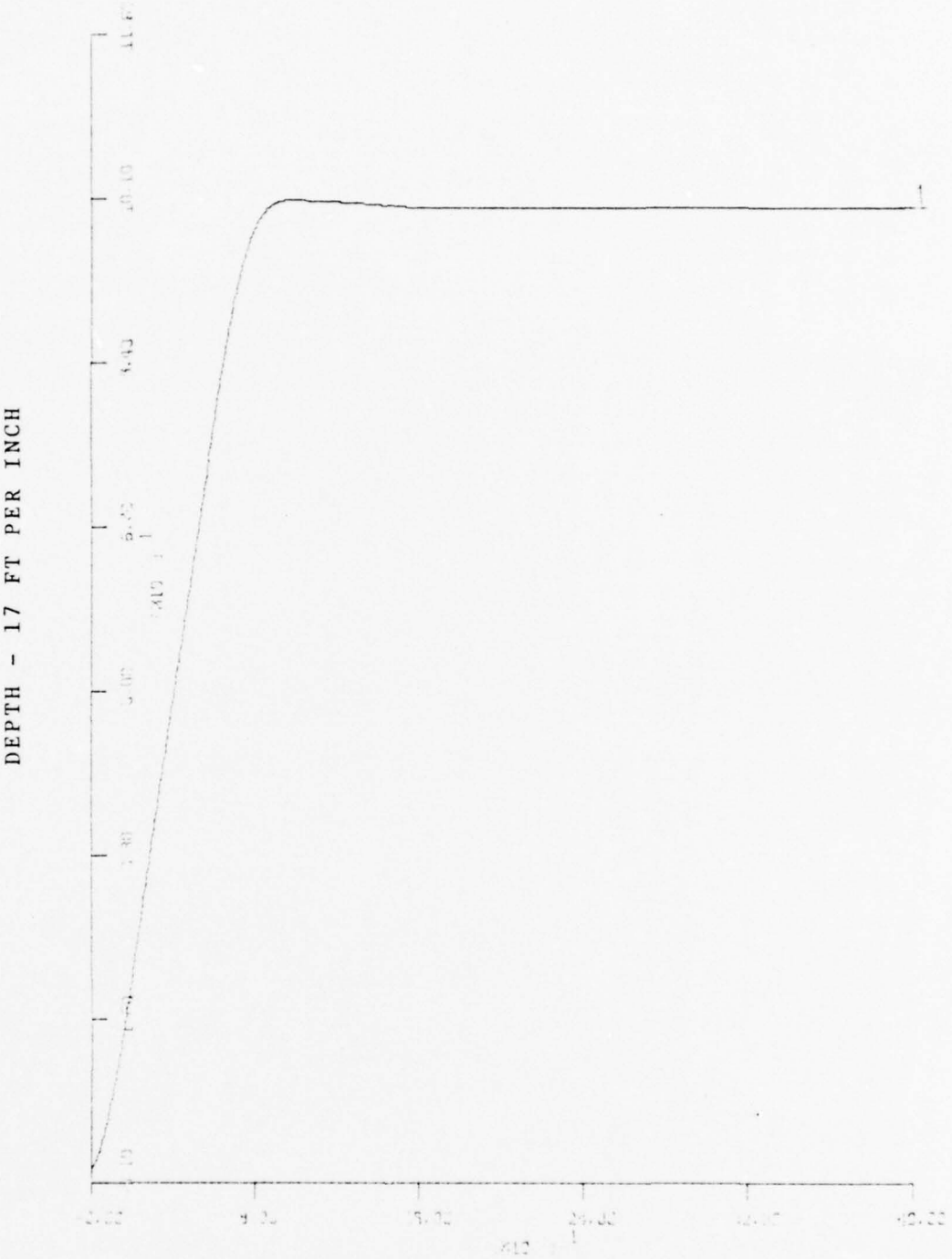

Figure 96 - RUN 4
100 FT DEPTH CHANGE, 13 KN

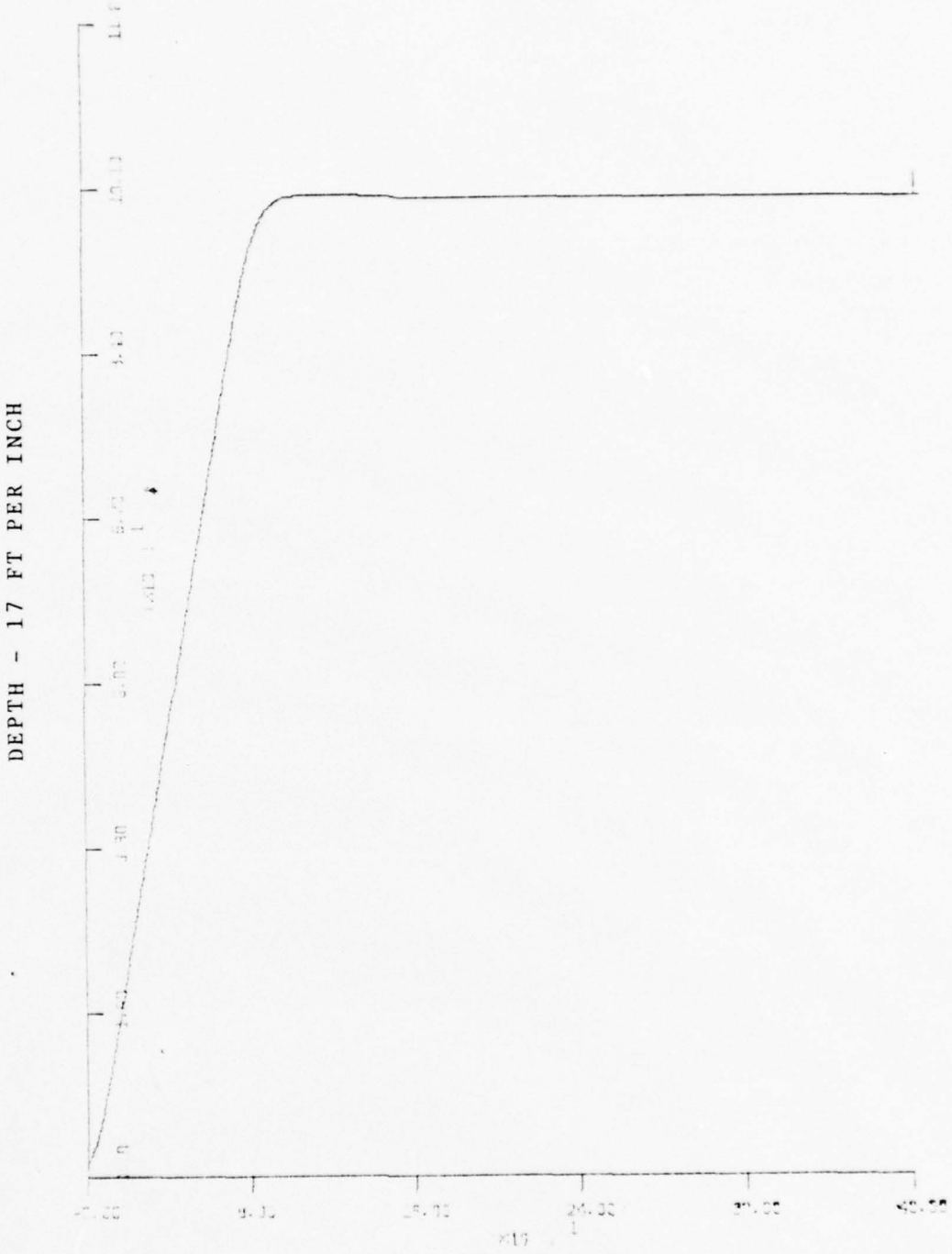

Figure 97 - RUN 5
100 FT DEPTH CHANGE, 15 KN

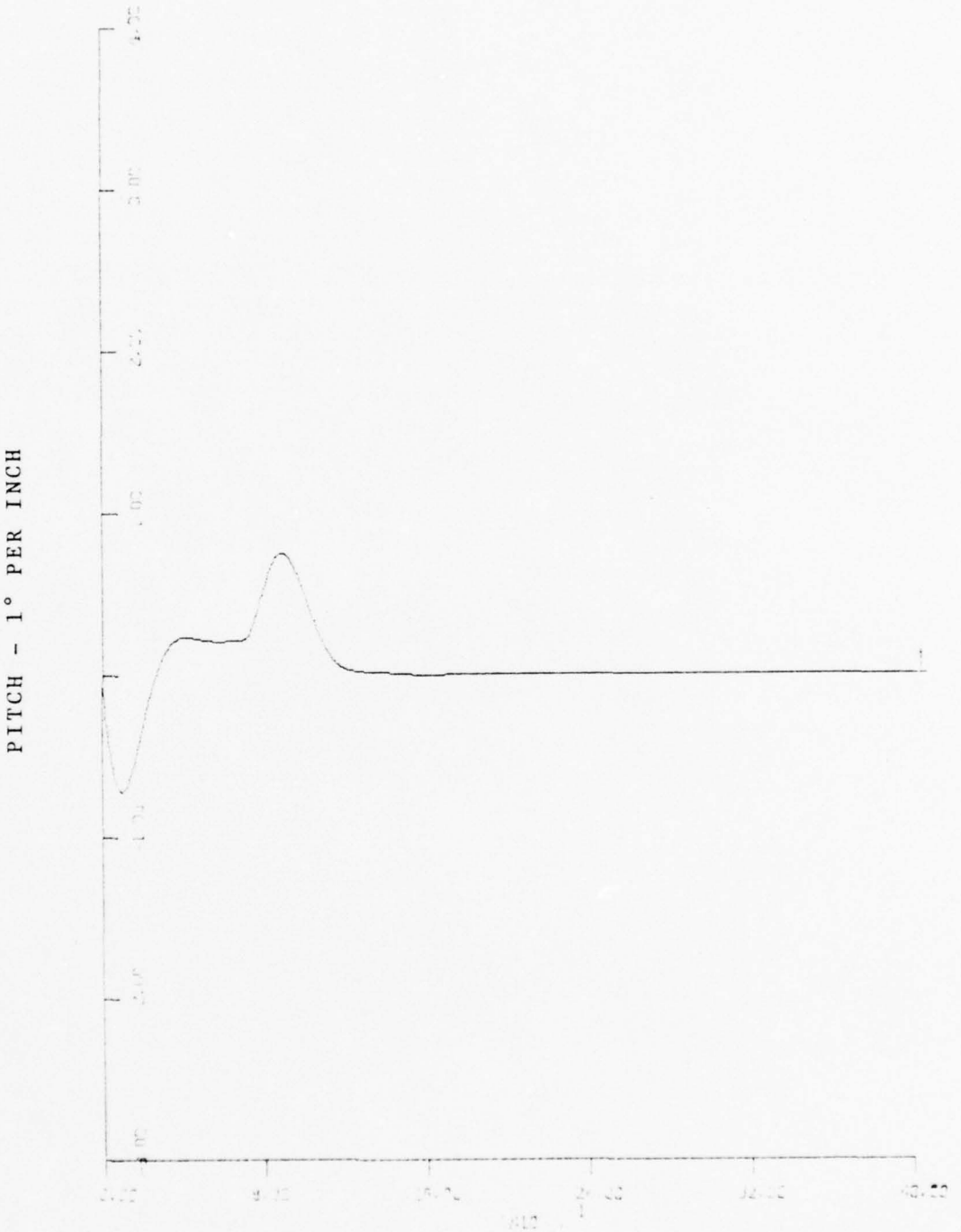

Figure 98 - RUN 5
100 FT DEPTH CHANGE, 15 KN

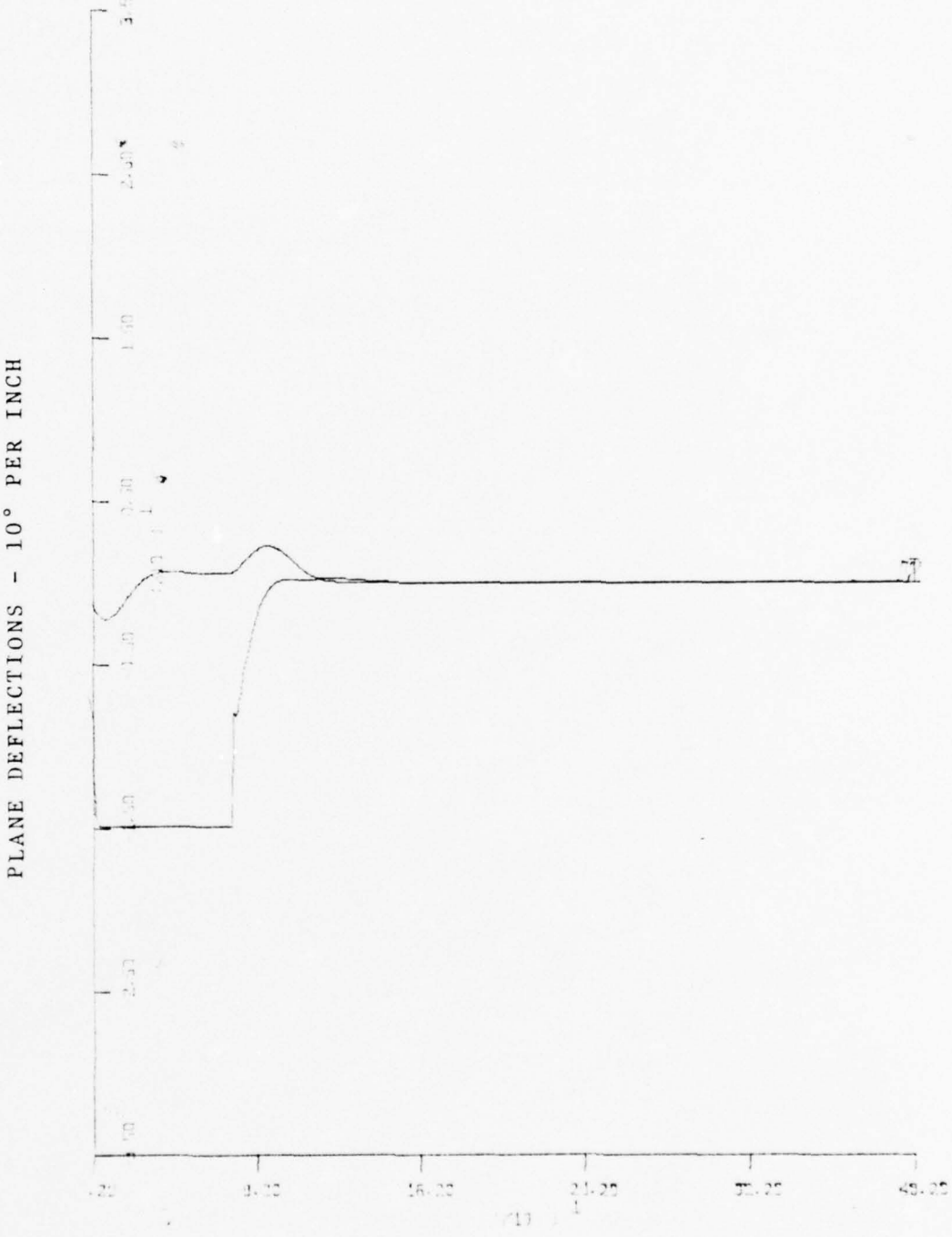

Figure 99 - RUN 5
100 FT DEPTH CHANGE, 15 KN

After an initial pitch the submarine approaches the ordered depth with constant plane deflections. Shortly before the depth is reached, opposite rudder angles are used to eliminate the depth rate.

Although it takes longer to reach the ordered depth initially the overall time to steady-state decreases with increasing speed.

This completes the design for the speed range from 7 kn to 15 kn and all possible depth changes. From here on the behavior of the compensated non-linear model will be investigated under special conditions, like turns, out of trim conditions,etc.
The final block diagram and the DSL-Program are shown in App. D.

C. TOTAL DECOUPLING

The previous design led to a steady-state decoupled system, where both outputs were influenced by a single input during the dynamic period. In our case the pitch encountered was small. In order to keep the submarine at even keel for zero pitch input at all times the system has to be totally decoupled. One method to achieve this behaviour for a multivariable system will be analysed and applied to the linear model.

The system configuration chosen for this design is:

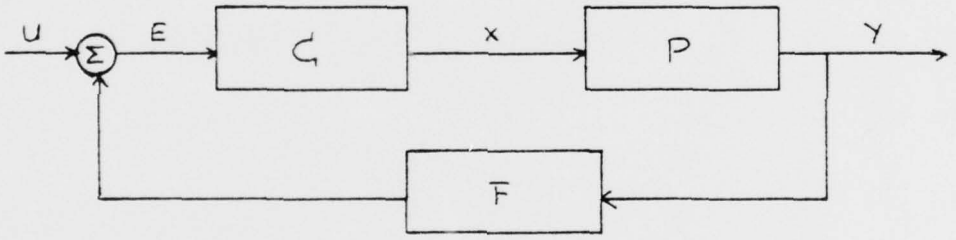

The closed loop system can be represented by:

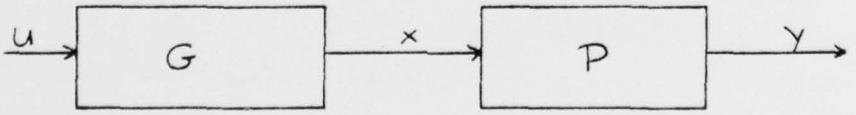

which can be combined to, as will be shown:

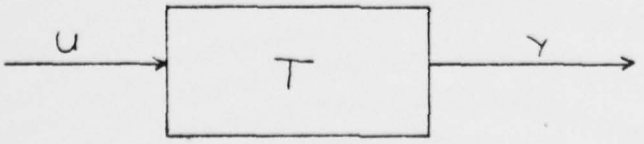

T is the desired overall transfer function which determines the desired overall respones.

Therefore

$$T = PG$$

thus

$$G = P^{-1}T$$

Frcm the block diagrams:

$$Y = TU$$

$$Y = PX$$

$$X = CE$$

$$E = U-FY$$

Thus

$$Y = PC[U-FY]$$

or

$$Y = [I + PCF]^{-1}PCU$$

and

$$T = [I + PCF]^{-1}PC = PG$$

solving for compensator C results in

$$C = G[I - FT]^{-1}$$

In the compensation used for this design the feedback gain matrix is the identity matrix, thus

$$C = G[I-T]^{-1}$$

$$= P^{-1}T[I-T]^{-1}.$$

Thus the compensator is determined by the plant, which is known, and the desired overall transfer function T.

In order to determine the compensator which decouples the system at all times, one has to:

- define the desired response according to the system specifications. This determines the overall transfer function T.
- find $G = P^{-1}T$ and check for realizability.
- determine $C = G[I - T]^{-1}$.

Applying unity feedback and using casade compensation as outlined the blockdiagram for the linear model becomes:

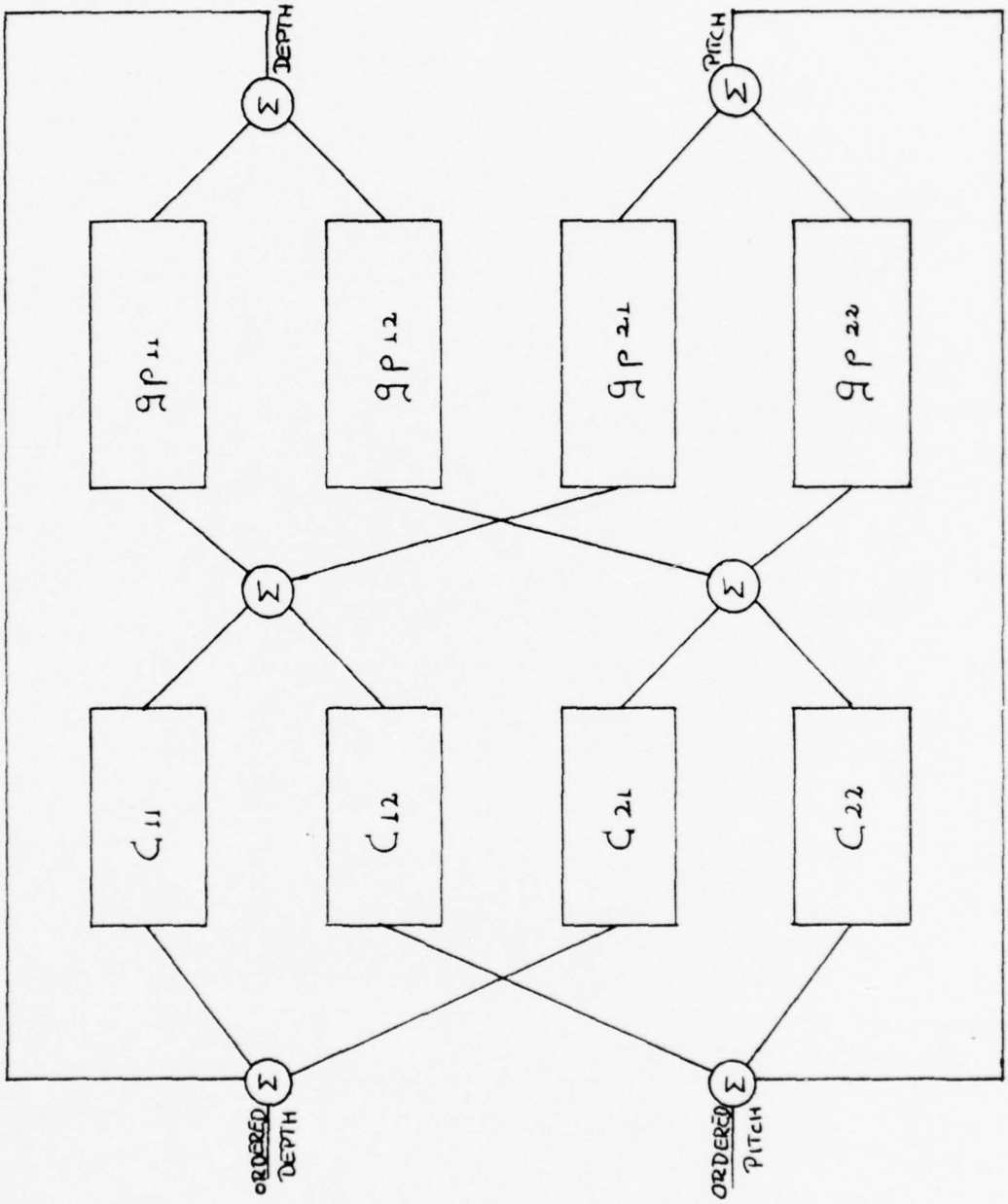

Figure 100 - BLOCK DIAGRAM

As can be seen from the block diagram the requirements for total decoupling can be stated in a different way.

It is required that

$$c_{11} g_{p21} = -c_{21} g_{p22} \tag{26}$$

and

$$c_{12} g_{p11} = -c_{22} g_{p12}. \tag{27}$$

Single loop methods can be applied to design the compensators c_{11} and c_{22} to guarantee the desired response. Once c_{11} and c_{22} are determined the compensators c_{12} and c_{21} can be calculated from (26) and (27).

As Ref. 15 shows C is realizable if G and $[I - T]^{-1}$ are realizable. A rational function in s is physically realizable as a voltage transfer function, if the following conditions are met:

- the coefficients of the function must be real.
- the order of the numerator must be less or equal to the order of the denominator.
- there are no poles in the right half plane and poles on the imaginary axis must be simple.

1. Design

It is desired that the transient response has no overshoot and has an acceptable rise time. The following transfer function is chosen for both outputs

$$t_{11} = t_{22} = \left[\frac{\alpha}{s+\alpha}\right]^2$$

$t_{12} = t_{21} = 0$, because the system is to be decoupled.

Following the previously outlined design steps, $P^{-1}*T$ has to be determined.

The plant matrix has the following elements

$$g_{p11} = k_{11}(\text{zeros } g_{p11})/s\gamma$$

$$g_{p12} = k_{12}(\text{zeros } g_{p12})/s\gamma$$

$$g_{p21} = k_{21}(\text{zeros } g_{p21})/\gamma$$

$$g_{p22} = k_{22}(\text{zeros } g_{p22})/\gamma$$

Thus

$$P^{-1} = \frac{\begin{bmatrix} k_{22}(\text{zeros } g_{p22})/\gamma & -k_{12}(\text{zeros } g_{p12})/\gamma s \\ -k_{21}(\text{zeros } g_{p21})/\gamma & k_{11}(\text{zeros } g_{p11})/\gamma s \end{bmatrix}}{g_{p11}g_{p22} - g_{p12}g_{p21}}$$

It can be shown that

$$g_{p11}g_{p22} - g_{p12}g_{p21} = 1/s\gamma$$

Therefore

$$P^{-1} = \begin{bmatrix} k_{22}(\text{zeros } g_{p22})s & -k_{12}(\text{zeros } g_{p12}) \\ -k_{21}(\text{zeros } g_{p21})s & k_{11}(\text{zeros } g_{p11}) \end{bmatrix}$$

$$= \begin{bmatrix} p_{11} & p_{12} \\ p_{21} & p_{22} \end{bmatrix}$$

and

$$G = P^{-1}T = [\alpha^2(s+\alpha)^2]P^{-1}$$

The next step is to find

$$[I-T]^{-1} = \frac{\begin{bmatrix} 1-t_{22} & 0 \\ 0 & 1-t_{11} \end{bmatrix}}{(1-t_{11})(1-t_{22})}$$

$$= \begin{bmatrix} (s+\alpha)^2/s(s+2\alpha) & 0 \\ 0 & (s+\alpha)^2/s(s+2\alpha) \end{bmatrix}$$

Finally the compensator matrix C can be determined:

$$C = G[I-T]^{-1}$$

$$= \begin{bmatrix} c_{11} & c_{12} \\ c_{21} & c_{22} \end{bmatrix}$$

where

$$c_{11} = \alpha^2 k_{22} (\text{zeros } g_{p22}) / (s+2\alpha)$$

$$c_{12} = -\alpha^2 k_{12} (\text{zeros } g_{p12}) / s(s+2\alpha)$$

$$c_{21} = -\alpha^2 k_{21} (\text{zeros } g_{p21}) / (s+2\alpha)$$

$$c_{22} = \alpha^2 k_{11} (\text{zeros } g_{p11}) / s(s+2\alpha)$$

The elements of the compensator for this specific design consist of the zeros of the plant transfer function and poles which depend on the desired response. As the zeros of the plant and probably the time constants of the desired response depend on the speed of the submarine, it can be expected that the compensator is highly dependent on speed.

The realizability of C is guaranteed, if G and $[I - T]^{-1}$ are realizable. It can easily be seen that for all

elements of G and $[I - T]^{-1}$ all three above mentioned conditions are satisfied.

2. Simulation

In order to check the design the system was simulated for a speed of 9 kn. The choice of the overall transfer function

$$t_{11} = t_{22} = .2^2/(s+.2)^2$$

$$t_{12} = t_{21} = 0$$

should lead to an overdamped response, which reaches the ordered depth in about 60 sec. From Tables 06 - 10 and the defined overall T it follows :

$$c_{11} = -.31945\ 10^{-1}(25.452s+1)/(2.5s+1)$$

$$c_{12} = -.38194(-5.1921s+1)(18.671s+1)/s(2.5s+1)$$

$$c_{21} = .15017\ 10^{-2}(-117.87s+1)/(2.5s+1)$$

$$c_{22} = -.29056\ 10^{-1}(5.6338s+1)(131.23s+1)/s(2.5s+1)$$

* Unconstrained trials:

In the first simulation the submarine had to change the depth by 10 ft at even keel. The simulation showed the

expected response, i.e. the depth was reached after 50 sec. without overshoot. The pitch was of the order of $\pm 10^{-5}$. This deviation can be explained by round-off and truncation.
In the design the physical constraints on the planes were neglected. As it turned out these constraints were exceeded by far. Due to the step input of the ordered depth the fairwater plane angle increased initially to 117° and exceeded the limit of 30° for about 4.5 sec. The max. stern plane angle was about 25°. Obviously further compensation is necessary.

Another important aspect is the sensitivity w.r.t. speed. Therefore the submarine was run with the same compensator for 7 and 11 kn.
For 7 kn the depth response was oscillatory with an overshoot of 7.6%. The pitch oscillated with a amplitude of .1°.
For 11 kn the depth response was oscillatory with an overshoot of 1%. The pitch oscillated with an amplitude of .09°. As expected the system is no longer decoupled, because the "correct" compensator depends among others on the zeros of the system, which in turn vary with speed. As the depth response deviates significantly from the desired response with change in speed, it can be concluded that the compensator, designed for a specific speed, covers only a relatively small interval.

* Implementation of constraints :

The two constraints are the rate limit of the planes and the max. angle allowed for a specific speed. The rate limit is taken care of by the actuator. The angle can be kept within its limits (ca. 30° for 9 kn) using either a limit on the signal applied at the actuator or error limitation. For a

Figure 101 - TOTAL DECOUPLING
10 FT DEPTH CHANGE, 9 KN

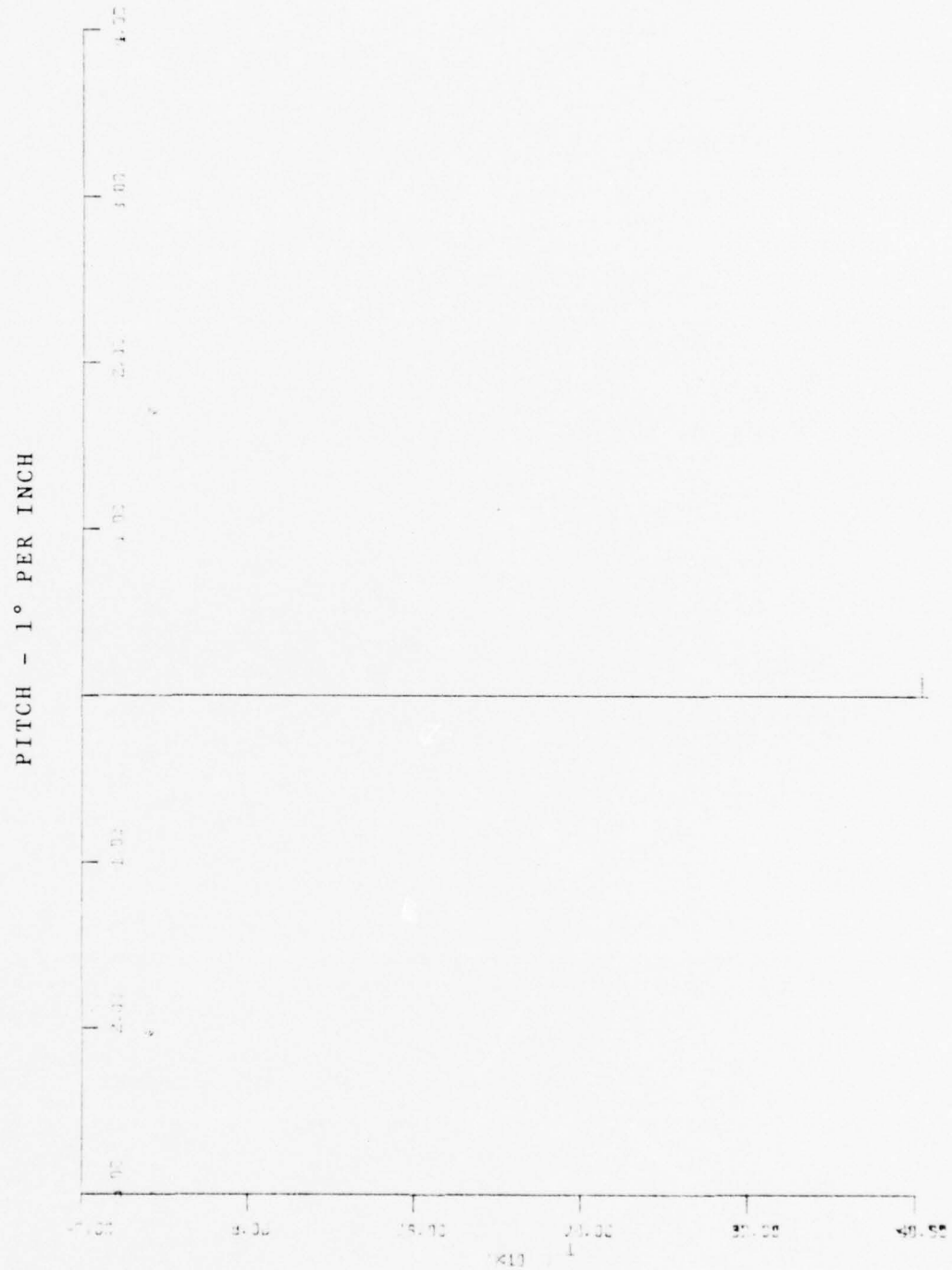

Figure 102 - TOTAL DECOUPLING
10 FT DEPTH CHANGE, 9 KN

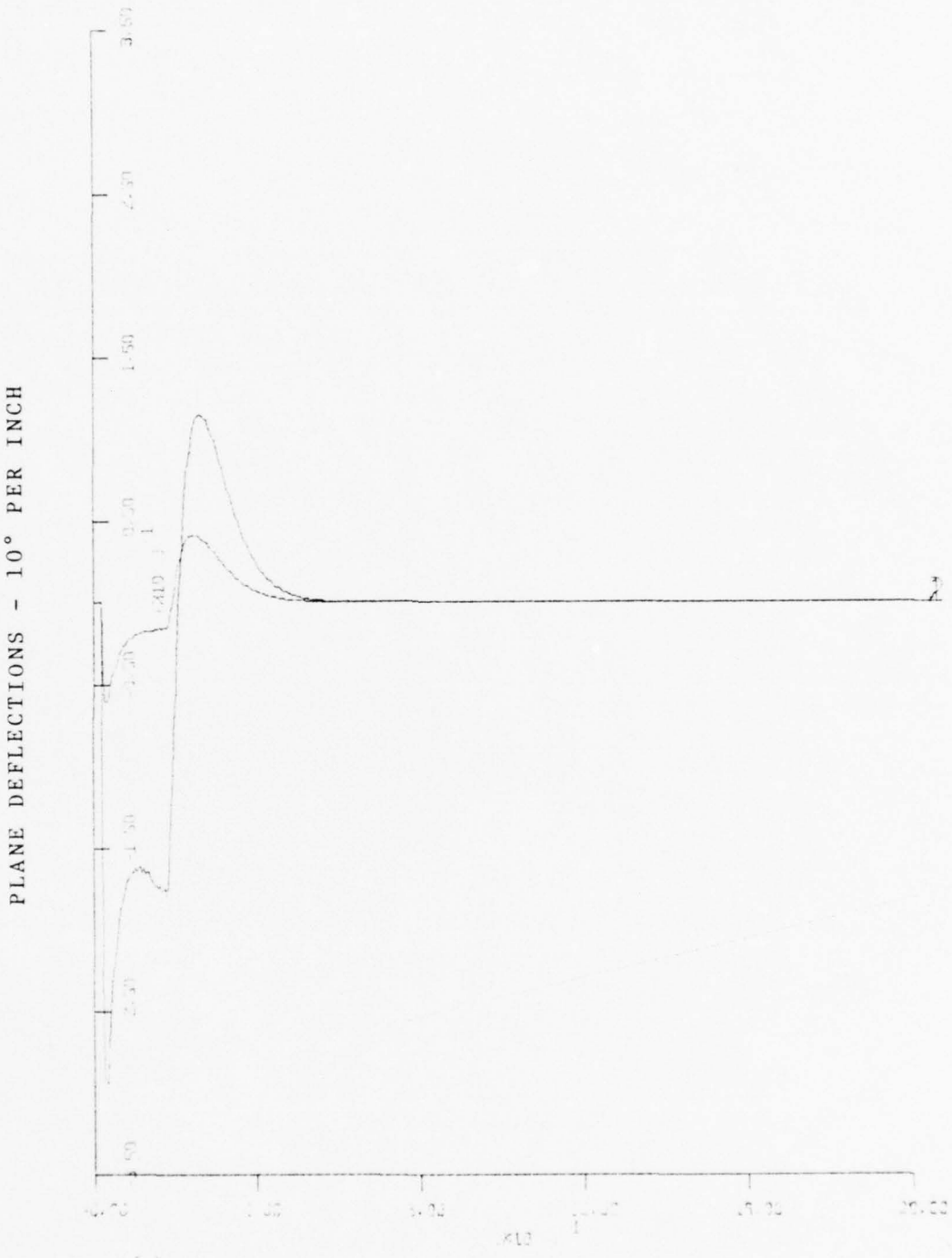

Figure 103 - TOTAL DECOUPLING
10 FT DEPTH CHANGE, 9 KN

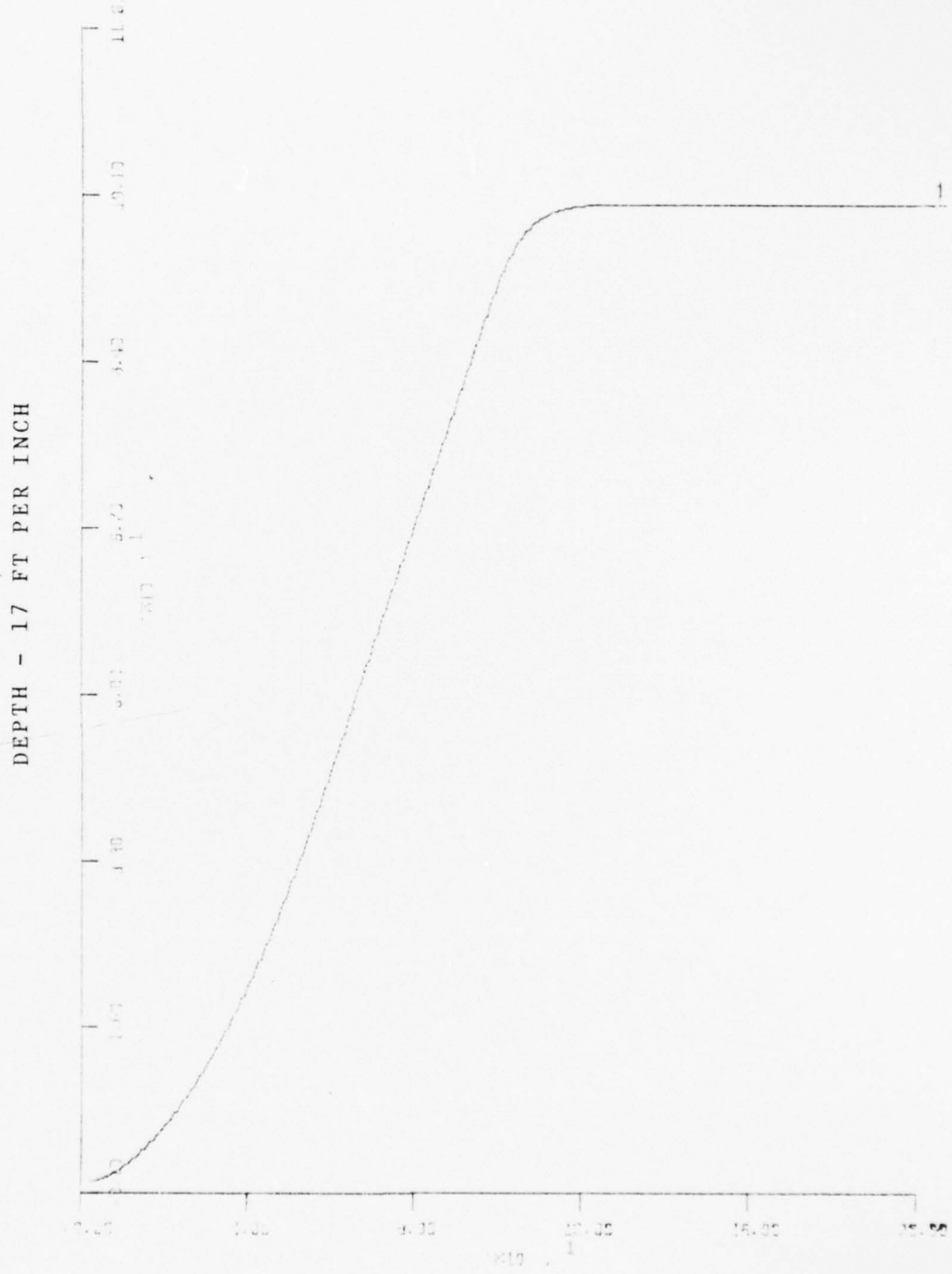

Figure 104 - TOTAL DECOUPLING
100 FT DEPTH CHANGE, 9 KN

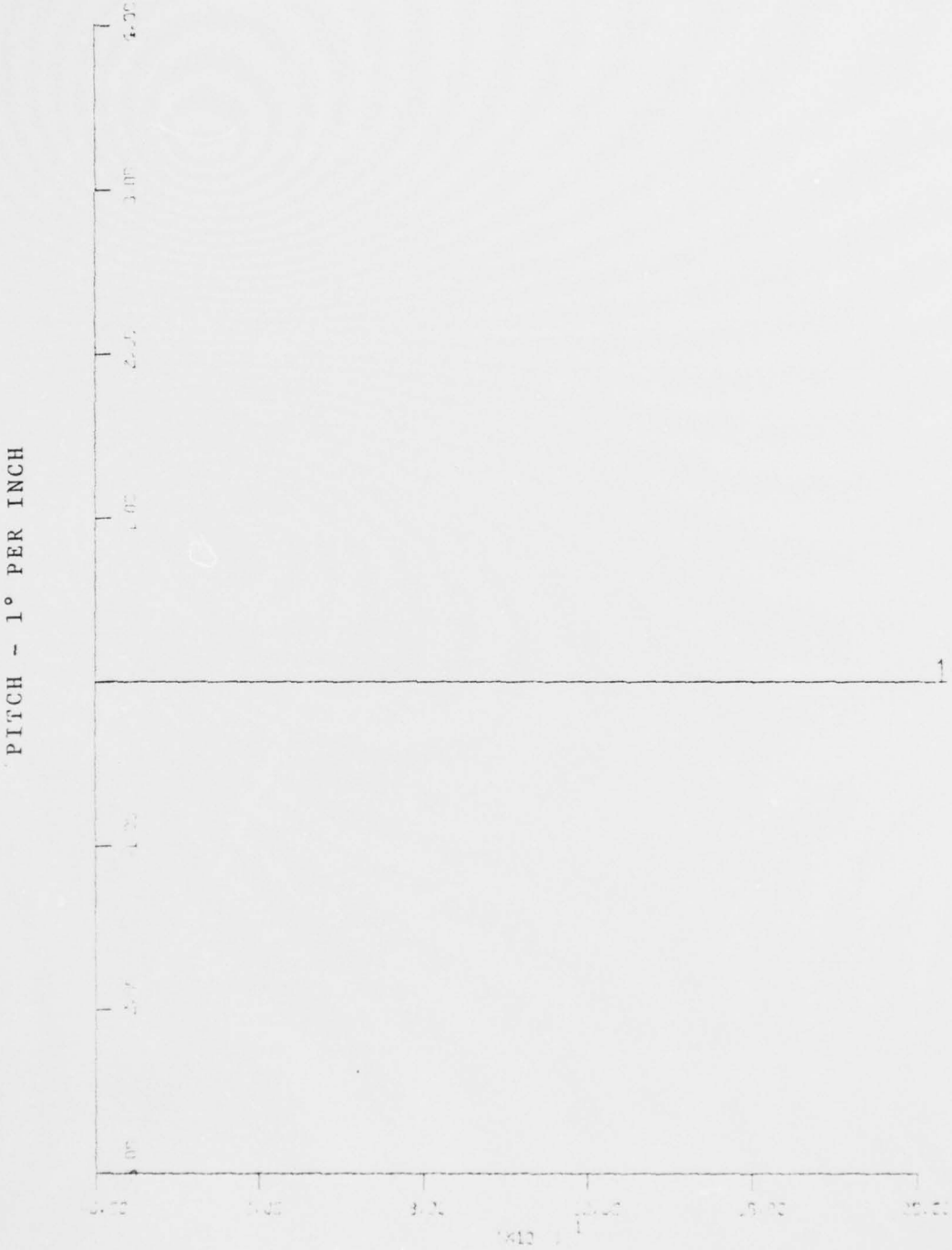

Figure 105 - TOTAL DECOUPLING
100 FT DEPTH CHANGE, 9 KN

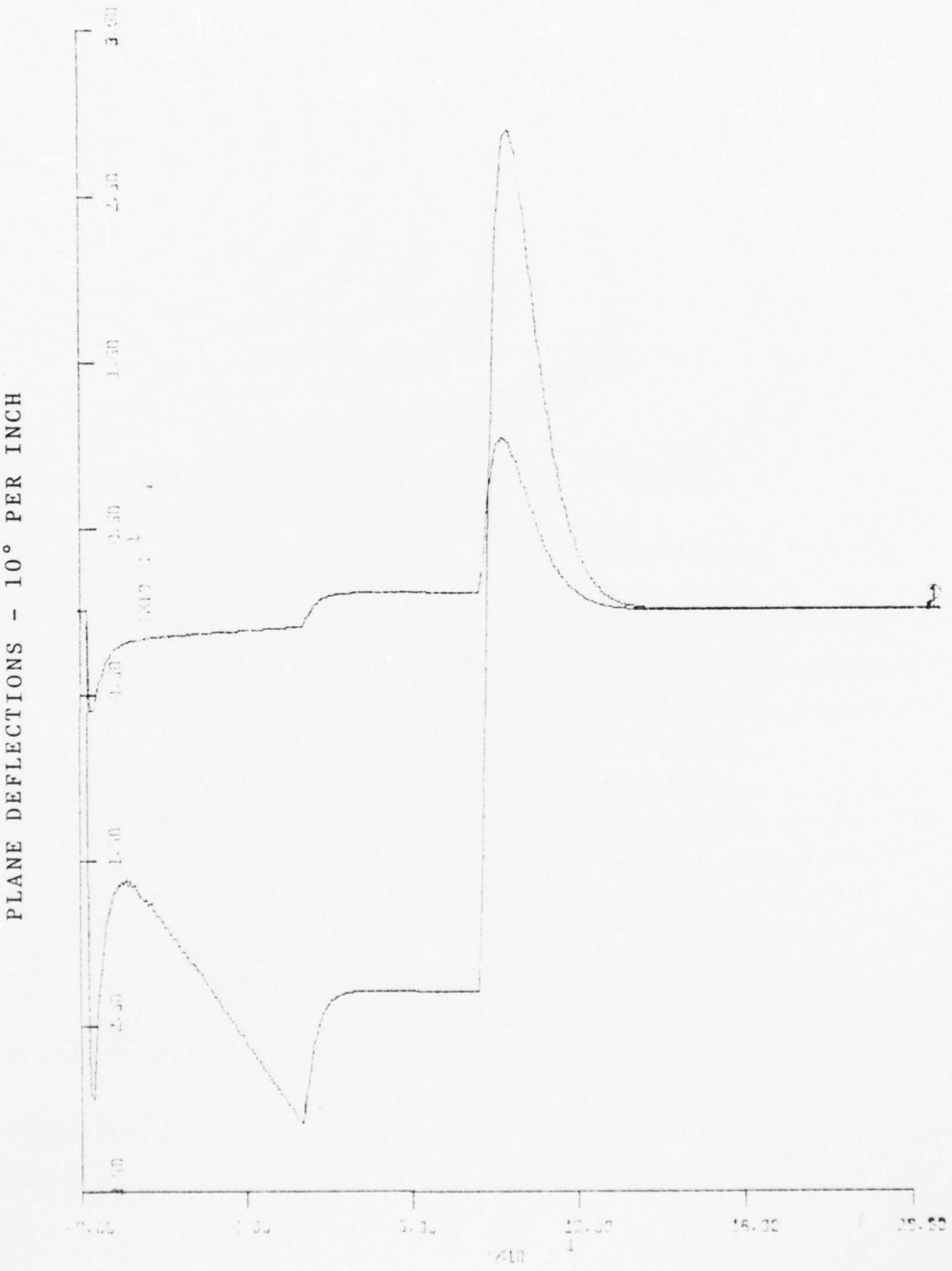

Figure 106 - TOTAL DECOUPLING
100 FT DEPTH CHANGE, 9 KN

depth change, generally the required fairwater plane deflections are much larger than the stern plane deflections. As soon as only one plane limiter is saturated, the achieved decoupling is disturbed as can be seen from Fig. 100. This saturation occurs for a small depth change of only 3 ft. Obviously this scheme is not acceptable.

The error limitation eliminates these problems. When the depth error is limited to 2.5 ft. the initial fairwater plane angle stays within the specifications. On the other hand the "steady-state" angle for large depth changes turned out to be too small (4.5°), which leads to an unacceptable response time. To achieve both an acceptable initial and "steady-state" angle, the limit was kept at 2.5 ft for 1.5 sec and then increased to a final value of 12.5 ft at a constant rate.
The limiting function used is

$$LIM = 2.5 \text{ ft} \qquad t < 1.5$$

$$LIM = .2*(TIME-1.5)+2.5 \text{ ft} \qquad 1.5 \leq t \leq 53.5$$

$$LIM = 12.5 \text{ ft} \qquad t > 53.5$$

The final block diagram and the DSL-Program are given in App. D

Fig. 101 to 106 show a 10 ft and 100 ft depth change. In both cases the depth response is overdamped and satisfies the time requirements. The pitch is decoupled and the submarine remains at even keel.

It has been shown that this design approach has the following disadvantages:

- Speed range which is covered by individual

controller is very small. If the speed deviates too much from the design speed the system is no longer totally decoupled.

- The high speed dependence requires a complex controller with varying pole-zero combinations dependent on the speed variations (system dynamics).

Additionally the " Total decoupling scheme " is disturbed by the non-linear terms in the non-linear model, which are not contained in the linear approximation. Therefore this design approach will not be pursued further.

V. SIMULATION OF THE COMPENSATED NON-LINEAR MODEL

A. MODIFICATIONS FOR NON-LINEAR MODEL

Two of the linearizing assumptions were, that the forward speed is constant and that the submarine is always in trim.

The purpose of this chapter is to investigate the deviations from these assumptions and their influence on the behavior of the submarine during basic maneuvers like depth changes, turns, and turns during depth changes.
Generally trim is a moment, but it is commonly used in a different context :
- "In trim" has the meaning that the submarine maintains depth at a given speed with the desired pitch angle.
- "Out of trim" conditions are heavy or light forward, heavy or light aft, heavy or light overall, and combinations of these.
- "To trim" means to change the contents of the tanks by shifting water between tanks, flooding tanks from sea, or pumping water from tanks to sea.

The arrangement of depth control or auxiliary and trim tanks in the assumed submarine are such that any change in the depth control tank does not produce a moment, i.e. the depth control tank is at the center of gravity. The trim tanks are arranged as shown in Fig. 107.

1. Trim

From experience it is known that a submarine, which is in neutral conditions for a certain speed, " gains buoyancy"

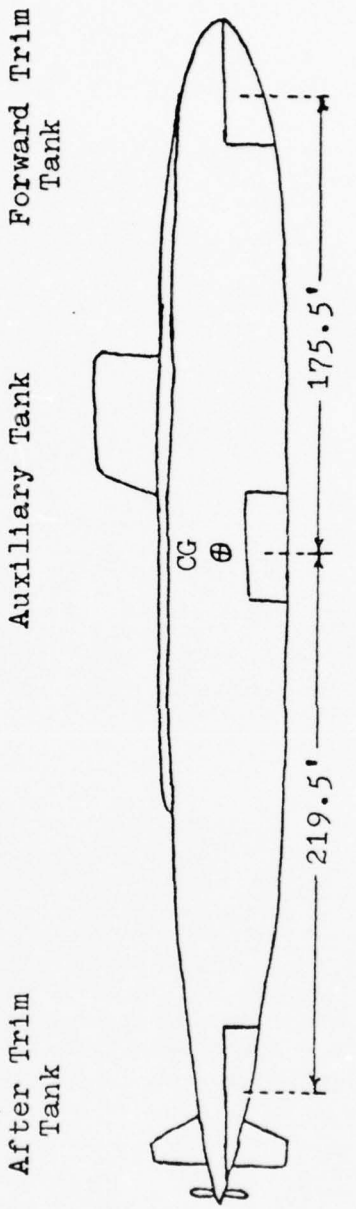

Figure 107 - CONFIGURATION OF TANKS

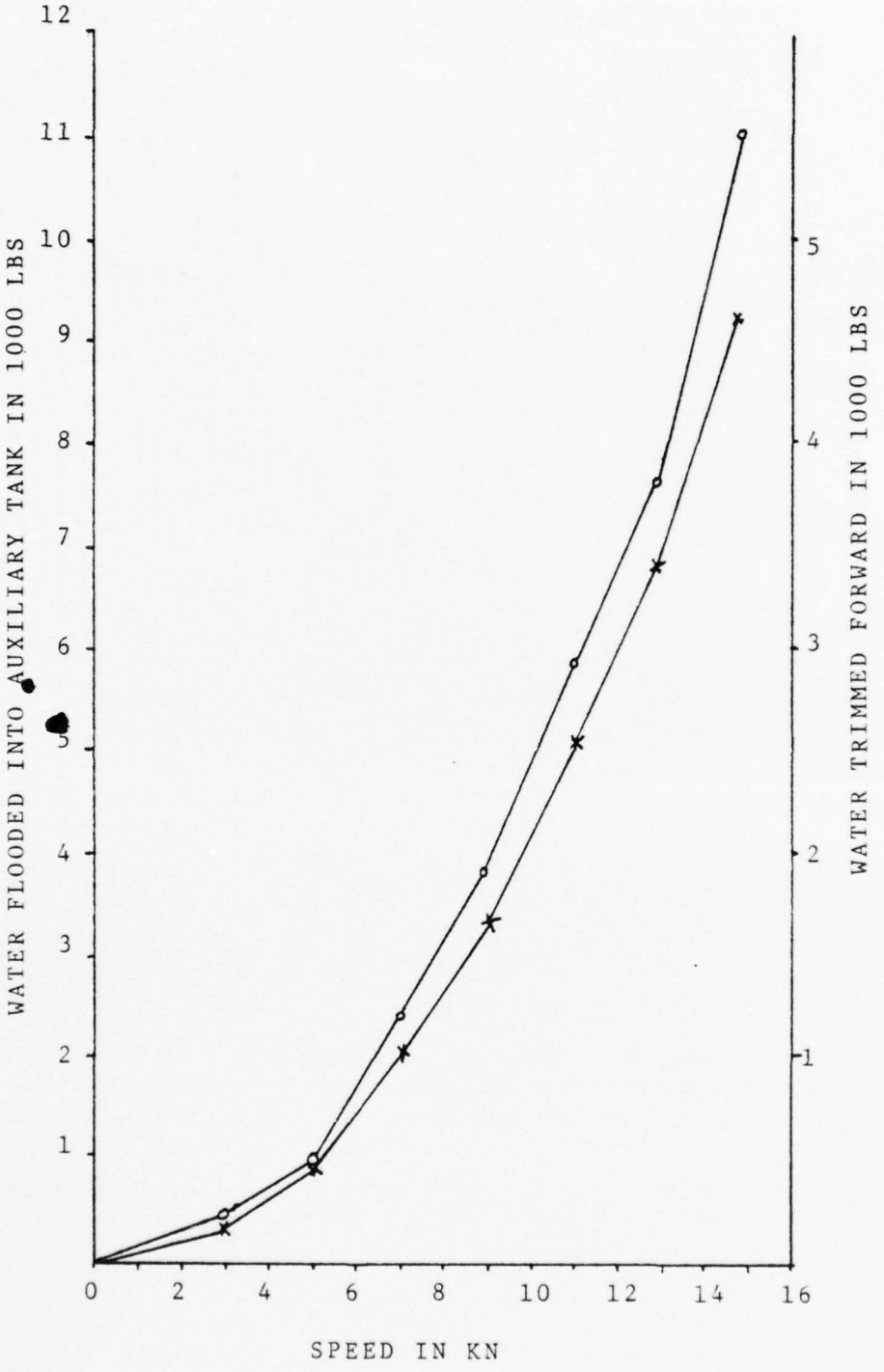

Figure 108 - CORRECTIONS FOR TRIM

and pitches up with increasing speed and vice versa due to dynamic forces acting on the hull, and therefore is no longer in trim as defined above.

Generally a submarine should be in trim at any time for a given commmand speed to avoid initial plane deflections. This guarantees availability of the full range of the planes for maneuvering. Although it is nearly impossible tc get the exact trim, it certainly is helpful to knew the corrections for different speeds.

Assuming neutral conditions for 0 kn speed, the corrections for trim were found by trial and error. The values shcwn in Fig. 108 guarantee an approximately neutral trim.

The results confirmed the tendencies observed in practice.

2. Mechanical constraints

The design specifications define the maximum plane deflections as a function of speed. While the ordered revolutions of the shaft remain constant, the actual forward speed (in direction of the x-axis of the body-fixed coordinate system) decreases during maneuvers due to drag, which is produced by the deflected planes, the pitch, the roll, and the yaw.

A feedback of the actual forward speed U instead of the ordered speed UC modifies the error limiter to

$$LIM = -1.6655*U + 59.6875$$

and allows the use of the maximum plane deflections as a function of the actual speed.

B. TEST RUNS

For the test runs to follow the designed compensator, the modified limiter, and the trim values for the ordered speed according to Fig. 108 are implemented in the non-linear model.
The program and final block diagram are given in App. D.

1. 100 ft depth changes

Table 14 lists the results of the simulations from 7-15 kn. Comparing these results with Table 13 it is obvious that the dynamic behavior of both the linear and the non-linear model are essentially the same.
Due to the initially large plane deflections the speed decreases by more than 1 kn for all initially ordered speeds until the ordered depth is reached. At this time the plane deflections get small and the submarine accelerates to the original speed. As predicted, the initial plane angles are increased with decreasing speed.
Although the reduced speeds cause slightly increased overshoots, the designed controller is still able to satisfy all the design specifications.

2. Turns

One of the more difficult maneuvers with a submarine is to change the depth and the course simultaneously. It is of interest to study the behavior of the submarine in a turn

first without depth change, because the flow dynamics in a turn change significantly.

The transverse motion of the submarine causes cross flow velocities. If the submarine had no appendices this crossflow would produce no pitch or other forcing moment on the hull. But due to the conning tower and other appendices the flow over the upper portion of the hull slows down. A wake shed from the conning tower also effects the velocity distribution aft.

Table 14 - 100 ft depth change

Run	Speed	Depth reached after sec	Overshoot in ft	Max Pitch in ^{o}	Max DB in ^{o}	Max DS in ^{o}	Figure
1	7	126.0	6.10	1.43	34.38	4.33	109-111
2	9	99.0	4.46	1.52	33.5	4.6	112-114
3	11	86.0	3.1	1.39	28.7	4.2	115-117
4	13	83.0	1.68	1.17	23.5	3.57	118-120
5	15	87.0	0.90	0.91	17.7	2.78	121-123

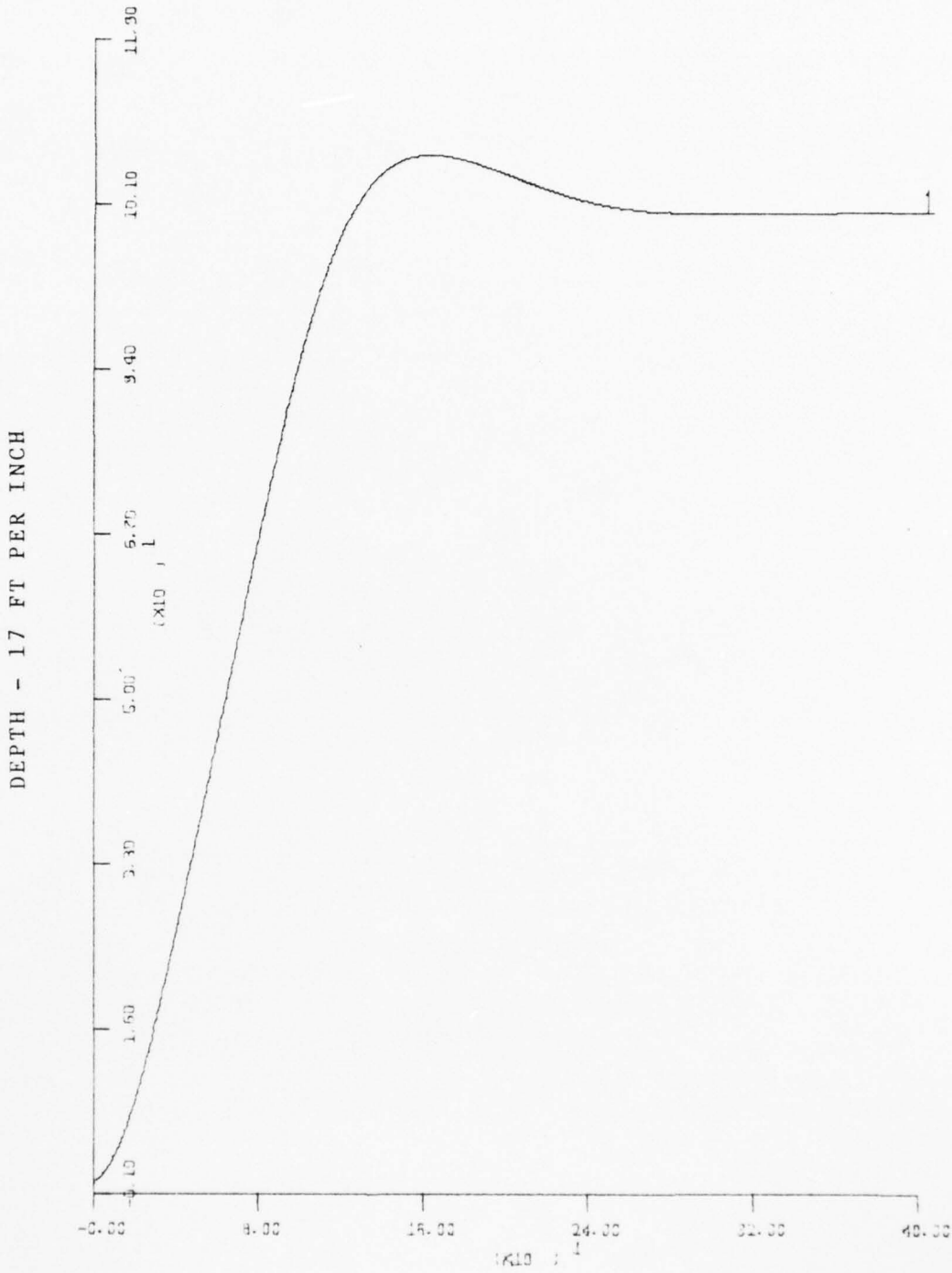

Figure 109 - RUN 1
100 FT DEPTH CHANGE, 7 KN

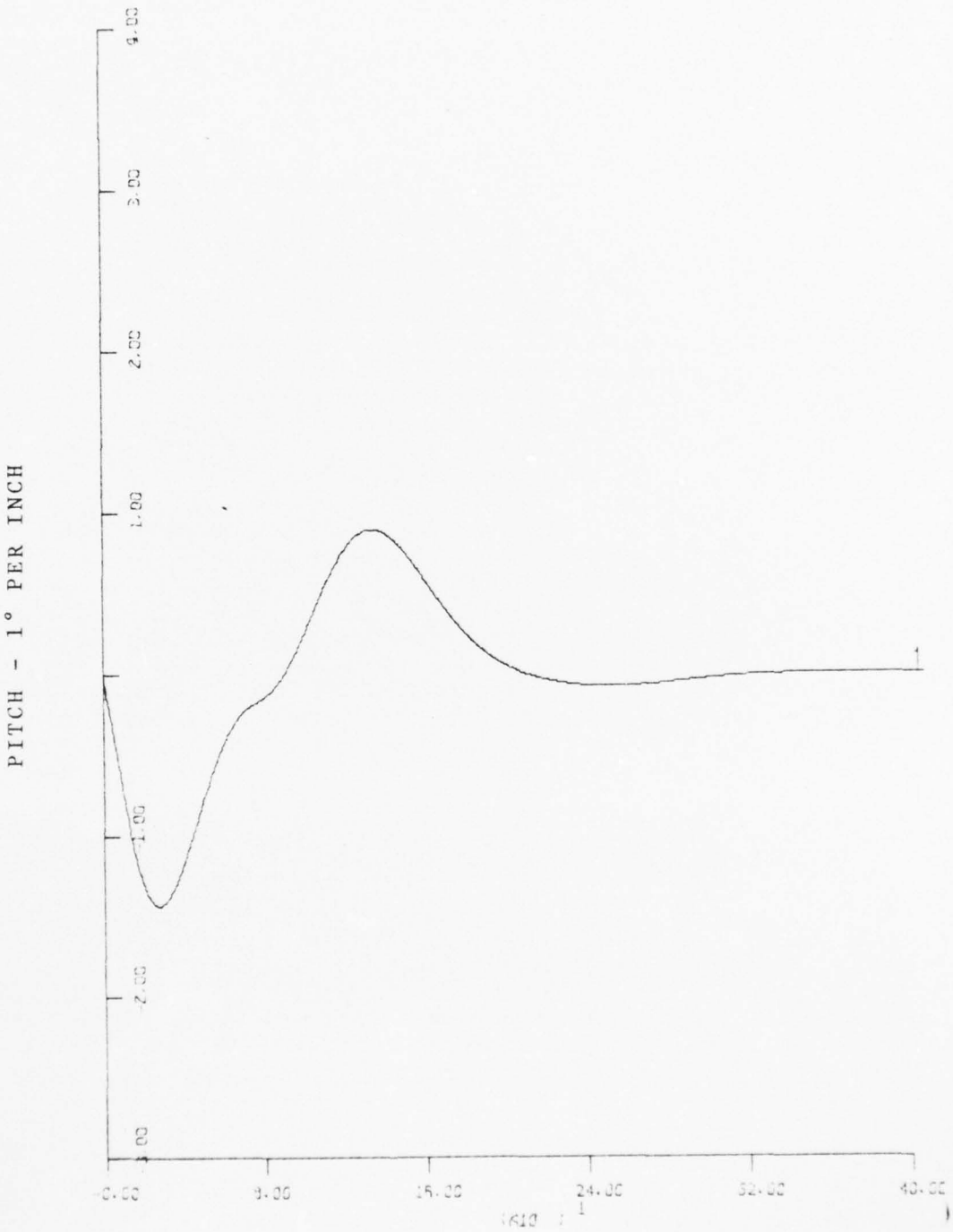

Figure 110 - RUN 1
100 FT DEPTH CHANGE, 7 KN

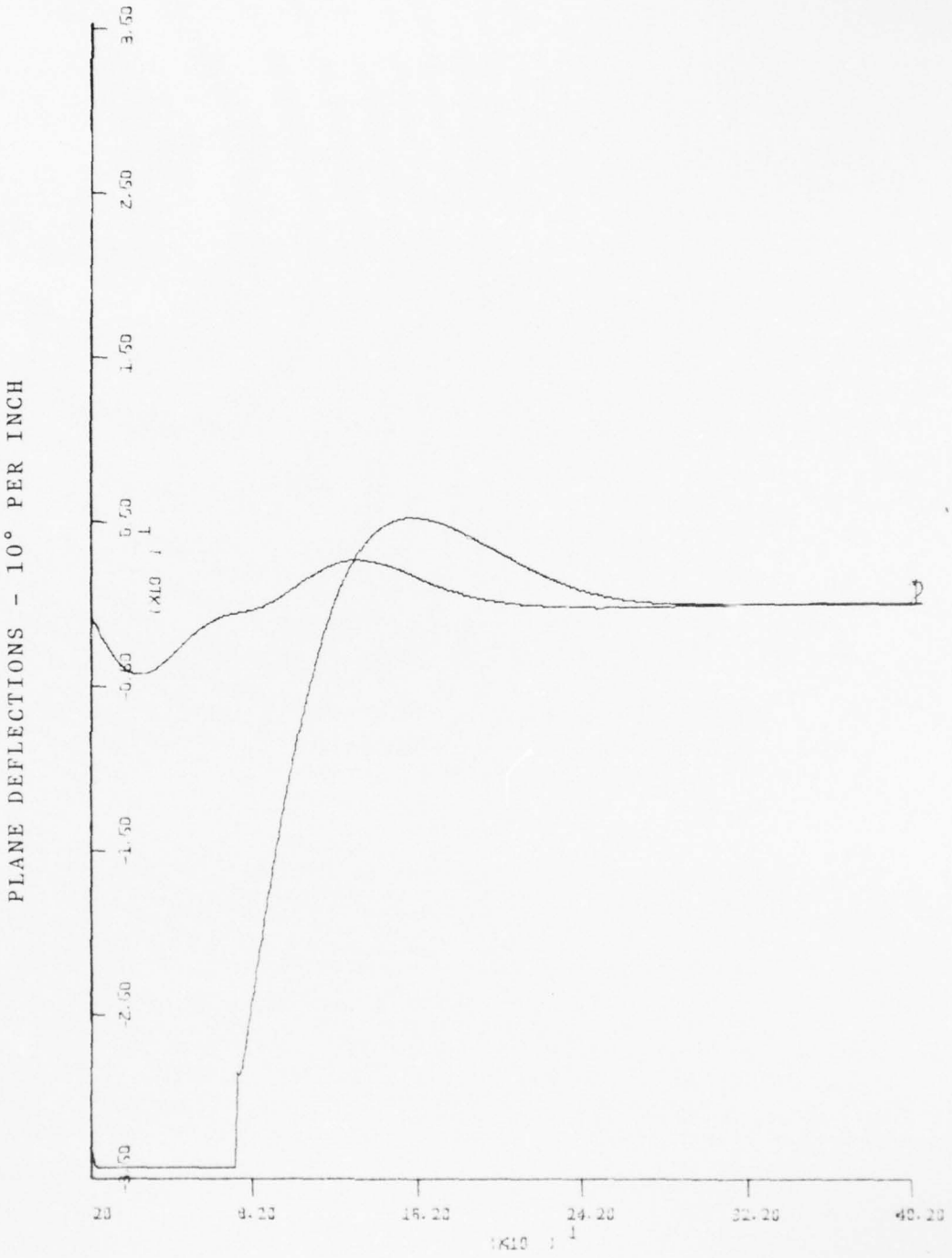

Figure 111 - RUN 1
100 FT DEPTH CHANGE, 7 KN

AD-A038 758 NAVAL POSTGRADUATE SCHOOL MONTEREY CALIF F/G 13/10.1
AUTOMATIC DEPTH AND PITCH CONTROL FOR SUBMARINES.(U)
DEC 76 V NITSCHE, K J LUESSOW

UNCLASSIFIED NL

3 OF 3
AD A038758

END

DATE FILMED
5-77

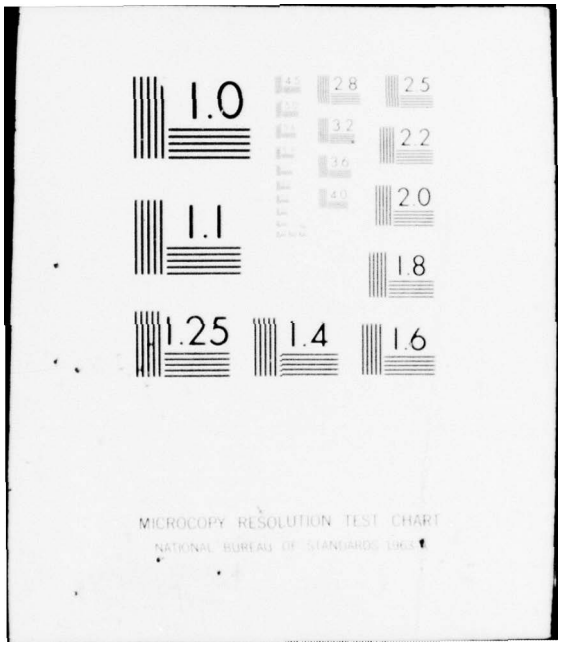
1.0
1.1
1.25
1.4
1.6
2.8
2.5
3.2
2.2
3.6
2.0
4.0
1.8
MICROCOPY RESOLUTION TEST CHART
NATIONAL BUREAU OF STANDARDS 1963-A

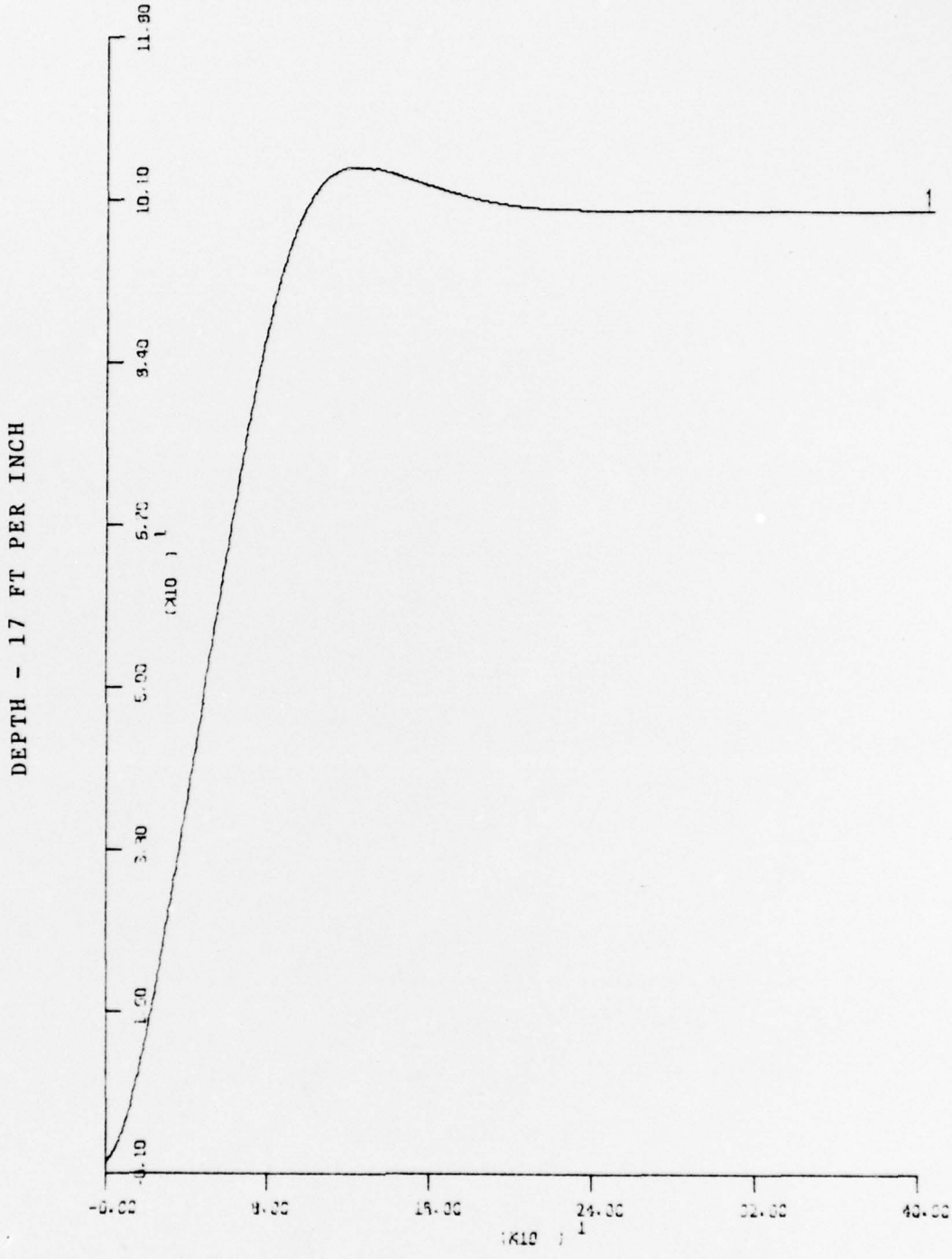

Figure 112 - RUN 2
100 FT DEPTH CHANGE, 9 KN

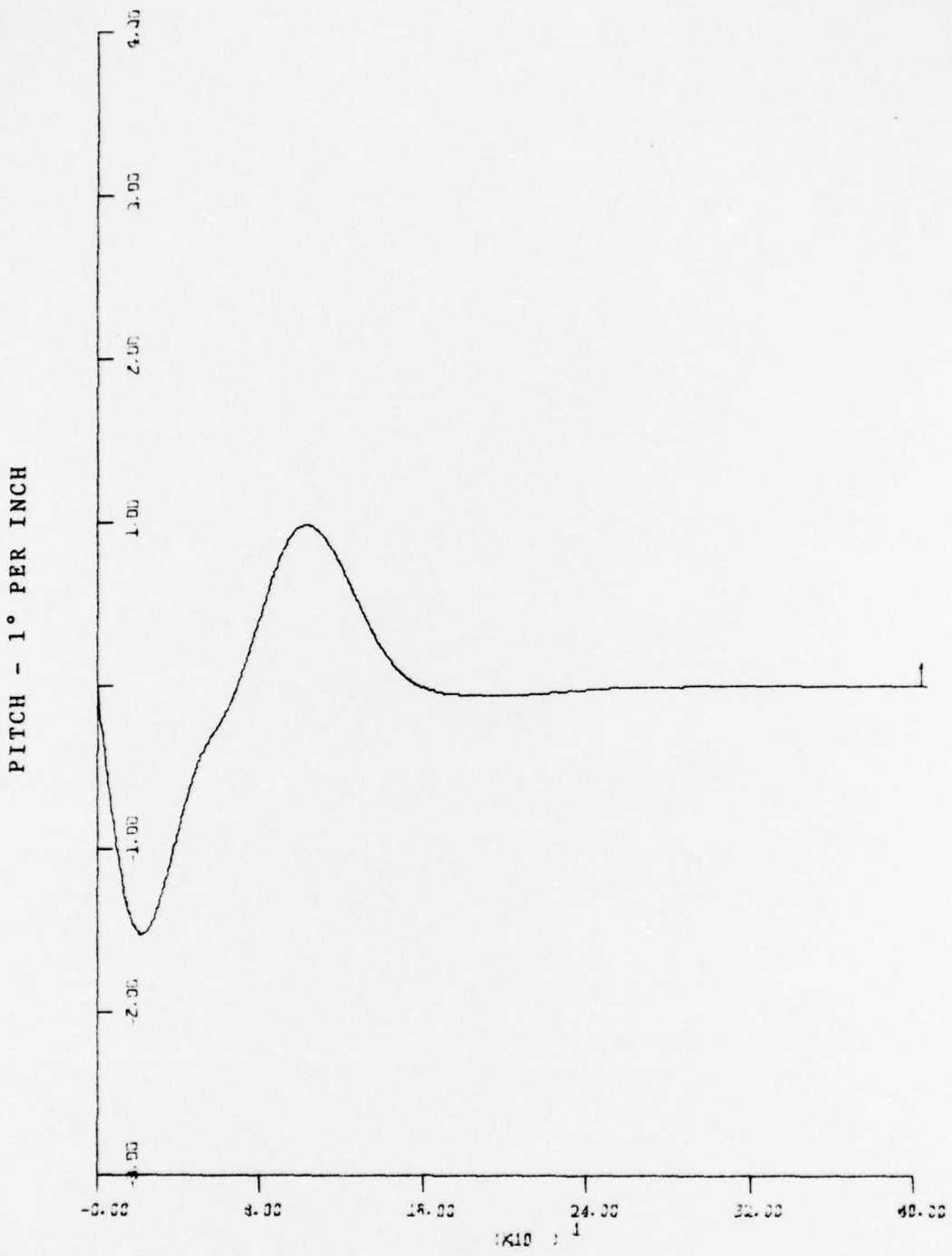

Figure 113 - RUN 2
100 FT DEPTH CHANGE, 9 KN

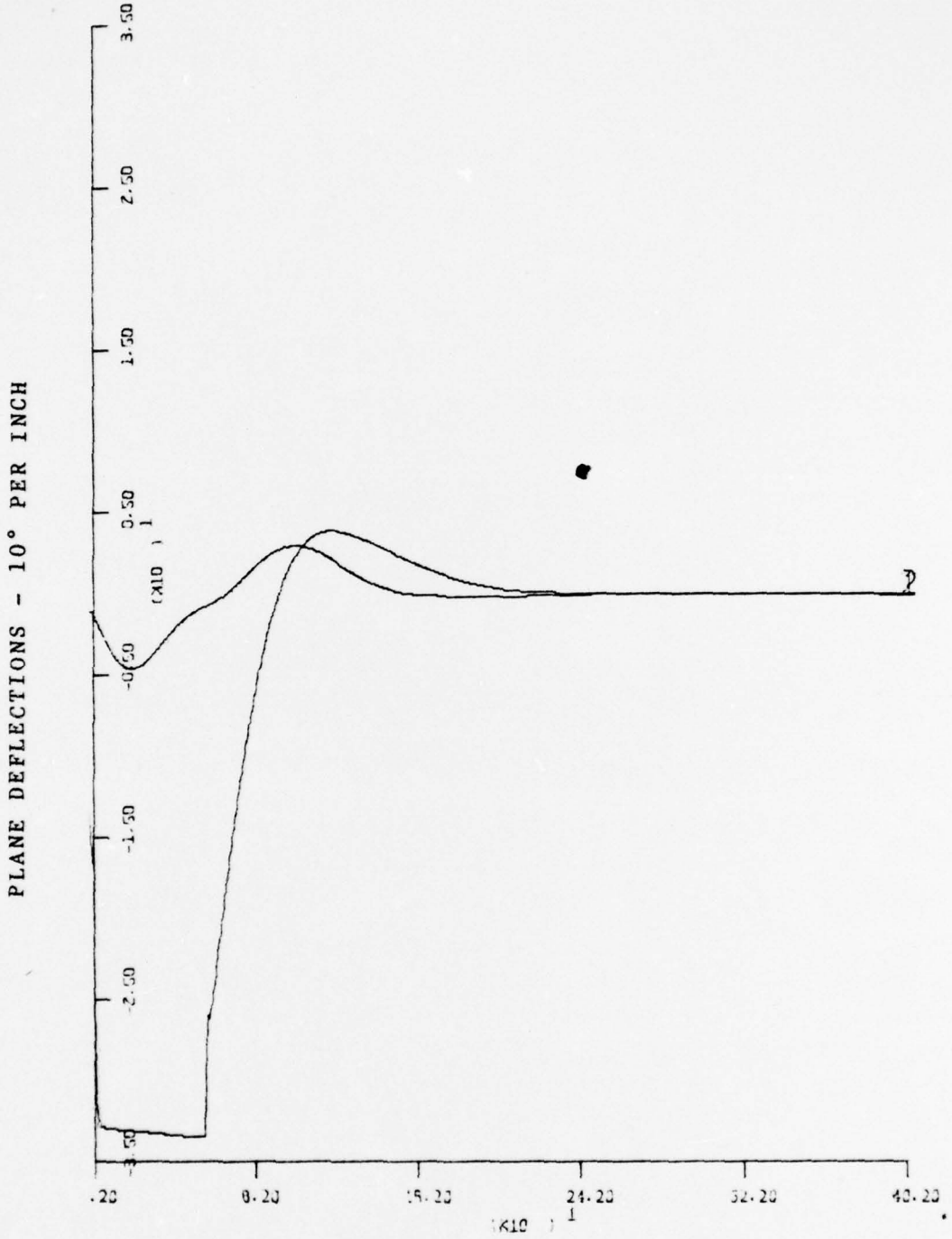

Figure 114 - RUN 2
100 FT DEPTH CHANGE, 9 KN

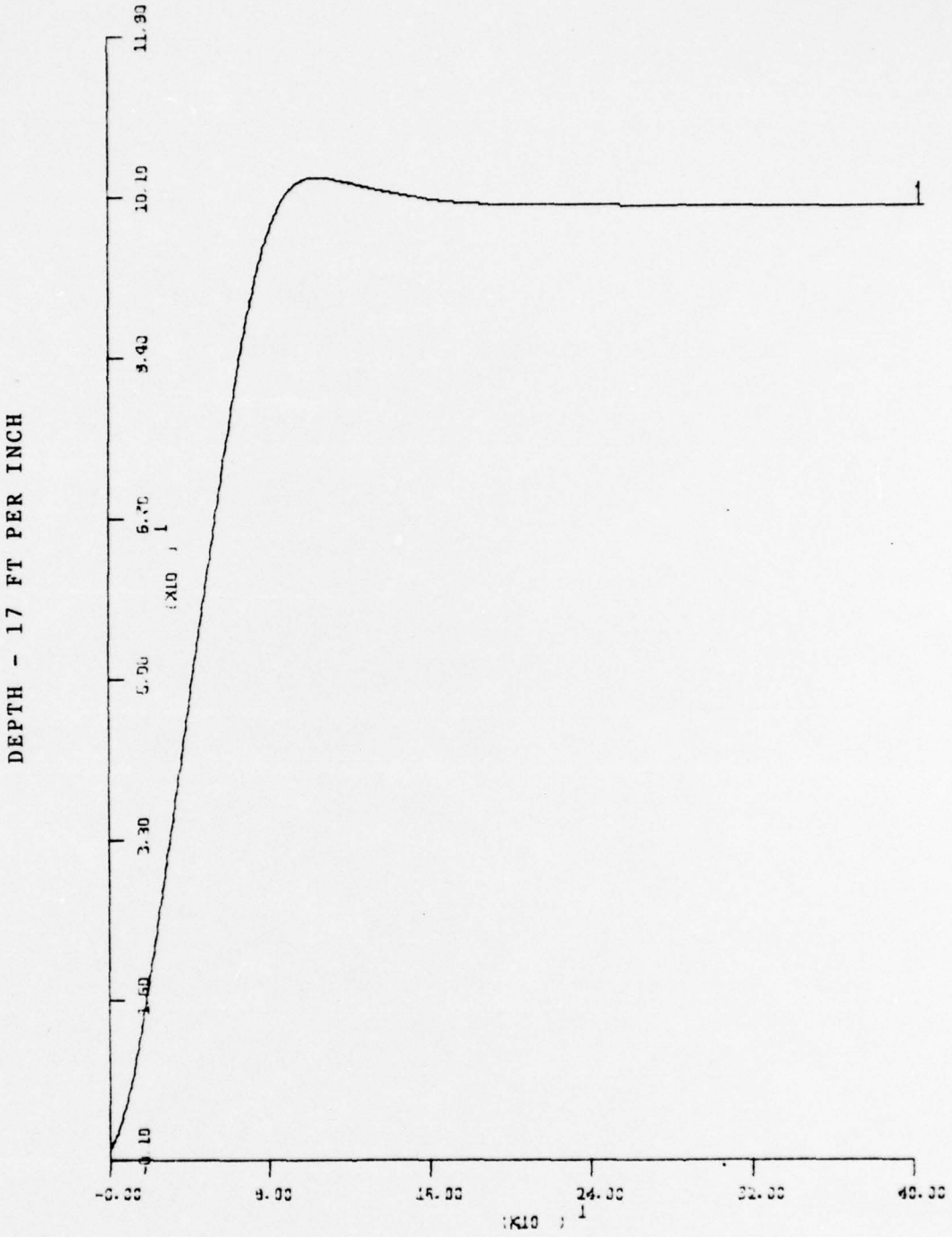

Figure 115 - RUN 3
100 FT DEPTH CHANGE, 11 KN

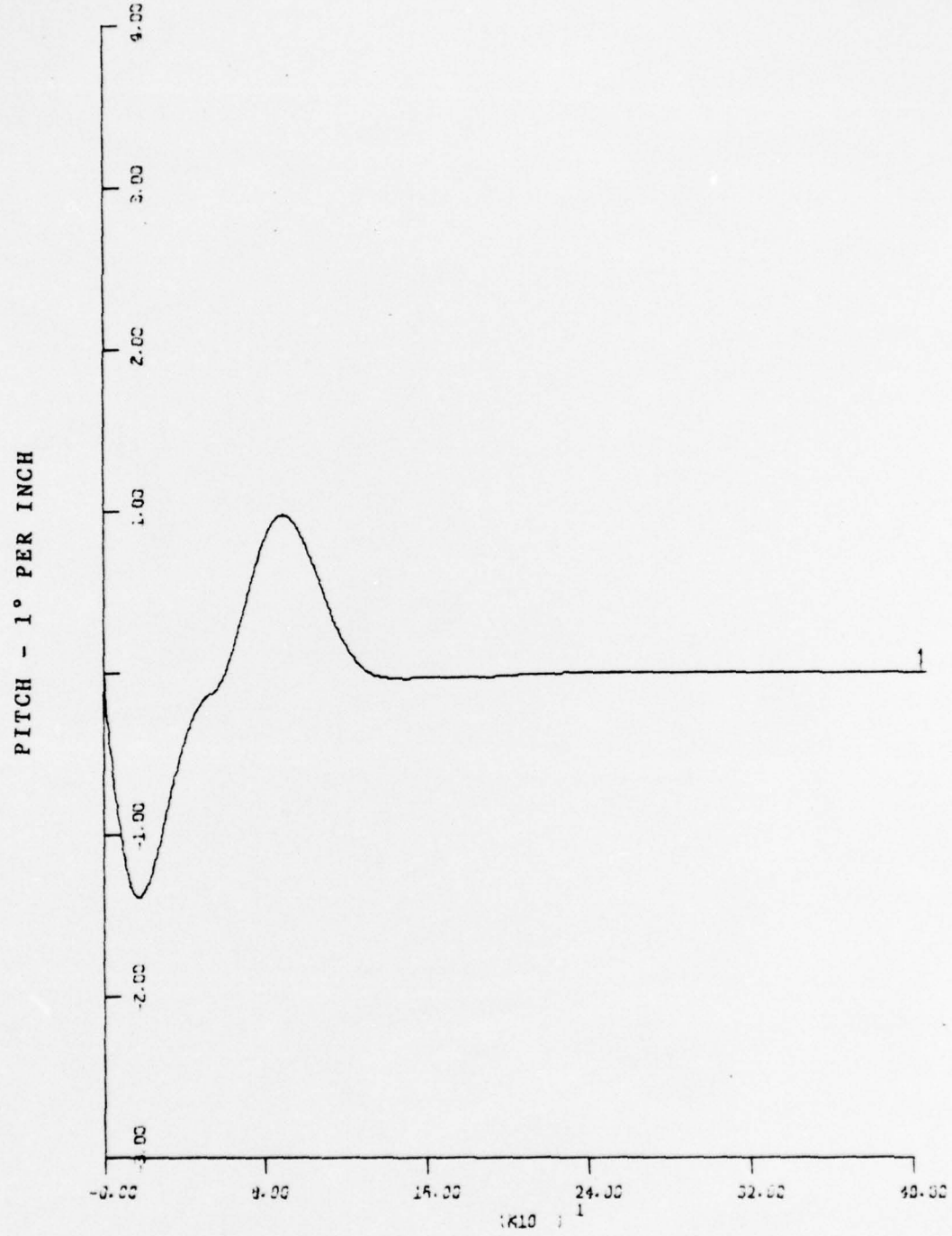

TIME - 80 SEC PER INCH

Figure 116 - RUN 3
100 FT DEPTH CHANGE, 11 KN

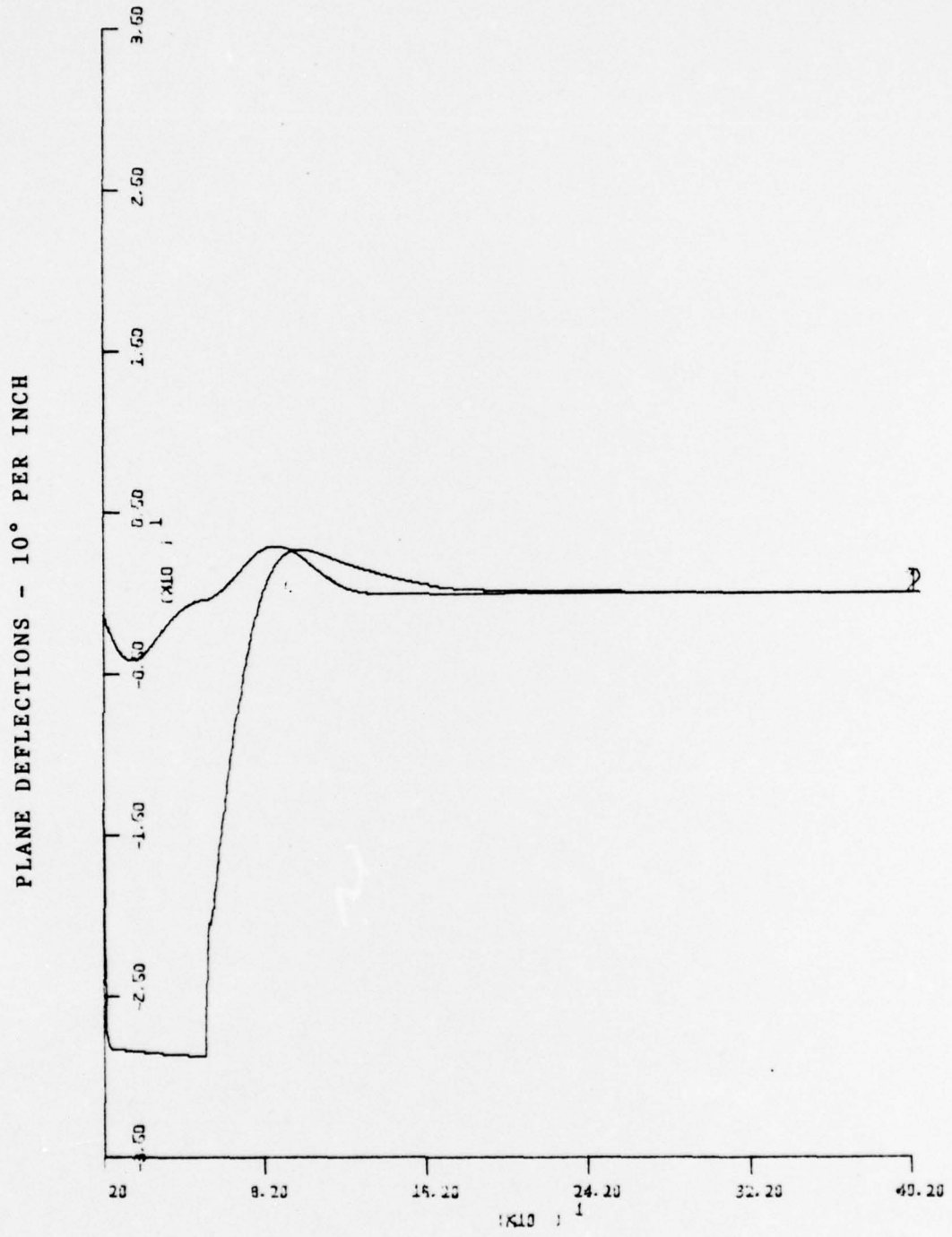

Figure 117 - RUN 3
100 FT DEPTH CHANGE, 11 KN

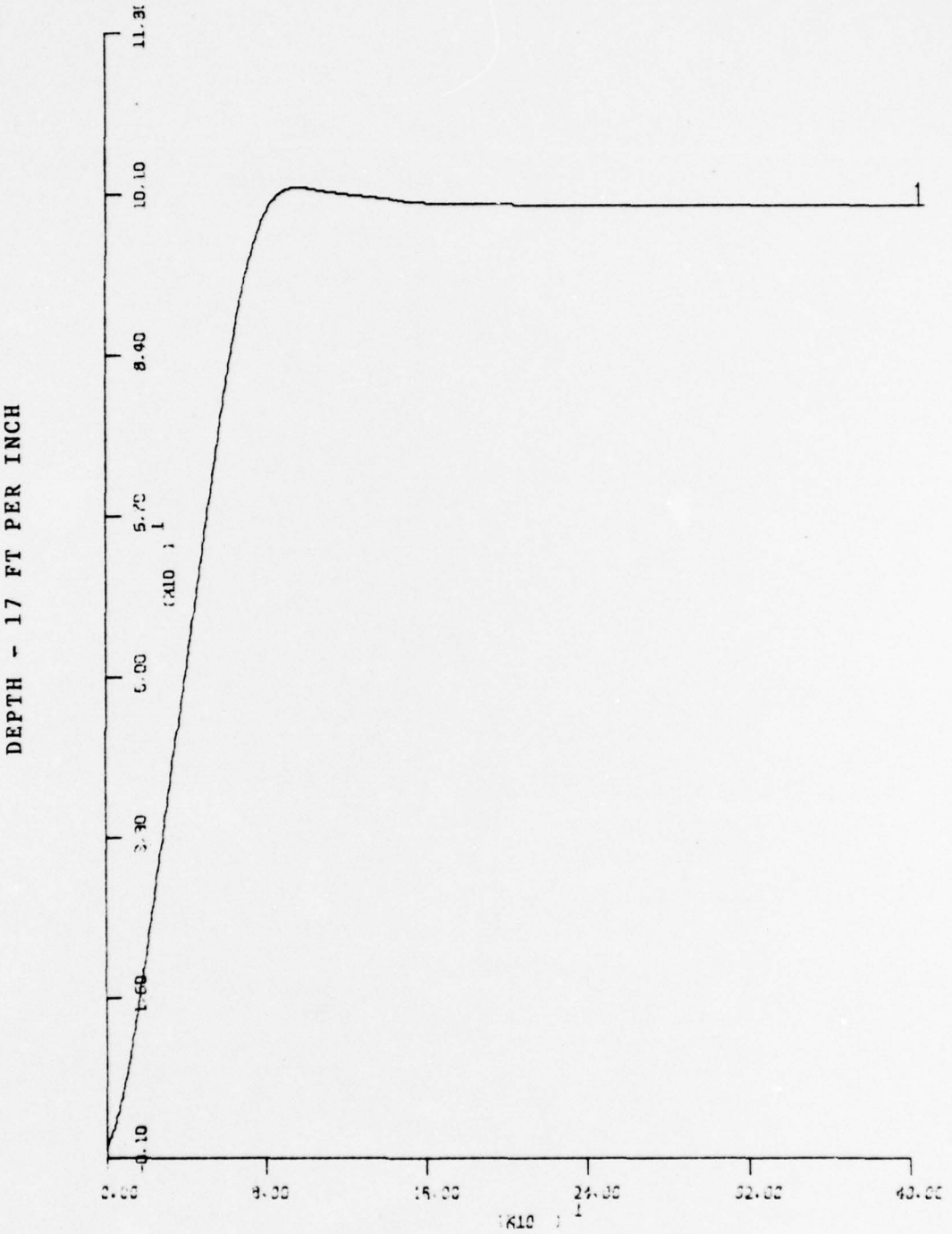

Figure 118 - RUN 4
100 FT DEPTH CHANGE, 13 KN

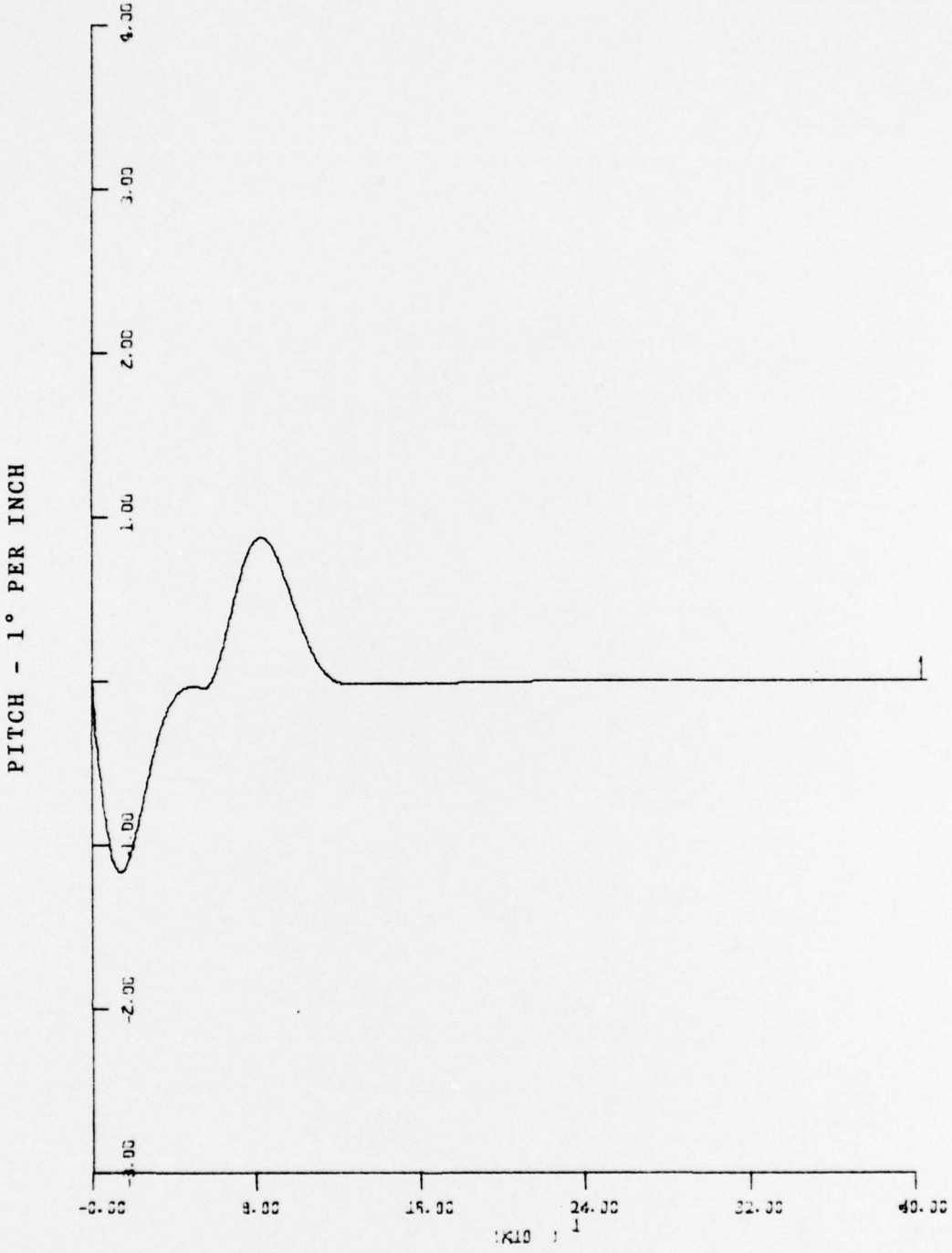

Figure 119 - RUN 4
100 FT DEPTH CHANGE, 13 KN

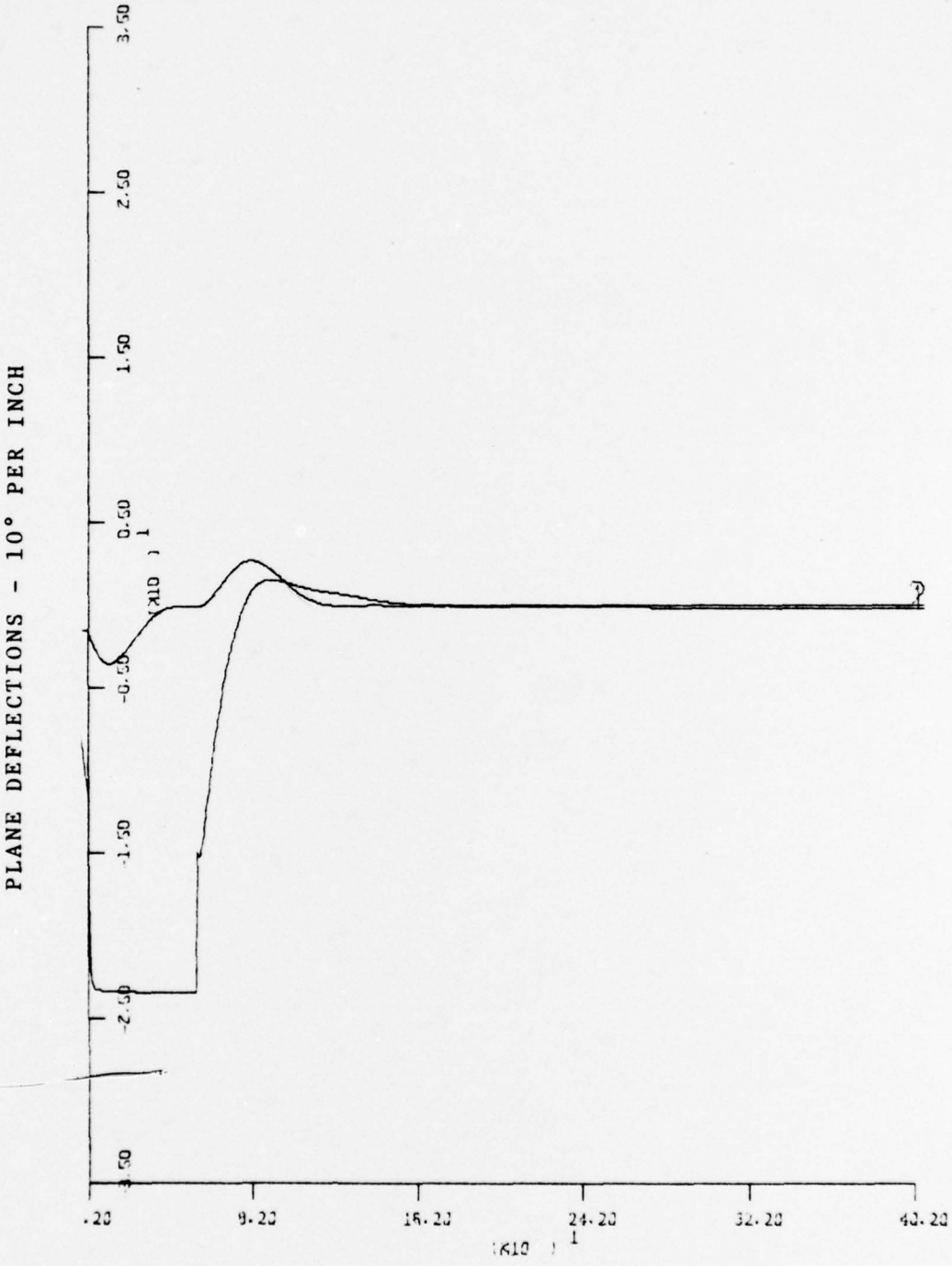

Figure 120 - RUN 4
100 FT DEPTH CHANGE, 13 KN

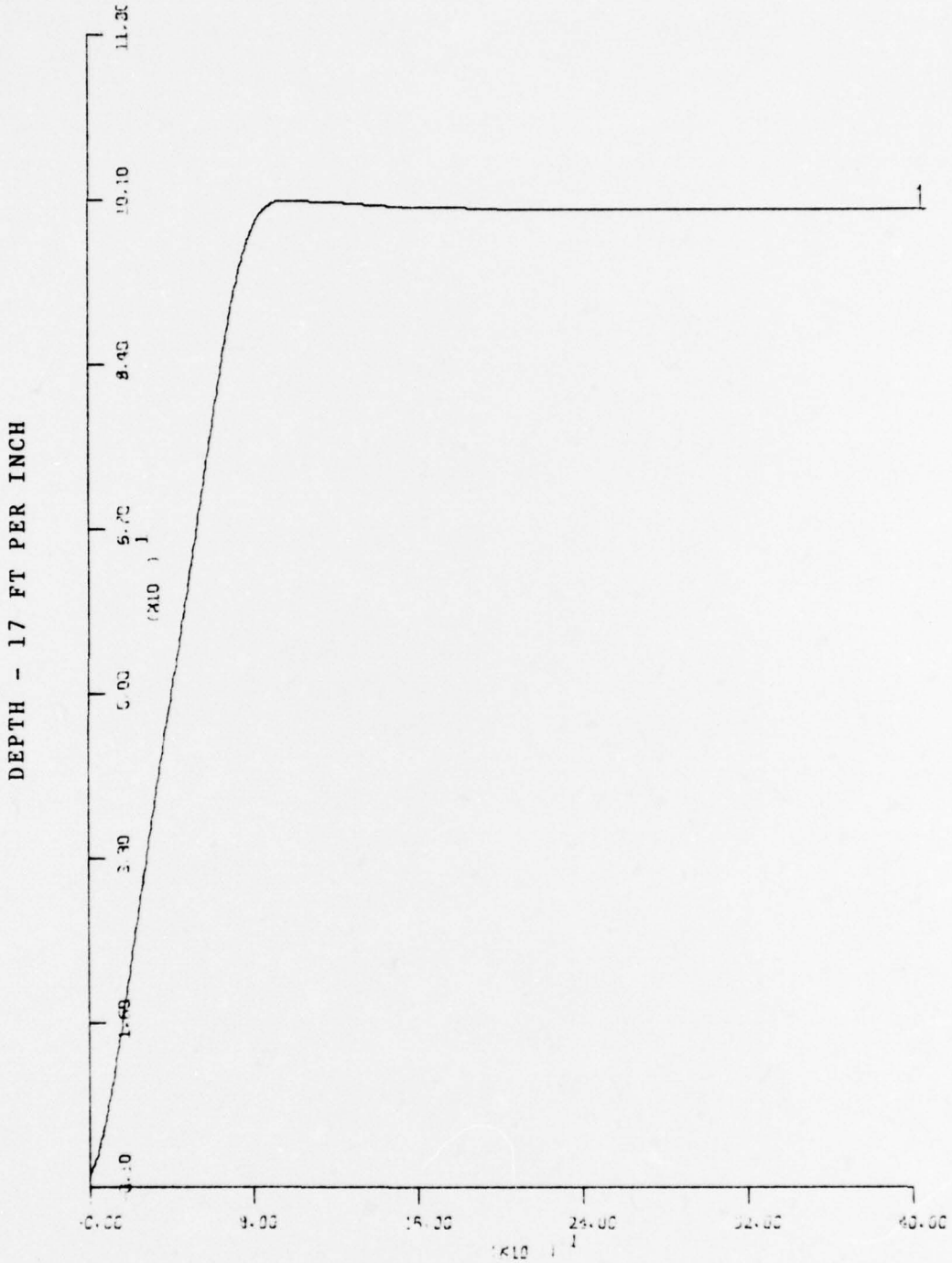

Figure 121 - RUN 5
100 FT DEPTH CHANGE, 15 KN

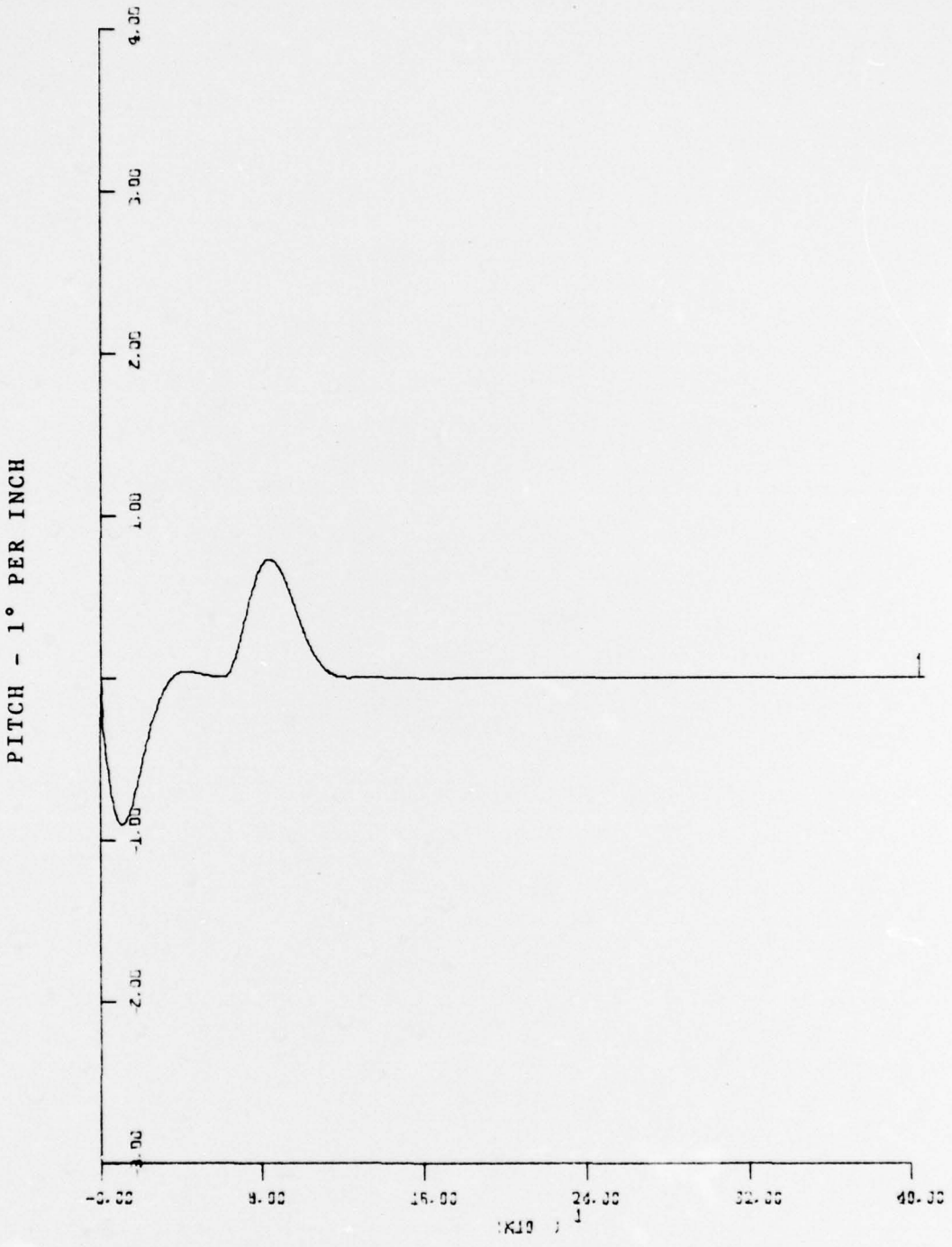

Figure 122 - RUN 5
100 FT DEPTH CHANGE, 15 KN

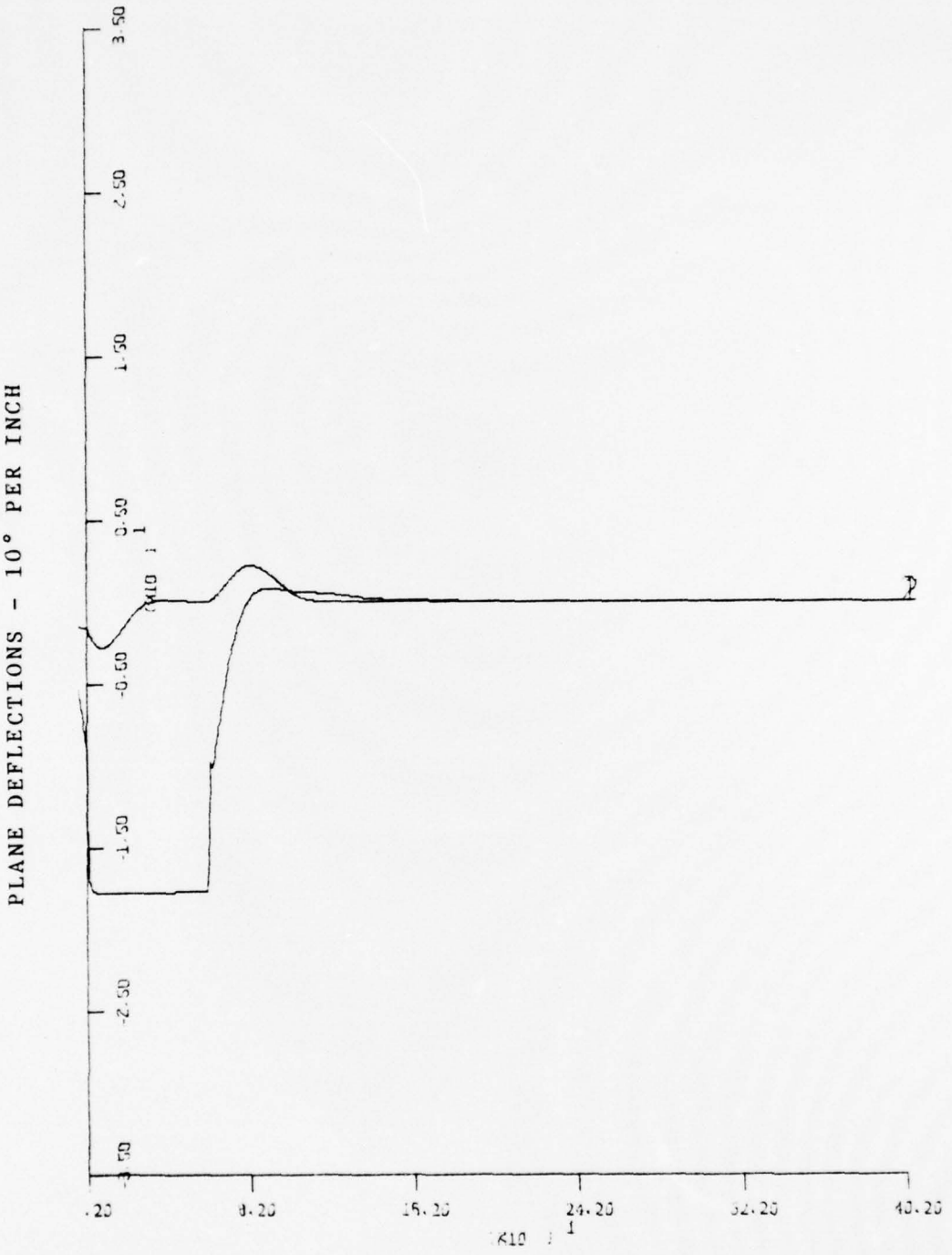

Figure 123 - RUN 5
100 FT DEPTH CHANGE, 15 KN

These effects combine to cause vertical forces and pitching moments. Another important factor is the loss of speed. The deflected rudder causes additional drag, the hull is moving at an angle of attack to the flow, where the drag is larger than at zero angle of attack, and finally, the propeller is operating at a higher loading and therefore is less efficient.

At an ordered speed of 11 kn three different rudder angles were applied over a period of 100 s and then reset to zero. The results are shown in Table 15. The above discussed effects are reflected in Fig. 124-135. The submarine pitches up to a steady-state angle, the depth is kept with a small steady-state error, and the speed decreases significantly. All deviations from the equilibrium state increase with increasing rudder deflection. When the rudder is reset to zero pitch, depth, and speed return to their original values.

Table 15 - Course changes

Rudder angle in °	Maximal deviation in			Yaw in °
	Speed in kn	Depth in ft	Pitch in °	
10	1.37	1.5	1.4	92.6
20	2.89	3.1	3.2	124.0
30	4.05	3.9	5.1	140.5

Judging from our experience on manually controlled

submarines the performance of the controller even for hard turns is very satisfactory.

After both maneuvers have been studied independently the combination of them leads to Fig. 136-141 and Table 16. It is obvious that both parts of the combined maneuver influence each other. The time required to reach the ordered depth increased with increasing rudder angle. At the same time the yaw-angle reached after 400 s decreased by about 20° compared to a turn without depth change. The overshoot experienced stayed still within the design specifications.

Table 16 - Course and depth change of 100 ft

Rudder angle in °	Depth reached in sec	Max pitch in °	Overshoot in ft	Max speed deviation in kn	Yaw in °
10	89	1.54	2.97	2.08	70.7
20	94	2.51	3.32	2.94	102.8
30	98	3.27	4.77	3.91	120.3

3. Cut of trim conditions

All test runs performed indicated that the speed was reduced due to additional drag introduced by all maneuvers. From Fig. 108 one must conclude that the submarine is not in trim during maneuvers. This out of trim condtion has clearly an effect on the performance of the submarine. But as the controller is capable of handling these deviations it is not advisable to try to trim the boat temporarily during

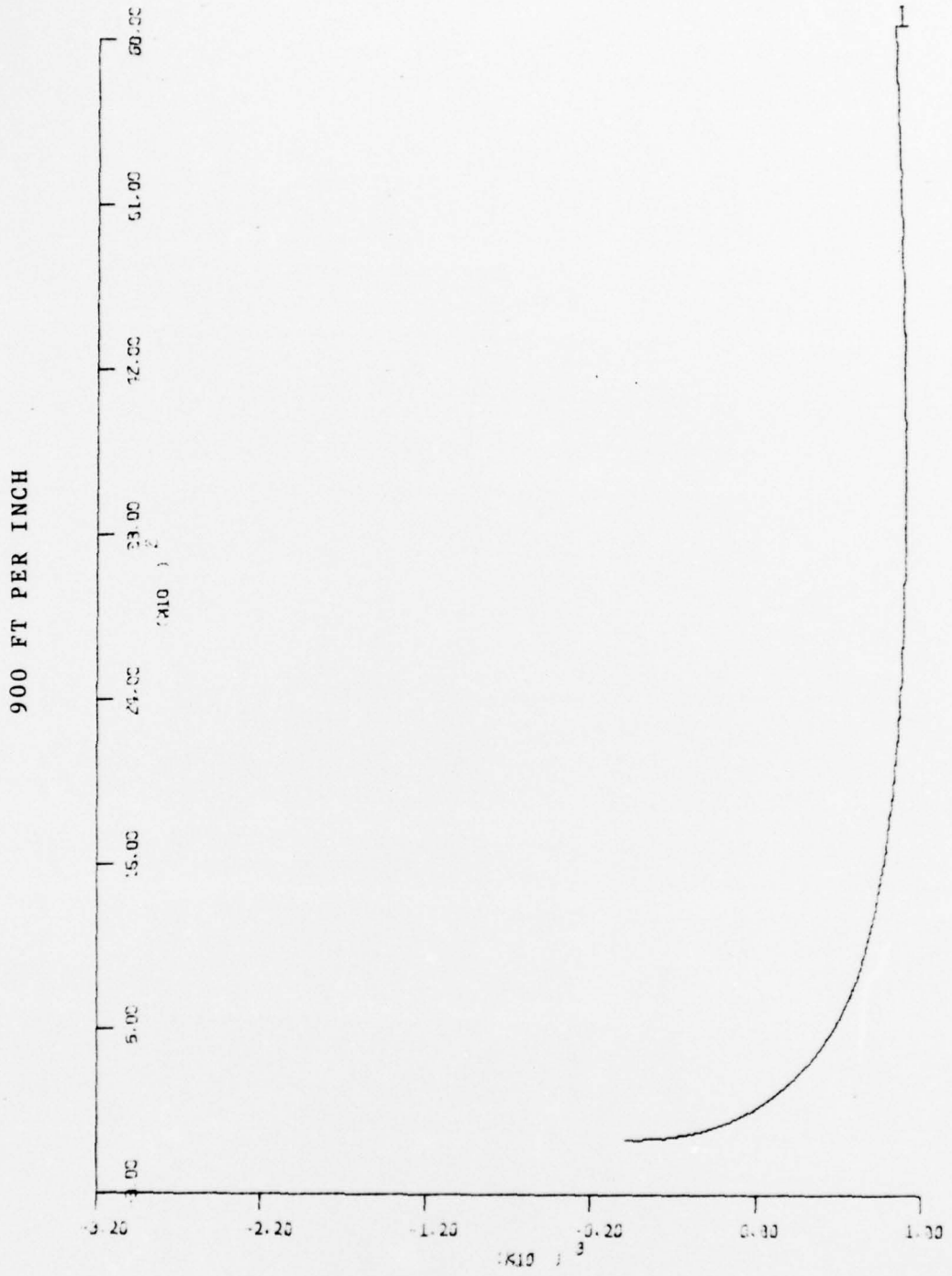

Figure 124 - COURSE CHANGE, HORIZONTAL PLANE
RUDDER ANGLE = 10°, SPEED = 11 KN

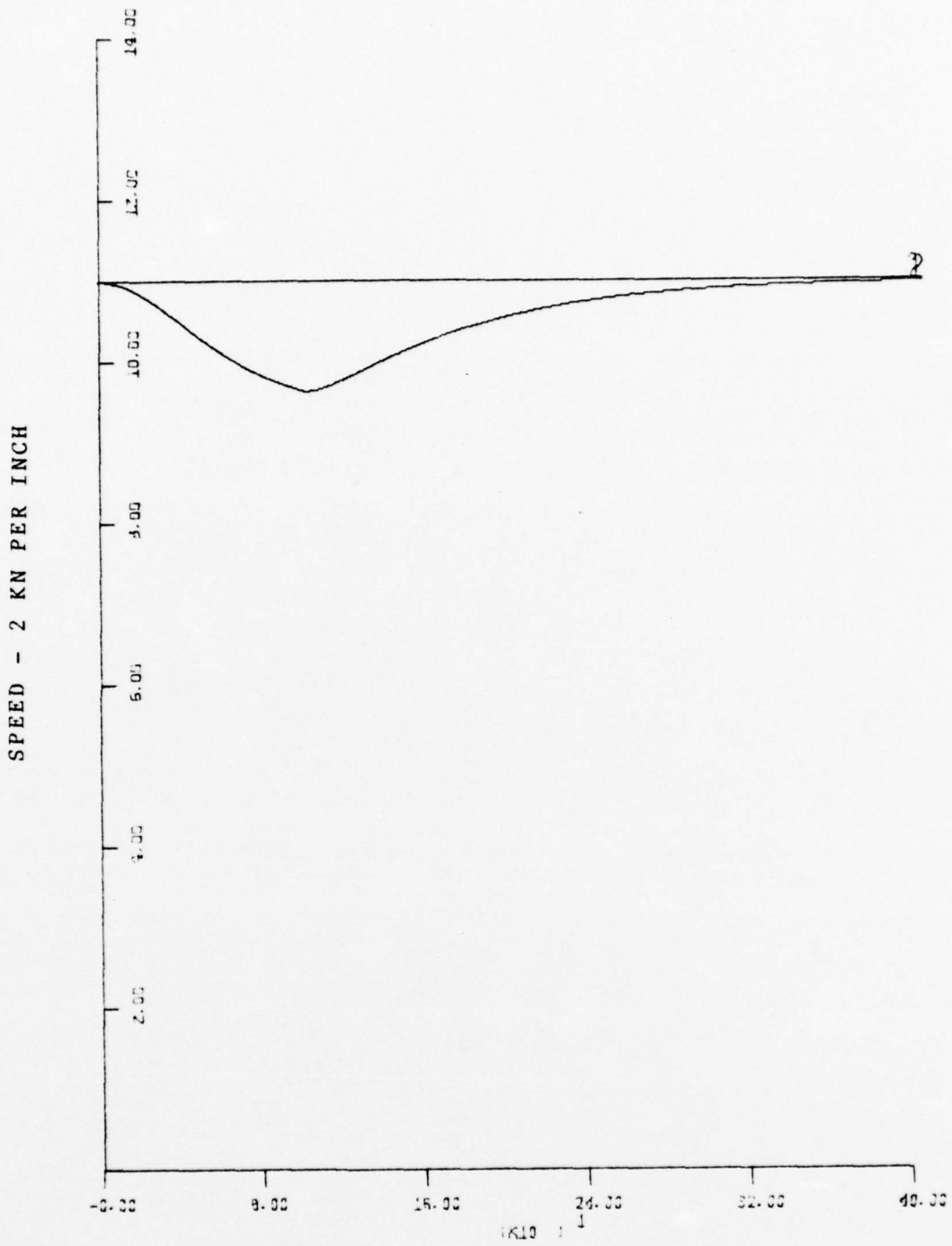

Figure 125 - COURSE CHANGE
RUDDER ANGLE = 10°, SPEED = 11 KN

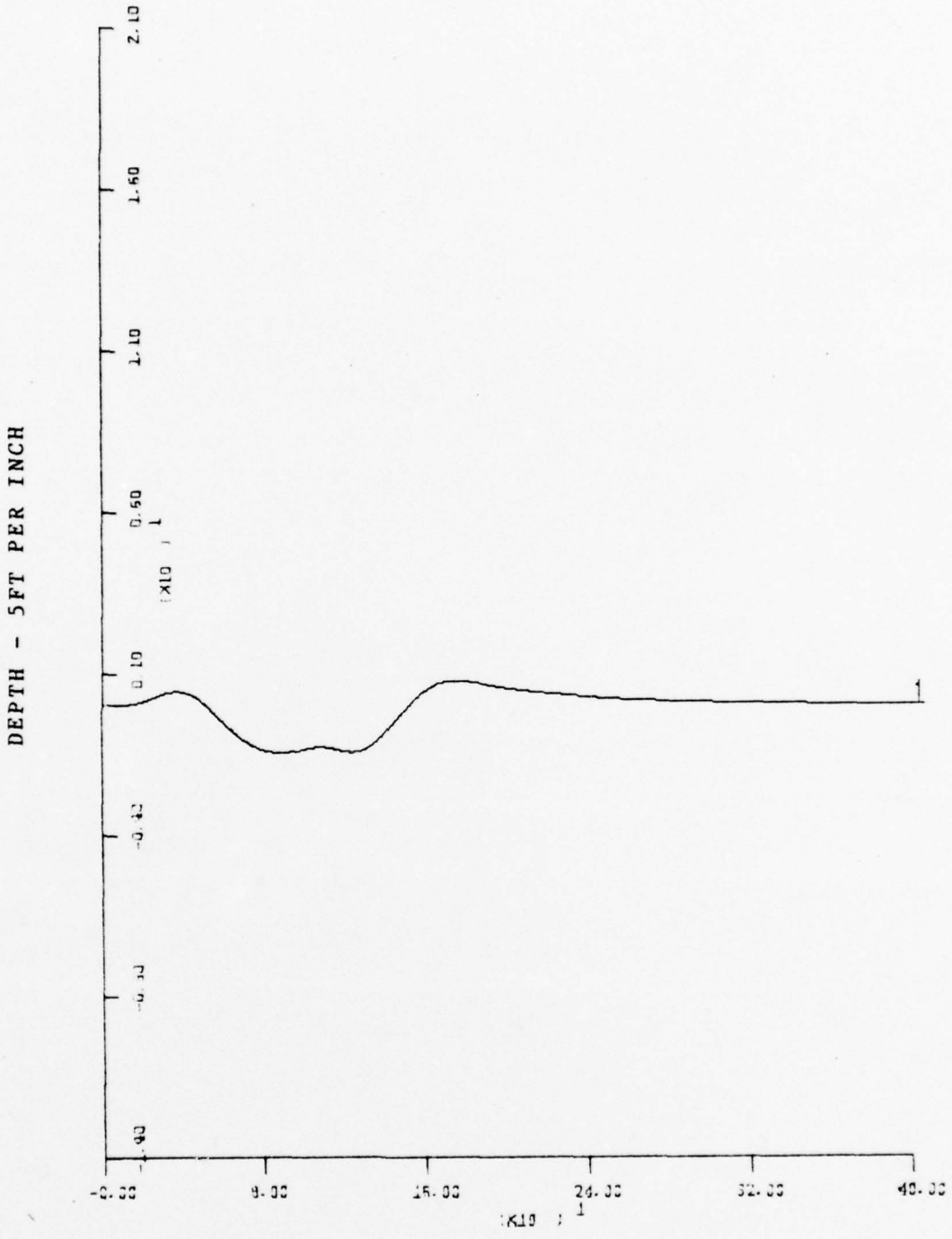

Figure 126 - COURSE CHANGE
RUDDER ANGLE = 10°, SPEED = 11 KN

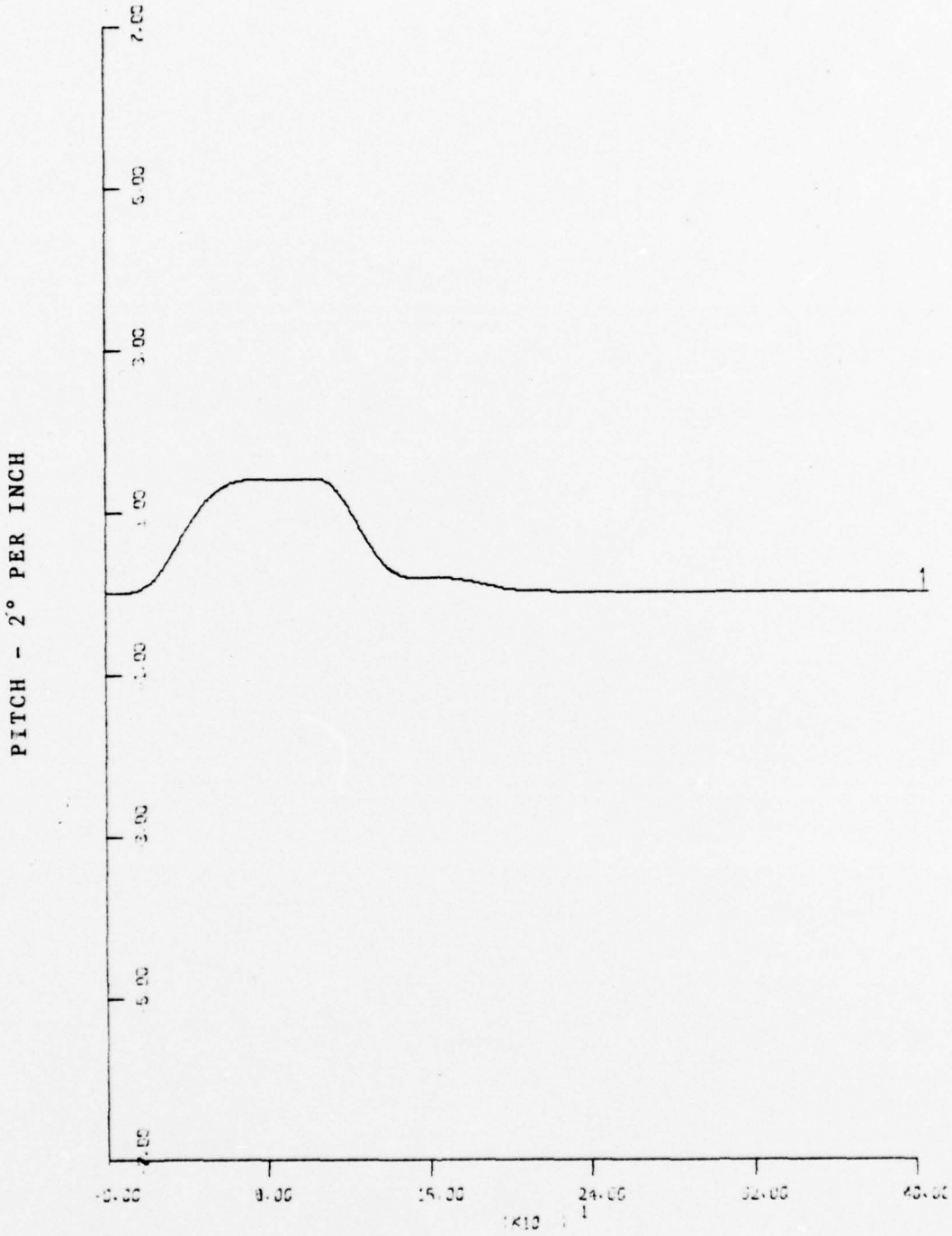

Figure 127 - COURSE CHANGE
RUDDER ANGLE = 10°, SPEED = 11 KN

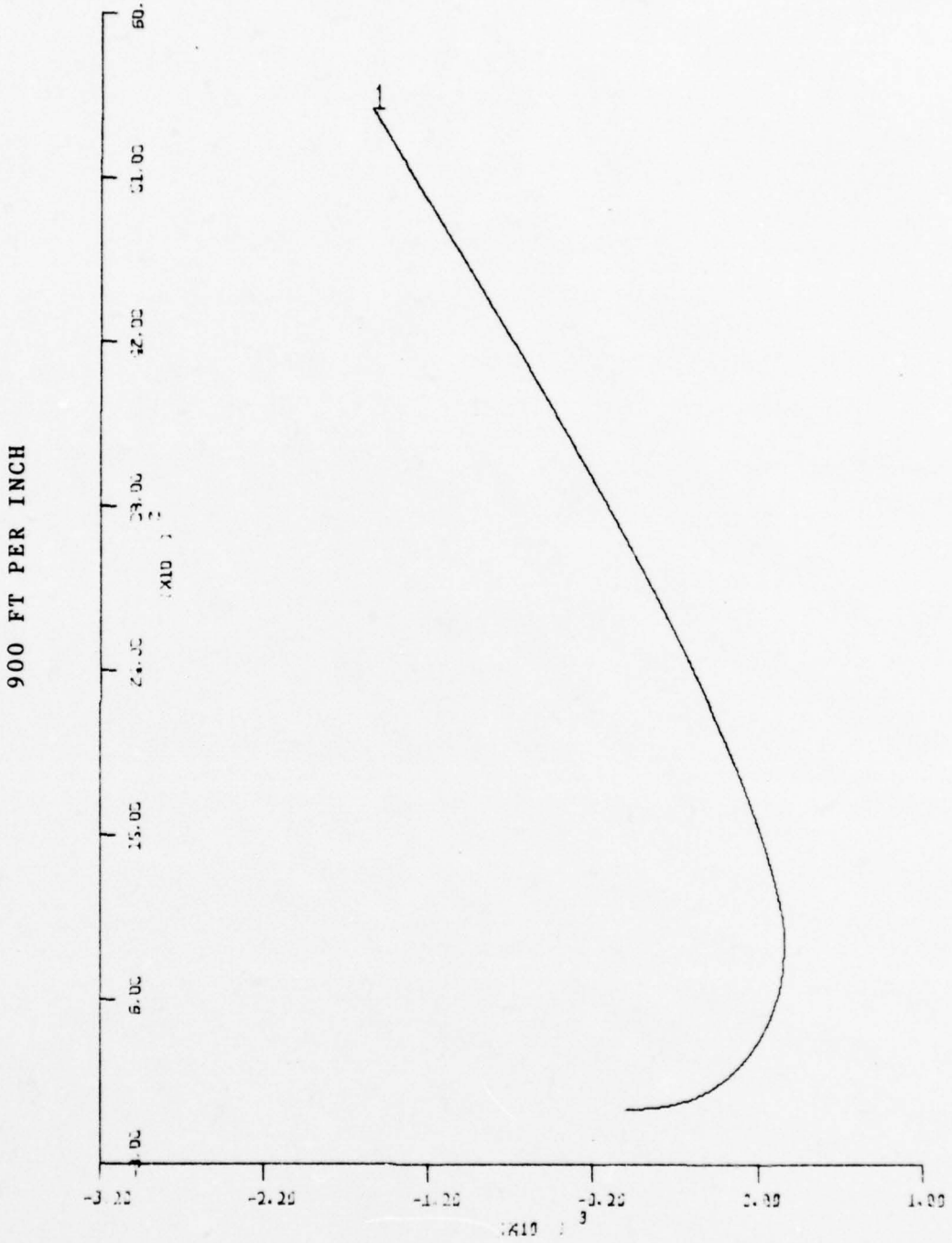

Figure 128 - COURSE CHANGE, HORIZONTAL PLANE
RUDDER ANGLE = 20°, SPEED = 11 KN

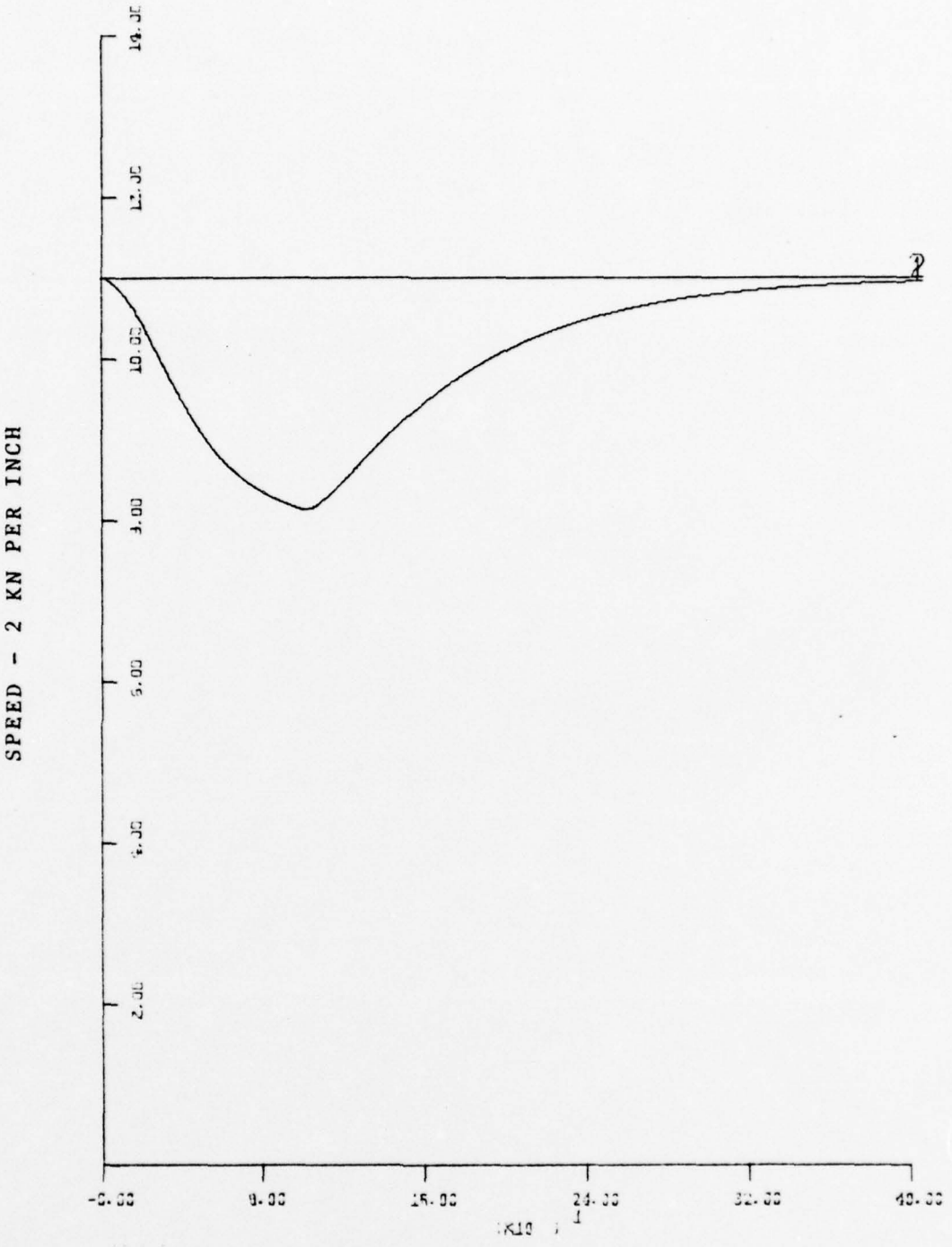

Figure 129 - COURSE CHANGE
RUDDER ANGLE = 20°, SPEED = 11 KN

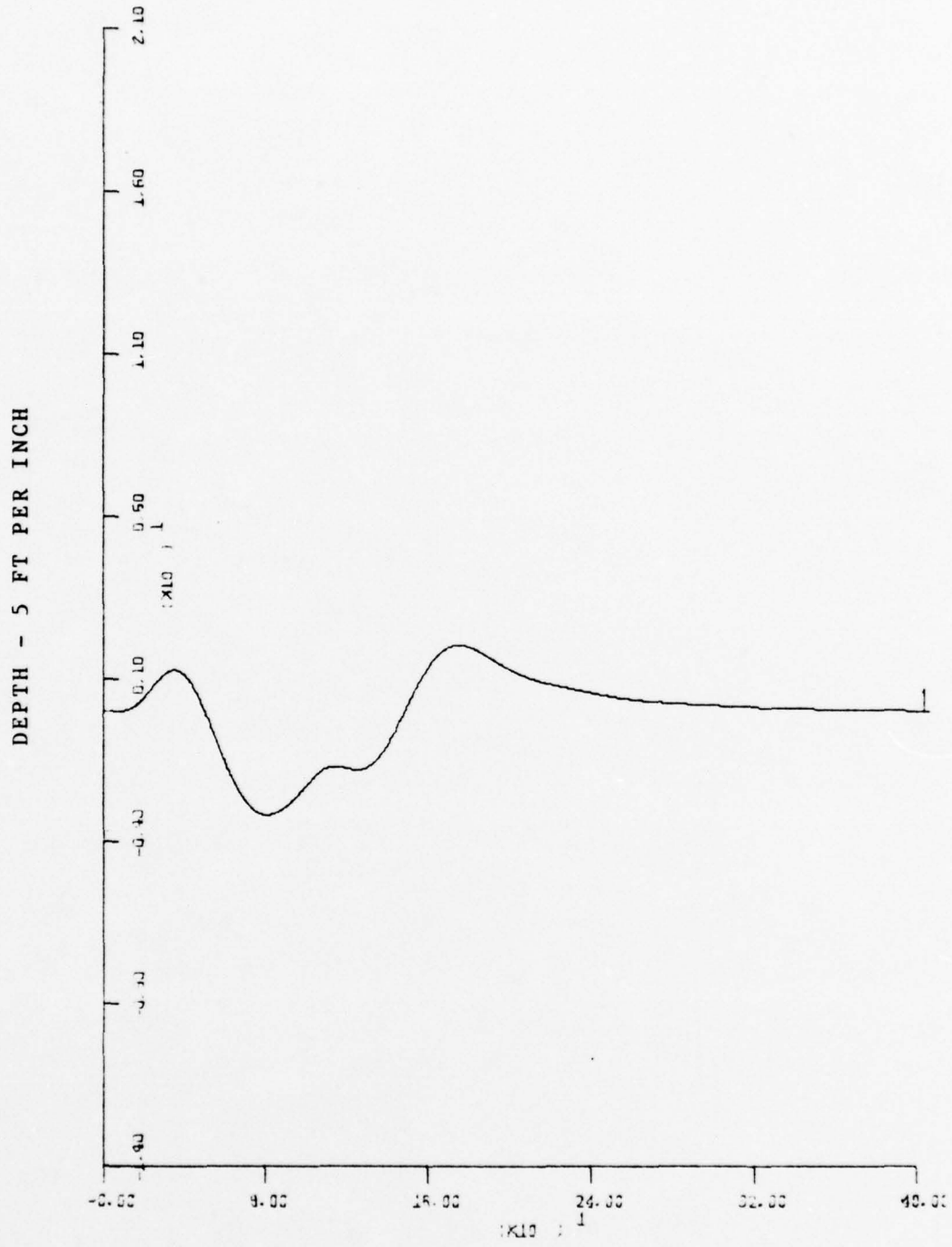

Figure 130 - COURSE CHANGE
RUDDER ANGLE = 20°, SPEED = 11 KN

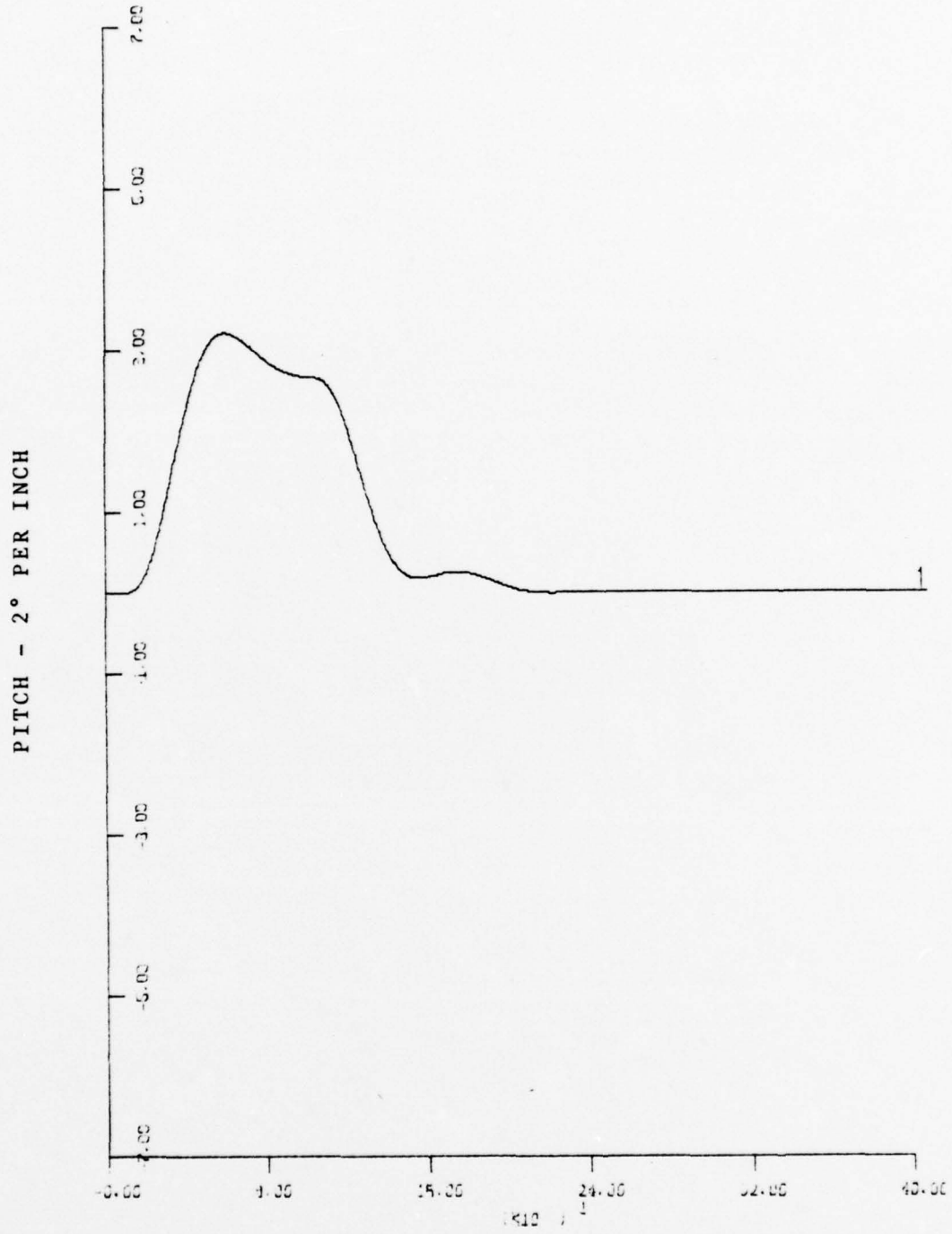

Figure 131 - COURSE CHANGE
RUDDER ANGLE = 20°, SPEED = 11 KN

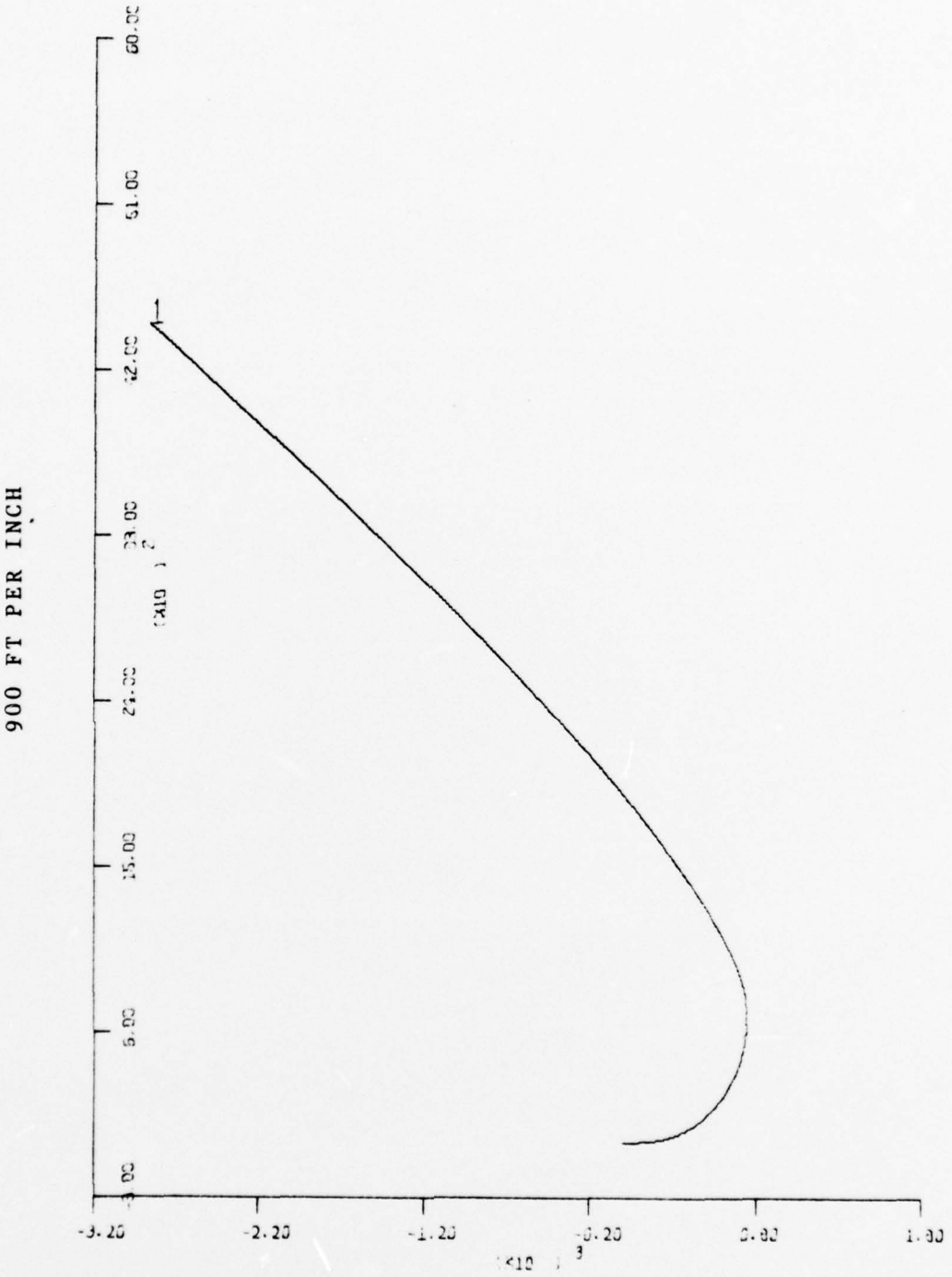

Figure 132 - COURSE CHANGE, HORIZONTAL PLANE
RUDDER ANGLE = 30°, SPEED = 11 KN

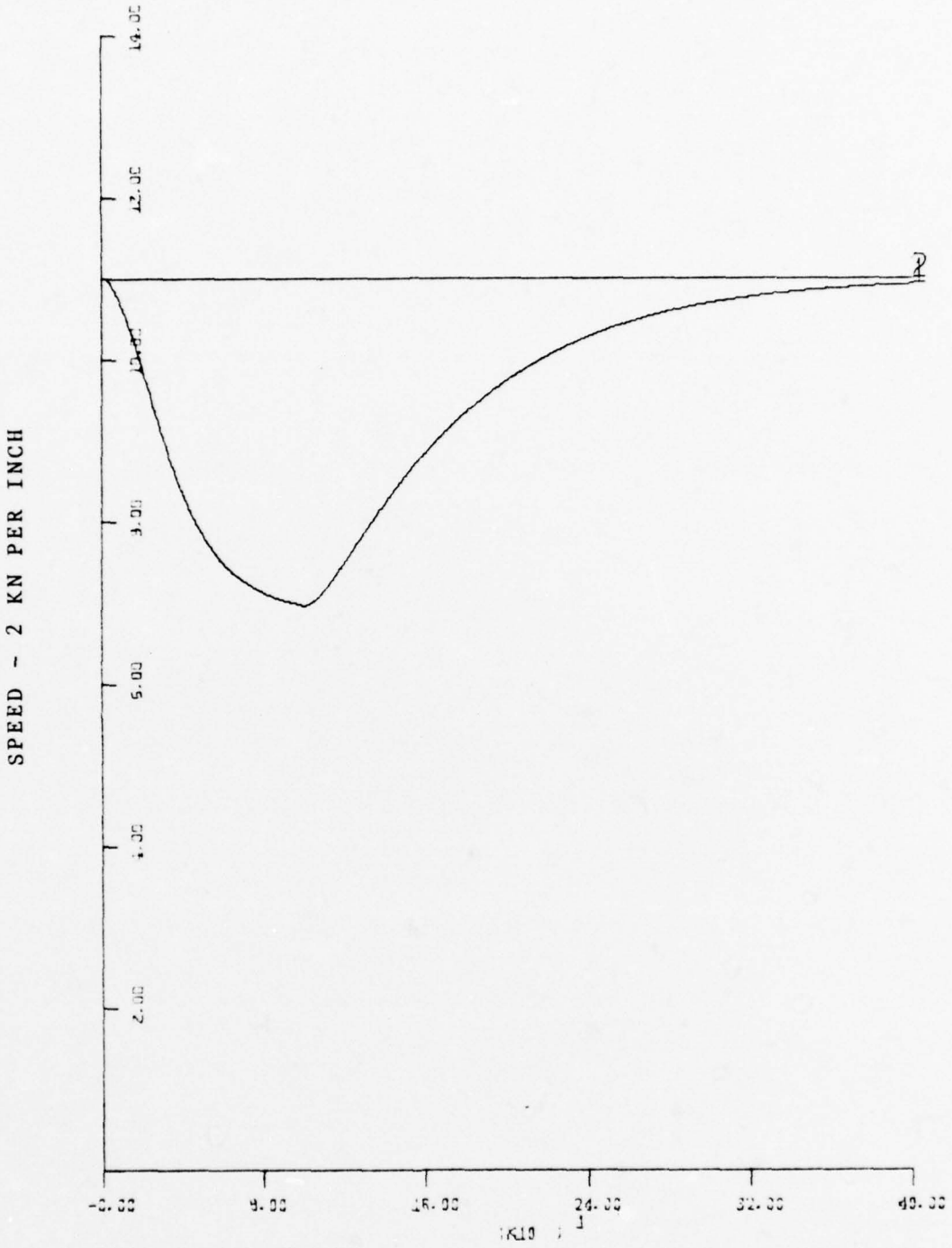

Figure 133 - COURSE CHANGE
RUDDER ANGLE = 30°, SPEED = 11 KN

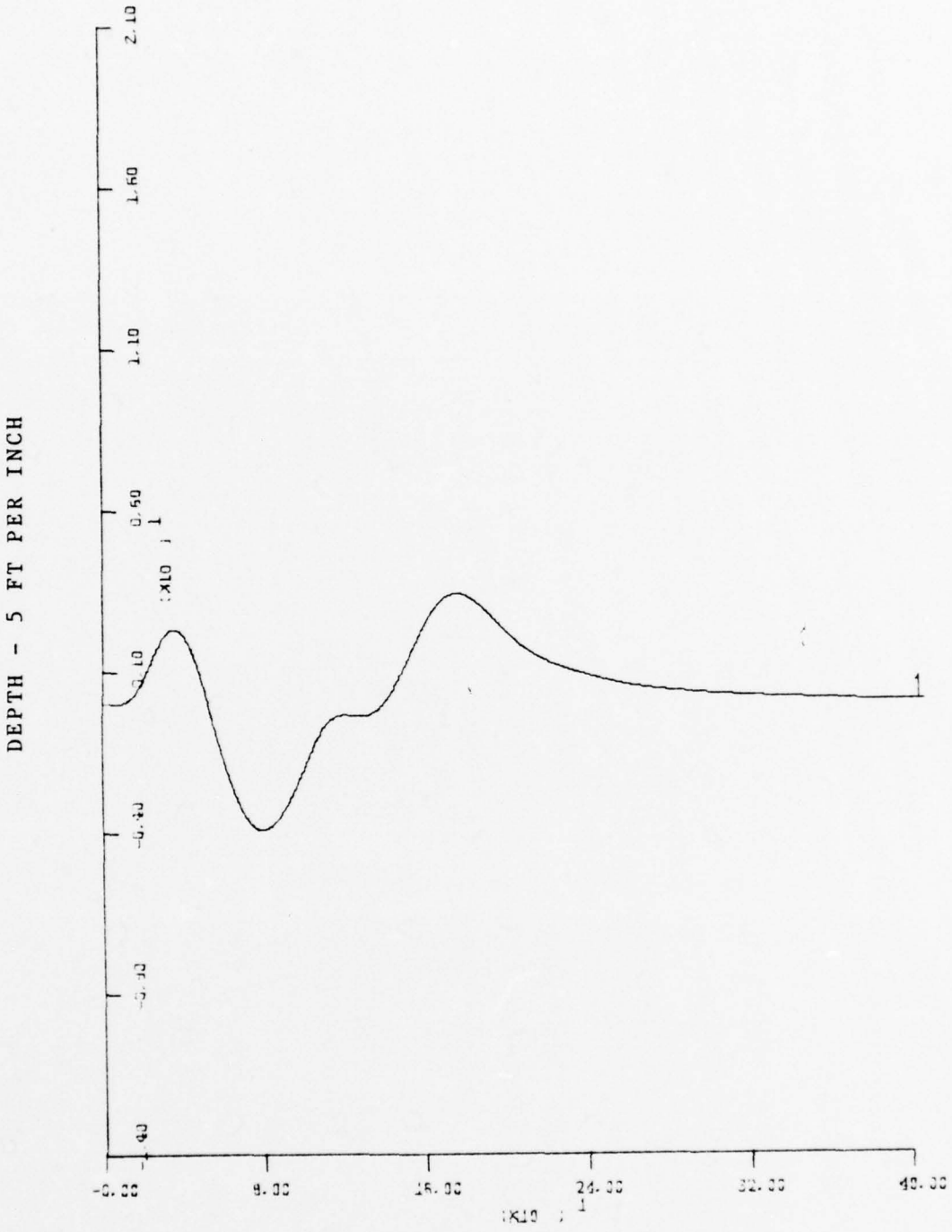

Figure 134 - COURSE CHANGE
RUDDER ANGLE = 30°, SPEED = 11 KN

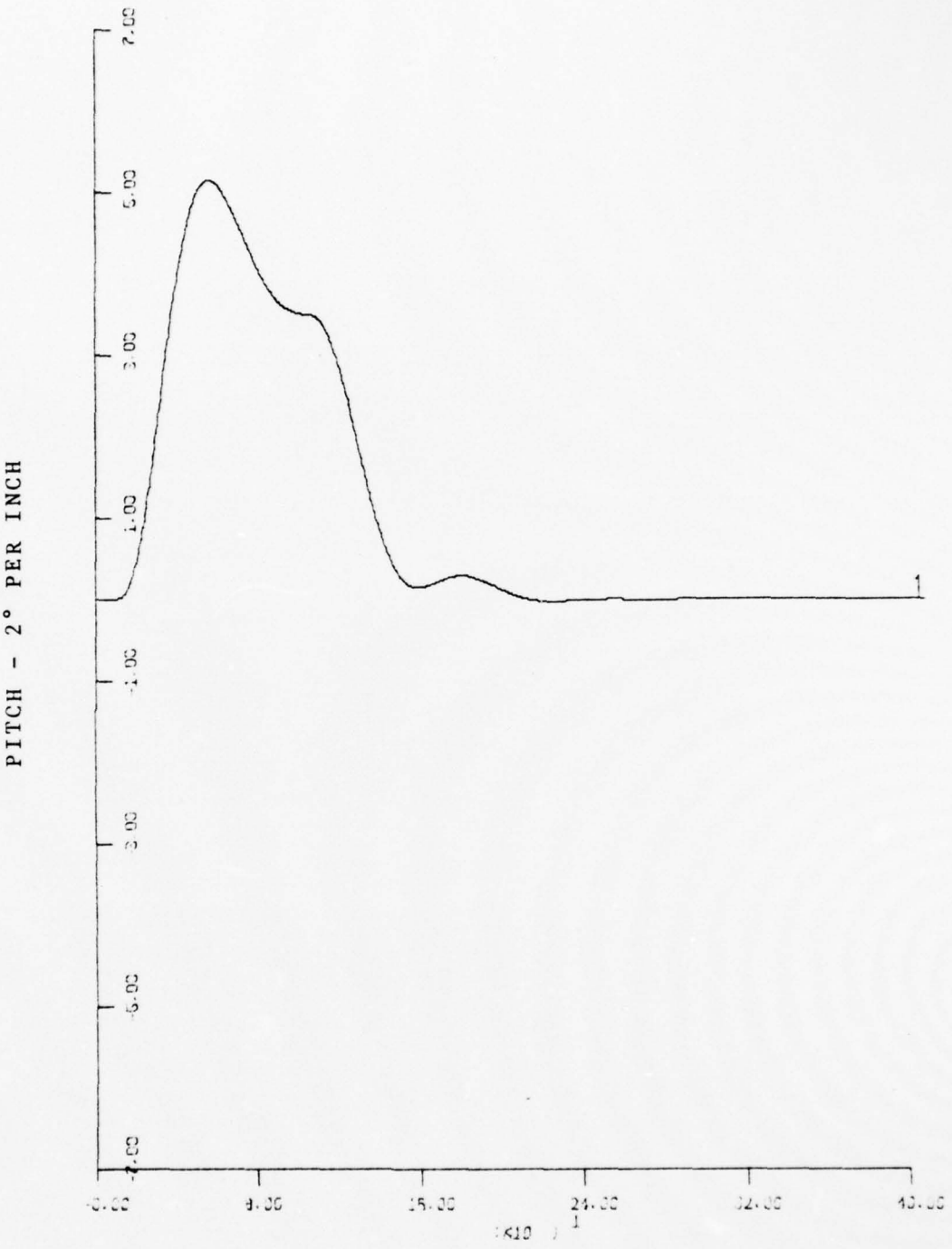

Figure 135 - COURSE CHANGE
RUDDER ANGLE = 30°, SPEED = 11 KN

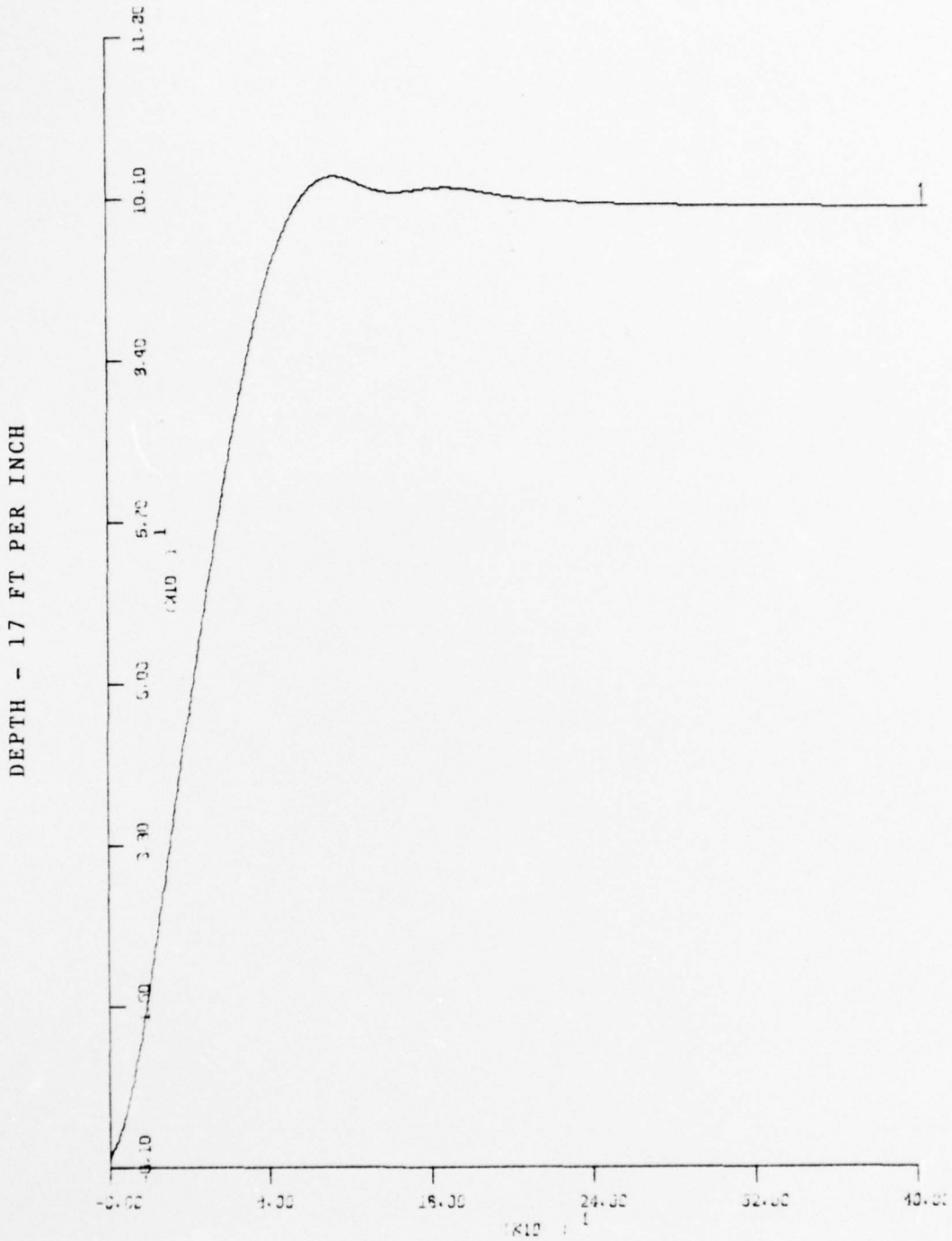

Figure 136 - COURSE AND 100 FT DEPTH CHANGE
RUDDER ANGLE = 10°, SPEED = 11 KN

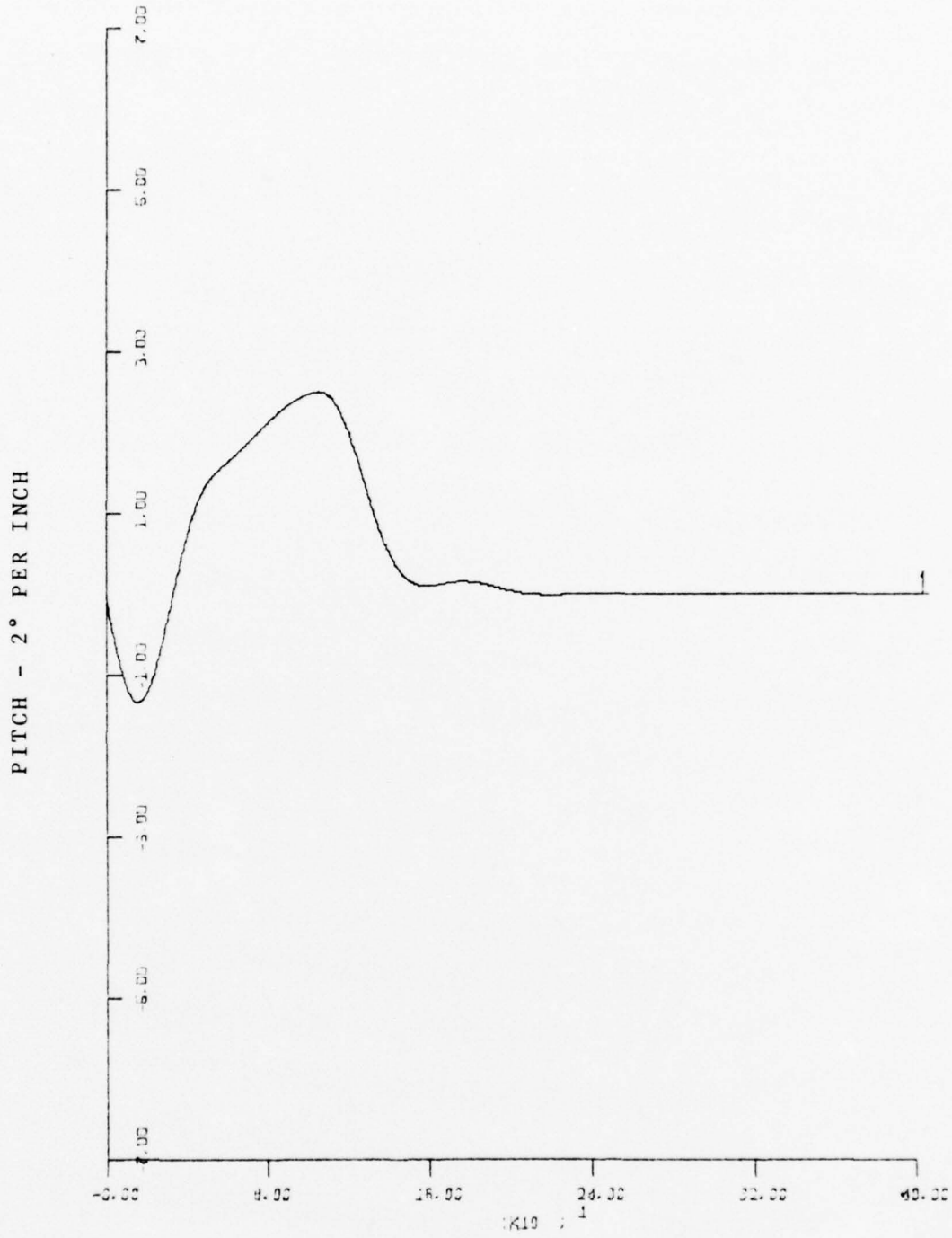

Figure 137 - COURSE AND 100 FT DEPTH CHANGE
RUDDER ANGLE = 10°, SPEED = 11 KN

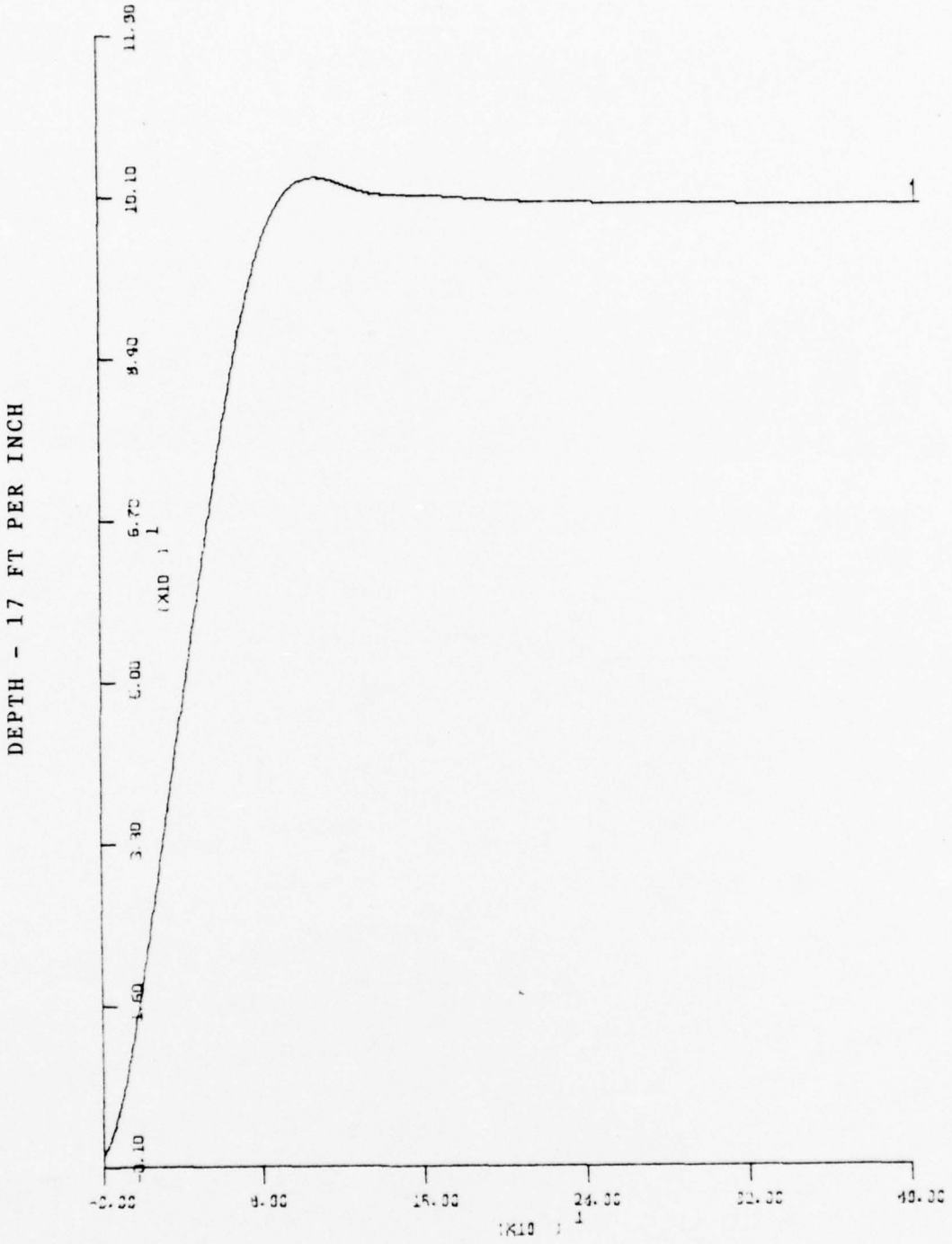

Figure 138 - COURSE AND 100 FT DEPTH CHANGE
RUDDER ANGLE = 20°, SPEED = 11 KN

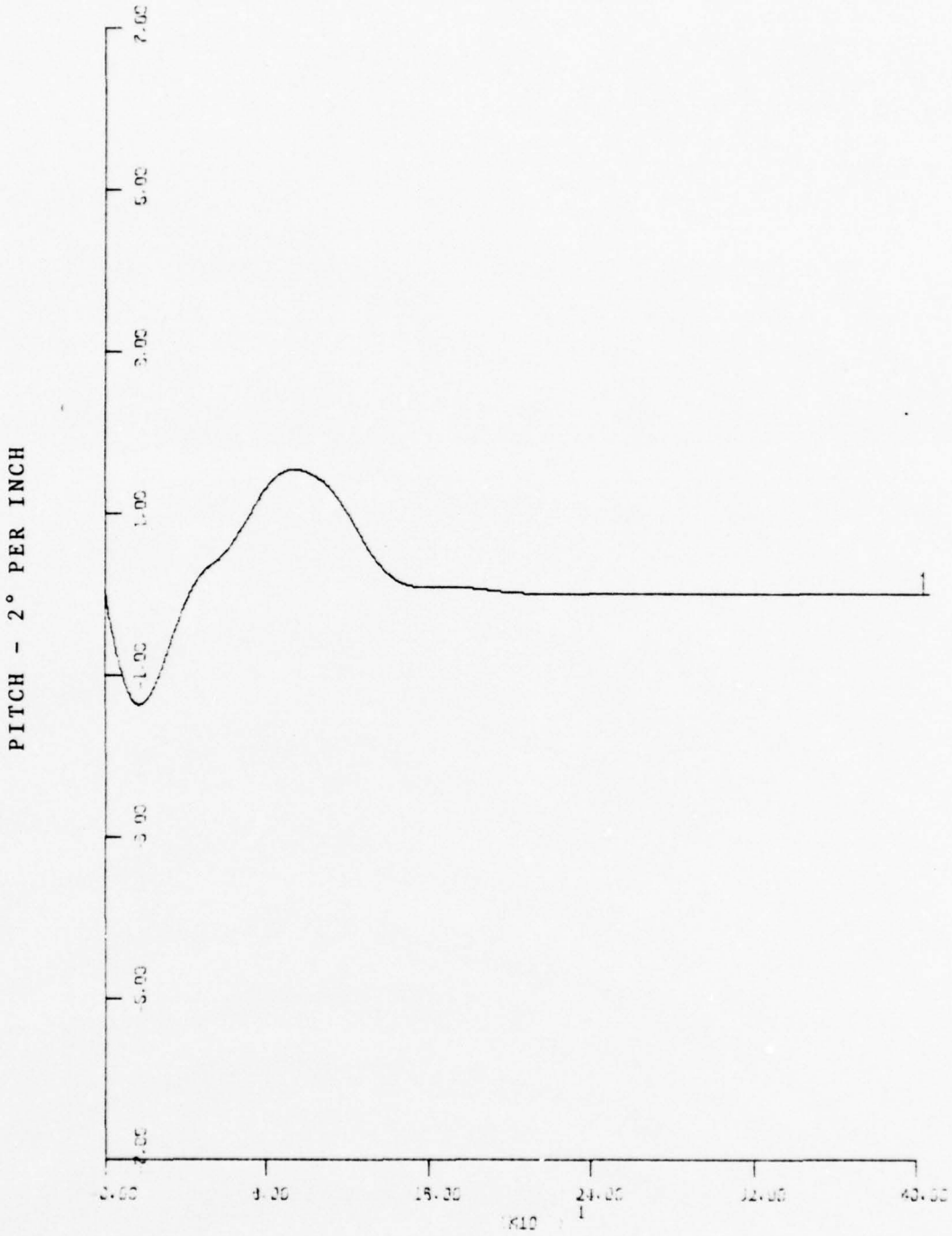

Figure 139 - COURSE AND 100 FT DEPTH CHANGE
RUDDER ANGLE = 20°, SPEED = 11 KN

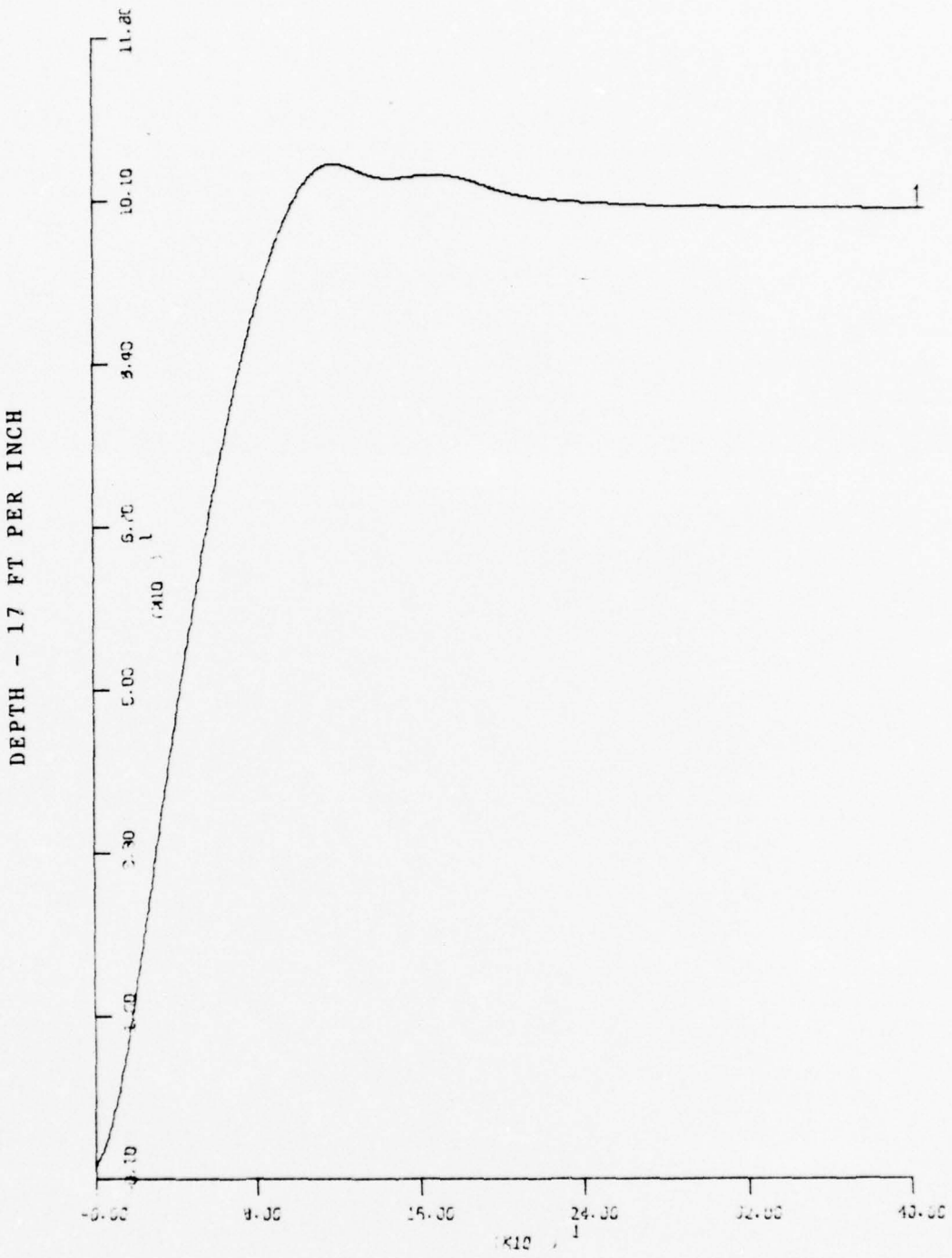

Figure 140 - COURSE AND 100 FT DEPTH CHANGE
RUDDER ANGLE = 30°, SPEED = 11 KN

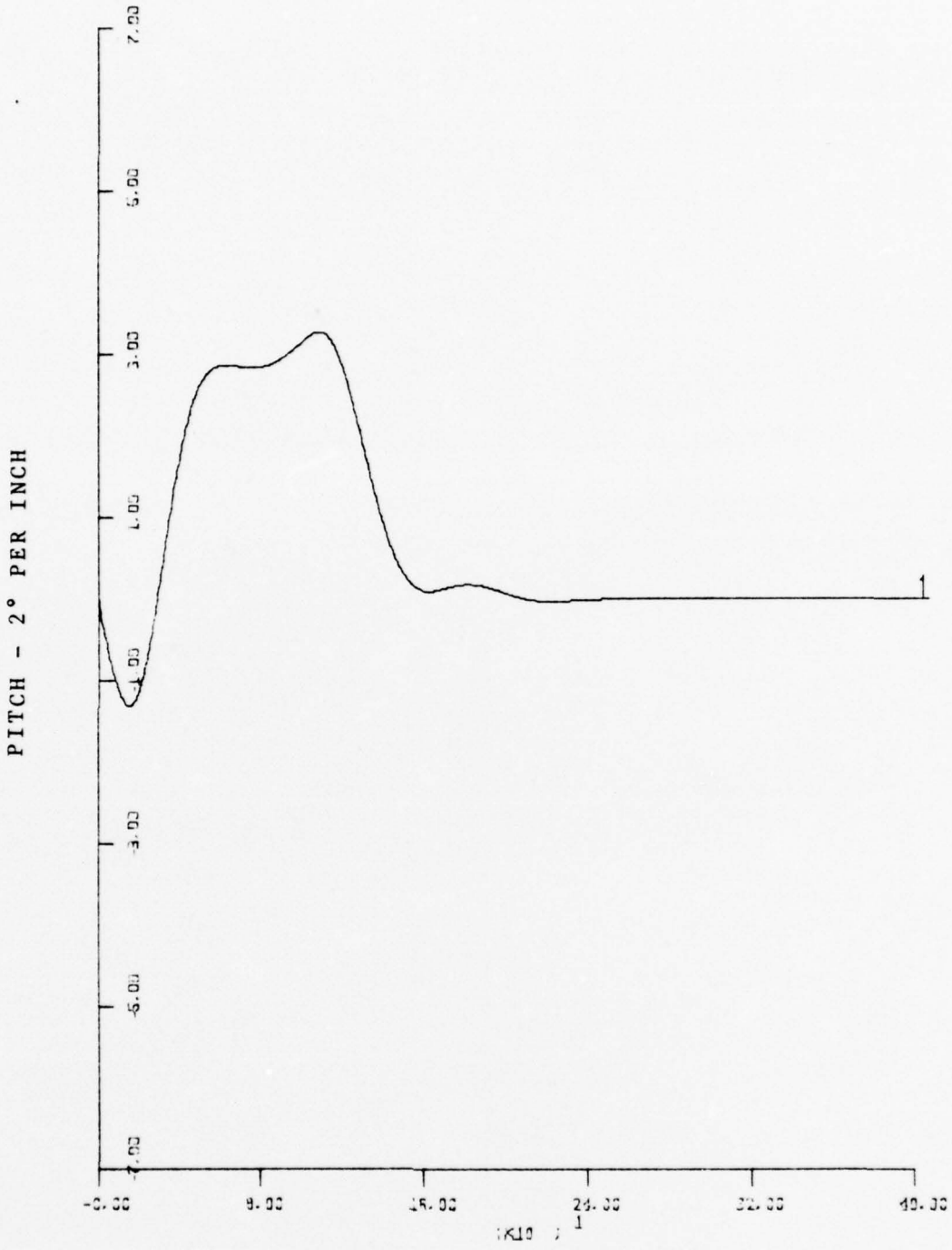

Figure 141 - COURSE AND 100 FT DEPTH CHANGE
RUDDER ANGLE = 30°, SPEED = 11 KN

maneuvers.

To demonstrate the influence of the out of trim conditions 100 ft depth changes were simulated. First, the ccrrect forward and aft trim for the ordered speed of 11 kn was maintained while the submarine was too heavy or too light overall. Seccnd, the correct overall weight was used and forward and aft trim changed by the same amount, but opposite in sign.

Table 17 - Incorrect overall weight

Weight error in lbs	Depth reached in sec	overshoot in ft	Steady-state error in	
			pitch in °	depth in ft
+2000	84.0	3.72	0.035	0.440
+1000	85.0	3.41	0.018	0.210
0	86.0	3.10	0.000	0.000
-1000	87.5	2.76	-0.018	-0.315
-2000	89.0	2.45	-0.037	-0.516

Tables 17 and 18 show the influence of trim changes. A change in the overall weight of 2000 lb and a transfer of 800 lb frcm the aft to the forward trim tank cr vice versa is required for the adjacent 2 kn intervals. The overshoot behaves as expected, i.e. when the boat is too heavy overall or the bow is too heavy the overshoot increases. Vice versa the overshoot decreases when the submarine is too light. During all maneuvers the speed decreases, which causes according tc Fig. 108 too heavy overall and too heavy forward conditions. This explains the increased overshoot observed for the depth changes simulated before.

Table 18 - Incorrect forward trim

Forward trim in lbs	Depth reached in sec	overshoot in ft	Steady-state error in	
			pitch in °	depth in ft
+800	83.0	4.17	-0.067	0.790
+400	85.0	3.63	-0.034	0.380
0	86.0	3.10	0.000	0.000
-400	87.0	2.56	0.034	-0.434
-800	90.0	2.00	0.067	-0.840

A new feature experienced during these trials is a steady-state error in depth as well as in pitch after the submarine has regained its original ordered speed. These steady-state errrors are small for relatively great out of trim conditions as 2000 lb in overall weight and 800 lb heavy forward. If the disturbances become greater it is clearly necessary to prevent these steady-state errors. There are basically two alternatives. First, correct the trim. Second, increase the sensitivity, i.e. the gains of the compensator for small depth and pitch errors.

VI. CONCLUSIONS

The system under investigation was a multivariable non-linear system with six degrees of freedom. Linearizing assumptions decoupled the vertical plane, now a two-dimensional multivariable linear system. Comparative test runs of the open-loop linear and non-linear model justified the utilization of the linear model for the design. The objective was to design a depth controller with a limited number of feedback states. Two approaches using cascaded transfer function matrices were investigated.

A. STEADY-STATE DECOUPLING

It has been shown that the steady-state decoupling scheme can be successfully applied to this submarine problem.

Using output feedback, steady-state decoupling depends only on the pure integrators the number of which is easy to determine by applying the final value theorem. But the actual design of the compensator is a matter of trial and error. Although single loop techniques, here the root-locus design, can be applied systematically, it still is a laborious and iterative process which requires either experience or many trials.

Design for stability and desired dominant roots was possible, but only simulation verified the dominance assumption. As the desired characteristics fixed the gain of the compensator matrix larger depth changes led to excessive plane deflections. Therefore limiters were required to keep the planes within the physical constraints.

The controller, designed on the basis of the linear model dynamics for 9 kn, showed the following performance, when implemented in the non-linear model:

a.) The design specifications for a speed range from 7 - 15 kn were satisfied.

b.) Out of trim conditions led to small steady-state errors.

c.) When operated in depth keeping mode in a turn the controller performed satisfactorily.

The compensated system is rather insensitive to speed. Thus all problems related to gain switching, like chattering and discontinuities in command plane angles, are avoided. This is especially important because the speed changes significantly during maneuvers.

The design was only concerned with the derivation of the transfer functions for the cascaded compensator. When implemented in hardware it has the following desirable features:

* Minimal instrumentation

As no rate information is required only simple sensors for depth and pitch angle are necessary, i.e. no inertial guidance system.

* Low cost, weight, and size

The simplicity of the compensator transfer functions makes them easily realizable in physical hardware at low manufacturing cost. Weight and size requirements are very small, another important factor especially for small coastal submarines.

* Reliability

The automatic controller can be realized with a set of physical components with a well known high reliability. High

component reliability and a small number of components will generally result in a high system reliability.

B. TOTAL DECOUPLING

As for the steady-state decoupling scheme the total decoupling is based on the linear model. The determination of the compensator matrix is an easy mathematical process, once the desired response dynamics have been defined in form of an overall transfer function matrix. At the first glance this method seems to be very appealing but it has some limitations:

a.) The realizability of the compensator is not always guaranteed, as the poles and zeros of the compensator matrix among others are determined by the plant singularities.

b.) Changes in the plant dynamics require changes in the compensator matrix.

The realizability of the compensator was no problem for the system under investigation. The second limitation presented serious problems. As the system dynamics change with speed, the compensator theoretically covers only a specific speed. Test runs showed that a compensator calculated for one speed was capable of covering a very small speed interval. In order to cover a large speed range as required in our problem the compensator has to be very complex because the gain and the root-locations have to be adjusted in very small step sizes. The influence of non-linearities was not considered as these will disturb the total decoupling scheme even more.

As result of this investigation it is concluded that the total decoupling scheme seems not to be practical. The

cascade compensation, using the steady-state decoupling method, is possible and practical for automatic pitch and depth control of small submarines.

APPENDIX A

STANDARD EQUATIONS OF MOTION

A. AXIAL FORCE

$$
\begin{aligned}
m(\dot{u} - vr + wq) = {} & \frac{\rho}{2} \ell^4 \left[X_{qq'} q^2 + X_{rr'} r^2 + X_{rp'} rp \right] \\
& + \frac{\rho}{2} \ell^3 \left[X_{\dot{u}'} \dot{u} + X_{vr'} vr + X_{wq'} wq \right] \\
& + \frac{\rho}{2} \ell^2 \left[X_{uu'} u^2 + X_{vv'} v^2 + X_{ww'} w^2 \right] \\
& + \frac{\rho}{2} \ell^2 u^2 \left[X_{\delta r \delta r'} \delta_r^2 + X_{\delta s \delta s'} \delta_s^2 + X_{\delta b \delta b'} \delta_b^2 \right] \\
& + \frac{\rho}{2} \ell^2 X_{vvn'} (n' - 1) v^2 \\
& + \frac{\rho}{2} \ell^2 X_{wwn'} (n' - 1) w^2 \\
& + \frac{\rho}{2} \ell^2 u^2 X_{\delta s \delta sn'} (n' - 1) \delta_s^2 \\
& + \frac{\rho}{2} \ell^2 u^2 X_{\delta r \delta rn'} (n' - 1) \delta_r^2 \\
& - \Sigma W_i \sin \theta \\
& + (F_x)_P
\end{aligned}
$$

B. LATERAL FORCE

$$m(\dot{v} - wp + ur) = \frac{\rho}{2} \ell^4 \left[Y_{\dot{r}}' \dot{r} + Y_{\dot{p}}' \dot{p} \right]$$

$$+ \frac{\rho}{2} \ell^4 \left[Y_{pq}' pq + Y_{p|p|}' p|p| \right]$$

$$+ \frac{\rho}{2} \ell^3 \left[Y_{\dot{v}}' \dot{v} + Y_{wp}' wp + Y_{v|r|}' \frac{v}{|v|} |(v^2 + w^2)^{\frac{1}{2}}| \, |r| \right]$$

$$+ \frac{\rho}{2} \ell^3 \left[Y_r' ur + Y_{|r|\delta r}' u|r|\delta r + Y_p' up \right]$$

$$+ \frac{\rho}{2} \ell^3 \, Y_{rn'}' (n' - 1) ur$$

$$+ \frac{\rho}{2} \ell^2 \left[Y_*' u^2 + Y_v' uv + Y_{v|v|}' v|(v^2 + w^2)^{\frac{1}{2}}| \right]$$

$$+ \frac{\rho}{2} \ell^2 u^2 \, Y_{\delta r}' \delta_r$$

$$+ \frac{\rho}{2} \ell^2 u^2 \, Y_{\delta r n'}' (n' - 1) \delta_r$$

$$+ \frac{\rho}{2} \ell^2 \, Y_{vn'}' (n' - 1) uv$$

$$+ \frac{\rho}{2} \ell^2 \, Y_{v|v|n'}' (n' - 1) v|(v^2 + w^2)^{\frac{1}{2}}|$$

$$+ \frac{\rho}{2} \ell^2 \, Y_{wv}' wv\#$$

$$+ \frac{\rho}{2} \ell^2 (F_y)_{vs} \frac{v^2 + w^2}{U} (-w) \sin \omega t$$

$$+ \Sigma W_i \sin \phi \cos \theta$$

\# Multiplied by $\frac{u}{U}$ for large angles of attack near -90°

C. NORMAL FORCE

$$m(\dot{w} - uq + vp) = \frac{\rho}{2} \ell^4 Z_{\dot{q}}' \dot{q}$$

$$+ \frac{\rho}{2} \ell^4 \left[Z_{rr}' r^2 \# + Z_{rp}' rp\# \right]$$

Note 1

$$+ \frac{\rho}{2} \ell^3 \left[Z_{\dot{w}}' \dot{w} + Z_{vr}' vr\# + Z_{vp}' vp + \delta Z_{vp}' vp\# \right]$$

$$+ \frac{\rho}{2} \ell^3 \left[Z_q' uq + Z_{|q|\delta s}' u|q|\delta s + Z_{w|q|} \frac{w}{|w|} (v^2 + w^2)^{\frac{1}{2}} |q| \right]$$

$$+ \frac{\rho}{2} \ell^3 Z_{qn'}' (n' - 1) uq$$

$$+ \frac{\rho}{2} \ell^2 \left[Z_*' u^2 + Z_w' uw + Z_{w|w|}' w|(v^2 + w^2)^{\frac{1}{2}}| \right]$$

$$+ \frac{\rho}{2} \ell^2 \left[Z_{|w|}' u|w| + Z_{ww}' |w (v^2 + w^2)^{\frac{1}{2}}| + Z_{vv}' v^2 \# \right]$$

$$+ \frac{\rho}{2} \ell^2 u^2 \left[Z_{\delta s}' \delta s + Z_{\delta b}' \delta b \right]$$

$$+ \frac{\rho}{2} \ell^2 \left[Z_{wn'}' (n' - 1) uw + Z_{w|w|n'}' (n' - 1) w|(v^2 + w^2)^{\frac{1}{2}}| \right]$$

$$+ \frac{\rho}{2} \ell^2 u^2 Z_{\delta s n'}' (n' - 1) \delta_s$$

$$+ \frac{\rho}{2} \ell^2 (F_z)_{vs} \frac{v^2 + w^2}{U} v \sin \omega t$$

$$+ \Sigma W_i \cos \theta \cos \phi$$

\# Multiplied by $\frac{u}{U}$ for large angles of attack near -90°

Note 1
when not multiplied by $\frac{u}{U}$ add to Z_{vp}'

D. ROLLING MOMENT

$$I_x\dot{p} + (I_z - I_y)\,qr = \frac{\rho}{2}\ell^5\left[K_{\dot{p}}\,'\dot{p} + K_{qr}\,'qr + K_{\dot{r}}\,'\dot{r} + K_{p|p|}\,'p|p|\right]$$

$$+ \frac{\rho}{2}\ell^4\left[K_{p}\,'up + K_{r}\,'ur + K_{\dot{v}}\,'\dot{v} + K_{wp}\,'wp\right]$$

$$+ \frac{\rho}{2}\ell^3\left[K_{*}\,'u^2 + K_{v}\,'uv + K_{v|v|}\,'v|(v^2 + w^2)^{\frac{1}{2}}|\right]$$

$$+ \frac{\rho}{2}\ell^3\,K_{vw}\,'vw$$

$$+ \frac{\rho}{2}\ell^3\,u^2K_{\delta r}\,'\delta_r$$

$$+ Bz_B \sin\Phi \cos\theta$$

E. PITCHING MOMENT

$$
\begin{aligned}
I_y\dot{q} + (I_x - I_z)\,rp \;=\; & \frac{\rho}{2}\ell^5\left[M_{\dot{q}}{}' \dot{q} + M_{rr}{}' r^2\# + M_{rp}{}' rp + \Delta M_{rp}{}' rp\#\right] \qquad \text{Note 1} \\
& + \frac{\rho}{2}\ell^4\left[M_{q}{}' uq + M_{|q|\delta s}{}' u|q|\delta s + M_{|w|q}{}' |(v^2 + w^2)^{\frac{1}{2}}|q\right] \\
& + \frac{\rho}{2}\ell^4\left[M_{\dot{w}}{}' \dot{w} + M_{vr}{}' vr\# + M_{vp}{}' vp\#\right] \\
& + \frac{\rho}{2}\ell^4 M_{qn'}{}' (n' - 1)\,uq \\
& + \frac{\rho}{2}\ell^3\left[M_{*}{}' u^2 + M_{w}{}' uw + M_{w|w|}{}' w|(v^2 + w^2)^{\frac{1}{2}}|\right] \\
& + \frac{\rho}{2}\ell^3\left[M_{|w|}{}' u|w| + M_{ww}{}' |w(v^2 + w^2)^{\frac{1}{2}}| + M_{vv}{}' v^2\#\right] \\
& + \frac{\rho}{2}\ell^3 u^2\left[M_{\delta s}{}' \delta_s + M_{\delta b}{}' \delta_b\right] \\
& + \frac{\rho}{2}\ell^3 M_{wn'}{}' (n' - 1)\,uw \\
& + \frac{\rho}{2}\ell^3 M_{w|w|n'}{}' (n' - 1)\,w|(v^2 + w^2)^{\frac{1}{2}}| \\
& + \frac{\rho}{2}\ell^3 u^2 M_{\delta sn'}{}' (n' - 1)\,\delta_s \\
& + Bz_B \sin\theta \\
& - \Sigma W_i x_{ti} \cos\theta\cos\phi
\end{aligned}
$$

\# Multiply by $\frac{u}{U}$ for large angles of attack near -90°

Note 1
when not multiplied by $\frac{u}{U}$ add to $M_{rp}{}'$

F. YAWING MOMENT

$$I_z \dot{r} + (I_y - I_x)\, pq = \frac{\rho}{2} \ell^5 \left[N_{\dot{r}}' \dot{r} + N_{pq}' pq + N_{\dot{p}}' \dot{p} \right]$$

$$+ \frac{\rho}{2} \ell^4 \left[N_r' ur + N_{|r|\delta r}' u|r|\delta r + N_{|v|r}' |(v^2 + w^2)^{\frac{1}{2}}|r \right]$$

$$+ \frac{\rho}{2} \ell^4 \left[N_p' up + N_{\dot{v}}' \dot{v} + N_{wp}' wp \right]$$

$$+ \frac{\rho}{2} \ell^4 \; N_{rn'}' (n' - 1) ur$$

$$+ \frac{\rho}{2} \ell^3 \left[N_*' u^2 + N_v' uv + N_{v|v|}' v|(v^2 + w^2)^{\frac{1}{2}}| \right]$$

$$+ \frac{\rho}{2} \ell^3 \; u^2 N_{\delta r}' \delta_r$$

$$+ \frac{\rho}{2} \ell^3 \; u^2 N_{\delta r n'}' (n' - 1) \delta_r$$

$$+ \frac{\rho}{2} \ell^3 \; N_{vn'}' (n' - 1) uv$$

$$+ \frac{\rho}{2} \ell^3 \; N_{v|v|n'}' (n' - 1) v|(v^2 + w^2)^{\frac{1}{2}}|$$

$$+ \frac{\rho}{2} \ell^3 \; N_{wv}' wv\#$$

$$+ \Sigma W_i x_{ti} \cos\theta \sin\phi$$

\# Multiply by $\frac{u}{U}$ for large angles of attack near -90°

G. AUXILIARY EQUATIONS

$$\dot{\phi} = p + \dot{\psi}\sin\theta$$

$$\dot{\theta} = (q - \dot{\psi}\cos\theta\sin\phi) / \cos\phi$$

$$\dot{\psi} = (r + \dot{\theta}\sin\phi) / \cos\theta\cos\phi$$

$$\dot{x}_o = u\cos\theta\cos\psi + v(\sin\phi\sin\theta\cos\psi - \cos\phi\sin\psi) + w(\sin\phi\sin\psi + \cos\phi\sin\theta\cos\psi)$$

$$\dot{y}_o = u\cos\theta\sin\psi + v(\cos\phi\cos\psi + \sin\phi\sin\theta\sin\psi) + w(\cos\phi\sin\theta\sin\psi - \sin\phi\cos\psi)$$

$$\dot{z}_o = -u\sin\theta + v\cos\theta\sin\phi + w\cos\theta\cos\phi$$

$$U = (u^2 + v^2 + w^2)^{\frac{1}{2}}$$

$$(F_x)_p = \frac{\rho}{2} \ell^2 u^2 \left[a_1' + a_2' n' + a_3' n'^2 \right] \quad \text{when} \quad k_1 < n'$$

$$= \frac{\rho}{2} \ell^2 u^2 \left[b_1' + b_2' n' + b_3' n'^2 \right] \quad \text{when} \quad k_2 < n' < k_1$$

$$= \frac{\rho}{2} \ell^2 u^2 \left[c_1' + c_2' n' + c_3' n'^2 \right] \quad \text{when} \quad k_3 < n' < k_2$$

$$= \frac{\rho}{2} \ell^2 u^2 \left[d_1' + d_2' n' + d_3' n'^2 \right] \quad \text{when} \quad n' < k_3$$

a_1', a_2', a_3'
b_1', b_2', b_3'
c_1', c_2', c_3'
d_1', d_2', d_3'

Sets of non-dimensional coefficients used in the propulsion equation above. The set which will be in effect at any time during a simulated maneuver will depend on the value of n' and the numbers k_1, k_2, k_3.

APPENDIX B

NOMENCLATURE

SYMBOL	DEFINITION
$\dot{}$	A dot over any symbol signifies differentiation with respect to time.
B	Buoyancy force which is positive upwards.
m	Mass of the submarine including the water in the free flooding spaces.
ℓ	Overall length of the submarine
U	Linear velocity of origin of body axes relative to an earth-fixed axis system.
u	Component of U along the body x-axis.
v	Component of U along the body y-axis.
w	Component of U along the body z-axis.

u_c	Command speed: A steady value of u for a given propeller rpm when α, β and control surface angles are zero. Sign changes with propeller reversal.
x	Longitudinal axis of the body fixed coordinate axis system.
y	Transverse axis of the body fixed coordinate axis system.
z	Vertical axis of the body fixed coordinate axis system.
x_o	Distance along the x_o axis of an earth-fixed axis system.
y_o	Distance along the y_o axis of an earth-fixed axis system.
z_o	Distance along the z_o axis of an earth-fixed axis system.
p	Component of angular velocity about the body fixed x-axis.
q	Component of angular velocity about the body fixed y-axis.
r	Component of angular velocity about the body fixed z-axis.
z_B	The z coordinate of the center of buoyance (CB) of the submarine.

α	Angle of attack.
β	Angle of drift.
δb, D_b	Deflection of bowplane (or sailplane)
δr, D_r	Deflection of rudder.
δs, D_s	Deflection of sternplane.
n'	The ratio u_c/u.
θ	Pitch angle.
Ψ	Yaw angle.
ϕ	Roll angle.
ρ	Mass density of sea water.
w_i	Weight of water blown from a particular ballast tank identified by the integer assigned to the index i.
ω	Angular velocity.
t	Time.
x_{ti}	Location along the body x-axis of the center of mass of the i^{th} ballast tank when this tank is filled with sea water.

$(F_x)_p$	Propulsion force (see auxiliary equations and relationships).
I_x	Moment of inertia of a submarine about the x-axis.
I_y	Moment of inertia of a submarine about the y-axis.
I_z	Moment of inertia of a submarine about the z-axis.
$K_{\dot{p}}'$, K_p', $K_{p\|p\|}'$, K_{qr}', K_r', $K_{\dot{r}}'$, $K_{\dot{v}}'$, K_{wp}', K_*', K_v', $K_{v\|v\|}'$, K_{vw}', $K_{\delta r}'$	Non-dimensional constants each of which is assigned to a particular force term in the equation of motion about the body x-axis.
$M_{\dot{q}}'$, M_{rr}', M_{rp}', $\Delta M_{rp}'$, M_q', $M_{\|q\|\delta s}'$, $M_{\|w\|q}'$, $M_{\dot{w}}'$, M_{vr}', M_{vp}', M_{qn}', M_*', M_w', $M_{w\|w\|}'$, $M_{\|w\|}'$, M_{ww}', M_{vv}', $M_{\delta s}'$, $M_{\delta b}'$, M_{wn}', $M_{w\|w\|n}'$, $M_{\delta sn}'$	Non-dimensional constants each of which is assigned to a particular force term in the equation of motion about the body y-axis.

$N_{\dot{r}}'$, N_{pq}', $N_{\dot{p}}'$, N_r', $N_{|r|\delta r}'$, $N_{|v|r}'$,

N_p', $N_{\dot{v}}'$, N_{wp}', N_{rn}', N_δ', N_v',

$N_{v|v|}'$, $N_{\delta r}'$, $N_{\delta rn}'$, N_{vn}', $N_{v|v|n}'$,

N_{wv}'

Non-dimensional constants each of which is assigned to a particular force term in the equation of motion about the body z-axis.

X_{qq}', X_{rr}', X_{rp}', $X_{\dot{u}}'$, X_{vr}', X_{wq}',

X_{uu}', X_{vv}', X_{ww}', $X_{\delta r\delta r}'$, $X_{\delta s\delta s}'$,

$X_{\delta b\delta b}'$, X_{vvn}', X_{wwn}', $X_{\delta s\delta sn}'$,

$X_{\delta r\delta rn}'$

Non-dimensional constants each of which is assigned to a particular force term in the equation of motion along the body x-axis.

$Y_{\dot{r}}'$, $Y_{\dot{p}}'$, Y_{pq}', $Y_{p|p|}'$, $Y_{\dot{v}}'$, Y_{wp}',

$Y_{v|r|}'$, Y_r', $Y_{|r|\delta r}'$, Y_p', Y_{rn}',

Y_δ', Y_v', $Y_{v|v|}'$, $Y_{\delta r}'$, $Y_{\delta rn}'$,

Y_{vn}', $Y_{v|v|n}'$, Y_{wv}', $(F_y)_{vs}$

Non-dimensional constants each of which is assigned to a particular force term in the equation of motion along the body y-axis

$Z_{\dot{q}}'$, Z_{rr}', Z_{rp}', $Z_{\dot{w}}'$, Z_{vr}, Z_{vp}',

$\Delta Z_{vp}'$, Z_q', $Z_{|q|\delta s}$, $Z_{w|q|}'$,

Z_{qn}', Z_δ', Z_w', $Z_{w|w|}'$, $Z_{|w|}'$,

Z_{ww}', Z_{vv}', $Z_{\delta s}'$, $Z_{\delta b}'$, Z_{wn}',

$Z_{w|w|n}'$, $Z_{\delta sn}'$, $(F_z)_{vs}$

Non-dimensional constants each of which is assigned to a particular force term in the equation of motion along the body z-axis

APPENDIX C

HYDRODYNAMIC COEFFICIENTS OF SIMULATION MODEL

XQQ = -.20000E-03	YP/P/= 0.		0.		KP/P/= -.80000E-06			0.				0.	
XRR = -.90000E-04	YPQ = .26000E-03	ZRR = -.15000E-02	KQR = -.10000E-03	MRR = -.55000E-03	NPQ = -.40000E-03								
XRP = .25000E-03	0.	ZRP = -.90000E-03	0.	MRP = .15000E-03	0.								
0.	YPDOT= -.30000E-03	ZQDOT= -.20000E-03	KPDOT= -.30000E-05	MQDOT= -.40000E-03	NPDOT= -.70000E-05								
0.	YRDOT= .90000E-04	0.	KRDOT= -.70000E-05	M+RP = 0.	NRDOT= -.50000E-03								
XUDOT= -.15000E-03	YVDOT= -.11000E-01	ZWDOT= -.75000E-02	KVDOT= -.25000E-03	MWDOT= -.20000E-03	NVDOT= .30000E-03								
XVR = .11000E-01	YV/R/= -.73000E-02	ZVR = -.80000E-02	0.	MVR = -.40000E-02	N/V/R= -.45000E-02								
XWQ = -.75000E-02	YWP = .75000E-02	ZW/Q/= -.60000E-02	KWP = .25000E-03	M/W/Q= -.20000E-02	NWP = -.20000E-03								
0.	YR = .30000E-02	ZQ = -.45000E-02	KR = -.40000E-04	MQ = -.25000E-02	NR = -.30000E-02								
0.	YRDR = 0.	ZQDS = 0.	0.	MQDS = 0.	NRDR = 0.								
0.	YP = -.70000E-03	0.	KP = -.35000E-04	MVP = .90000E-03	NP = -.20000E-05								
0.	0.	ZVP = -.70000E-02	0.	0.	0.								
0.	0.	Z+VP = 0.	0.	0.	0.								
0.	0.	0.	0.	0.	0.								
XUU = 0.	YUU = 0.	ZUU = -.10000E-03	KUU = 0.	MUU = .40000E-04	NUU = 0.								
XVV = .65000E-02	YV/V/= -.60000E-01	ZVV = .65000E-01	KV/V/= -.90000E-03	MVV = .15000E-01	NV/V/= .14000E-01								
XWW = .20000E-02	YV = -.21000E-01	ZW/W/= -.30000E-01	KV = -.70000E-03	MW/W/= -.50000E-02	NV = -.75000E-02								
XDRDR= -.28000E-02	YDR = .62000E-02	ZW = -.11000E-01	KDR = .70000E-04	MW = .30000E-02	NDR = -.30000E-02								
XDSDS= -.25000E-02	YWV = -.65000E-01	ZDS = -.50000E-02	KWV = .35000E-02	MDS = -.25000E-02	NWV = .15000E-01								
XDBDB= -.26000E-02	0.	ZDB = -.25000E-02	0.	MDB = .50000E-03	0.								
0.	0.	0.	0.	0.	0.								
0.	0.	Z/W/ = 0.	0.	M/W/ = 0.	0.								
0.	0.	ZWW = 0.	0.	MWW = 0.	0.								
0.	0.	0.	0.	0.	0.								
0.	YVS = 0.	ZVS = 0.	0.	0.	0.								
0.	0.	0.	0.	0.	0.								
0.	YRN = 0.	ZQN = 0.	0.	MQN = 0.	NRN = 0.								
0.	0.	0.	0.	0.	0.								
XVVN = 0.	YVN = 0.	ZWN = 0.	0.	MWN = 0.	NVN = 0.								
XWWN = 0.	YVAVN= 0.	ZWAWN= 0.	0.	MWAWN= 0.	NVAVN= 0.								
XDR2N= 0.	YDRN = 0.	ZDSN = 0.	0.	MDSN = 0.	NDRN = 0.								
XDS2N= 0.	0.	0.	0.	0.	0.								
0.	0.	0.	0.	0.	0.								
0.	0.	0.	0.	0.	0.								
	A1 = -.10000E-02	B1 = -.10000E-02	C1 = -.10000E-02	D1 = -.10000E-03									
	A2 = -.95000E-03	B2 = 0.	C2 = 0.	D2 = .25000E-03									
	A3 = .19500E-02	B3 = .10000E-02	C3 = -.40000E-03	D3 = -.12500E-02									

APPENDIX D

DSL-PROGRAMS AND BLOCK DIAGRAMS

A. COMPENSATED LINEAR MODEL
(STEADY-STATE DECOUPLING)

B. COMPENSATED LINEAR MODEL
(TOTAL DECCUPLING)

C. COMPENSATED NON-LINEAR MODEL
(STEADY-STATE DECOUPLING)

COMPENSATED LINEAR MODEL (STEADY-STATE DECOUPLING)

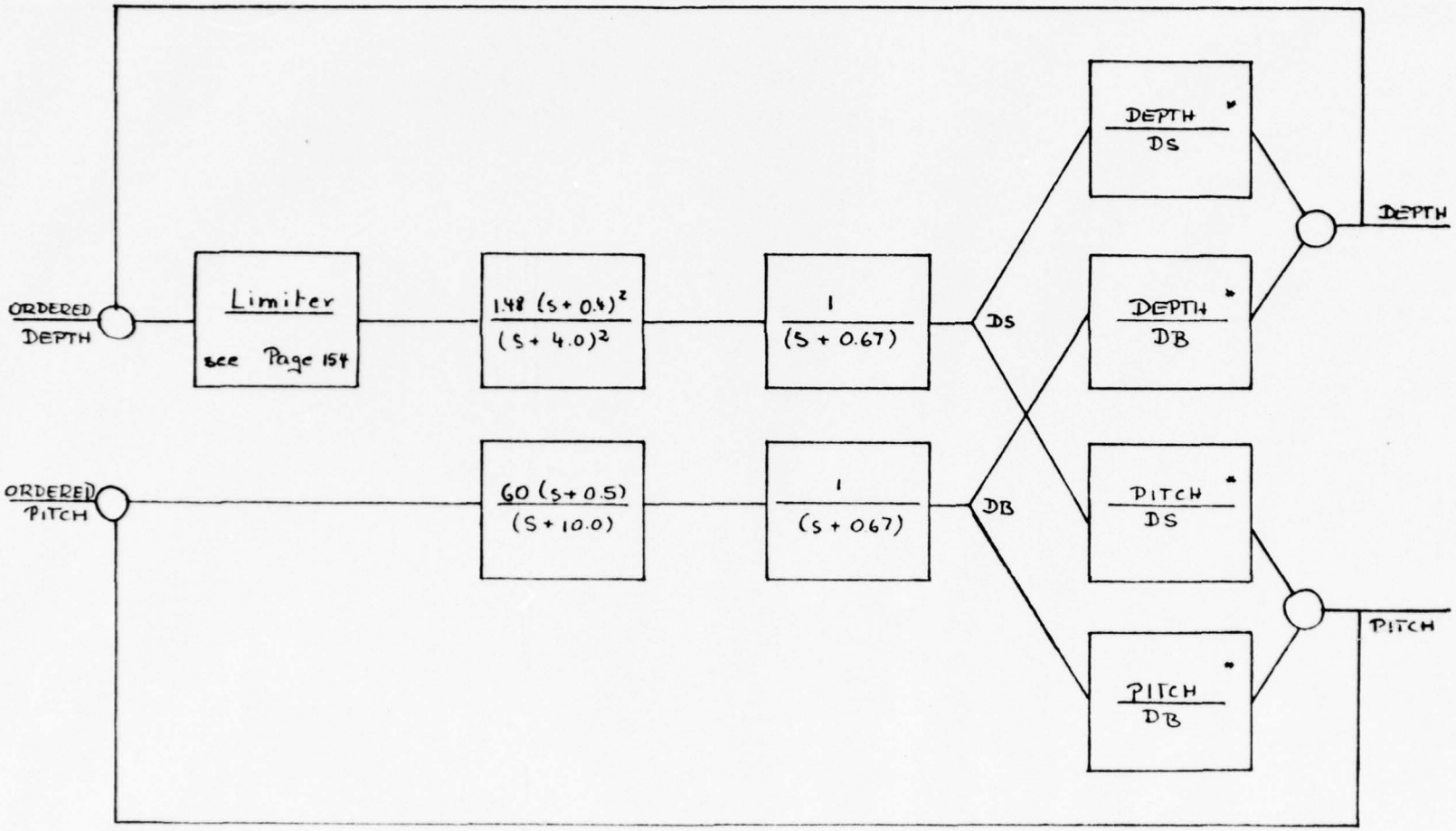

* See Table 06 -10 , Page 103 - 107

```
                    COMPENSATED LINEAR MODEL (STEADY-STATE DECOUPLING)
*
*
*
*
* THIS PROGRAM SIMULATES THE LINEARIZED COMPENSATED SUBMARINE IN THE
* VERTICAL PLANE.
*
*
*
* NOMENCLATURE:
*
*          K1      = GAIN OF COMPENSATOR GC11
*          K2      = GAIN OF COMPENSATOR GC22
*          UC      = COMMAND SPEED IN FT/S
*          LCZCR   = ORDERED DEPTH IN FT
*          LCPCR   = ORDERED PITCH IN RAD
*          LCZER   = DEPTH ERROR
*          LCPER   = PITCH ERROR
*          LDSGRA  = STERNPLANE ANGLE IN DEG
*          LDBGRA  = FAIRWATER PLANE ANGLE IN DEG
*          LQ      = ANGULAR PITCH VELOCITY
*          LQDOT   = ANGULAR PITCH ACCELERATION
*          LZDOT   = DEPTH CHANGE
*          LZDDOT  = VERTICAL ACCELERATION
*
*
*
TITLE SUBMARINE SIMULATION LUESSOW-NITSCHE
PARAM K1 = .015
PARAM K2 = 3.
PARAM UC = 25.33
PARAM LCZCR=100.
INTGER NPLOT
CONST NPLOT=1
*
* COEFFICIENTS OF STATE EQUATIONS
*
CONST A11=-1.728E-03,A12=-0.7062, A13=0.01289 ,A14=-1.728E-03
CONST A21=1.884E-05, A22=-6.365E-03,A23=1.884E-05,A24=-2.522E-03
CONST B11=-6.668E-04,B12=-3.871E-04, B21=-1.465E-05,B22=3.190E-06
CONTRL FINTIM=400. ,DELT=.01,DELS=.5
PRINT 0.5,UC,LZDOT,LPITCH,LDEPTH,LDBGRA,LDSGRA
INITIAL
*
* ERROR LIMIT CALCULATION
*
      IF(UC.LT.11.82) LIM = 40.
```

```
      IF(UC.GE.11.82) LIM = -1.6655*UC + 59.6875
DERIVATIVE
*
* STATE EQUATIONS
*
      LPITCH = INTGRL(0.0,LQ)
      LDEPTH = INTGRL(0.0,LZDOT)
      LQ = INTGRL(0.0,LQDOT)
      LZDOT = INTGRL(0.0,LZDDOT)
      LZDDOT = A11*UC*LZDOT + A12*UC*LQ + (A13 +A14*UC**2)*LPITCH ...
      + (B11*LDS + B12*LDB)*UC**2
      LQDOT = A21*UC*LZDOT + A22*UC*LQ + (A23*UC**2 + A24)*LPITCH ...
      + (B21*LDS + B22*LDB)*UC**2
*
* ERROR CALCULATION
*
      LZER = LZCR - LDEPTH
      LPER = LPCR - LPITCH
      LZERR = LIMIT(-LIM,LIM,LZER)
*
* COMPENSATOR GC11
*
      LC1A = -K1*LZERR
      LC1B = LEDLAG(0.,2.5,.25,LC1A)
      LC1C =LEDLAG(0.,2.5,.25,LC1B)
      LDB  = REALPL(0.,.667,LC1C)
*
* COMPENSATOR GC22
*
      LC2A = -K2*LPER
      LC2B = LEDLAG(0.,2.,.1,LC2A)
      LDS  = REALPL(0.,.667,LC2B)
      LDSGRA = 57.296*LDS
      LDBGRA = 57.296*LDB
      LPITGR = 57.296*LPITCH
SAMPLE
      CALL DRWG(1,1,TIME,LDEPTH)
      CALL DRWG(2,1,TIME,LPITGR)
      CALL DRWG(3,1,TIME,LDBGRA)
      CALL DRWG(3,2,TIME,LDSGRA)
TERMINAL
      CALL ENDRW(NPLOT)
END
```

COMPENSATED LINEAR MODEL (TOTAL DECOUPLING)

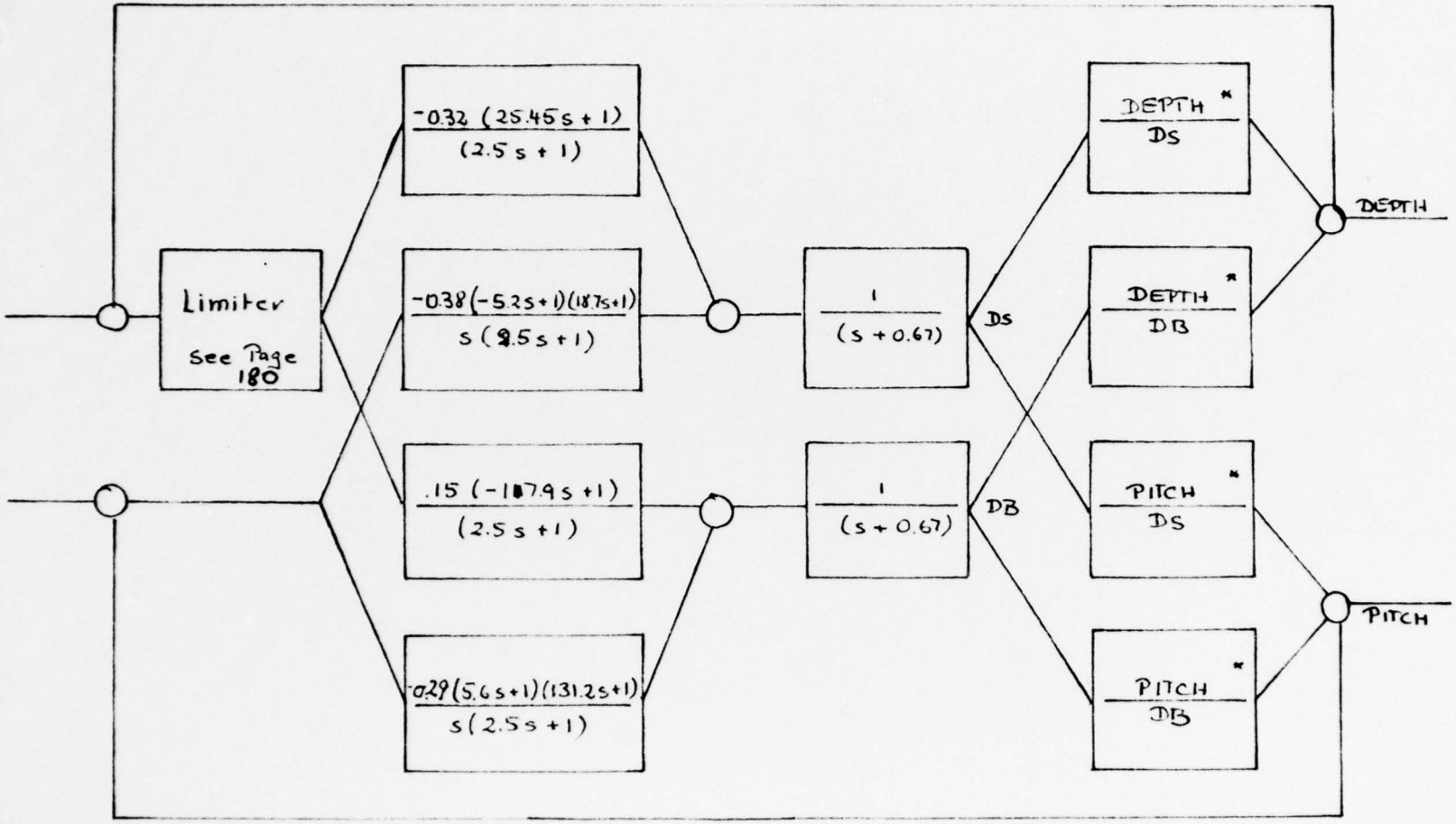

* See Table 06-10, Page 103-107

```
                    COMPENSATED LINEAR MODEL (TOTAL DECOUPLING)
*
*
*
*
* THIS PROGRAM SIMULATES THE LINEARIZED COMPENSATED SUBMARINE IN THE
* VERTICAL PLANE.
*
*
*
* NOMENCLATURE:
*
*
*          UC      = COMMAND SPEED IN FT/S
*          ZOR     = ORDERED DEPTH IN FT
*          LOPOR   = ORDERED PITCH IN RAD
*          LOZER   = DEPTH ERROR
*          LOPER   = PITCH ERROR
*          LDSGRA  = STERNPLANE ANGLE IN DEG
*          LDBGRA  = FAIRWATER PLANE ANGLE IN DEG
*          LQ      = ANGULAR PITCH VELOCITY
*          LQDOT   = ANGULAR PITCH ACCELERATION
*          LZDOT   = DEPTH CHANGE
*          LZDDOT  = VERTICAL ACCELERATION
*
*
TITLE SUBMARINE SIMULATION LUESSOW-NITSCHE
PARAM UC= 15.2
PARAM ZOR=100.
INTGER NPLOT
CONST NPLOT=1
*
* COEFFICIENTS OF STATE EQUATIONS
*
CONST A11=-1.728E-03,A12=-0.7062, A13=0.01289 ,A14=-1.728E-03
CONST A21=1.884E-05, A22=-6.365E-03,A23=1.884E-05,A24=-2.522E-03
CONST B11=-6.668E-04,B12=-3.871E-04, B21=-1.465E-05,B22=3.190E-06
CONTRL FINTIM=400. ,DELT=.01,DELS=.5
PRINT 0.5,UC,LZDOT,LPITCH,LDEPTH,LDBGRA,LDSGRA
DYNAMIC
*
* ERROR LIMIT CALCULATION
*
      LIM = 2.5
      IF(TIME.GE.3.5) LIM = .2  *(TIME - 3.5) +2.5
      IF(TIME.GE.53.5) LIM = 12.5
DERIVATIVE
*
```

```
*  STATE EQUATIONS
*
      LPITCH = INTGRL(0.,LQ)
      LDEPTH = INTGRL(0.0,LZDOT)
      LQ = INTGRL(0.0,LQDOT)
      LZDOT = INTGRL(0.,LZDDOT)
      LZDDOT = A11*UC*LZDOT + A12*UC*LQ + (A13 +A14*UC**2)*LPITCH ...
      + (B11*LDS + B12*LDB)*UC**2
      LQDOT = A21*UC*LZDOT + A22*UC*LQ + (A23*UC**2 + A24)*LPITCH ...
      + (B21*LDS + B22*LDB)*UC**2
*
*  ERROR CALCULATION
*
      LCZOR = STEP(2.)
      LCZCR = ZCR*LCCZCR
      LCCZER = LCZOR - LDEPTH
      LCZER = LIMIT(-LIM,LIM,LCCZER)
      LCPER = LCPCR - LPITCH
*
*  COMPENSATOR C11
*
      LC11 = LEDLAG(0.,25.452,2.5,LCZER)
*
*  COMPENSATOR C12
*
      LC12A= LEDLAG(0.,18.671,2.5,LCPER)
      LC12B= INTGRL(0.,.1926*LC12A)
      LC12C= LC12A - LC12B
*
*  COMPENSATOR C21
*
      LC21 = LEDLAG(0.,-117.87,2.5,LCZER)
*
*  COMPENSATOR C22
*
      LC22A= LEDLAG(0.,131.234,2.5,LCPER)
      LC22B= INTGRL(0.,.1775*LC22A)
      LC22C= LC22A + LC22B
*
*  PLANE ANGLE GENERATION
*
      LDDS = .0015017*LC21 - .1637*LC22C
      LDDB = -.031945*LC11 + 1.9831*LC12C
      LDB  = REALPL(0.,.667,LDDB)
      LDS  = REALPL(0.,.667,LDDS)
      LDSGRA = 57.296*LDS
      LDBGRA = 57.296*LDB
      LPITGR = 57.296*LPITCH
```

```
SAMPLE
      CALL DRWG(1,1,TIME,LDEPTH)
      CALL DRWG(2,1,TIME,LPITGR)
      CALL DRWG(3,1,TIME,LDBGRA)
      CALL DRWG(3,2,TIME,LDSGRA)
TERMINAL
      CALL ENDRW(NPLOT)
END
```

```
          COMPENSATED NON-LINEAR MODEL (STEADY-STATE DECOUPLING)
*
*
*
* THIS PROGRAM SIMULATES THE NON-LINEAR SUBMARINE IN SIX DEGREES
* OF FREEDOM.
*
*
*
* NOMENCLATURE:
*
*
*          K 1     = GAIN OF COMPENSATOR GC 11
*          K 2     = GAIN OF COMPENSATOR GC 22
*          UC      = COMMAND SPEED IN FT/S
*          CZOR    = ORDERED DEPTH IN FT
*          CZER    = DEPTH ERROR
*          LCZERR  = LIMITED DEPTH ERROR
*          CPOR    = ORDERED PITCH IN RAD
*          CPER    = PITCH ERROR
*          DRC     = ORDERED RUDDER ANGLE IN RAD
*          DSGRA   = STERNPLANE ANGLE IN DEG
*          DBGRA   = FAIRWATER PLANE ANGLE IN DEG
*          DRGRA   = RUDDERANGLE IN DEG
*          AT      = NORMALIZED CONTENT OF AFT TRIM TANK
*          FT      = NORMALIZED CONTENT OF FORWARD TRIM TANK
*          AU      = NORMALIZED CONTENT OF AUXILIARY TANK
*
*
TITLE SUBMARINE SIMULATION LUESSOW-NITSCHE
PARAM K1 = .015
PARAM K2 = 3.
PARAM UC = 18.58
PARAM CZOR = 100.
PARAM DRC = .3491
PARAM AT = -3.477 E-5
PARAM FT =  3.477 E-5
PARAM AU = 8.226E-5
*
* PRECALCULATED COFACTORS
*
PARAM DEL=.18901E-16,COFAA=.212502E-14,COFAB=0.0,COFAC=C.C
PARAM COFAD=0.0,COFAE=0.0,COFAF=0.0,COFEA=0.0
PARAM COFBB=.153152E-14,COFBC=0.0,COFBD=-.186106E-10
PARAM COFEE=0.0,COFBF=.17543E-12,COFCA=C.0,COFCB=C.C
PARAM COFCC=.11665E-14,COFCD=0.0,COFCE=-.999506E-13
PARAM COFCF=C.0,COFDA=0.C,COFDB=-.905797E-16,COFDC=0.0
```

```
PARAM CCFDD=.294191E-11,CCFDE=0.0,COFDF=-.224359E-13
PARAM CCFEA=0.0,COFEB=0.0,COFEC=-.58035E-18,COFED=0.0
PARAM CCFEE=.19562E-13,CCFEF=0.0,COFFA=0.0,COFFB=.162929E-17
PARAM CCFFC=0.0,COFFD=-.318591E-13,CCFFE=0.0,CCFFF=.179521E-13
*
* HYDRODYNAMIC COEFFICIENTS AND SUBMARINE CHARACTERISTICS
*
PARAM LC=415.0,ML=.0087445,A1=-.001,A2=-.00095,A3=.CC195
PARAM IX=7.3114E-06,IY=5.6867E-04,IZ=5.6867E-04
PARAM XLDDT=-.0C015,XVR=.C11,XWQ=-.0C75,XVV=.0C65,XWW=.C02,XDRDR=-.C028
PARAM XDSDS=-.0025,XDBDB=-.0026,XQQ=-.0002,XRR=-.C0C09,XRP=.0CC25
PARAM YVDDT=-.011,YWP=.0C75,YV=-.021,Y1V1V=-.06,YF=.003,YV1R1=-.0073
PARAM YP=-.0007,YRDOT=.0C0C9,YPDOT=-.CCC3,YDR=.0C62,YPQ=.CCC2
PARAM YWW=-.065
PARAM ZWDDT=-.0075,ZVP=-.007,ZS=-.0001,ZW=-.011,ZW1W1=-.03,ZVV=.065
PARAM ZQ=-.0045,ZW1Q1=-.006,ZVR=-.008,ZRR=-.0015,ZDS=-.0C5,ZDB=-.0025
PARAM ZQDDT=-.0002,Z1W1=0.0,ZWW=0.0,ZRP=-.0009
PARAM KPDDT=-3.0E-06,KQR=-.0001,KRDOT=-7.0E-06,K1P1P=-8.0E-07,KV=-.C007
PARAM K1V1V=-.0009,KP=-3.5E-05,KR=-4.0E-05,KVDDT=-.00025,KVW=.CC35
PARAM KDR=7.0E-05,KWP=2.5E-04
PARAM MDDDT=-.00C4,MRP=.C0015,MS=4.0E-05,MW=.003,M1W1W=-.0C5,MVV=.015
PARAM MQ=-.0025,M1W1Q=-.002,MVR=-.004,MRR=-.00055,MWDOT=-.CC02
PARAM MDS=-.0C25,MDB=.0005,M1W1=0.0,MVP=.0009
PARAM NRDDT=-5.0E-04,NPQ=-4.0E-04,NPDOT=-7.0E-06
PARAM NV=-.0C75,N1V1V=.014
PARAM NR=-.003,N1V1R=-.0045,NP=-2.0E-06,NVDOT=.00C3,NDR=-.CC3
PARAM NWV=.015,NWP=-.0002
PARAM E2E=1.C11413E-03
INTEGER NFLDT
INCON YADDT=0.0,RDDOT=0.0,PIDDT=0.0
INCON DS=C.,DB=0.
CONST NFLDT=1
CONTRL FINTIM=400. ,DELT=.01,DELS=.5
PRINT T.,L,DEPTH,YAWGRA,PITGRA,DBGRA,DSGRA
*
INITIAL
*
      LC2=LC**2
      IZX=IZ-IX
      IYX=IY-IX
      IZY=IZ-IY
*
DYNAMIC
*
* ERROR LIMIT CALCULATION
*
      IF(L.LT.11.82) LIM = 40.
      IF(L.GE.11.82) LIM = -1.6655*U + 59.6875
```

```
DERIVATIVE
*
* PRECALCULATION FOR EQUATIONS OF MOTION
*
      FA1=XDRDR*L*U*DR*DR/LC
      FA2=XDSDS*U*U*DS*DS/LC
      FA3=XDEDE*U*U*DE*DE/LC
      FB1=YDR*U*L*DR/LC
      FC2=ZDS*U*U*DS/LC
      FC3=ZDE*U*U*DE/LC
      FD1=KDR*U*L*DR/LC2
      FE2=MDS*U*U*DS/LC2
      FE3=MDE*U*L*DE/LC2
      FF1=NDR*U*U*DR/LC2
      FA=FA1+FA2+FA3
      FB=FB1
      FC=FC2+FC3
      FD=FD1
      FE=FE2+FE3
      FF=FF1
      AEV=ABS(V)
      AEW=ABS(W)
      AEP=ABS(P)
      AEQ=ABS(Q)
      AER=ABS(R)
      VVWW=V*V+W*W
      AVW=SQRT(VVWW)
      AEWF=FCNSW(W,-1.0,0.0,1.0)
      AEVF=FCNSW(V,-1.0,0.0,1.0)
      SA1=+LC*(XQQ*Q**2+XRR*R**2+XRP*R*P)
      SA2=+(ML*V*R+XVR*V*R+XWQ*W*Q-ML*W*Q)
      SA3=+(XVV*V**2+XWW*W**2)/LC-SIN(PITCH)*(AT+FT+AU)
      SA4=+(A1*U**2+A2*U*UC+A3*UC**2)/LC
      SB1=+LC*YPQ*P*Q
      SB2=+(YWP*W*P+YV1R1*ABR*AVW*ABVP+ML*W*P-ML*L*R)
      SB3=+(YWV*W*V+Y1V1V*AVW*V)/LC+SIN(ROLL)*COS(PITCH)...
      *(AT+FT+AU)
      SB4=(YR*R+YP*P+YV*V/LC)*U
      SC1=LC*R*(ZRR*R+ZRP*P)
      SC2=+(ZVP*V*P+ZVR*V*R+ZW1Q1*ABQ*AVW*ABWP+ML*U*Q-ML*P*V)
      SC3=+(ZWW*W**2+ZVV*V**2+ZW1W1*W*AVW+U*Z1W1*ABW+U*U*ZS)/LC
      SC4=ZQ*U*Q+ZW*U*W/LC+COS(PITCH)*COS(ROLL)*(AT+FT+AU)
      SD1=+(KCR*C*R+K1P1P*ABP*P)-IZY*C*R
      SD2=(KWP*W*P-BZB*SIN(ROLL)*COS(PITCH))/LC
      SD3=+(K1V1V*V*AVW+KVW*V*W+KS*U**2)/LC2
      SD4=((KP*P+KR*R)/LC+KV*V/LC2)*U
      SE1=(MRP*P+MRR*R+IZX*P)*R
      SE2=((MVR*R+MVP*P)*V+M1W1Q*AVW*Q-EZB*SIN(PITCH))/LC
```

```
      SE3=(MVV*V**2+MWW*W**2+M1W1W*AVW*W+M1W1*L*AVW+U**2*MS)/LC2
      SE4=MQ*U*Q/LC+(MW*U*W-(175.5*FT-219.5*AT)*COS(PITCH)...
      *COS(ROLL))/LC2
      SF1=(NPQ-IYX)*P*Q
      SF2=+(NWP*W*P+N1V1R*AVW*R)/LC
      SF3=(NWV*W+N1V1V*AVW)*V/LC2
      SF4=(NP*P+NR*R)*U/LC+(NV*U*V+(175.5*FT-219.5*AT)*...
      COS(PITCH)*SIN(ROLL))/LC2
      SA=SA1+SA2+SA3+SA4
      SB=SB1+SB2+SB3+SB4
      SC=SC1+SC2+SC3+SC4
      SD=SD1+SD2+SD3+SD4
      SE=SE1+SE2+SE3+SE4
      SF=SF1+SF2+SF3+SF4
      ZA=SA+PA
      ZB=SB+PB
      ZC=SC+PC
      ZD=SD+PD
      ZE=SE+PE
      ZF=SF+PF
*
* EQUATIONS OF MOTION
*
      UDOT=(CCFAA*ZA+COFAB*ZB+COFAC*ZC+COFAD*ZD+CCFAE*ZE+CCFAF*ZF)/DEL
      VDOT=(CCFBA*ZA+CCFBB*ZB+COFBC*ZC+CCFBD*ZD+CCFBE*ZE+CCFBF*ZF)/DEL
      WDOT=(COFCA*ZA+COFCB*ZB+COFCC*ZC+CCFCD*ZD+CCFCE*ZE+CCFCF*ZF)/DEL
      PDOT=(CCFDA*ZA+COFDB*ZB+COFDC*ZC+CCFDD*ZD+CCFDE*ZE+CCFDF*ZF)/DEL
      QDOT=(CCFEA*ZA+COFEB*ZB+COFEC*ZC+CCFED*ZD+CCFEE*ZE+CCFEF*ZF)/DEL
      RDOT=(CCFFA*ZA+COFFB*ZB+COFFC*ZC+COFFD*ZD+CCFFE*ZE+CCFFF*ZF)/DEL
*
* AUXILIARY EQUATIONS
*
      ZDOT=-U*SIN(PITCH)+V*COS(PITCH)*SIN(ROLL)...
      +W*COS(PITCH)*COS(ROLL)
      PIDOT=Q*COS(ROLL)-R*SIN(ROLL)
      YADOT=(R*COS(ROLL)+Q*SIN(ROLL))/COS(PITCH)
      RDOT=P+YADOT*SIN(PITCH)
      U=INTGRL(UC ,UDOT)
      V=INTGRL(0.,VDOT)
      W=INTGRL(0.,WDOT)
      P=INTGRL(0.,PDOT)
      Q=INTGRL(0.,QDOT)
      R=INTGRL(0.,RDOT)
      DEPTH=INTGRL(0.0,ZDOT)
      ROLL=INTGRL(0.0,RODOT)
      PITCH = INTGRL(PITCHO,PIDOT)
      YAW=INTGRL(0.0,YADOT)
      DEGRA=DE*57.296
```

```
      DSCRA=DS*57.296
      DRCRA=DR*57.296
      PITCRA = PITCH*57.296
      RCLCRA=ROLL*57.296
      YAWCRA=YAW*57.296
*
* ERROR CALCULATION
*
      CZER = CZCR - DEPTH
      CPER = CPCR - PITCH
      LCZERR = LIMIT(-LIM,LIM, CZER)
*
* COMPENSATOR GC11
*
      LC1A = -K1*LCZERR
      LC1B = LEDLAG(0.,2.5,.25,LC1A)
      LC1C =LEDLAG(0.,2.5,.25,LC1B)
      DE=REALPL(0.,.667,LC1C)
*
* COMPENSATOR GC22
*
      LC2A = -K2* CPER
      LC2B = LEDLAG(0.,2.,.1,LC2A)
      DS   = REALPL(0.,.667,LC2B)
SAMPLE
      CALL DRWG(1,1,TIME,DEPTH)
      CALL DRWG(2,1,TIME,PITCRA)
TERMINAL
      CALL ENDRW(NPLOT)
END
```

LIST OF REFERENCES

1. R.W. Richard, User's Guide NSRDC Digital Program for simulating Submarine motion, NSRDC Report No P-433-M-01,June 1971

2. H.L. Drurey,Automatic Control of Submarine Depth, Pitch and Trim, Thesis NPS, September 1975

3. E. Romero, Mathematical Models and Computer Solution for the Equations of Motion of Surface Ships and Submarines, in Six Degrees of Freedom, Thesis NPS,June 1972

4. G.J.Thaler and J.-Y. Huang, Steady-State Decoupling and Design of Linear Multivariable Systems, Research Report Grant No. NGR 05-017-010 University of Santa Clara, June 1972-June 1974

5. J.R. Ware,Trident Automatic course and depth Keeping Controller(U), NAVSHIPS Report No. C-510-H-05,June 1973

6. M.A.S. MacNamara, A New Parameter Optimization Method Applied to Autopilot Design, Thesis NPS, March 1975

7. M. Gertler and G.R. Hagen, Standard Equations of Motion for Submarine Simmulation, NSRDC Report No. 2510,June 1967

8. K. Ogata, Modern Control Engineering, Prentice-Hall, Inc., 1970

9. G.J. Thaler, Design of Feedback Systems, Dowden,Huchinson and Ross, Inc., 1973

10. J.G. Truxal, Introductory Systems Engineering, McGraw-Hill Book Company, 1972

11. H.H. Rosenbrock, State-Space and multivariable Theory, JohnWiley and Sons, Inc., 1970

12. W.A. Wolovich, Static Decoupling, Joint Automatic control conference, 1973

13. C.T. Chan, Stability of Linear Multivariable Feedback Systems, Proc. IEEE, Vol. 116, p. 1929-1936, 1969

14. C.H.Hsu and C.T. Chen, A Proof of the Stability of Multivariable Feedback Systems, Proc. IEEE, Nov. 1968

15. G.J. Thaler and B.T. Rung,On the Realization of Linear Multivariable Control Systems, NPS Research Paper No. 39, August 1963

INITIAL DISTRIBUTION LIST

		No. Copies
1.	Defense Documentation Center Cameron Station Alexandria, Virginia 23314	2
2.	Library, Code 0212 Naval Postgraduate School Monterey, California 93940	2
3.	Department Chairman, Code 62 Department of Electrical Engineering Naval Postgraduate School Monterey, California 93940	2
4.	Professor G. Thaler, Code 62 Tr Department of Electrical Engineering Naval Postgraduate School Monterey, California 93940	5
5.	Marineamt -A 1- 294 Wilhelmshaven Federal Republic of Germany	1
6.	Dokumentationszentrale der Bundeswehr (See) Friedrich-Ebert-Allee 34 53 Bonn Federal Republic of Germany	1
7.	Dr. John Ware Operations Research Inc. 1400 Spring Street Silver Spring, Maryland	1

8. William E. Smith, Code 1576 — 1
NSRDC
Bethesda, Maryland 20034

9. LCDR Volkmar Nitsche, FGN — 2
Eckener Str. 13 b. Weck
239 Flensburg
Federal Republic of Germany

10. LCDR Klaus J.C. Luessow, FGN — 2
Besenheide 10
22 Elmshorn
Federal Republic of Germany


FILM
5